Utility of hepatocellular systems to measure drug transport and metabolism for prediction of *in vivo* drug clearance

A thesis submitted to the University of Manchester for the degree of Doctor of Philosophy in the Faculty of Biology, Medicine and Health

2017

James A R Harrison

Division of Pharmacy and Optometry

Table of Contents

Final Word Count: 60,995

List of Figures

List of Tables

List of Abbreviations

5-CDFDA	5-Carboxy-2',7'-Dicholofluorescein Diacetate
ABC	ATP-Binding Cassette
ABT	1-Aminobenzotriazole
ADME	Absorption, Distribution, Metabolism And Excretion
ANOVA	Analysis of variance
AUC	Area under the curve
BCRP	Breast-Cancer Resistant Protein
BDDCS	Biopharmaceutics Drug Disposition Classification System
C_0	Initial Substrate Concentration In The Media
CDF	Carboxydichlorofluorescein
CDSF	Clearance-Derived Scaling Factors
CL_{active}	Active Uptake Clearance
CL_{bile}	Biliary Efflux Clearance
CL_{efflux}	Total Efflux Clearance
CL_H	Hepatic Clearance
CL_{int}	Intrinsic Clearance
$CL_{int,app}$	Apparent Intrinsic Clearance
$CL_{int,\ in\ vitro}$	*In Vitro* Intrinsic Clearance Scaled To The Level Of The Body
$CL_{int,\ in\ vivo}$	*In Vivo* Intrinsic Clearance
$CL_{int,\ ML}$	Media Loss Intrinsic Clearance
$CL_{int,\ total}$	Total Intrinsic Clearance
CL_{met}	Metabolic Intrinsic Clearance
CL_p	Plasma Clearance
$CL_{passive}$	Passive Uptake Clearance (Passive Diffusion)
CL_R	Renal Clearance
CL_{uptake}	Total Uptake Clearance
CYP	Cytochrome P450
DDI	Drug-Drug Interactions
ER	Endoplasmic Reticulum
$CL_{sinusoidal}$	Sinusoidal Efflux Clearance
FDA	Food And Drug Administration
fu_b	Fraction Of Unbound Drug In The Blood
fu_{cell}	Fraction Of Unbound Drug In The Cell
fu_p	Fraction Of Unbound Drug In The Plasma
GLKB	Gram Liver Per Kg Bodyweight
GMFE	Geometric Mean Fold Error
GST	Glutathione S-Transferase
HBSS	Hank's Balanced Salt Solution
HPGL	Hepatocytes Per Gram Liver
IVIVE	*In Vitro* to *In Vivo* Extrapolation
k_1	Elimination Rate Constant In The First Phase
k_2	Elimination Rate Constant In The Second Phase
K_{el}	Elimination Rate Constant
K_i	Inhibitory Constant

K_m	Michaelis Constant
Kp	Hepatocyte To Medium Partition Coefficient For Total Drug
Kp_u	Hepatocyte To Medium Partition Coefficient For Unbound Drug
LC-MS/MS	Liquid Chromatography In Tandem With Mass Spectrometry
MAPEG	Membrane Associated Proteins In Eicosanoid And Gluthathione Metabolism
ML	Media Loss
ML:C	Ratio Of CL_{int} Between The Media Loss And Conventional Assay
MMPPGL	Mg Microsomal Protein Per Gram Liver
MPPGL	Mg Protein Per Gram Liver
MRP2	Multidrug Resistance Protein 2
MT	Methyltransferase
NAT	N-Acetyltransferase
NCE	New Chemical Entities
NSAID	Non-Steroidal Anti-Inflammatory Drugs
NTCP	Na^+-Taurocholate Co-Transporting Polypeptide
OAT	Organic Anion Transporters
OATP	Organic Anion Transporting Polypeptide
OCT	Organic Cation Transporters
PBPK	Physiologically-Based Pharmacokinetic
PBS	Phosphate Buffered Saline
P-gp	P-Glycoprotein/Multidrug Resistance Protein 1
PK	Pharmacokinetics
Q_H	Hepatic Blood Flow
R_b	Blood To Plasma Ratio
Rfc	Rifamycin SV
RMMA	Relative Mean Microsomal Abundance
RMSE	Root Mean Squared Error
S_{cell}	Substrate Concentration In The Cell
SCH	Sandwich Cultured Hepatocytes
SDE	Soluble Dimeric Enzyme
SLC	Solute Carrier Superfamily
S_{med}	Substrate Concentration In The Media
SULT	Sulfotransferase
TMT	Thiol Methyltransferase
TPMT	Thiopurine S-Methyltransferase
UGT	UDP-Glucuronosyltransferase
V_{cell}	Cell Volume
$V_{cell,app}$	Apparent Cell Volume
V_{max}	Maximal Velocity
V_{med}	Media Volume
WME	Williams' Medium E

Abstract

Predictive pharmacokinetics now forms a critical part of the drug discovery process. However, metabolic data has been demonstrated to under-predict *in vivo* clearance, while no large scale analysis has been performed for hepatic uptake data. The primary aim of this thesis was therefore to investigate the utility of various clearance parameters generated in hepatocellular assays for the prediction of *in vivo* clearance.

Large scale literature analyses were performed for uptake data in both rat and human hepatocytes. In the rat, it was highlighted that over-prediction was the predominant issue for suspension and media loss hepatocyte assays. Conversely, monolayer and SCH assays suffered from under-prediction. However, in human hepatocytes under-prediction was observed in all assay formats. Use of empirical scaling factors improved predictions in both species, and are recommended for future use.

The media loss assay, a method described by Soars et al[1], was further developed in rat hepatocytes through inclusion of transporter and metabolic enzyme inhibitors. Using a two-compartment model, individual clearance parameters (CL_{met}, CL_{active} and $CL_{passive}$) were estimated, and were also used to estimate binding and partitioning terms (Kp, Kp_u and fu_{cell}). IVIVE of data produced from this assay resulted in a lower bias than had been noted from literature data. However, it was hypothesised that additional clearance parameters could be used in a mechanistic approach to further improve predictions.

SCH assays were performed to generate estimates of uptake rates, as well as efflux rates from both the sinusoidal and canalicular membranes. Combining clearance terms from both the media loss and SCH assays using the $CL_{int,total}$ term led to less bias when predicting *in vivo* clearance than observed using uptake or metabolism data alone. Additionally, the use of empirical scaling factors identified from the literature analysis led to further reduction in prediction bias. Future work must now focus on the application of this research to human hepatocytes.

It is concluded that the work presented in this thesis provides evidence for the usefulness of both uptake and extended clearance terms, in conjunction with empirical scaling methods, for the prediction of *in vivo* clearance. Adaptation of the media loss assay allowed the estimation of several key pharmacokinetic parameters. Although some of these are not always useful in a quantitative fashion, they remain essential properties of a compound that must be considered when predicting behaviour within the body.

Declaration

No portion of the work referred to in the thesis has been submitted in support of an application for another degree or qualification of this or any other university or other institute of learning

Copyright Statement

Acknowledgements

First and foremost, I would like to thank my supervisor Professor J. Brian Houston for providing me with the opportunity to undertake this Ph.D. project, as well as for the guidance, knowledge and freedom you have given over my time at CAPKR. I am also thankful to my supervisors, both past and present, who have been instrumental to the success of this Ph.D. project at different stages. To Dr Carina Cantrill; for your time, patience and knowledge as I started out on my journey, with little experience and a lot of questions! To Dr Tom De Bruyn; for your expertise and enthusiasm, as well as the confidence you instilled when I needed it most. To Dr Adam Darwich; for your time, effort and expertise which formed such an essential part of this project, and for putting up with my demands without complaint. Special thanks is owed to Dr David Hallifax and Susan Murby for your time and assistance with LC-MS/MS analysis, as well as keeping the machines running!

To my colleagues, past and present at CAPKR, I'm grateful for your friendship and advice. I'd especially like to thank Francesca, Shelby and Laura for being such huge sources of encouragement, advice and laughter – I wouldn't have survived without you!

To my family, I'm thankful for your love, support and belief through all stages of life, without which none of this would have been possible. I'm especially grateful to my wife, Claire. You've always been there to provide encouragement, support and a listening ear whenever it has been needed, and are a constant source of inspiration.

Chapter 1. General Introduction

The development of new chemical entities (NCEs) is becoming an increasingly lengthy and expensive process. Current cost estimates from target identification to launch are in the region of £1.2 billion, of which £569 million is out of pocket expense[2]. Early termination of candidate molecules destined to fail in clinical trials has been suggested as an effective strategy to reduce overall costs of drug development[3]. It is believed as much as £178-484 million could be saved in this manner, depending on the stage at which development is terminated[2]. Between 1964 and 1991, poor pharmacokinetics (PK) was cited as the primary reason for the failure of drug development in around 40% of cases[3]. This prompted a push for predictive methods to determine absorption, distribution, metabolism and excretion (ADME) properties of a compound early in development. Initial attempts focused on the use of allometric scaling following administration of drugs to animals *in vivo*. While it was hoped that PK parameters could be directly scaled between species, it quickly became apparent that the method had several variables, depending on drug properties and/or species of animal, leading to inaccurate results[4]. As an alternative, *in vitro* assays were developed using liver homogenates and later hepatocytes in order to generate predictions of *in vivo* metabolic clearance[5, 6]. This principle was based on the use of liver models, which encompass the contribution of several parameters and physiology of the liver to describe the overall rate of hepatic clearance[7]. Combined with increasing knowledge of both enzymes and transporters, as well as the advent of physiology-based pharmacokinetic (PBPK) modelling, the field of predictive pharmacokinetics experienced an exponential growth in predictive capabilities. This has contributed to a fall in the number of NCEs failing due to poor PK to just 10% by the year 2000[8], and now guides compound design, lead compound selection and preclinical studies.

This introduction focuses on the liver, the primary site of drug elimination. Hepatocellular processes, including hepatic transport, metabolism and efflux will be outlined, along with detailed descriptions of *in vitro* techniques and data analysis commonly applied within the field.

1.1. The Liver

In humans, the liver is the second largest organ of the body, weighing approximately 1.4kg in the average male. Histologically, the liver has three key components (hepatocytes, bile canaliculi and hepatic sinusoids) arranged into lobules (Figure 1). Hepatocytes are highly specialised cells which account for approximately 80% of the organ volume and perform a large number of metabolic and secretory tasks. They are arranged in hepatic laminae, a complex three-dimensional structure, which ensures a one cell thick border lines the hepatic sinusoids. Sinusoids allow oxygenated blood from the hepatic artery to mix with the nutrient rich blood from the portal vein. Each sinusoid flows into the central vein, which leads to the hepatic vein and is finally transported to the rest of the body via the inferior vena cava. Bile canaliculi are ducts present between hepatocytes which collect bile, a substance used for both secretion and excretion of various products into the gastrointestinal tract. As with the blood flow, a series of connections are formed from the bile canaliculi, eventually connecting to the gall bladder in humans to form the common bile duct, which leads into the small intestine.

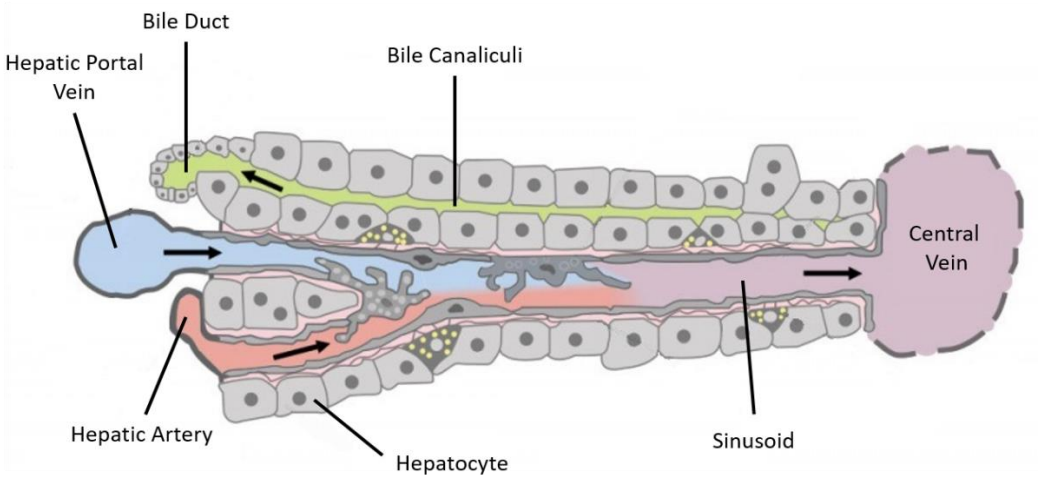

Figure 1 – Diagram of the histological components of the liver[9].

The liver is responsible for a number of highly important functions in vertebrates, including carbohydrate, lipid and protein metabolism, protein synthesis, production of digestive substances and detoxification and elimination of both exogenous and endogenous substances from the body. The lobule structure ensures two distinct hepatocyte membranes; the sinusoidal (basolateral) membrane in contact with the blood

flow, and the canalicular (apical) membrane in contact with the bile duct. This structure allows drug elimination through hepatic uptake (transport), metabolism and/or biliary efflux.

1.2. Hepatic Transport

1.2.1. Uptake Transporters

While it is possible for substances to cross the plasma membrane of hepatocytes via passive diffusion, many cannot do so efficiently without being facilitated by transporter proteins. These transporters are members of the solute carrier superfamily (SLC), which consists of a number of subfamilies. Of particular interest to drug transport are the organic anion transporting polypeptide (OATP), organic cation transporters (OCT), organic anion transporters (OAT) and Na^+-taurocholate co-transporting polypeptide (NTCP). Specific transporters within these subfamilies are known to be responsible for the transport of many drugs, and will be discussed in detail. For the most part, rat orthologs are highly similar to that of the human transporters, and are identified by the use of lowercase letters within the transporter names (i.e. Oatp)[10, 11].

1.2.1.1. Organic Anion Transporting Polypeptide (OATP)

Members of the OATP family have been identified as being the major transporter of a large number of drugs. Eleven members of the OATP family have been identified in humans, seven of which have been determined to be expressed in the liver through detection of their respective mRNA[12]. Structure and function of these transporters have been extensively reviewed by Hagenbuch and Gui[13], whose findings are summarised here. At present, structural information for these transporters are limited to predictions from computational modelling. While it is estimated that they contain 9-12 domains, it is generally accepted within the literature that there are likely 12 domains. Additional extracellular loops act as N-glycosylation sites, believed to be important for both function and localisation of the transporters. OATPs are typically involved in the uptake of hydrophobic anions with molecular weights above 450 Da. However, substrate range is broad and includes organic amphiphilic substances (bile salts, hormones, conjugates and various drugs, see Table 1). While the exact mechanism of these transporters has yet to be fully elucidated, it is believed that they function as anion exchangers[14, 15]. OATP1B1,

1B3 and 2B1 have been identified as the family members of most importance to hepatic drug disposition in human, while in rat it is Oatp1b2 (the rat ortholog of human OATP1B1/1B3) and Oatp2b1 (summarised in Table 1). While OATP1B1/1B3 and Oatp1b2 are almost exclusively located on the basolateral membrane of hepatocytes, OATP2B1/Oatp2b1 has been found in almost all tissues, indicating a much broader role[12].

With such a wide range of substrates and inhibitors, the effects of drug-drug interactions (DDI) and genetic polymorphisms on these transporters must be considered, as both can lead to important clinical implications. For example, a study performed on patients co-dosed with cyclosporine and repaglinide (an OATP1B1 inhibitor and substrate, respectively) resulted in area under the curve (AUC) increases of 244% for repaglinide[16]. Although a reduction in metabolism of repaglinide was suspected, the inhibition caused by cyclosporine was reduced by 42% in patients with a *SLCO1B1* reduced function gene mutation, which codes for OATP1B1, strongly suggesting that the inhibition of the transporter was the predominant cause of the AUC increase[16]. The effect of cyclosporine and transporter mutations, have also been observed to affect exposure to many statins[15, 17], which are well known substrates of OATPs.

1.2.1.2. Organic Cation Transporter (OCT)

OCTs have been identified as having a range of substrates and are present in multiple tissues. OCTs belong to the SLC22 family of transporters, and are divided into subtypes of 1-3. As with OATPs, the exact structure of OCTs are unknown, however it is predicted that they too have 12 transmembrane domains with extracellular loops. OCT function is driven by an electrochemical gradient, independent of sodium (Na^+). As such, transport can be bidirectional and is driven by the direction of the electrochemical gradient[18].

Only OCT1 (Oct1 in rat) appears to be relevant to drug uptake in the liver. OCT1 has been identified in many mammalian species, and is localised to the basolateral membrane of hepatocytes. Endogenous substrates include neurotransmitters, choline, creatinine and guanidine. Generally, exogenous substrates are hydrophilic, low molecular weight and organic cations, however some weak bases have also been identified. Examples include

cimetidine, acyclovir and metformin (see Table 1)[18]. Inhibitors have a tendency to be highly lipophilic, large molecular weights and a net positive charge[15], while *in vitro* evidence exists for strong inhibition caused by clonidine, fenfluramine and imipramine[19]. Several cases have been published demonstrating DDIs arising from the inhibition of OCT1, however these typically involve reductions in renal excretion, rather than hepatic uptake[20]. OCT1 polymorphisms have been recorded, and are believed to lead to reduced function. For example, reduced therapeutic action of metformin has been noted in some patients with such polymorphisms, and is thought to be caused by a decrease in hepatic uptake[21]. Additionally, O-desmethyltramadol, the active metabolite of the opioid analgesic tramadol, has recently been observed at significantly higher concentrations in the plasma of patients carrying a loss of function polymorphism in OCT1 than that of control patients[22]. This is believed to be due to reduced hepatic uptake of the metabolite. It should be considered, therefore, that reduction of hepatic uptake due to DDIs involving OCT1 may be clinically relevant.

1.2.1.3. Organic Anion Transporter (OAT)

OATs also belong to the SLC22 family, with OAT1-4 being the most significant human isoforms. It is predicted that the transporters consist of 12 transmembrane domains and functions via an exchange of intracellular 2-oxoglutarate for the substrate, resulting in transport being bidirectional in some instances[15].

Only OAT2 (Oat2 in rat) has high expression in the liver and is localised on the basolateral membrane, while OAT1 and 3 are highly expressed in the basolateral membrane, and OAT4 in the apical membrane of the kidney proximal tubule cells[12]. Examples of OAT2 substrates include allopurinol, methotrexate, and bumetanide[23] (Table 1), while probenecid has been suggested to inhibit OAT2[24]. In cases where OATs are thought to be involved with DDIs, this is due to reduced renal clearance caused by inhibition of renal OAT1, 3 and 4[15], while no clinically relevant interactions have been attributed to OAT2.

1.2.1.4. Na^+-taurocholate co-transporting polypeptide (NTCP)

NTCP (Ntcp in rat) is localised on the basolateral membrane of hepatocytes. Thought to consist of seven transmembrane domains and an extracellular loop essential for correct function of the transporter, NTCP utilise the Na^+ gradient to drive transport of substrates

into the cell, requiring two Na^+ atoms per molecule of substrate[25]. NTCP is responsible for the majority of bile acid uptake into hepatocytes, and so regulates the correct removal of bile acids from the blood. It is this role that must be considered for possible clinical implications arising from drug administration. Cyclosporine A and bumetanide inhibit NTCP and have been demonstrated to lead to cholestatic liver injury if administered for extended periods of time[25]. As well as bile acids, there is evidence that NTCP contributes to the active transport of micafungin[26] and rosuvastatin in humans, but not rats[27]. NTCP has also been identified as the cellular receptor for Hepatitis B virus, allowing its entry into the hepatocyte[28].

1.2.2. Efflux Transporters

Active transport of substrates from hepatocytes into the bile canaliculi is mediated by the ATP-binding cassette (ABC) family of transporters. As the name suggests, these transporters utilise ATP hydrolysis to drive transport. While 48 ABC genes have been identified in human, three are of particular importance to hepatic disposition; breast cancer resistance protein (BCRP), multidrug resistance-associated protein 1 or P-glycoprotein (P-gp) and multidrug resistance-associated protein 2 (MRP2).

1.2.2.1. Breast Cancer Resistance Protein (BCRP)

BCRP (Bcrp in rat) is expressed in a range of tissues, acting to efflux substrates out of the cell from the apical membrane. BCRP structure differs from that of other transporters, in that the gene codes for half of a transporter. This includes six transmembrane domains and an extracellular loop. It is believed that disulphide bonds form between two of these protein structures to make a complete transporter[29]. Its main physiological role in the liver appears to be the extrusion of porphyrins from hepatocytes[15], but *in vitro* assays have demonstrated an affinity for a broad range of exogenous substrates (summarised in Table 1). Significant changes to PK profiles due to effects of DDIs or genetic polymorphisms on BCRP has prompted several drug regulatory bodies to recommend that drugs be tested as both substrates and inhibitors[30]. Rosuvastatin has been identified as the most appropriate probe for BCRP, while curcumin and lapatinib were identified as the most potent inhibitors[30].

1.2.2.2. P-glycoprotein (P-gp)

P-gp, also known as Multidrug Resistance Protein 1 (MDR1 in human, Mdr1a/b in rat), has been studied extensively due to its ubiquitous tissue distribution and broad substrate range, making it highly influential on the kinetic profile of many drugs. P-gp has been imaged to a resolution of 3.4 Ångströms in *Caenorhabditis elegans*, and is thought to be 46% identical to human P-gp. It is therefore estimated that human P-gp possesses 12 transmembrane domains, as well as intracellular loops thought to be involved in drug binding, or to act as hinges allowing the opening of the transporter, a structure believed to be similar across all ABC transporters[31]. It is hypothesised that the main physiological function of the transporter is to protect tissues from toxic substances through extrusion from the cell[32]. However, the influence of the transporter on drug profiles became apparent following the discovery that, along with other transporters, efflux of anti-cancer drugs from the targeted cancerous cells was one of the main causes of chemoresistance[33]. It is now evident that P-gp can influence distribution and elimination of many drugs throughout the body[32]. In respect of the liver, P-gp is expressed at the apical membrane where it acts to eliminate substrates via biliary excretion. Substrates are typically amphiphilic cations or anionic conjugates, and there is considerable substrate overlap with BCRP[32] (see Table 1). DDIs have been noted for compounds primarily eliminated via P-gp mediated biliary excretion. For example, digoxin has been observed to have a reduction in non-renal clearance when co-dosed with the P-gp inhibitor quinidine[34]. In addition, it is believed that genetic polymorphisms of the P-gp gene are responsible for population differences in expression and activity of the transporter. This can have significant effects on the ADME of P-gp substrates. For example, plasma digoxin levels have been observed to be significantly higher in patients possessing the $C_{3435}T$ single nucleotide polymorphism, which results in lower P-gp expression[35, 36].

1.2.2.3. Multidrug Resistance-Associated Protein 2 (MRP2)

MRP2 (Mrp2 in rat) has been localised to the apical membrane of cells in the liver, kidney, placenta and small intestine where it acts as an ATP-dependent export pump[37]. Computational models have predicted the transporter to contain 17 transmembrane domains[38], which signifies a key difference between the MRP family and other ABC-transporters[37]. Physiological roles include the extrusion of endogenous substances into the bile or urine, such as conjugated forms of bilirubin[39, 40], as well as having several

identified drug substrates, including methotrexate and a number of statins[41, 42] (see Table 1). MRP2 is potently inhibited by elavirdine, efavirenz, and emtricitabine *in vitro*[43], however no significant DDIs appear to have been identified. There are several examples of genetic polymorphisms leading to altered kinetic profiles. Single nucleotide polymorphisms (SNPs) in the MRP2 gene have been associated with increased exposure to pravastatin[44], methotrexate[42] and doxorubicin[45].

Table 1 – Summary of localisation, direction of transport, substrates and inhibitors of hepatic uptake and efflux transporters

Transporter (Human)	Transporter (Rat)	Membrane Localisation	Direction of transport	Driving Force [11, 46]	Example Substrate(s)	Example Inhibitor(s)	Reference(s)
OATP1B1	Oatp1b2	Basolateral	Unidirectional	Under investigation. ATP- and Na^+ independent	Statins Repaglinide Valsartan	Saquinavir Cyclosporine Rifampicin	[32]
OATP1B3		Basolateral	Unidirectional		Statins Digoxin Fexofenadine Valsartan	Ritonavir Cyclosporine Rifampicin	[32]
OATP2B1	Oatp2b1	Basolateral	Unidirectional		Statins Fexofenadine	Cyclosporine Rifampicin	[32]
OCT1	Oct1	Basolateral	Bidirectional	Electrochemical	Cimetidine Acyclovir Metformin	Clonidine Imipramine	[18, 19]
OAT2	Oat2	Basolateral	Bidirectional	α-ketoglutarate exchange	Allopurinol Methotrexate Bumetanide	Probenecid	[23, 24]
NTCP	Ntcp	Basolateral	Unidirectional	Na^+ co-transport	Rosuvastatin	Cyclosporine	[25, 27]
BCRP	Bcrp	Apical	Bidirectional	ATP	Rosuvastatin	Curcumin Lapatinib	[15, 30]
P-gp	Mdr1a/b	Apical	Unidirectional	ATP	Digoxin Fexofenadine	Quinidine Verapamil Cyclosporine	[32]
MRP2	Mrp2	Apical	Unidirectional	ATP	Etoposide Methotrexate Statins	Elavirdine Efavirenz Emtricitabine	[40, 43]

1.3. Hepatic Metabolism

Metabolism allows removal of drugs from the body through modification of the parent compound to a biochemical structure which favours their entry into either bile or urine. Traditionally, metabolism has been split into two sequential phases, phase I and II[47].

1.3.1. Phase I Metabolism

Phase I includes three main enzymatic reactions: oxidation, reduction or hydrolysis. Metabolites formed in phase I reactions are much more polar, and therefore hydrophilic, than the parent compound. Some drug metabolites are sufficiently hydrophilic after phase I metabolism to be removed in the urine[48]. Cytochrome P450 (CYP) enzymes are responsible for the vast majority of phase I drug metabolism, and are the most extensively studied molecules in drug metabolism[49]. The liver contains a number of CYP isoforms, which are localised to the endoplasmic reticulum (ER) within hepatocytes, and relative proportions of each subfamily protein expression are demonstrated in Figure 2.

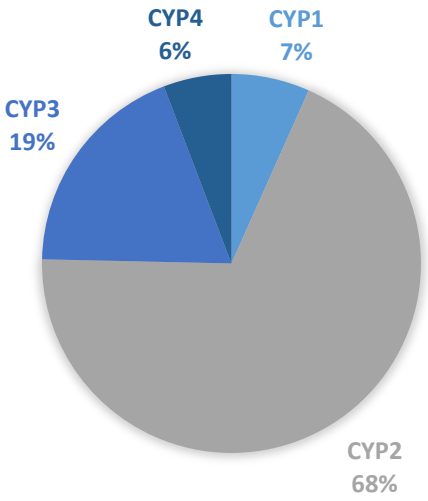

Figure 2 – Relative protein expression of drug metabolising enzyme subfamilies within liver microsomal fractions[50]

It should be noted that a number of tissues express CYPs and are able to metabolise drugs, including the lung, kidney and brain, however the majority of metabolism occurs in the liver[51]. 57 CYP genes have been identified in humans[52], however it is believed that

only certain members of the CYP subfamilies are responsible for the metabolism of most drugs (Table 2). A number of substances are also known to cause either inhibition or induction of CYP enzyme family, which may lead to clinical implications. The catalytic cycle of CYP enzymes follow several steps, and inhibition can arise when any one of these steps is hindered or prevented. Most frequently, this can occur at the start of the cycle through prevention of binding to the active site, but can also include steps that allow binding of oxygen and the oxygenation of the substrate[53]. Typically clinical inhibition will follow reversible behaviour, which occurs when there is competition between two substrates for the active site. However, in some cases irreversible inhibition may occur if catalytic binding forms a permanent bond between the substrate and the haem group within the CYP enzyme[53]. A number of inhibitors are listed for each CYP isoform in Table 2. *In vivo*, inhibition of CYPs may lead to increased exposure to a drug, which may have both therapeutic and toxicological implications. In some cases, this method has been used purposely in order to "boost" a drug which otherwise has poor bioavailability due to extensive metabolism. This has been used to great effect in HIV therapy, where ritonavir is frequently co-dosed with other, more effective antiretroviral drugs due to its known inhibitory effect on CYP3A4[54].

CYP induction is a much slower process, and is often regarded as a physiological adaptation in order to protect the body from chronically administered substances. Typically this is due to an increase in transcription leading to higher enzyme expression, but may also involve stabilization of the enzyme or its mRNA[55]. This phenomenon can lead to the loss of therapeutic effect of drugs, since clearance is increased. St. John's Wort is a prominent example, which has been recorded to reduce the AUC of midazolam by 79% due to induction of CYP3A4[56].

Members of the CYP2 and CYP3A account for the vast majority of CYP expression, and so warrant further introduction. Since many preclinical studies are performed in rats, it is important to note that although orthologs exist across species, the specificity of each is not necessarily identical to those in human, and will be discussed in further detail in 1.3.1.3.

1.3.1.1. CYP2 Family

The CYP2 family consists of 16 genes, the three largest of which contain the sub-families most important for drug metabolism, specifically CYP2A6, 2B6, 2C8, 2C9, 2C19 and 2D6. The family as a whole account for approximately 68% of the total hepatic CYP protein in humans (Figure 2)[50] and are responsible for the metabolism of a number of compounds (examples and further breakdown of hepatic expression provided in Table 2).

CYP2A6 is highly expressed within the liver, accounting for approximately 15% of the total hepatic CYP content. It has been credited as the major enzyme involved in the metabolism of nicotine and coumarin (see Table 2)[57, 58]. Rifampicin and phenobarbital are known to induce CYP2A6 through activation of pregnane X receptors, which stimulate expression of the CYP2A6 mRNA[59]. There is little evidence to suggest that increased enzyme expression has any impact on clinically administered drugs, however there are links to increased nicotine dependence and severity of withdrawal in individuals who smoke[60]. Reduced CYP2A6 activity caused by polymorphisms or inhibitors have been implicated in the reduced bioavailability of the prodrug tegafur, which is primarily metabolised to its active form by CYP2A6[61], while inhibitors have also been suggested as a supplement to anti-smoking therapy through inhibition of nicotine metabolism[62].

CYP2B6, while only accounting for approximately 2% of the total hepatic CYP pool, has a diverse range of substrates, including clinically prescribed drugs (for example S-mephenytoin and cyclophosphamide, see Table 2), recreational drugs (for example 3,4-methylenedioxymethamphetamine) and a number of pesticides, chemicals and pollutants[57, 63]. As with other enzymes, polymorphisms have been identified that lead to either increased or decreased activity or expression. For example, CYP2B6*4 has higher activity towards efavirenz, while CYP2B6*27 has up to 85% reduced activity, and is associated with extreme elevations in efavirenz plasma concentrations[57, 64]. Inhibitors and inducers are listed in Table 2, but have little clinical relevance.

The CYP2C subfamily has several highly homologous genes encoding for CYP2C8, 2C9 and 2C19, accounting for approximately 30% of the total hepatic CYP pool[50]. Despite sharing greater than 80% of DNA and protein sequencing[57], each of the enzymes display a

diverse range of substrate specificity. Due to the number of 2C family members, I refer to Zanger and Schwab[57] for a comprehensive review of substrates, genetic polymorphisms and clinical impacts, summarised in Table 2.

Despite forming only 5% of the total hepatic CYP pool, CYP2D6 is believed to metabolise between 15-25% of all clinically administered drugs, spanning a vast array of drug classes[57]. CYP2D6 has been extensively investigated in the field of pharmacogenetics, due to the number of polymorphic variants discovered and the degree of influence these have on *in vivo* pharmacokinetics of substrates. As a result, carriers of polymorphisms are classified as poor, intermediate or rapid/extensive metabolisers, depending on the effect. For example, CYP2D6*4 leads to incorrect splicing, ultimately resulting in the complete loss of expression from the liver, and the phenotype of a poor metaboliser[65]. At the other end of the spectrum, rapid or extensive metabolisers are typically found to have duplications of the CYP2D6 gene, leading to much higher expression of the enzyme, and hence a higher activity towards substrates[65, 66]. Substrates, inhibitors and inducers of CYP2D6 are listed in Table 2, however no clinically relevant DDIs have been noted.

1.3.1.2. CYP3A Family

CYP3A family members are accredited with the metabolism of approximately 50% of clinically prescribed drugs[67]. Subfamily members expressed in the adult liver include CYP3A4, 3A5, and, in approximately 20% of the population[67], 3A7[51, 68]. Members within the CYP3A subfamily share greater than 85% of their sequence identity and span large sections of DNA[51], and, on average, account for around 19% of total P450 protein expression (Figure 2)[50].

At approximately 85% of the total CYP3 microsomal protein expression[50], CYP3A4 is the most abundantly expressed in the liver. However, substantial variability exists within the population, and has been linked with a correlation to overall P450 expression levels[69]. It is also found at high levels within the intestinal cells, where it contributes significantly to the first-pass effect[70]. Due to both the size and flexibility of the active site, CYP3A4 has a broad substrate range including both large and small molecules (for example cyclosporine and midazolam, respectively; see Table 2)[71]. A number of substances are also known to

cause either inhibition or induction of CYP3A4, with suitable examples outlined in 1.3.1. Identified polymorphisms now run into the hundreds, and are thought to be minor contributors to the large degree of variability in activity observed throughout the human population[67]. Only one mutation, CYP3A4*20, results in a complete loss of enzyme activity[72]. The patient in which this was identified had approximately 2-fold lower clearance of midazolam compared to other patients. Other polymorphisms appear to have limited clinical impact, likely due to overlap of substrates between CYP3A family members[57, 67].

CYP3A5 has much lower expression within the liver compared to CYP3A4, and is also expressed within the gastrointestinal tract where it contributes to the first-pass effect[57]. Expression appears to be particularly low in Caucasians, and higher in Africans/African Americans[67]. Since CYP3A4 and 3A5 share almost identical substrates, it is believed that CYP3A4 is able to adequately metabolise administered drugs, should CYP3A5 be compromised via genetic polymorphisms, thereby preventing serious clinical implications[57]. Equally, inhibition and induction of CYP3A5 have not been noted to have any clinical effect.

CYP3A7 is a foetal enzyme that is typically silenced after birth[73]. However, in some cases a mutation in the CYP3A7 gene leads to continued expression into adulthood[57]. However, due to a large substrate overlap, it is not believed to be clinically relevant.

Table 2 - Hepatic CYP isoforms along with their Relative Mean Microsomal Abundance (RMMA) and examples of identified substrates, inhibitors and inducers in humans. Adapted from [47, 53, 74, 75].

CYP	RMMA (%)	Substrate(s)	Inhibitor(s)	Inducer(s)
1A2	6.7	Caffeine Phenacetin Acetaminophen Theophylline	Furafylline α-Napthoflavone	β-Napthoflavone
2A6	15.0	Coumarin Nicotine	Tranylcypromine Methoxsalen	Rifampicin Phenobarbital
2B6	1.8	S-Mephenytoin Cyclophosphamide	Phencyclidine	Phenobarbital
2C8	8.0	Taxol Amiodarone	Montelucast Quercetin	Rifampicin
2C9	20.3	Diclofenac Tolbutamide S-Warfarin	Sulfaphenazole Fluconazole	Rifampicin
2C19	1.4	Propranolol Mephenytoin Diazepam	Ticlopidine	Rifampicin
2D6	4.6	Bufuralol Dextromethorphan Imipramine Codeine	Quinidine Fluoxetine	Paracetamol
2E1	17.6	Dextromethorphan Phenobarbital	Cimetidine Diclofenac	Diazepam
3A4	16.1	Midazolam Cyclosporine Erythromycin Lovastatin Verapamil	Ketoconazole Troleondomycin Itraconazole	Dexamethasone Rifampicin Carbamazepine

1.3.1.3. Cross-species differences in rat P450 specificity

Although rat orthologs of human hepatic transporters share similar substrate specificity, the same is not true of the P450 enzymes. This is exemplified by a study by Kobayashi et al.[76], who analysed the catalytic activity of rat CYPs against well characterised probe substrates for specific human CYP isoforms. Differences in CYP specificity are displayed in Table 3. Differences have also been documented in levels of expression and activity, and so caution must be exercised for any study intended to predict effects in human using rat data, such as toxicity screening or DDI predictions[77].

Table 3 – Comparison of primary CYP isoforms responsible for the metabolism of a selection of drugs in rat and human, demonstrating cross-species differences[76].

Human CYP Isoform	Drug	Rat CYP Isoform
1A2	Phenacetin 7-Ethoxyresorufin	1A2/2C6
2A6	Coumarin	2A2/2C6/2C12/2D2/3A1/3A2
2C9	Diclofenac	2C6
2C19	*S*-Mephenytoin	None detected
2D6	Dextromethorphan Bufuralol	2D2
2E1	*p*-Nitrophenol Chlorzoxazone	2E1
3A4	Midazolam	3A1/3A2
3A5	Midazolam	3A1/3A2

1.3.2. Phase II Metabolism

Phase II metabolism comprises of conjugation reactions, where groups are added to the molecule in order to further increase polarity and molecular weight, while toxicity caused by drugs is typically reduced through prevention of activity[78]. The increase in weight and charge to the molecule often necessitates the contribution of transporter proteins to allow passage across cellular membranes. Phase II reactions are controlled by the transferase enzymes and are split into methylation, sulphation, acetylation, glucuronidation and glutathione or glycine conjugation reactions. Due to significant overlap of substrates, clinically relevant DDIs mediated by inhibition or induction of phase II enzymes are rare[78].

Table 4 - Hepatic phase II enzyme isoforms relevant to drug metabolism in humans, along with the reactions they catalyse, cell localisation and examples of substrates[79].

Enzyme	Isoform	Reaction	Cell Localisation	Substrate(s)
UGT	1A2	Glucuronidation	ER	Bilirubin, Paracetamol
	1A3		ER	NSAID, Chloropromazine
	1A4		ER	NSAID
	1A6		ER	Paracetamol
	1A9		ER	NSAID, Paracetamol
	2B7		ER	Opioids, NSAID
SULT	1A1	Sulfation	Cytosol	Paracetamol, Minoxidil
GST	SDE	Glutathione conjugation	Cytosol	Busulfan
	MAPEG		ER	Busulfan
NAT	1	Acetylation	Cytosol	Sulfamethoxazole, Caffeine
	2		Cytosol	Isoniazid, Hydralazine
MT	TMT	Methylation	ER	Captopril, D-penicillamine
	TPMT		Cytosol	6-mecaptopurine, Azathioprine

UGT, UDP-glucuronosyltransferase; SULT, Sulfotransferase; GST, Glutathione S-Transferase; NAT, N-Acetyltransferase; MT, Methyltransferase; SDE, Soluble Dimeric Enzyme; MAPEG, Membrane Associated Proteins in Eicosanoid and Glutathione metabolism; TMT, Thiol methyltransferase; TPMT, Thiopurine S-methyltransferase ER, Endoplasmic Reticulum (membrane bound); NSAID, Non-Steroidal Anti-Inflammatory Drugs

1.4. Experimental methods for prediction of hepatic drug disposition

In vitro hepatocellular systems have been developed over several decades, intended to provide predictions of drug pharmacokinetic properties at the discovery stage of drug research and development, prior to *in vivo* animal studies. Traditionally, these methods have been designed to investigate individual elimination mechanisms. In some cases, however, multiple clearance parameters can be determined from a single assay. This section will provide an overview of the common techniques that are applied.

1.4.1. Microsomal Fractions

Liver microsomal fractions are a simple *in vitro* tool to examine drug metabolism by metabolic enzymes found in the ER. They enable the exposure of test compounds to a metabolic environment similar to that seen *in vivo*, since the complete array of hepatic CYPs and UGTs are present. However, due to the loss of a tightly controlled cellular environment, the addition of cofactors is required for enzymatic reactions to occur. Microsomes are prepared by differential centrifugation of liver homogenate, resulting in the precipitation of the vast majority of cellular material into a solid pellet. After several spin cycles at increasing speeds, the remaining pellet contains only hepatic enzymes from the ER. Fractions can be stored at -80°C without loss of activity for 2 years, making them highly convenient[80, 81]. Typical uses of fractions include the identification of CYP involvement in metabolism, to determine inhibitors of CYPs and for the prediction of metabolic intrinsic clearance (CL_{met})[5, 57, 81].

To identify the contribution of individual CYPs to the metabolism of a drug, potent and specific inhibitors are required for each isoform. Knowledge of the specific enzyme(s) contributing to the metabolism of a drug can be used to predict the risk of clinical DDIs and prevent their occurrence. Typically inhibition is measured using the inhibitory constant (K_i), defined as the concentration of inhibitor required to reduce the reaction rate of a probe substrate by half. Generally, K_i values less than 1 µM represent strong inhibitors, while greater than 20 µM are considered weak inhibitors; values falling between are typically open to interpretation[81].

Microsomal fractions are most commonly used for the prediction of CL_{met}, with pharmaceutical companies now utilising automated high-throughput screening processes at the initial stages of drug discovery[82]. The most common method measures loss of the parent compound from the media at low concentrations (≤1 μM) over a period of time [82]. Use of low concentrations prevents excess inhibition from metabolites or through enzyme saturation. If a measure of the maximal velocity (V_{max}) or Michaelis constant (K_m) is desired, metabolite formation studies are typically used[82]. This approach is less common due to the additional complications involved with quantifying specific metabolites.

In terms of predicting *in vivo* clearance, microsomes are often seen to produce under-predictions[83]. In particular, poor predictions have been noted for drugs that are accumulated in the hepatocytes through either active transport or trapping processes[84]. This limits their use for novel compounds, where some of these aspects may be unknown.

1.4.2. Hepatocytes in Suspension

The use of primary liver cells is seen as a more physiologically relevant approach compared to microsomal fractions, since they retain an intact plasma membrane, express the full range of phase I and II metabolic enzymes (both ER-bound and cytosolic) and co-factors, and have functional basolateral membrane transporters[82]. In suspension studies, this allows prediction of both passive and active uptake rates along with rates of metabolism to determine intrinsic clearance[85]. Hepatocytes must first be isolated from the liver, typically performed using a well-established collagenase perfusion method developed by Berry and Friend[86]. Cells are suspended in media or buffer and viability is established. For freshly isolated hepatocytes, the cut off for acceptable viability ranges between 80-90%[84, 87-94], since values below this range generally indicate a poor isolation procedure, and could result in inconsistent results and a higher degree of non-specific binding of drugs. From this point, protocols vary depending on the methodology of individual groups.

For uptake studies, the most common method is a two-step method to determine uptake kinetics. Uptake is initiated by the addition of drug solution to cells at both 37°C and 4°C.

At designated time points the experiment must be ceased rapidly by centrifugation through a layer consisting of a mixture of silicone oils, followed by snap freezing to allow separation of the cells and media[84, 95, 96]. At 4°C, active transport is prevented due to a lack of ATP generation and protein activity, giving a measurement of passive uptake clearance ($CL_{passive}$). $CL_{passive}$ is subtracted from the total rate of uptake clearance (CL_{uptake}) noted at 37°C to leave a measurement of active uptake clearance (CL_{active}). A more recent adaptation of this technique uses pan inhibitors of transporter proteins, such as cyclosporine and rifampicin, to replace the need to incubate cells at 4°C to determine $CL_{passive}$[97]. Evidence exists that plasma membrane characteristics vary depending on temperature[85], which may influence $CL_{passive}$ at 4°C compared to 37°C, potentially resulting in inaccurate measurements. At present there are no inhibitors or substrates available that are both potent and specific to individual transporter isoforms, which prevents the identification of specific transporters involved in the active transport of a compound using suspended hepatocytes. Additionally, since hepatocytes are believed to rapidly internalise some apical efflux transporters, this system cannot be used to assess biliary efflux[98]. This does not exclude passive efflux from the membrane, as well as active efflux from basolateral efflux transporters, which should be considered when interpreting uptake rates[85].

For metabolism studies, as with microsomes, measuring depletion of the parent compound from the incubation is the most commonly employed method to evaluate rate of metabolism[82]. Metabolite formation studies can still be performed, however the presence of phase II enzymes must be considered. Without adequate steps to release the metabolite from the conjugate, for example by hydrolysis using β-glucuronidase[87], total rate of metabolism is likely to be under-predicted. Metabolism studies in suspension are initiated by addition of substrate to cells, and are ceased by snap freezing in liquid nitrogen, dry ice, or cooled ethanol[87, 99], or by quenching in suitable solvents (for example methanol or acetonitrile). Samples can then be analysed in the same fashion as uptake studies to estimate CL_{met}. Addition of specific probe substrates and inhibitors can also be used in suspension to determine the inhibitory effect of drugs on metabolic enzymes, and has been used to provide comparable results to those obtained using microsomal fractions[84].

The media loss assay, developed by Soars et al[1], can be used to estimate both hepatic uptake and metabolism using hepatocytes in suspension. In this methodology, dual incubations are performed. In one set of incubations, the conventional parent depletion assay, used to determine drug metabolism, is performed. In the second set of incubations, samples are centrifuged immediately prior to sampling of the media. This step allows for analysis of total loss from the media alone, and therefore reflects both metabolic and uptake clearances. The methodology was further investigated by Jigorel and Houston[88]. In this study, the authors were able to estimate values for the K_m, and using a two-compartment model further separated CL_{uptake} into its active and passive components.

A drawback of hepatocytes in suspension formats is the rapid decline in cell viability and enzyme function, leading to the recommendation that experiments be completed within 4 hours of hepatocyte isolation[100]. This prevents the use of hepatocytes in suspension for drugs with low metabolism or uptake clearance, as well as reducing reliability of results the longer experiments continue. In comparison to microsomes, hepatocytes in suspension are seen to generate comparable CL_{met}[101, 102], however fold under-predictions tend to increase for high clearance compounds (where *in vivo* intrinsic clearance ($CL_{int, in\ vivo}$) >1000 mL/min/kg) [83]. Recent evidence has suggested that this may be due to rate-limiting diffusion through the unstirred water layer and/or plasma membrane[103].

1.4.3. Hepatocytes in monolayer cultures

Plated or monolayer hepatocytes follow the same principles as suspended hepatocytes, creating a system with an intact plasma membrane, as well as a full array of hepatic enzymes and functional basolateral transporter proteins. Although falling short of the full 3D structure of the liver, culturing hepatocytes recreates an environment more akin to that seen *in vivo*. As a result hepatocytes retain their morphological shape and cell-cell contacts, in turn leading to increased life-span following isolation[104]. Hepatocytes, isolated as described in 1.4.2, are diluted to an appropriate density and plated at a known number of cells per well. As an example, Ménochet et al. [97] used 240,000 viable cells per

well in a 24-well plate. Cells are left for a minimum of 2 hours to allow adhesion, after which they can be used for experimentation.

Uptake transporter expression reduces over time in culture in both human and rat primary hepatocytes in monolayer. After 3 days in culture rat Oatp1a2/1b1/1b3/2b1, Oct1, Oat2 and Ntcp mRNA expression has been observed to be below 20% of that found in freshly isolated hepatocytes. In humans, mRNA expression was maintained to a greater degree than that seen in rat, but reductions were still substantial for some of the transporters[105]. After 3 days significant reductions in transporter function are also noted, determined through reduced accumulation of transporter probe compounds[105]. For rats, significant reductions in tetraethylammonium and taurocholate accumulation (Oct1 and Ntcp substrates, respectively) were seen after 24 hours when compared to 4 hours[105]. Expression of efflux transporters is believed to be reduced to a low level following isolation and after 1 hour in culture, although they are still present in areas of the cell membrane in contact with other cells[98]. It should be noted, however, that this observation is disputed by authors who demonstrate function and activity of these transporters after isolation[106, 107]. CYP expression is also seen to reduce dramatically across multiple species, with a 50-80% reduction after 24 hours reported for rat hepatocytes compared to that obtained from the intact liver[108].

Overall, monolayer systems offer some advantages over hepatocytes in suspension, such as a simpler experimental technique and an extended duration of hepatocyte viability. There is currently a lack of a holistic assessment of their capability to predict *in vivo* clearance using metabolism or uptake rates, and so it is not known if they are suitable for this purpose.

1.4.4. Hepatocytes in sandwich culture

Sandwich culture hepatocytes (SCH) are a further adaptation of the monolayer system, generated through the addition of a gel overlay following adherence of hepatocytes. Hepatocytes adopt the typical cuboidal shape observed *in vivo*, and re-establish many features that are lost in both monolayer and suspension formats. Of particular interest is the formation of functional bile canaliculi and tight junctions. SCH therefore allow the

measurement of uptake, metabolism and efflux within the same system. Furthermore, SCH improves the length of time cells are able to survive in culture, particularly with the addition of a second collagen overlay[109]. Methodology and culture conditions for this system (such as type of gel, media, plating density and recommended supplements), have been reviewed extensively by De Bruyn et al[110], and are paramount to produce high quality cultures. In general, it is accepted that using Biocoat™ (type I collagen gel) as the basement gel with a Matrigel™ overlay produces hepatocyte cultures that best mimic the 3D shape and cytoskeletal structures seen *in vivo*, with well-formed bile canaliculi.

Uptake clearance can be determined in SCH by assessment of total accumulation of compound into the cells and canaliculi, while biliary efflux clearance (CL_{bile}) must be determined through use of a Ca^{2+}-free buffer. Ca^{2+}-free buffer causes tight junctions to become disrupted, thereby exposing the bile canaliculus to the media. Compound recovered from these studies are therefore accumulated within the cells only. The concentration of compound found in the bile is calculated by subtracting the concentration in cells, obtained in Ca^{2+}-free buffer, from that obtained in standard buffer. In practice, *in vivo* biliary clearance is often under-predicted using SCH, likely due to reduced expression of both uptake and efflux transporters, similar to that seen in monolayer cultures[110-112]. To address this issue, correction factors have been suggested to improve the accuracy of *in vitro* predictions[111]. Despite the absolute values leading to under-prediction of *in vivo* biliary clearance, correlations have been noted between *in vitro* and *in vivo* values, as well as some success in prediction of rank order. A selection of sartans and statins studied by Abe et al. [113] displayed good correlation between *in vitro* biliary clearance and published *in vivo* biliary excretion data, while Ghibellini et al.[114] reported good correlation of *in vitro* and *in vivo* biliary excretion data for Tc-99m sestamibi, Tc-99m mebrofenin and piperacillin. Overall, while there have been a number of successful predictions of biliary clearance in relation to rank order or in terms of their correlation to *in vivo* values, SCH may be limited by the amount of time required for correct formation of cultures. This delay results in reduced expression of transporters, and may be the reason for the under-prediction of biliary clearance values.

SCH can also be used to determine sinusoidal efflux ($CL_{sinusoidal}$) from the basolateral surface through preincubation of cells with the compound of interest. Once the cells are preloaded, media is removed and standard buffer is applied to cells. Aliquots of buffer can be taken over time periods to determine concentration, which can then be analysed much like accumulation studies to determine the rate of efflux[110].

SCH also have many other applications, which have been reviewed extensively by Swift et al.[110] and De Bruyn et al.[112]. SCH have allowed the study of active uptake, metabolism and biliary excretion within the same assay[115], and in some cases with additional consideration of basolateral efflux processes[116]. The assay has also proven to be useful for compounds that undergo phase II metabolism, such as morphine and naloxone[117, 118]. Elevation of bile acid levels in the blood have been correlated with hepatic damage caused by hepatotoxic drugs[119], which has been shown to be, at least in part, due to inhibition of efflux transporters[120]. SCH therefore has the potential to be a tool for identification of hepatotoxic drugs early in development processes. Traditional CYP and uptake transporter DDI studies can be performed in SCH, using the same methods as other *in vitro* systems[121]. Overall, SCH are a promising and useful system, however it has limitations due to poor transporter and enzyme expression, low throughput and variability caused by differences in culture conditions which may in turn cause differences between results obtained in different laboratories. As with other hepatocellular systems, an extensive overview regarding the performance of the assay in the prediction of *in vivo* clearance is currently lacking, which prevents a true assessment of its utility.

1.4.5. Summary of in vitro systems

Current hepatic *in vitro* systems generally follow a continuum for their throughput and physiological relevance. Microsomal fractions are the most economical and highest throughput, but are limited only to estimations of metabolic clearance, and require cellular conditions to be artificially generated in order to function. Suspended hepatocytes maintain the cellular environment, and allow measurement of both uptake, metabolism and sinusoidal efflux. However, the free movement of hepatocytes differs greatly to 3D structures observed in the liver. Plated hepatocytes and SCH attempt to bridge this gap, using hepatocytes that are attached to a surface, which better reflects the

in vivo environment. Both assays can be used to measure uptake, sinusoidal efflux and, to a lesser extent, metabolism. SCH can additionally provide predictions of biliary clearance, due to the reformation of bile canaliculi. However, the additional culture time causes both systems to suffer from a reduction in enzyme and transporter expression/function, as well as reducing throughput.

1.5. Methods of *in vitro* to *in vivo* extrapolation (IVIVE)

The purpose of IVIVE is the conversion of *in vitro* or *in vivo* clearances into a common term, allowing a comparison to be made between the two. Since *in vivo* clearance comprises of several processes, simple allometric scaling is now avoided in favour of more physiologically based methods involving models of the liver.

1.5.1. Scaling from assay to whole body

Since *in vivo* clearance is representative of the whole body, units of *in vitro* data must be scaled in order to be comparable. All methods begin with the scaling of *in vitro* data from that of the cellular level to that of the whole organ. This requires known values for hepatocellularity (10^6 cells/g liver, HPGL), protein content of hepatocytes (mg protein/g liver, MPPGL) or, when using microsomes, the microsomal recovery (mg microsomal protein/g liver, MMPPGL). The weight of the liver relative to the total bodyweight (g liver/kg bodyweight, GLKB) for the species in question can then be used to make the step from the level of the organ to that of the whole body. A number of papers have produced estimates for scaling values, which are species specific, and are commonly used when performing IVIVE[122-125].

1.5.2. Liver Clearance Models

Following this initial conversion, although data are presented in the same units (mL/min/kg), *in vitro* CL_{int} is not directly comparable to the *in vivo* hepatic clearance (CL_H). To bridge this gap, liver clearance models are applied to take into account factors which, along with intrinsic clearance (CL_{int}), determine CL_H. This includes physiological parameters such as hepatic blood flow (Q_H) and the fraction of unbound drug in the blood (fu_b). Three liver clearance models have been developed, known as the well-stirred,

parallel tube and dispersion model. Each model assumes that distribution into the liver is perfusion limited, is unrestricted by barriers, that only unbound drug is available for entry into the hepatocytes by transporter and diffusion processes, and that transporter proteins and metabolic enzymes are evenly distributed throughout the whole liver[126].

The well-stirred model presents a scenario whereby drug distribution in the liver is instantaneous, representing the liver as a single compartment with an equal concentration throughout[126], shown in Equation 1.

$$CL_H = \frac{Q_H \cdot fu_b \cdot CL_{int}}{Q_H + fu_b \cdot CL_{int}} \qquad \textbf{Equation 1}$$

The parallel tube model encompasses a much different view in regards to the physiology of the liver. Instead of a whole compartment, the liver is represented as a series of tubes, each surrounded by hepatocytes. Since each hepatocyte has equal capacity for drugs to enter and for metabolism to occur, the concentration is presumed to decline exponentially from the beginning of the tube to the end, reflected in Equation 2.

$$CL_H = Q_H \left(1 - e^{\left[\frac{fu_b \cdot CL_{int}}{Q_H}\right]}\right) \qquad \textbf{Equation 2}$$

The dispersion model is mathematically much more complex than both the well-stirred and parallel tube models, and was developed by engineers to be consistent with liver physiology by combining the concepts of both the well-stirred and parallel tube model. However, a study by Houston and Carlile[126] analysed the utility of each model in terms of providing accurate *in vivo* predictions, and found there to be no inherent advantage to any of the models across all compounds. In light of this, the dispersion model will not be considered. The well-stirred model has typically been the most popular choice, due to its mathematical simplicity.

1.5.3. Extended Clearance Terms

For the purpose of IVIVE, *in vitro* CL_{int} is the general term used to describe a clearance process, and can relate to uptake or metabolism depending on the assay performed. An alternative method is the use of so called extended clearance terms, which integrate multiple clearance parameters to determine a total CL_{int} value ($CL_{int,total}$). Taking into account all clearance processes, and based on a recirculating liver perfusion model, $CL_{int,total}$ is determined using Equation 3[127-130],

$$CL_{int,total} = CL_{uptake} \cdot \frac{CL_{met} + CL_{bile}}{CL_{met} + CL_{bile} + CL_{sinusoidal}} \qquad \textbf{Equation 3}$$

where CL_{uptake} is the total uptake clearance, CL_{met} is the metabolic clearance, CL_{bile} is the biliary clearance and $CL_{sinusoidal}$ is the sinusoidal efflux clearance. The widespread use of $CL_{int,total}$ is generally hampered by the relatively large amount of *in vitro* data required. As an alternative, apparent intrinsic clearance ($CL_{int,app}$) can be used, described by Equation 4,

$$CL_{int,app} = CL_{met} \cdot \frac{CL_{active} + CL_{passive}}{CL_{met} + CL_{passive}} \qquad \textbf{Equation 4}$$

where CL_{active} is the active uptake clearance and $CL_{passive}$ is the passive uptake clearance. Equation 4 is a derivative of Equation 3, assuming efflux clearances to be negligible. This term is typically applied to data from suspension, media loss or monolayer assays, where there is evidence that apical efflux transporters are rapidly internalised[98]. While $CL_{int,total}$ has been demonstrated to result in improved *in vivo* predictions[129], further application of both terms is required to properly assess if they are beneficial for the prediction of *in vivo* clearance.

Chapter 2. Aims

For several decades, *in vitro* metabolism was the key focus of scientists attempting to predict *in vivo* clearance at an early developmental stage. However it has been frequently demonstrated that use of metabolic clearance data generally under-predicts *in vivo* clearance[83, 131]. The importance of uptake transporters to the clearance of some drugs has now been well documented, and has led to a surge in papers using *in vitro* uptake assays for many different applications. Despite the abundance of uptake data now available, there is a clear lack of a holistic analysis, similar to that performed for metabolism data, in order to determine the overall prediction tendencies of the assays. Additionally, the lack of a high throughput uptake system has severely limited the feasibility of using these assays at the early stages of drug development. As our knowledge of cellular processes grows, it is becoming increasingly apparent that a simple cellular approach, where data are scaled directly from *in vitro* assays, may be insufficient for the accurate prediction of drug pharmacokinetics. A more mechanistic approach, taking into account several factors affecting the overall clearance of a drug, may be instead be required. The overall aim of this thesis, therefore, was to further refine current *in vitro* assays and data analysis procedures in order improve the accuracy of predictive pharmacokinetic data they provide, and to explore the merits of cellular and mechanistic approaches to predict *in vivo* clearance.

The first aim (Chapter 3) was to provide the first large scale assessment of the prediction of *in vivo* clearance using *in vitro* uptake data. Since multiple assay formats are available to measure uptake clearance, each were compared to establish differences and determine their applicability. In addition, empirical data scaling techniques were investigated in an attempt to improve predictions.

The second aim (Chapter 4) was to further investigate the utility of the media loss assay from the observations of Jigorel and Houston[88] Initially, the assay will be transitioned into a higher throughout system. This was intended to address the current issues surrounding the low-throughput nature of uptake assays, and to allow the inclusion of inhibitors of both CYP-mediated metabolism and OATP-mediated uptake. An *in silico*

model was developed in order to estimate several individual clearance parameters, in turn allowing an estimate of binding and partitioning properties of the compound. Initially, a cellular scaling approach was used to assess the predictions compared to that seen previously in Chapter 3.

The final aim (Chapter 5) was to integrate both biliary and sinusoidal efflux data, generated using SCH, into data obtained in Chapter 4. This was done using the total intrinsic clearance term, which utilises multiple clearance parameters to determine an overall intrinsic clearance. It was hypothesised that this approach, in conjunction with data scaling techniques investigated in Chapter 3, would further improve predictions of *in vivo* clearance.

Chapter 3. Assessment of the predictive ability of CL_{uptake}

3.1. Introduction

As highlighted in Chapter 1, prediction of *in vivo* drug PK has become an important aspect of the drug discovery process, leading to the development of an array of *in vitro* methodologies aimed at generating accurate predictions of *in vivo* clearance, as well as assessing the potential for clinical implications such as DDIs. Houston[5] was the first to assess this cellular approach, using *in vitro* metabolic clearance data to predict *in vivo* clearance in the rat. Whilst it appeared successful initially, recent literature analyses have demonstrated *in vitro* assays typically generate a clearance-dependent under-prediction of *in vivo* clearance, both in human and rat microsomes/hepatocytes[83, 132]. In addition, the changing environment of the drug discovery process has led towards a tendency for metabolically stable compounds. As such, the utility of metabolic assays alone to predict *in vivo* clearance has declined. In cases where metabolic clearance plays a minor role, hepatic uptake has become widely appreciated as being a more accurate indicator of *in vivo* clearance[15].

In vitro uptake assays have allowed quantitative clearance predictions and, with the application of Michaelis-Menten kinetics, aid in determining the compound's route of entry into the cell, being via transporter-mediated and/or passive diffusion processes. With increased awareness of the importance of drug transport, as well as several well documented cases of DDIs caused by transporter inhibition, the Food and Drug Administration (FDA) has now implemented recommendations and guidance for *in vitro* testing of NCEs in order to identify transporter substrates. *In vitro* transport assays are now routinely performed to determine the affinity of NCEs for particular drug transporters, to evaluate the potential risk of DDIs and to provide predictions of *in vivo* clearance. In terms of drug clearance, several methods have been investigated and are continuing to advance in complexity, including novel approaches such as 3D cultured systems. However, despite the increase in literature data it is apparent that a holistic analysis, similar to that performed for metabolism data over two decades ago by Houston[5], is currently lacking for uptake clearance data.

Without a comprehensive analysis of literature *in vitro* uptake data, it is impossible to properly assess the utility of current *in vitro* methodologies. While many studies provide a

comparison to *in vivo* clearance for their own data, much larger data sets are required to assess the overall accuracy of the various *in vitro* systems, as well as to identify trends and to understand why they may occur. This information is vital for the selection of an appropriate *in vitro* assay for novel compounds, and for aiding the interpretation of *in vitro* data.

3.2. Aims

The primary objective of this chapter was to assess the utility of *in vitro* uptake data as a predictor of *in vivo* hepatic clearance. In order to do this, uptake clearance data will be compiled from *in vitro* studies using both rat and human hepatocytes and IVIVE performed. Since multiple assay formats are available to determine uptake clearance, statistical analysis and comparisons will be performed for each of the selected assay formats to allow an assessment of their performance. This information is intended to fill the current gap in knowledge that is evident from the literature. In addition, studies will be further sorted by either their ionisation character or grouping within the Biopharmaceutics Drug Disposition Classification System (BDDCS)[133], to determine if specific groups of compounds have any trends in their predictions. If such patterns were to exist, it may be informative for future selection of *in vitro* assay, or interpretation of *in vitro* data.

A secondary objective was to attempt to improve *in vivo* clearance predictions using various scaling methods. Of particular interest is the use of empirical scaling factors, which will be implemented and analysed for their effects on the bias and precision of each assay format. In addition to static empirical scaling factors, data will be analysed for trends in the magnitude of their required empirical scaling factor relative to their *in vitro* uptake clearance. It is hypothesised that the use of trendline equations may allow for specific scaling factors to be generated for drugs based on their *in vitro* clearance.

Finally, the uptake clearance predictions will be combined with other available literature datasets in order to test the apparent intrinsic clearance term ($CL_{int,app}$). This parameter incorporates multiple clearance processes into one intrinsic clearance value for a drug[91]. The utility of this parameter with both uptake and metabolism data will be investigated. It is hypothesised that this it is more reflective of the total hepatic *in vivo* clearance, and will

result in less bias and greater prediction accuracy compared to using a single clearance parameter.

3.3. Methods

3.3.1. Data Collation

3.3.1.1. Rat

For *in vitro* data collection, CL_{uptake} was defined as the total uptake clearance, which is a summation of both the active and passive processes. Data were obtained from drug uptake assays using hepatocytes freshly isolated from rats in suspension (31 drugs, 50 entities), media loss (12 drugs, 15 entities), monolayer (18 drugs, 33 entities) and SCH (17 drugs, 41 entities) formats. No restriction was placed on the use of a single or range of concentrations. Data for media loss assays were only included if a distinction was made between uptake and metabolism. *In vivo* PK parameters were collated for rats dosed intravenously via a bolus or infusion. Parameters collated, where available, included plasma clearance (CL_p), unbound fraction in the plasma (fu_p), blood clearance (CL_b), unbound fraction in the blood (fu_b) blood to plasma ratio (R_b) and renal clearance (CL_R). See Table 30 (Appendix 7.1) and Table 31 (Appendix 7.2) for full list of values and sources.

3.3.1.2. Human

Data collation was performed as described in 3.3.1.1, with the exception that cryopreserved, rather than freshly isolated, hepatocytes were included. Data were collected from suspension (21 drugs; 81 entities), monolayer (12 drugs; 26 entities) and SCH (11 drugs; 30) assay formats. No *in vitro* studies were identified that performed the media loss assay using human hepatocytes. See Table 32 (Appendix 7.3) and Table 33 (Appendix 7.4) for full list of values and sources.

3.3.2. Basic IVIVE of CL_{int}, in vitro and Determination of in vivo CL_{int}

3.3.2.1. Rat

CL_{int} was scaled to that of the whole body ($CL_{int,\ in\ vitro}$) and converted to units of mL/min/kg using Equation 5,

$$CL_{int,in\ vitro} = \frac{CL_{int} \cdot MPPGL \cdot GLKB}{1000} \qquad \textbf{Equation 5}$$

Where MPPGL is the mg protein/g liver and GLKB is the grams of liver/kg bodyweight. Standard physiological scaling factors were defined as values of 200mg protein/g liver and 40 g liver/kg bodyweight[123, 125] for MPPGL and GLKB, respectively. To convert CL_{int} values in µL/min/10^6 cells to µL/min/mg protein, a Bradford protein assay was performed which determined that 1 mg protein was equal to 1x10^6 cells.

3.3.2.2. Human

IVIVE was performed as described in 3.3.2.1 using standard physiological scaling factors defined by values of 120 mg protein/g liver and 21.4 g liver/kg bodyweight[125, 134] for MPPGL and GLKB and where necessary CL_{int} expressed in µL/min/10^6 cells was converted to µL/min/mg protein assuming 1 mg protein/10^6 cells[89].

3.3.2.3. In Vivo CL_{int}

All blood clearance data were initially corrected for renal clearance. *In vivo* CL_{int} ($CL_{int,\ in\ vivo}$) was then calculated from *in vivo* CL_b, fu_b and hepatic blood flow (Q_H, set at 100 and 20.7 mL/min/kg[135] for rat and human, respectively) using the well-stirred model (Equation 6). Where necessary, CL_b and fu_b were calculated using R_b (CL_p/R_b and fu_p/R_b, respectively).

$$CL_{int,in\ vivo} = \frac{CL_b}{fu_b \cdot \left(1 - \frac{CL_b}{Q_H}\right)} \qquad \textbf{Equation 6}$$

It is important to note that the $CL_{int,\ in\ vivo}$ term does not resolve the contribution of individual processes to the clearance of a drug. For this analysis, it is assumed that uptake is the predominant process.

3.3.3. Variation in Scaling Factor and Effect on Determination of $CL_{int,\ in\ vivo}$

Literature data regarding the hepatocellularity, protein content of the liver, weight of the liver relative to the bodyweight and conversion factor between protein content per million cells were collated for both rat and human. From this, a maximum and minimum scaling factor was determined and applied to the data sets. Data were then analysed as described in 3.3.6. See Table 34 (Appendix 7.5) for values.

3.3.4. Data and Clearance-Derived Scaling Factors

All observed $CL_{int,\ in\ vivo}$ data were divided by the corresponding experimental CL_{int} data to determine the required empirical scaling factor for each study, individually. For data-derived scaling factors, the arithmetic mean and median was determined from all empirical scaling factors for each assay format. All clearance values were then scaled using the arithmetic mean or median scaling factor, with bias and precision calculated as described in 3.3.6.

For clearance-derived scaling factors, the drug specific required empirical scaling factor was plotted against *in vitro* CL_{uptake}, and a trend line fitted using least squares regression of the power function. The equation of this line was then used to generate an empirical scaling factor for each compound individually, based on the measured *in vitro* clearance.

3.3.5. Application of apparent intrinsic clearance

$CL_{int,app}$ is derived from the extended clearance term (see 1.5.3), and incorporates multiple clearance parameters (Equation 4)[91],

$$CL_{int,app} = CL_{met} \cdot \frac{CL_{active} + CL_{passive}}{CL_{met} + CL_{passive}} \qquad \textbf{Equation 4}$$

where CL_{met} is the total metabolic clearance rate, CL_{active} is the active uptake rate and $CL_{passive}$ is the passive transmembrane diffusion rate. Only the suspension assay was analysed using this approach, as it is well documented that CYP activity is reduced in cultured (monolayer and SCH) assay formats[99], which has led to a lack of metabolism data, and there is no consistent distinction between active and passive transport in the media loss assay. In this study, CL_{met} data were acquired from a database assembled by Wood et al[131]. Where possible CL_{met} data were taken from suspended hepatocytes,

however where this information was lacking, data from microsomes were used instead. Uptake data collected in 3.3.1 were used to determine CL_{active} and $CL_{passive}$, where possible. In this instance, efflux clearance was assumed to be negligible given the current lack of data in this area, as well as previous evidence to suggest internalisation of efflux transporters following isolation[98]. Predictions were compared between uptake or metabolism data alone and when combined within the $CL_{int, app}$ term.

In addition, $CL_{int, app}$ was analysed using clearance parameters scaled using the methods described in 3.3.3 and 3.3.4 to determine if further improvements could be made. For CL_{met}, no correlations were noted between *in vitro* CL_{int} and required scaling factor. As a result, mean and median required scaling factors were calculated as described in 3.3.4.

3.3.6. Calculation of Prediction Bias and Precision

The bias and precision of $CL_{int, in\ vitro}$ to $CL_{int, in\ vivo}$ for each system was assessed using the absolute geometric mean fold error (GMFE, Equation 7) and the root mean squared error (RMSE, Equation 8), respectively [83]. Qualitative assessment of predictions were judged as being well predicted when $CL_{int, in\ vitro}$ fell within 2-fold of the observed $CL_{int, in\ vivo}$. $CL_{int, in\ vitro}$ values above or below this threshold were determined to be over-predicted and under-predicted, respectively.

$$GMFE = 10^{\left[\frac{1}{n}\sum log\frac{CL_{int,in\ vitro}}{CL_{int,in\ vivo}}\right]} \qquad \textbf{Equation 7}$$

$$RMSE = \sqrt{\frac{1}{n}\sum(predicted - observed)^2} \qquad \textbf{Equation 8}$$

3.4. Results

3.4.1. Basic IVIVE and calculation of $CL_{int,\ in\ vivo}$

3.4.1.1. Rat Hepatocytes

3.4.1.1.1. Suspension

In the suspension format, $CL_{int,\ in\ vitro}$ ranged over several orders of magnitude (10 – 23,800 mL/min/kg, n=50) using standard physiological scaling factors. Of the $CL_{int,\ in\ vitro}$ data collected, only 20% resulted in an accurate prediction of $CL_{int,\ in\ vivo}$, while 60% were over-predicted and 20% under-predicted (Figure 3). A high degree of bias was evident (GMFE = 4.08), while precision (RMSE = 3688) was low relative to other assay formats and methods of analysis seen throughout this study. For summary of data, see Table 5.

Data were further inspected for trends in both the BDDCS (being class 1-4, as defined by Benet et al[133]) and the ionisation character (being acidic, basic, neutral or zwitterionic), and is also summarised in Table 5. When grouped based on BDDCS, class 2 compounds had a clear tendency toward over prediction (81% of data). No other clear trend was noted. This analysis is hindered by the relative lack of data on both class 1 and 4 compounds, which accounted for only a small proportion of the dataset.

Grouped by ionisation character, over predictions of both basic and neutral compounds were identified. Too few basic compounds were available to substantiate any findings, however there were sufficient neutral compounds to suggest the trend towards over prediction should be considered. It is also interesting to note that neutral compounds would be expected to have a high degree of passive permeability, a characteristic also associated with BDDCS class 2 compounds. It was observed that of the 10 studies using class 2 neutral compounds, all were over-predicted.

3.4.1.1.2. Media Loss

$CL_{int,\ in\ vitro}$ ranged between 15 – 17,300 mL/min/kg (n=15) for the media loss assay, similar to that seen in suspension. Predictions also remained consistent with suspension, with 13% of data being accurately predicted, 60% over-predicted and 27% under-predicted (Figure 3). Substantial bias was noted within the assay format (GMFE = 5.83), as well as

poor precision compared to other formats in the rat (RMSE = 6443). Data are summarised in Table 5.

No BDDCS class 1 compounds and only one class 4 compound were recorded for media loss, which prevented any insight into the patterns of their prediction. As was seen previously with suspension, a trend towards over-prediction was noted for class 2 compounds. Neutral compounds also had a high proportion of over predictions. Further analysis again determined that class 2 neutral compounds were over-predicted. However in this case, only two compounds were identified, and so the link cannot be substantiated.

3.4.1.1.3. Monolayer

Monolayer $CL_{int,\ in\ vitro}$ had a narrower range of 21 – 6,000 mL/min/kg (n=33) in comparison to both suspension and media loss assays. Monolayer was seen to be the most accurate of the four rat hepatocytes assays tested in this study, with 40% of studies accurately predicting $CL_{int,\ in\ vivo}$. Unlike suspension and media loss, there was a tendency for under prediction of clearance (48%), while only 12% were over-predicted (see Figure 3). Less bias and higher precision were noted for monolayer (GMFE = 3.41, RMSE = 2897) compared to both suspension and media loss. See Table 5 for summary of data.

Studies in monolayer were more evenly distributed across BDDCS classes 1, 2 and 3, compared to previous assay formats. Class 1 compounds were particularly well predicted, while proportions of under-predictions increased for each of the remaining classes. The vast majority of studies using acidic compounds were under-predicted. Although fewer in number, the remaining ionisation character saw even distributions between under-predictions and successful predictions, as summarised in Table 5.

3.4.1.1.4. Sandwich Cultured Hepatocytes

SCH displayed the narrowest range of $CL_{int,\ in\ vitro}$ of between 0.4 – 780 mL/min/kg (n=41), representing a maximum value approximately 8-fold lower than that seen in monolayer, and 22-fold lower than both suspension and media loss. As a result, 93% of data resulted in an under prediction of $CL_{int,\ in\ vivo}$, while 7% were predicted well (Figure 3). With such a clear bias towards under prediction, bias was the highest of the four assay formats (GMFE

= 14.5). Despite this, precision was the highest of the four assay formats in rat (RMSE = 1032). Empirical scaling of the data may therefore be a viable option to correct for the heavy bias towards under-prediction.

On inspection of BDDCS groups, it is apparent that the proportion of data collected on class 3 and 4 compounds is higher in SCH than had been seen in other assay formats. It is likely that the application of the SCH assay to measure efflux may lend to the tendency to select compounds which are known to be substrates of efflux transporters, which are predicted properties of class 3 and 4 compounds. Beyond this there are no clear patterns observed for either BDDCS group or ionisation character, since almost all compounds are under-predicted regardless of classification, or have too few data entries (see Table 5 for summary).

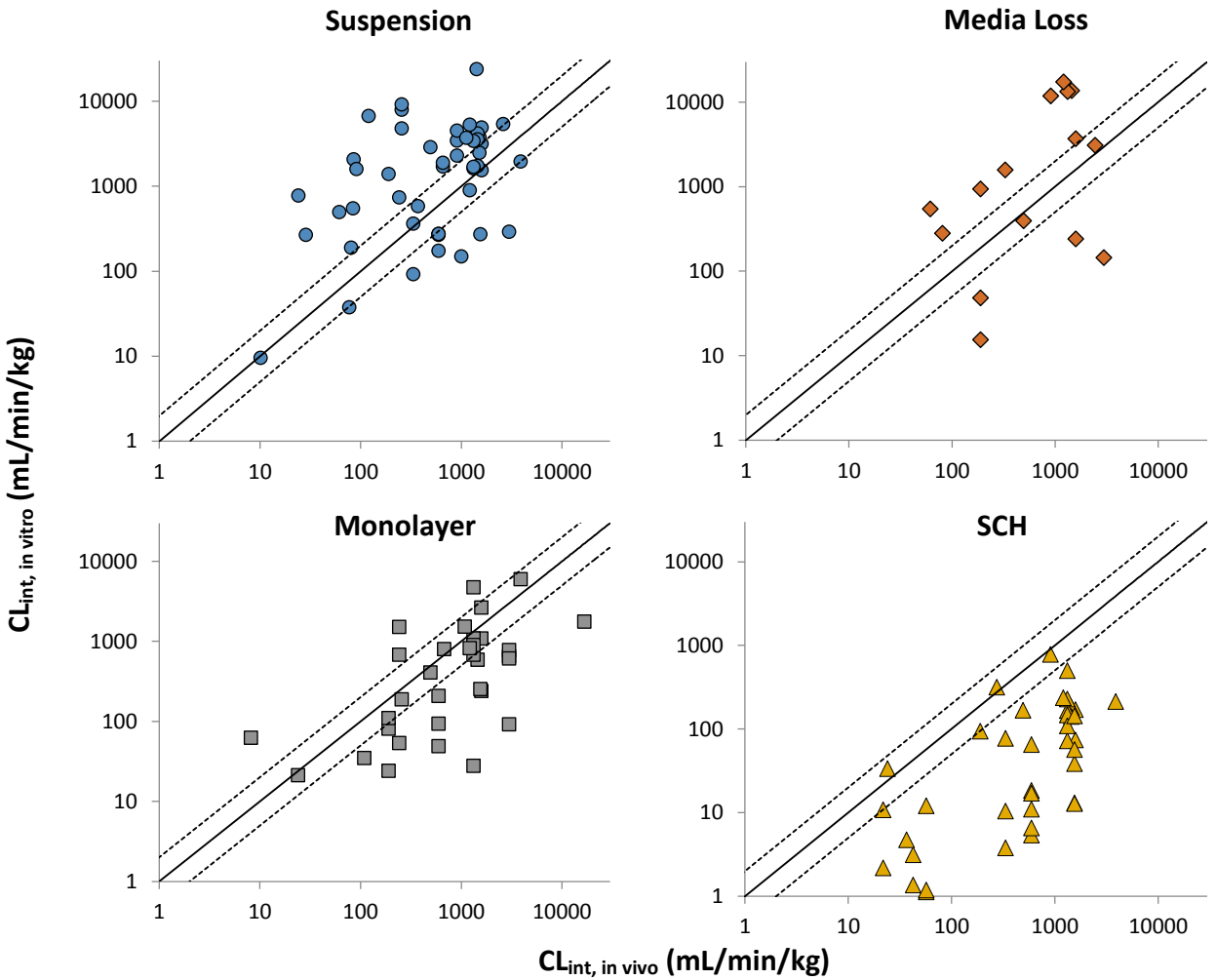

Figure 3 – Predicted $CL_{int,\ in\ vitro}$ against observed $CL_{int,\ in\ vivo}$ for compounds in rat suspension (n=50), media loss (n=15), monolayer (n=33) and SCH (n=41) assays scaled using standard physiological scaling factors. Line of unity (solid line), and 2-fold under and over-prediction (dashed line) are displayed.

Table 5 - Summary of drug predictions in rat hepatocyte assays and when grouped by BDDCS class and ionisation character.

	Suspension					Media Loss					Monolayer					SCH				
Number of drugs	31					12					18					17				
Number of entities	50					15					33					41				
GMFE (RMSE)	4.08 (3688)					5.83 (6443)					3.41 (2897)					14.5 (1032)				
Range (mL/min/kg)	10 – 23,800					15 – 17,300					21 – 6,000					0.4 – 780				
% well predicted	20					13					40					7				
% over-predicted	60					60					12					0				
% under-predicted	20					27					48					93				
BDDCS group	***1***	***2***	***3***	***4***	**N/C**	***1***	***2***	***3***	***4***	**N/C**	***1***	***2***	***3***	***4***	**N/C**	***1***	***2***	***3***	***4***	**N/C**
% of studies	6	52	32	6	4	0	53	33	7	7	12	36	36	3	13	18	29	41	6	6
% well predicted	33	15	25	33	-	0	13	0	0	-	75	42	42	0	-	20	14	5	0	-
% over-predicted	33	81	31	33	-	0	63	60	100	-	0	8	8	0	-	0	0	0	0	-
% under-predicted	33	4	44	33	-	0	24	40	0	-	25	50	50	100	-	80	86	95	100	-
Ionisation character	***A***	***B***	***N***	***Z***		***A***	***B***	***N***	***Z***		***A***	***B***	***N***	***Z***		***A***	***B***	***N***	***Z***	
% of studies	58	4	28	10	-	53	7	40	0	-	73	6	15	6	-	65	12	17	6	-
% well predicted	28	0	0	40	-	25	0	0	0	-	33	50	60	50	-	0	33	67	0	-
% over-predicted	41	100	100	40	-	50	100	67	0	-	17	0	0	0	-	0	0	0	0	-
% under-predicted	31	0	0	20	-	25	0	33	0	-	50	50	40	50	-	100	67	33	100	-

N/C; Not Classified, A; Acid, B; Base, N; Neutral, Z; Zwitterion

3.4.1.2. Human Hepatocytes

3.4.1.2.1. Suspension

As was seen for rat data, $CL_{int,\ in\ vitro}$ ranged over several orders of magnitude from 2 – 1,580 mL/min/kg (n=81) in human suspension assays. $CL_{int,\ in\ vitro}$ data predicted $CL_{int,\ in\ vivo}$ accurately in 28% of studies, while 31% were over-predicted and 41% under-predicted (Figure 4). Although the majority of studies resulted in under-prediction, the proportions of accurate, under- and over-predictions were more equally distributed than were observed with assays performed using rat hepatocytes. Bias remained relatively high (GMFE = 4.3), while precision was better than that observed in the rat (RMSE = 1855). Data are summarised in Table 6.

Compounds studied in human hepatocytes were evenly distributed among BDDCS groups. Predictions appear to be uniform across most of the BDDCS classes (
Table 6), with the exception of class 3 compounds, which have a larger proportion of under-predictions.

When grouped based on ionisation character, acidic compounds formed the majority of the dataset. Both basic and neutral compounds appeared to have tendencies to successfully predict *in vivo* clearance, although only a small number of studies used drugs from these species. Acidic and zwitterionic drug had no clear prediction trends.

3.4.1.2.2. Monolayer

With $CL_{int,\ in\ vitro}$ ranges of between 2 – 340 mL/min/kg (n=26), human monolayer cultures appear consistent with their rat counterparts in that the range is both lower than suspension and spans only two orders of magnitude. Data from monolayer assays were more heavily biased (GMFE = 4.73) than that observed for suspension assays, while precision was almost identical (RMSE = 1835). Patterns of prediction also remained broadly consistent with rat hepatocytes, with a clear tendency towards under-prediction (66% of studies). The remainder were split between good and over predictions (19% and 15%, respectively; Figure 4). Data are summarised in Table 6.

Studies largely appeared to focus on class 2 and 3 compounds, which accounted for 42% and 33%, respectively, of the studies using the monolayer assay. Class 3 compounds were

seen to almost exclusively under-predict *in vivo* clearance, an observation that remains consistent with both human suspension and rat monolayer assays. Under-prediction predominated for all three of the ionisation character for which there was data, while no basic compounds were studied. Data are summarised in
Table 6.

These patterns agree with observations in rat monolayer cultures, indicating a degree of similarity between species. In particular it highlights a potential issue with under-prediction of both low and high permeability compounds expected to have some degree of affinity for uptake transporters (i.e. class 2 and 3 compounds). This is contested by the majority of studies using class 4 compounds being well predicted, however the number of studies is much lower.

3.4.1.2.3. SCH

SCH $CL_{int,\ in\ vitro}$ ranged between 0.9 – 370 mL/min/kg (n=30) which, unlike rat hepatocytes, remained equivalent to that seen in human monolayer cultures despite the additional culture time required. Although an improvement, the $CL_{int,\ in\ vitro}$ range remains an order of magnitude lower than that seen for hepatocytes in suspension. Under-prediction was evident for the majority of studies using SCH (73%). However, with 23% of studies predicting *in vivo* clearance successfully and 7% being over-predicted, human hepatocytes appear less affected by the extended culture period than their rat counterparts (Figure 4). A high degree of bias was observed within the system (GMFE = 6.91), although not to the extent seen in rat hepatocytes, as well as the lowest precision of the three human hepatocyte systems (RMSE = 1948). Data are summarised in Table 6.

With such clear bias towards under-prediction, it is not possible to identify any patterns in prediction based on either BDDCS classes or ionisation character (
Table 6). Only class 2 compounds appeared to have a smaller proportion of under-predictions, with all of these studies found to be using acidic compounds, a pattern that was also observed in monolayer.

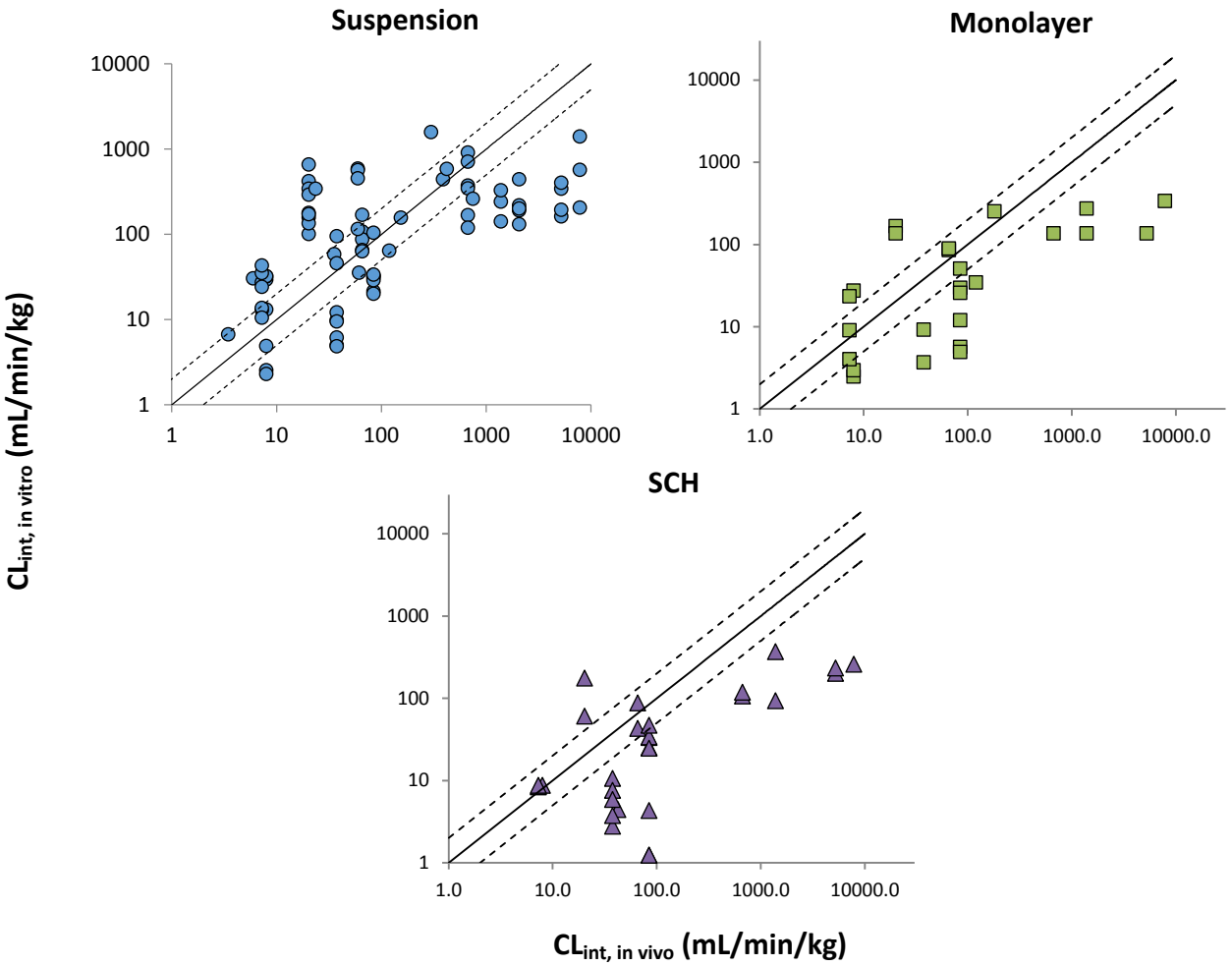

Figure 4 - Predicted $CL_{int,\ in\ vitro}$ against observed $CL_{int,\ in\ vivo}$ for compounds in human suspension (n=81), monolayer (n=26) and SCH (n=30) assays scaled using standard physiological scaling factors. Line of unity (solid line), and 2-fold under and over-prediction (dashed line) are displayed.

Table 6 - Summary of drug predictions in human hepatocyte assays when grouped by BDDCS class and ionisation character.

	Suspension				Monolayer				SCH			
Number of drugs	21				12				11			
Number of entities	81				26				30			
GMFE (RMSE)	4.3 (1855)				4.73 (1835)				6.91 (1948)			
Range (mL/min/kg)	2 – 1,580				2 – 340				0.9 – 370			
% well predicted	28				19				23			
% over-predicted	31				15				7			
% under-predicted	41				66				73			
BDDCS group	***1***	***2***	***3***	***4***	***1***	***2***	***3***	***4***	***1***	***2***	***3***	***4***
% of studies	19	39	32	10	7	33	48	12	18	36	36	10
% well predicted	47	18	23	50	0	33	8	33	0	29	6	100
% over-predicted	6	44	19	50	0	23	8	33	0	29	0	0
% under-predicted	47	38	58	0	100	44	84	33	100	43	94	0
Ionisation character	***A***	***B***	***N***	***Z***	***A***	***B***	***N***	***Z***	***A***	***B***	***N***	***Z***
% of studies	67	7	14	12	58	0	25	17	73	0	9	18
% well predicted	20	50	45	40	21	-	20	0	20	-	100	0
% over-predicted	34	33	36	0	16	-	20	0	8	-	0	0
% under-predicted	46	17	18	60	63	-	60	100	72	-	0	100

A; Acid, B; Base, N; Neutral, Z; Zwitterion

3.4.2. Variations in Scaling Factor and Data Derived Scaling Factors

3.4.2.1. Rat Hepatocytes

3.4.2.1.1. Minimum and Maximum Literature Scaling Factors

Throughout the literature, various physiological values for liver protein content, hepatocellularity and liver weight were found to have been used to calculate scaling factors. Using these data, maximum and minimum scaling factors were determined using combinations of physiological values, summarised in Table 34 (Appendix 7.5). The maximum scaling factor was 15.5, and the minimum was 3.46.

Table 7 - Effect of varying physiological scaling factors on the bias and precision of $CL_{int,\ in\ vivo}$ predictions of rat hepatocytes.

Scaling Factor		Standard	Maximum	Minimum
	Scaling Value	8	15.5	3.46
Suspension	GMFE (RMSE)	4.17 (3782)	6.16 (4978)	3.23 (1549)
	% well predicted	21	19	40
	% over-predicted	60	77	32
	% under-predicted	19	4	28
Media Loss	GMFE (RMSE)	4.89 (6065)	6.72 (7943)	4.12 (2414)
	% well predicted	18	12	24
	% over-predicted	59	65	41
	% under-predicted	23	24	35
Monolayer	GMFE (RMSE)	3.25 (3012)	2.78 (2988)	5.75 (3211)
	% well predicted	38	38	17
	% over-predicted	10	28	7
	% under-predicted	52	34	76
SCH	GMFE (RMSE)	14.5 (1032)	6.84 (1090)	27.25 (1172)
	% well predicted	7	14	3
	% over-predicted	0	6	0
	% under-predicted	93	80	97

Data collated in 3.3.1.1 were reanalysed using both of these scaling factors, as displayed in Table 7 (see Figure 32 and Figure 33, Appendix 7.6 for corresponding graphs). Both suspension and media loss assays benefitted from the minimum scaling factor, which reduced both GMFE and RMSE in comparison to using standard physiological scaling factors. Use of the maximum scaling factor had the opposite effect, with the vast majority of compounds being over-predicted. Conversely, the monolayer and SCH formats benefitted from the use of the maximum scaling factor, with reductions in GMFE. However, in terms of the number of compounds that were predicted well, little change was seen. Use of the minimum scaling factor resulted in a heavy bias towards under-prediction in both assays, while RMSE remained consistent regardless of scaling factor.

3.4.2.1.2. Mean and Median Required Scaling Factor

The required scaling factor was determined for each data entry by dividing the observed $CL_{int,\ in\ vivo}$ value by the measured CL_{int} value from each *in vitro* assay. The mean and median values were calculated and applied to reanalyse the data from 3.3.1.1 for each assay format. Results are displayed in Table 8, and see Figure 34 and Figure 35 (Appendix 7.6) for corresponding graphs.

The mean scaling factor was found to be greater than the standard physiological scaling factor in all assay formats. For suspension and media loss, which had an overall tendency for over-predictions of *in vivo* clearance, this was due to the extent of under-predictions causing a skew in the required scaling factor. As a result, using the mean scaling factor led to increased bias and reduced precision in both the suspension and media loss assays, while causing a reduction in both for monolayer and SCH.

The median scaling factor was much lower than the mean in all cases, resulting in values below the standard scaling factor for suspension and media loss, while it remained higher for both monolayer and SCH assays. The median scaling factor reduced bias to a greater extent than the mean, as well as leading to an improvement in precision in all assay formats. In terms of successful predictions of *in vivo* clearance, only SCH saw a noticeable difference between any of the scaling factors. Use of the mean scaling factor increased the percentage of successful predictions from 7% to 29%, although at the expense of

producing a large proportion of over-predictions. Use of the median scaling factor produced more successful predictions (42%), with fewer over-predictions.

Table 8 - Effect of mean and median empirical scaling factors on the bias and precision of $CL_{int,\ in\ vivo}$ predictions in rat hepatocytes.

Scaling Factor		Standard	Mean	Median
Suspension	Scaling Value	8	9	3.2
	GMFE (RMSE)	4.17 (3782)	4.45 (4328)	3.21 (1438)
	% well predicted	21	28	38
	% over-predicted	60	62	30
	% under-predicted	19	11	32
Media Loss	Scaling Value	8	23	3.5
	GMFE (RMSE)	4.89 (6065)	8.28 (18632)	4.11 (2422)
	% well predicted	18	6	24
	% over-predicted	59	76	41
	% under-predicted	23	18	35
Monolayer	Scaling Value	8	33.9	18.9
	GMFE (RMSE)	3.25 (3012)	3.08 (5140)	2.76 (3361)
	% well predicted	38	41	41
	% over-predicted	10	48	31
	% under-predicted	52	10	28
SCH	Scaling Value	8	234	92.4
	GMFE (RMSE)	14.5 (1032)	3.96 (5152)	2.96 (1841)
	% well predicted	7	29	42
	% over-predicted	0	54	29
	% under-predicted	93	17	29

3.4.2.1.3. Clearance-Derived Scaling Factors

For all formats, a weak to moderate, negative but significant ($p < 0.05$) correlation was observed between $CL_{int,\ in\ vitro}$ and required empirical scaling factor (Figure 5), indicating that a lower scaling factor was required as $CL_{int,\ in\ vitro}$ increased. Using the equation of each trendline, scaling factors were then generated for each study individually, defined as

clearance-derived scaling factors (CDSF) and data were reanalysed as described in 3.3.6. Results of this analysis are displayed in Table 9, along with that of standard scaling factors for means of comparison. See Figure 36 (Appendix 7.6) for corresponding graphs. In all assay formats, both GMFE and RMSE were reduced, along with an increase in the number of successful predictions in each assay format.

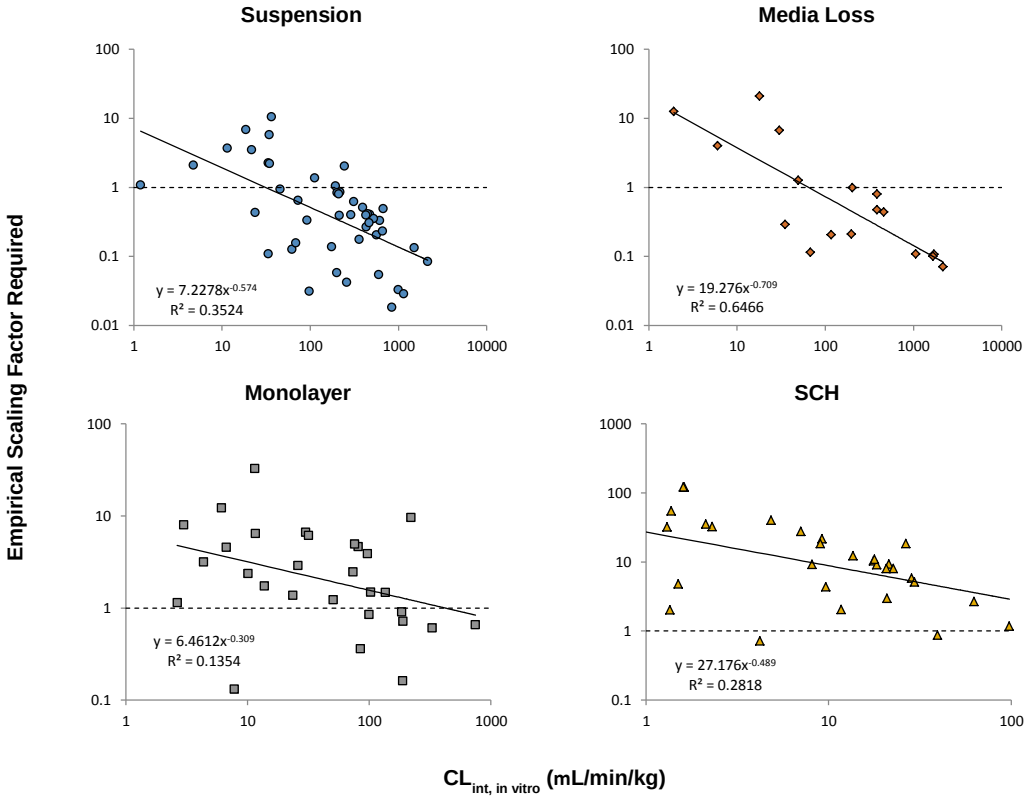

Figure 5 - Empirical Scaling factors required in addition to standard physiological scaling, plotted against $CL_{int,\ in\ vitro}$ for compounds in suspension, media loss, monolayer and SCH in rat hepatocytes. Line of best fit for required scaling factor (solid line) and the static physiological scaling factor (dashed) are displayed

Table 9 - Effect of CDSF on the bias and precision of $CL_{int,\ in\ vivo}$ predictions in rat hepatocytes.

Scaling Factor		Standard	CDSF
Suspension	GMFE (RMSE)	4.17 (3782)	2.69 (867)
	% well predicted	21	38
	% over-predicted	60	28
	% under-predicted	19	34
Media Loss	GMFE (RMSE)	4.89 (6065)	2.15 (880)
	% well predicted	18	53
	% over-predicted	59	24
	% under-predicted	23	24
Monolayer	GMFE (RMSE)	3.25 (3012)	2.42 (2893)
	% well predicted	38	55
	% over-predicted	10	14
	% under-predicted	52	31
SCH	GMFE (RMSE)	14.5 (1032)	2.54 (780)
	% well predicted	7	44
	% over-predicted	0	29
	% under-predicted	93	27

3.4.2.1.4. Application of apparent intrinsic clearance

Due to multiple studies being available for some compounds, average values for each drug were taken when necessary. As a result, 20 drugs were included in this analysis. Details of the individual studies can be found in Table 35 (Appendix 7.6). Using standard physiological scaling factors, $CL_{int,\ app}$ ranged from 28 – 11,300 mL/min/kg. Following IVIVE, the majority of compounds over-predicted *in vivo* clearance (Table 10). GMFE for $CL_{int,\ app}$ (4.85), was similar to that using uptake data alone (5.62), but was lower than metabolism alone (9.35). Precision remained comparable between the use of uptake data and $CL_{int,\ app}$ (RMSE = 3949 and 2975, respectively), while using metabolism data had the lowest precision recorded in this study (RMSE = 23,298). Each clearance parameter resulted in the over-prediction of *in vivo* clearance for the majority of the drugs in this analysis.

As a final exercise the various empirical scaling methods described in this chapter were applied to uptake data prior to input into the $CL_{int, app}$ term. These included mean, median and CDSF calculated in sections 3.4.2.1.1 - 3.4.2.1.3. For metabolism, similar analyses were performed on the metabolism database developed by Wood et al[131], however no relationship was identified between the required empirical scaling factor and *in vitro* clearance. As a result, only mean and median required scaling factors were investigated. The use of clearance-derived scaling factors for uptake, along with the median required scaling factor for metabolism data prior to the calculation of $CL_{int, app}$ produced predictions with the lowest bias (GMFE = 2.65). However, this was similar in terms of both bias and precision to using uptake data alone, scaled using CDSF (GMFE = 2.72). Results are summarised in Table 10, and see Figure 37 (Appendix 7.6) for corresponding graphs.

Table 10 - Summary of $CL_{int, app}$ in terms of bias and precision for the prediction of $CL_{int, in\ vivo}$ in rat hepatocytes.

Scaling		Standard	CDSF	Median	Mean
Metabolism	Scaling Value	8	N/A	34	274
	GMFE (RMSE)	9.35 (23298)	-	13.7 (101553)	39.5 (818922)
	% well predicted	20	-	6	11
	% over-predicted	45	-	61	78
	% under-predicted	35	-	33	11
Uptake	Scaling Value	8	Varied	3.2	9
	GMFE (RMSE)	5.62 (3949)	2.72 (903)	3.06 (1475)	6.17 (4505)
	% well predicted	10	42	53	6
	% over-predicted	80	32	37	83
	% under-predicted	10	26	11	11
$CL_{int, app}$	Scaling Value	8	Varied*	Varied	Varied
	GMFE (RMSE)	4.85 (2975)	2.65 (926)	2.83 (1361)	5.35 (4126)
	% well predicted	20	42	53	11
	% over-predicted	55	26	32	78
	% under-predicted	25	32	16	11

*CL_{met} scaled by median scaling factor

3.4.2.2. Human Hepatocytes

3.4.2.2.1. Minimum and Maximum Literature Scaling Factors

As with rat hepatocytes, a number of physiological values used to calculate scaling factors have been referenced for human hepatocytes within the literature, although with a narrower range. The maximum scaling factor was determined to be 3.47, and the minimum scaling factor was 1.18 (see Table 34, Appendix 7.5). Results of the application of these scaling factors to the data are displayed in Table 11 (see Figure 38 and Figure 39, Appendix 7.7 for corresponding graphs). The maximum scaling factor had little effect on the suspension assay, with only a 10% increase in the number of over-predicted studies. Monolayer and SCH saw improvements to both GMFE and RMSE, as well as an increase in successful *in vivo* predictions. The minimum scaling factor led to an increase in bias, and reduction in precision and number of successful predictions in all assay formats. This was particularly evident for monolayer and SCH, where under-predictions increased.

Table 11 - Effect of mean and median empirical scaling factors on the bias and precision of $CL_{int,\ in\ vivo}$ predictions in human hepatocytes.

Scaling Factor		Standard	Maximum	Minimum
	Scaling Value	2.57	3.47	1.18
Suspension	GMFE (RMSE)	4.04 (1466)	4.09 (1462)	4.85 (1490)
	% well predicted	31	24	22
	% over-predicted	28	38	24
	% under-predicted	41	38	54
Monolayer	GMFE (RMSE)	4.85 (1831)	3.71 (269)	7.98 (1908)
	% well predicted	20	24	16
	% over-predicted	16	19	8
	% under-predicted	64	57	76
SCH	GMFE (RMSE)	6.19 (1934)	5.81 (1924)	13.5 (1985)
	% well predicted	23	23	7
	% over-predicted	7	7	3
	% under-predicted	70	70	90

3.4.2.2.2. Mean and Median Required Scaling Factor

Mean and median scaling factors were calculated, as described in 3.3.4, and applied to the data as shown in Table 12 (see Figure 40 and Figure 41, Appendix 7.7 for corresponding graphs). The mean value exceeded that of the standard scaling factor in all assay formats, leading to a reduction in under-predictions. It also led to a reduction of the bias and an increase in precision, with the exception of the suspension assay, for which it had the opposite effect. The median value was lower than the mean in all assay formats, and in the case of suspension was slightly lower than the standard scaling factor. As a result, no changes were noted for the suspension assay in comparison to standard physiological scaling. Monolayer and SCH assays saw a more substantial improvement when using the median over the standard scaling factor, with reduced bias, improved precision and an increase in the number of successful predictions.

Table 12 - Effect of mean and median empirical scaling factors on the bias and precision of $CL_{int,\ in\ vivo}$ predictions in human hepatocytes.

Scaling Factor		Standard	Mean	Median
Suspension	Scaling Value	2.57	10.05	2.53
	GMFE (RMSE)	4.3 (1855)	5.5 (1757)	4.3 (1858)
	% well predicted	28	26	28
	% over-predicted	31	59	31
	% under-predicted	41	16	41
Monolayer	Scaling Value	2.57	19.05	9.4
	GMFE (RMSE)	4.73 (1835)	4.02 (1490)	3.27 (1671)
	% well predicted	19	35	42
	% over-predicted	15	50	31
	% under-predicted	66	15	27
SCH	Scaling Value	2.57	44.1	13.53
	GMFE (RMSE)	6.19 (1934)	4.9 (1329)	3.65 (1677)
	% well predicted	20	23	33
	% over-predicted	7	63	30
	% under-predicted	73	13	37

3.4.2.2.3. Clearance-Derived Scaling Factors

For human data, no significant correlations were noted between required empirical scaling factor and $CL_{int,\ in\ vitro}$ (Figure 6). Despite the lack of statistical significance, CDSF were tested as empirical scaling factors to determine if improvements could be made. CDSF resulted in a reduction in GMFE and an increase in successful predictions for monolayer and SCH, while precision saw no change (Table 13, see Figure 42, Appendix 7.7 for corresponding graphs). SCH had the largest improvement, where successful predictions were increased by 20%. Data from suspension remained relatively unchanged.

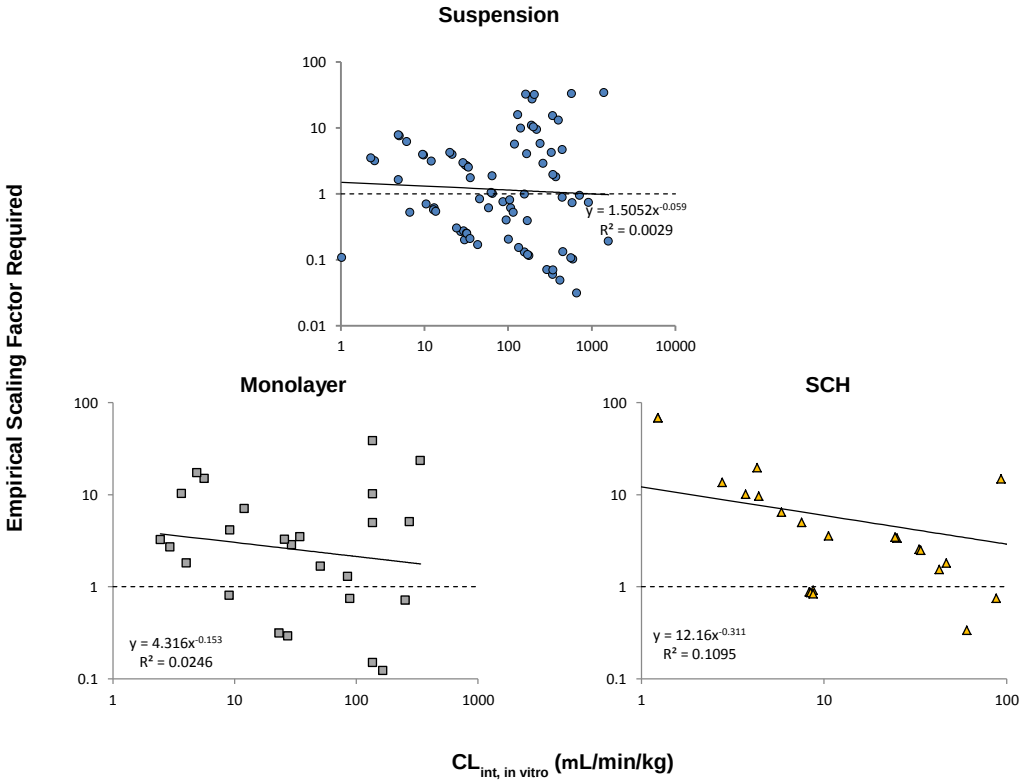

Figure 6 - Empirical Scaling factor required in addition to physiological scaling, plotted against $CL_{int,\ in\ vitro}$ for compounds in suspension, monolayer and SCH for human hepatocytes. Line of best fit for required scaling factor (solid line) and the static physiological scaling factor (dashed) are displayed.

Table 13 - Effect of CDSF on the bias and precision of $CL_{int,\ in\ vivo}$ predictions in human hepatocytes.

Scaling Factor		Standard	CDSF
Suspension	GMFE (RMSE)	4.3 (1855)	4.28 (1850)
	% well predicted	28	22
	% over-predicted	31	37
	% under-predicted	41	41
Monolayer	GMFE (RMSE)	4.73 (1835)	3.41 (1798)
	% well predicted	19	32
	% over-predicted	15	32
	% under-predicted	66	36
SCH	GMFE (RMSE)	6.91 (1947)	3.49 (1949)
	% well predicted	20	43
	% over-predicted	7	23
	% under-predicted	73	33

3.4.2.2.4. Application of apparent intrinsic clearance

A total of 15 drugs were identified which had sufficient data to calculate $CL_{int,\ app}$ (see Table 36, Appendix 7.7). Of these, only one required metabolism data from microsomes as no data were available from hepatocytes in suspension. Using standard physiological scaling factors, $CL_{int,\ app}$ ranged between 1.4 – 130 mL/min/kg. An overall tendency towards under-prediction was noted (Table 14, see Figure 43, Appendix 7.7 for corresponding graphs), with GMFE calculated as 6.32 for $CL_{int,app}$. This was substantially worse than using uptake data alone for this set of compounds (GMFE = 3.05), while using metabolism data alone resulted in the highest amount of bias (GMFE = 15.1). Precision remained relatively high regardless of the data that was used, with RMSE values of 516, 604 and 600 for uptake, metabolism and $CL_{int,app}$, respectively.

Table 14 - Summary of $CL_{int,\ app}$ in terms of bias and precision for the prediction of $CL_{int,\ in\ vivo}$ in human hepatocytes.

Scaling		Standard	CDSF	Median	Mean
Metabolism	Scaling Value	2.57	N/A	34.5	393
	GMFE (RMSE)	15.1 (605)	-	5.15 (615)	4.38 (579)
	% well predicted	20	-	47	47
	% over-predicted	7	-	33	33
	% under-predicted	73	-	20	20
Uptake	Scaling Value	2.57	Varied	2.56	9.63
	GMFE (RMSE)	3.05 (517)	3.1 (511)	3.05 (517)	6.16 (919)
	% well predicted	47	47	47	13
	% over-predicted	33	40	33	80
	% under-predicted	20	13	20	7
$CL_{int,\ app}$	Scaling Value	2.57	Varied*	Varied	Varied
	GMFE (RMSE)	6.32 (602)	3.46 (570)	3.57 (556)	4.17 (553)
	% well predicted	27	27	33	40
	% over-predicted	6	40	13	40
	% under-predicted	67	33	54	20

*CL_{met} scaled by median scaling factor, since no CDSF was available for CL_{met}

CDSF, mean and median scaling factors were used to assess if bias and number of successful predictions were improved, as described in 3.4.2.1.4. It was observed that the least degree of bias (GMFE = 3.05) was seen when using uptake data alone, scaled using the median required scaling factor or the standard physiological scaling factor. For $CL_{int,\ app}$, the lowest bias was noted when using uptake and metabolism data that had been scaled using CDSF and the median required scaling factor, respectively, prior to input into the equation. This resulted in a GMFE of 3.46, with a slight tendency towards over-prediction. Use of the mean required scaling factor resulted in a larger reduction in bias compared to using the median for metabolism only.

3.5. Discussion

The primary focus of this chapter was to compile and analyse literature data in order to provide an assessment of both the accuracy and precision of *in vitro* uptake data for the prediction of *in vivo* hepatic clearance. It is important to note that, for the broad purpose of this analysis, it is assumed that *in vivo* hepatic clearance is mediated by the uptake of drug into the liver. It is to be expected that, given the diversity of drugs covered, this is not always true. However, this method provides a platform to assess the utility of *in vitro* uptake data as a predictor of *in vivo* clearance, as well as allowing for comparisons between assay formats and investigating various methods of improving *in vivo* predictions using scaling factors.

3.5.1. Database overview and prediction of $CL_{int,\ in\ vivo}$

3.5.1.1. Rat Hepatocytes

In rat hepatocytes, the suspension format was identified as the most popular, both in the number of studies and the number of unique drugs covered within the literature. However, in general this assay had a clear tendency to over-predict *in vivo* clearance, an aspect also shared with the media loss assay, although less data are available in this format. Since hepatocytes are in the same suspended state in both the suspension and media loss assays, they are both termed “non-cultured” formats. The non-cultured formats displayed a large degree of bias, while precision was seen to be lower than that seen for monolayer and SCH.

From these observations, it would be implied that the non-cultured assay formats cause hepatocytes to display uptake rates above that which is typically seen *in vivo*. Inspection of the BDDCS grouping and ionisation character of the dataset suggests passive diffusion could be the process affected. Two observations have led to this hypothesis. First, in the suspension and media loss assay, 79% and 60% of the class 2 compounds had an over-prediction of their *in vivo* clearance, respectively. These compounds are typically expected to have high permeability and metabolism, but have the potential to be substrates of uptake transporters. Second, all neutral compounds were over-predicted in suspension, and the vast majority in media loss. Neutral compounds are known to be able to diffuse more readily across the plasma membrane and, taken with the BDDCS

observation, indicate that it is possible non-cultured assays exhibit higher rates of passive diffusion. This is further supported by the observation that all class 2 compounds that were also neutral were over-predicted in both assays (n=10 and n=2 for suspension and media loss, respectively). Although this provides a potential link, this hypothesis cannot be tested further with the current data set, since no distinction was made between active and passive uptake rates in many of the studies. This prevents analysis of the over-predicted compounds to determine if passive diffusion plays a significant role in their total uptake rate.

Both the monolayer and SCH assays require cells to be cultured for some time before commencing the experiment, and as such are termed "cultured" formats. The observations of the cultured formats directly contrasted that of the non-cultured formats, with predictions largely falling short of the observed *in vivo* values. In terms of overall bias, monolayer was seen to produce the lowest GMFE value (3.25) of the four assay formats, while SCH produced the highest (14.5). Precision was higher than the non-cultured formats for the monolayer assay, and SCH had the lowest observed RMSE value of the four assays. The concordance of the SCH assay would suggest that this system would benefit greatly from an empirical scaling factor.

In monolayer cultures, compounds with assumed higher permeability (BDDCS class 1 and 2) led to reasonable predictions of *in vivo* clearance, while low permeability compounds that are expected to rely on uptake transporters for entry into the cell (BDDCS class 3 and 4) typically produced under-predictions. No distinct patterns were observed when grouping based on ionisation character. It is therefore difficult to hypothesise the cause of under-prediction. Since class 1 and 2 compounds aren't seen to be over-predicted, an issue noted for non-cultured assays, it would seem likely that passive diffusion in monolayer cultures is more in line with that which occurs *in vivo*. The under-prediction of class 3 and 4 compounds may suggest that culture time could lead to a reduction in uptake transporters present at the cell membrane, and therefore a decreased uptake of actively transported compounds, as has been hypothesised previously[136]. However, without the distinction between active and passive uptake rates within this database, it is again difficult to pinpoint where the source of error is likely to originate from.

Due to the extent of under-prediction found in SCH, no particular patterns could be identified. SCH assays are typically very similar to the monolayer assay in terms of their culture and assay methodology, with the key difference of a much longer culture time prior to commencement of the assay. It has been demonstrated previously that over time in culture, the abundance of influx transporters in the membrane decreases[137], and is likely a key factor in the observed under-prediction of *in vivo* clearance.

Overall the monolayer assay appears to be useful for predicting *in vivo* clearance of BDDCS class 1 and 2 compounds, and on average produces the least amount of bias for any compound. Class 3 and 4 compounds will typically be expected to be under-predicted in this format, therefore a non-cultured format may be preferable. SCH in its current form is considered unsuitable for prediction of *in vivo* clearance, as compounds were almost exclusively under-predicted by several fold.

3.5.1.2. Human Hepatocytes

Analysis of data from human experiments displayed some clear differences to that which was seen in rat, as well as some similarities. No literature data were found for human hepatocytes in the media loss format. It is not clear if this is due to methodological incompatibilities, or simply due to the tendency to use hepatocytes in suspension by default when using human hepatocytes (particularly when considering the high financial cost and the novelty of the media loss assay). Hepatocytes in suspension again had the highest frequency in the literature, the majority of which resulted in an under-prediction of *in vivo* clearance. Despite this difference to rat hepatocytes, overall bias was found to be very similar, while precision was better in human. BDDCS class 1 compounds were particularly well predicted, while class 2 suffered the same over-prediction issues seen in the rat. Ionisation character did not appear to have any influence on predictions for human hepatocytes, unlike observations for neutral compounds in rat hepatocytes.

Human hepatocytes in monolayer maintained similar results to that in the rat, with a large majority of studies under-predicting *in vivo* clearance. Both bias and precision were found to be worse in human monolayer than the human suspension format. For both BDDCS and ionisation character no clear pattern to distinguish the cause of under-prediction was observed.

Similar to rat, human SCH saw the vast majority of studies resulting in an under-prediction of *in vivo* clearance. GMFE (6.19) was greater than both the suspension and monolayer formats, however, it was a marked improvement over that observed in the rat. SCH had the highest RMSE value, indicating the lowest precision, of the three human assay formats. As would be expected, all BBDCS classes tended to be under-predicted, with the exception of class 4 compounds which showed good predictions (although there was insufficient data within this class to draw any conclusions).

Overall, when using human hepatocytes the least amount of bias was noted when using the suspension format. Compared to rat, human hepatocytes tended to show an under-prediction of *in vivo* clearance. Human monolayers displayed more bias than was seen in their rat counterparts, however the percentage of good, over and under predictions remained similar, with a strong tendency towards under-prediction. Human SCH were again seen to heavily under-predict *in vivo* clearance, although not to the same degree as was seen in rat. Despite this, the assay appears to be inappropriate for estimating *in vivo* clearance as a standalone assay. Empirical scaling or integration with other systems would be required before this assay is suitable for use in such a manner. In this particular study, no comparison was made between common drugs within each assay format. This was due to data being tabulated individually, rather than through calculation of an average for each drug. As such, comparison of common drugs was not considered to be informative, given the disproportionate number of paired data relative to the actual number of common drugs.

3.5.2. Variability in scaling factor and the use of empirical values to improve $CL_{int,\ in\ vivo}$ predictions

3.5.2.1. Rat Hepatocytes

Analysis of data in 3.4.1 was performed using scaling factors reported in the literature. Physiological values of 200 mg protein/g liver and 40g liver/kg bodyweight were selected, which equated to a scaling factor of 8. However, during the construction of the database it became apparent that the choice of values for these scaling parameters varied substantially. As such, the next aim of this study was to determine to what extent the choice of values for the physiological scaling factor affected the outcome of predictions.

Using various combinations of physiological factors quoted in the literature, maximum (15.5) and minimum (3.46) scaling factors were calculated and applied to the data. As was expected, non-cultured assay formats, which were previously seen to produce over-predictions, benefitted from the use of the minimum scaling factor. Indeed, it was noted that the majority of studies in the literature that had performed IVIVE using data from hepatocyte suspensions or media loss assays opted for a scaling factor below that of which was selected for this study. Most commonly this would be composed of a hepatocellularity of 120 x 10^6 cells/g liver and a liver weight of 40 g liver/kg bodyweight, which results in a scaling factor of 4.8[91, 136, 138, 139]. Conversely, cultured formats benefitted more from the maximum scaling factor. It was particularly evident that IVIVE of SCH data more frequently opted for the physiological scaling factor of 8[111, 140-143], which was applied in this study.

Following from this initial analysis of physiological scaling, several methods were applied to generate empirical scaling factors, a principle that has been employed for some time in order to aid IVIVE. In particular, this method has been used in order to combat the clearance-dependent under-prediction of metabolic data[144, 145], but has also been used previously in smaller uptake datasets to improve accuracy of *in vivo* predictions[146, 147].

The first method employed in this study was to calculate the arithmetic mean and median required scaling factor for each assay format. This led to the unexpected result of non-cultured assay formats having a greater mean empirical scaling factor value (9 and 23 for suspension and media loss, respectively) than the standard physiological scaling factor value of 8. As a result, application of the mean empirical scaling factor led to an increase in GMFE, as well as a greater number of over-predictions for each of these assays. Upon further investigation, it became apparent that these high mean values were caused by a small number of studies which produced predictions which were in some cases greater than 100-fold lower than the observed *in vivo* clearance. In comparison, the largest over-prediction was only 7-fold greater than the observed *in vivo* clearance, which led to a skew in the mean value. In the case of both monolayer and SCH, the overall effect was an improvement in terms of bias, but at the expense of a decrease in precision and a large increase in the amount of over-predictions generated.

As an alternative to the mean scaling factor, the median value was also calculated in order to counteract the skew caused by extreme values. The resulting scaling factors for non-cultured formats were lower than the physiological scaling factor, while cultured formats had much higher values. This led to a reduction in bias for all assay formats, while precision increased for non-cultured formats but decreased for cultured formats. Overall, it would appear that the median required scaling factor would be the best choice for increasing accuracy, despite the mean or standard scaling factors in some cases leading to a higher percentage of successful predictions.

The second method employed was termed "clearance-derived" scaling factors (CDSF). This principle involved plotting the required scaling factor against the measured $CL_{int,\ in\ vitro}$. Upon fitting a trendline, it became apparent that for all assay formats, as $CL_{int,\ in\ vitro}$ increased, the required scaling factor to equal the observed $CL_{int,\ in\ vivo}$ decreased. This would mean that when using a static scaling factor, high clearance compounds were more likely to be over-predicted than lower clearance compounds. This directly contradicts findings that have been reported for metabolism data[131], where the scaling factor required increases as $CL_{int,in\ vivo}$ increases. For rat, it was found that all correlations between required scaling factor and the $CL_{int,\ in\ vitro}$ were significant for uptake data, but not for metabolism data. Using the line equations for each assay, scaling factors were then generated based on each compound's $CL_{int,\ in\ vitro}$. When applied, large improvements were noted to the bias, precision and percentage of successful predictions for each assay format. CDSF incorporated both an empirical scaling factor, as well as combating the observed clearance-based over-prediction. As a result, each of the assay formats displayed a similar degree of bias when predicting *in vivo* clearance.

3.5.2.2. Human Hepatocytes

A repeat of the analyses described in 3.5.2.1 were performed for data collected from human hepatocytes. In terms of literature scaling factors, human physiological parameters saw much less variation. Despite this, the fold difference between the minimum and maximum scaling factors, compared to the most frequent literature values, was very similar between human and rat.

In general, cultured formats benefitted from the use of the maximum scaling factor, which led to a reduction in bias and an increase to the proportion of successful predictions for both assay formats. The suspension assay was not heavily influenced by either scaling factor, with the standard scaling factor providing the most accurate results.

Overall it was concluded that the choice of physiological scaling factor had less impact when calculating human clearance than was noted in the rat. That being said, it would not be recommended to apply the lowest scaling factor, due to the negative effect on cultured formats. If using these assays, the maximum scaling factor would likely result in better outcomes for predictions.

In terms of the mean and median required scaling factors, the same occurrences were observed for human as for rat. When calculating the mean, extreme under-predictions again inflated the value of the mean, resulting in an increase in bias for the suspension assay, while both cultured formats saw modest improvements (at the expense of large increases to the proportion of over-predictions). The median required scaling factor was more suitable, resulting in the largest improvements to bias and successful predictions in the cultured formats. Interestingly, the median required scaling factor value was almost identical to the standard physiological value for the suspension assay, and as such no change was noted. As was shown in 3.5.2.1 it appears that the use of median scaling factors is preferable when generating static empirical scaling factors. With the huge variability in predictions, this approach helps to even out the skew caused by extreme values. In addition, use of the median scaling factor only had positive effects on the bias of each system tested in both rat and human, indicating it to be a very reliable method.

When generating CDSF in human, correlations between $CL_{int,\ in\ vitro}$ and required scaling factors were found not to be significant. Regardless of the lack of statistical significance, it was concluded that this method produces an empirical scaling factor, and could still therefore be useful. This was indeed seen to be the case for monolayer and SCH, as the application of a CDSF resulted in a greater improvement to bias and successful predictions than was noted for any of the previous empirical scaling methods. For suspension, no change was noted between use of the CDSF and the standard physiological scaling. It is therefore concluded that the use of CDSF appears to be an effective method to improve

$CL_{int,\ in\ vitro}$ predictions for all assay formats, as at worst they will produce the same predictions as using standard physiological scaling factors.

3.5.3. Use of the $CL_{int,\ app}$ term to improve $CL_{int,\ in\ vivo}$ predictions

3.5.3.1. Rat Hepatocytes

Although the focus of this chapter has been on the uptake of compounds, it is also acknowledged that in some cases the use of uptake data alone is inappropriate. Just as uptake rate-limited compounds are poorly predicted in metabolism assays, the same may be true for metabolism-rate limited compounds subjected to uptake assays. The $CL_{int,\ app}$ term was investigated as it incorporates multiple clearance parameters to provide an overall clearance rate. Using the uptake data gathered in this study, as well as metabolism data gathered previously by Wood et al[131] it was possible to calculate $CL_{int,\ app}$ for 20 compounds. Due to a lack of data, efflux rates were assumed to be negligible. This assumption is supported by previous reports which have found the presence of canalicular efflux transporters to be reduced substantially in non-cultured assay formats[98]. Sinusoidal efflux was assumed to be negligible due to the current lack of data for the drugs used in this study.

Using standard scaling factors, it was observed that for the set of 20 compounds $CL_{int,\ app}$ produced predictions with the highest precision, as well as with the lowest bias, compared to either uptake or metabolism alone. In addition, CDSF were applied to the data to assess if further improvements could be made to predictions. Marked improvements were observed after application of CDSF. It should be noted, however, that use of uptake data alone produced highly similar values in terms of GMFE, RMSE and percentage of successful predictions in both sets of analyses. It would therefore be recommended that $CL_{int,\ app}$ is applied if data are available, however use of the uptake data alone in this instance would also produce comparable results.

3.5.3.2. Human Hepatocytes

In human hepatocytes, $CL_{int,\ app}$ did not result in a reduction in prediction bias compared to other clearance terms. Use of uptake data alone produced the least bias and highest proportion of successful predictions for the vast majority scaling methods tested (the only exception being the mean required scaling factor). Metabolism remained the least

accurate parameter, with the highest GMFE value for each of the scaling methods. From this analysis, the $CL_{int, app}$ term is not recommended to be applied to human data.

3.6. Conclusion

In conclusion, this chapter has highlighted that the holistic analysis of *in vitro* uptake methodologies using data from the literature is of high importance to fully understand the limitations and bias of each assay, and to aid in the future interpretation of data. It should also be noted that the findings of this chapter are dependent on the dataset used. In rat, use of the monolayer assay provided the most accurate and precise results when using standard physiological scaling factors, while suspension assays were found to be the most accurate system using human hepatocytes. In terms of IVIVE, this analysis would suggest that these two assays are the best choices for each species when studying novel compounds. The use of various empirical scaling factors was found to be beneficial to both the accuracy and precision of *in vitro* uptake assays, and in the case of SCH is essential for any meaningful IVIVE to be performed. Finally, the $CL_{int, app}$ term was seen to provide a modest improvement to prediction accuracy in the rat, but was not beneficial in human. The results of this analysis will be considered when selecting appropriate assays for the subsequent chapters of this thesis. Since use of empirical scaling essentially made each assay format comparable, it was concluded that selection of assays could be based purely on specific parameters or assay features required.

Chapter 4. Development of the Media Loss Assay

4.1. Introduction

Chapter 3 provided an extensive analysis of current literature data for four commonly utilised hepatocellular uptake assays: suspension, media loss, monolayer and SCH. This analysis represents a cellular scaling approach for prediction of *in vivo* clearance, where data are extrapolated from the level of the cell to that of the whole body. In both rat and human hepatocytes, suspension assays were the most commonly utilised. This method is particularly labour intensive, requiring incubations to be performed in tubes containing a layer of oil which allows the separation of cells and media via centrifugation. Monolayer and SCH formats are less technically demanding, but require culture time before assays can commence. As well as reducing the throughput of the assays, it is argued that during this time transporter expression at the membrane declines, which may lead to under prediction of clearance[105], a theory supported by data in Chapter 3. The "media loss" assay was developed more recently and is capable of providing simultaneous estimations of uptake and metabolism[1]. Generation of multiple clearance parameters from a single assay has since been attempted in other hepatocyte systems, such as monolayer[97], and has allowed the use of more complex mechanistic models to generate *in vivo* clearance estimates[129].

While uptake rates are the most appropriate process to predict *in vivo* clearance for many types of compound, the low throughput nature of the assays has typically prevented their widespread use. To this end, a higher throughput method would be desirable. In addition, the ability to distinguish between active and passive uptake, as well as the rate of metabolism and degree of intracellular binding would also be advantageous for predictions *in vivo* clearance, allowing a full characterisation of drugs, as well as allowing a transition towards more complex, mechanistic predictions.

4.2. Aims

The media loss assay was selected for further study in this chapter using rat hepatocytes, due to: a) its potential to be developed into a higher throughput system b) its ability to

provide both uptake and metabolism data, simultaneously, and c) the potential of the assay to further split uptake into both active and passive rates.

As such, the first aim was to adapt the current methodology to allow the use of multi-well plates. This will open the assay up to a wide number of further applications, due to an increased number of samples that are able to be generated. Focus will be applied to the incorporation of inhibitors of both metabolic enzymes and uptake transporters, which will enable identification of the key processes in the clearance of a compound. In order to fully assess the utility of the assay, a range of drugs with differing characteristics will be required. To this end, drug uptake data and metabolism rates in rat hepatocytes (where available from data collated in Chapter 3) were used to divide drugs into groups (1-4) based on the contribution of active transport to their uptake, as well as their rate of metabolism (Figure 7). Descriptors were defined as follows: high active uptake (% active transport > 75), low active uptake (% active transport < 75), high metabolism (Metabolic $CL_{int,\ in\ vitro}$ > 100 mL/min/kg) and low metabolism (Metabolic $CL_{int,\ in\ vitro}$ < 100 mL/min/kg). A selection of compounds from each group were chosen for study (Table 15, Figure 7), and were intended to achieve a diversity in both rate of metabolism and extent of active transport to fully

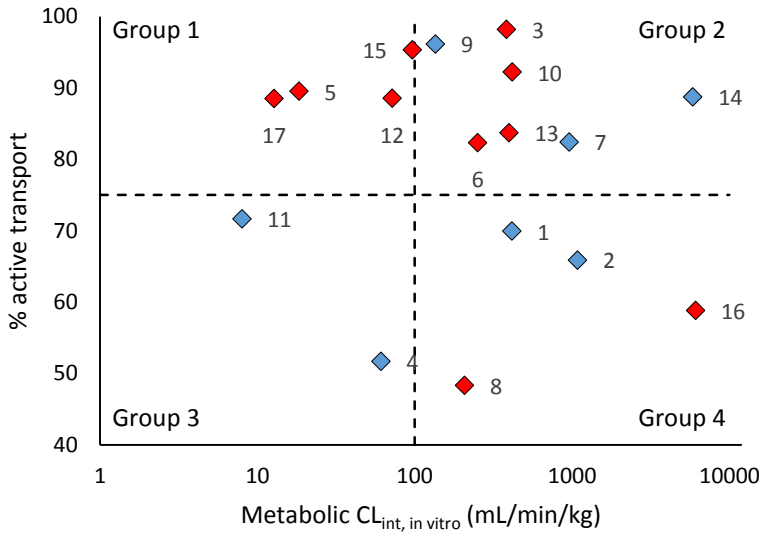

Figure 7 – Percentage Active Transport plotted against metabolic $CL_{int,\ in\ vitro}$ for the classification of drugs into groups 1-4. Data were taken from rat hepatocyte literature data listed in 7.2, where available. Metabolic clearance data were scaled using standard physiological scaling factors of 200 mg protein/g liver and 40 g liver/kg bodyweight. Labels are as follows: 1) Amprenavir, 2) Atazanavir, 3) Atorvastatin, 4) Bosentan, 5) Cerivastatin, 6) Clarithromycin, 7) Darunavir, 8)

Erythromycin, 9) Fexofenadine, 10) Indinavir, 11) Indomethacin, 12) Pitavastatin, 13) Repaglinide, 14) Ritonavir, 15) Rosuvastatin, 16) Saquinavir, 17) Valsartan. Red symbols indicate drugs that were selected for this study.

Table 15 - Overview of compounds selected for study, along with their group classification.

	Low Metabolism	**High Metabolism**
High Active Uptake	**Group 1** Cerivastatin Pitavastatin Rosuvastatin Valsartan	**Group 2** Atorvastatin Clarithromycin Indinavir Repaglinde
Low Active Uptake	**Group 3** Tolbutamide	**Group 4** Erythromycin Midazolam Saquinavir

assess the utility of the assay. Two compounds selected for study (midazolam and tolbutamide) are not present in Figure 7 as, although previous in house data has determined uptake to be predominantly via passive diffusion, no value for % active transport has been determined. These two compounds were intended to act as control compounds. Tolbutamide is well known to have very low rates of metabolism and uptake, and so would be expected to have almost no depletion over time in either the conventional or media loss assay. Conversely, midazolam is known to have very high rates of metabolism, and so would be expected to display similar (i.e. monophasic) profiles across both assay formats.

The second aim of this chapter was to develop a two-compartment mechanistic model to process the *in vitro* data generated, allowing for rates of metabolic and active/passive transport to be calculated, as well as various distribution and binding parameters. Finally, as a continuation of Chapter 3, a cellular IVIVE approach using single parameters (i.e. intrinsic clearance, metabolism or uptake) will be used to predict observed *in vivo* clearance.

4.3. Methods

4.3.1. Chemicals

Atorvastatin, indinavir, pitavastatin calcium, rosuvastatin and valsartan were purchased from Sequoia Research Products (Pangbourne, UK). Saquinavir and midazolam were purchased from Roche Products Ltd (Welwyn Garden City, UK). 1-Aminobenzotriazole (ABT), Rifamycin SV (Rfc), clarithromycin, erythromycin, tolbutamide, and Bradford reagent were purchased from Sigma-Aldrich (Dorset, UK). Cerivastatin and repaglinide were purchased from Carbosynth Limited (Berkshire, UK). All other reagents were obtained from Life Technologies (Paisley, UK).

4.3.2. Hepatocyte Isolation and Preparation

Rat hepatocytes were isolated from the livers of male Sprague-Dawley rats weighing between 250 – 300g (Charles River, Margate, Kent, UK). Rats were sacrificed using CO_2 overdose followed by cervical dislocation. Hepatocytes were prepared using an adaptation of the two-step collagenase perfusion method, as described previously[86]. After isolation, hepatocytes were suspended in phenol red-free Williams' medium E (WME), pH 7.4. Cell count and viability were determined using the trypan blue exclusion method. Only preparations exceeding 85% viability were used. Cells were diluted to a density of 2 x 10^6 cells/mL in WME before being split into aliquots. Inhibitors were added to the appropriate cell aliquots to give final concentrations of 1 mM ABT and 100 µM Rfc. Concentrations of inhibitor were selected based on previous evidence demonstrating extensive inhibition in rat of both CYP-mediated metabolism by ABT[148] and Oatp1, Oatp2 and Ntcp mediated uptake by Rfc[149].

4.3.3. Conventional Depletion Assay

Cell suspensions (125 µL) were transferred to a 96-well plate and pre-incubated for 10 minutes in a Heidolph Inkubator 1000 (Heidolph, Schwabach, Germany) at 37°C and 900 rpm. Experiments were performed in duplicate and the maximum organic solvent concentration in the incubation was 0.11% (v/v). To initiate the reaction, 125 µL of drug solution (2 µM) in WME was added to the cell suspension. At 9 specified time points, 75 µL aliquots were quenched in methanol containing relevant internal standard. Samples were stored at -20°C until analysis by liquid chromatography in tandem with mass

spectrometry (LC-MS/MS). Cell suspensions were frozen overnight to lyse cells, and a Bradford protein assay (Biorad, Hemel Hempstead, UK) was performed to determine protein concentrations in each well. See Figure 8 for illustration of method.

4.3.4. Media Loss Assay

The media loss assay, described previously[1, 88], was performed simultaneously with the depletion assay. Methodology remained identical to the depletion assay, except for the addition of a centrifugation step immediately prior to sampling of the media, using an Eppendorf Centrifuge 5804 (Stevenage, UK) at 1500 *g* for 15 s. See Figure 8 for illustration of method. All data were corrected for non-specific binding through addition of any measured depletion in wells containing no hepatocytes for both the conventional and media loss assay.

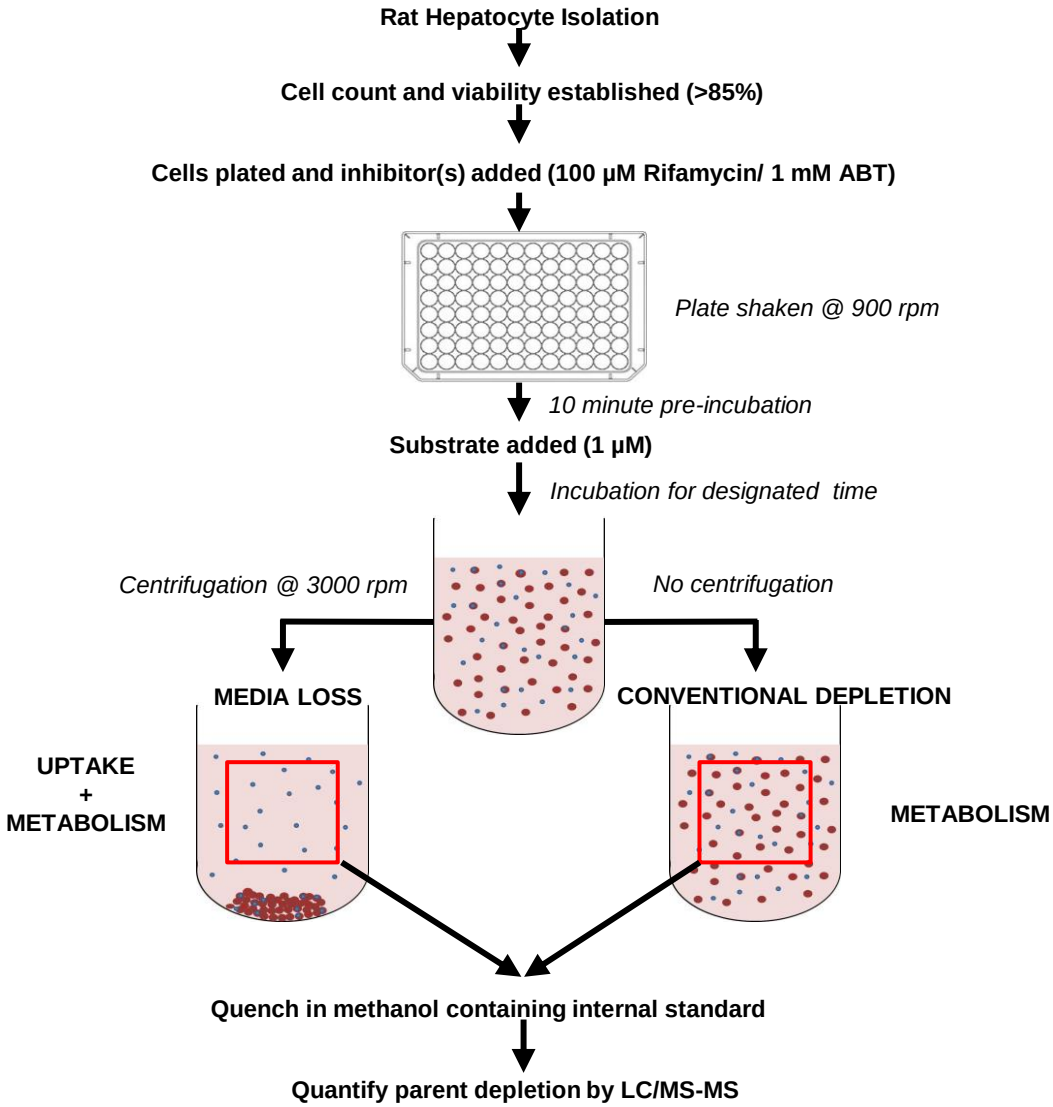

Figure 8 – Overview of the steps taken to perform the media loss and conventional depletion assays in rat hepatocytes.

4.3.5. LC-MS/MS Analysis

A Waters 2795 with a Micromass Quattro Ultima or Quattro Micro triple quadruple mass spectrometer (Waters, Milford, MA) was used for LC-MS/MS analysis. Analytes were centrifuged for 10 min at 2500 rpm and a 10 µL aliquot of the supernatant was analysed by LC-MS/MS. Four mobile phases (A, B, C and D) were used, the composition of each was as follows: A) 90% water; 10% methanol; 0.05% formic acid, B) 90% methanol; 10% water; 0.05% formic acid, C) 90% water; 10% methanol; 10 mM ammonium acetate, D) 90% methanol; 10% water, 10 mM ammonium acetate. A Luna C18 column (3 µm, 50 mm x 4.6 mm) or Luna Phenyl Hexyl column (5µm, 550 x 4.6 mm) was used for chromatographic separation of the analytes (Phenomenex, Torrance, CA), with the flow rate set at 1 mL/min split to 0.25 mL/min before entering the mass spectrometer. For detailed information regarding LC-MS/MS methods for each compound, see Appendix 7.8.

4.3.6. Data Analysis and Modelling

Data were fitted to a monophasic or biphasic exponential decay model, described in Equation 9 and Equation 10[88],

$$C(t) = C_0 \cdot e^{-k_{el}(t)} \qquad \textbf{Equation 9}$$

where C_0 is the initial media substrate concentration and k_{el} is the elimination rate constant.

$$\boldsymbol{C(t) = A \cdot e^{-k_1(t)} + B \cdot e^{-k_2(t)}} \qquad \textbf{Equation 10}$$

Where A and B represent the back-extrapolated drug concentration in the media in the first and second phase, respectively, and k_1 and k_2 are the elimination rate constants in the first and second phase, respectively. Following this, CL_{int} was calculated using Equation 11 and Equation 12 for monophasic and biphasic fits, respectively.

$$CL_{int} = \frac{V \cdot k_{el}}{P} \qquad \textbf{Equation 11}$$

$$CL_{int} = \left(\frac{C_0 \cdot V}{\left(\frac{A}{k_1} + \frac{B}{k_2} \right)} \right) \Big/ P$$ **Equation 12**

Where V is the incubation volume and P is the amount of protein in mg in each incubation. A single factor ANOVA and a post hoc Scheffe's test was used to determine if CL_{int} values were significantly different between conditions.

Data were also modelled using a two-compartment model, adapted from Jigorel et al[88] and implemented in Matlab R2014a (The MathWorks, Inc., Natick, MA) (courtesy of Dr. Adam Darwich, University of Manchester). The model fitted *in vitro* concentration-time points from both the conventional and media loss assay in each of the conditions studied, producing estimates for the rates of active uptake, bidirectional passive diffusion and metabolism. The model was found to be most successful when using a step-wise approach. The conventional assay was first modelled to obtain an estimation of metabolic clearance (CL_{met}), as well as to obtain interaction terms for each inhibitor condition acting on CL_{met} (Int_{ABT}, Int_{Rfc} and Int_{ABTRfc}) described in Equation 13,

$$CL_{met,app} = CL_{met} \cdot Int_{ABT}{}^{ABT} \cdot Int_{Rfc}{}^{Rfc} \cdot Int_{ABTRfc}{}^{ABTRfc}$$ **Equation 13**

Where $CL_{met,app}$ is the apparent metabolic clearance, and ABT, Rfc and ABTRfc are power constants of 0 (in the absence of inhibitor) or 1 (in the presence of inhibitor). In this instance, CL_{met} is a non-saturable clearance term, with interaction terms acting as proportionality scalars to determine the overall effect in Equation 14. For the purpose of data modelling, it was assumed that active transport was completely inhibited by Rfc. Parameters estimated based on the conventional assay were then fixed in the second step, where the media loss concentration-time profiles were modelled to estimate rates of CL_{active} and $CL_{passive}$ transport and the theoretical cell volume ($V_{cell,\ app}$). All results were normalised to the amount of protein within each well. A schematic overview of the steps taken for data modelling are displayed in Figure 9, while Figure 10 gives a diagram of the final model. The full model script can be found in Appendix 7.13.

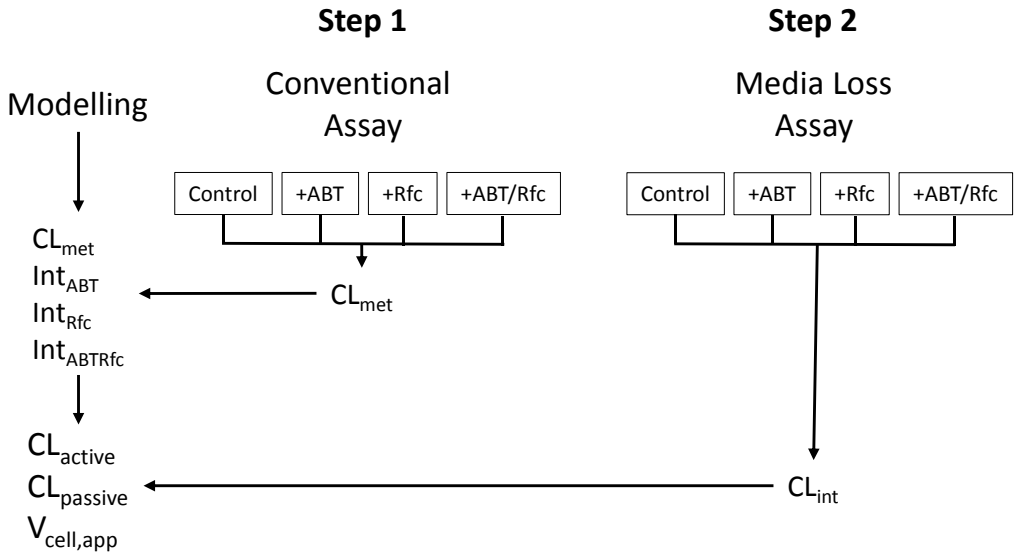

Figure 9 – Schematic outline of the steps taken in the modelling of data from both the media loss and conventional assay.

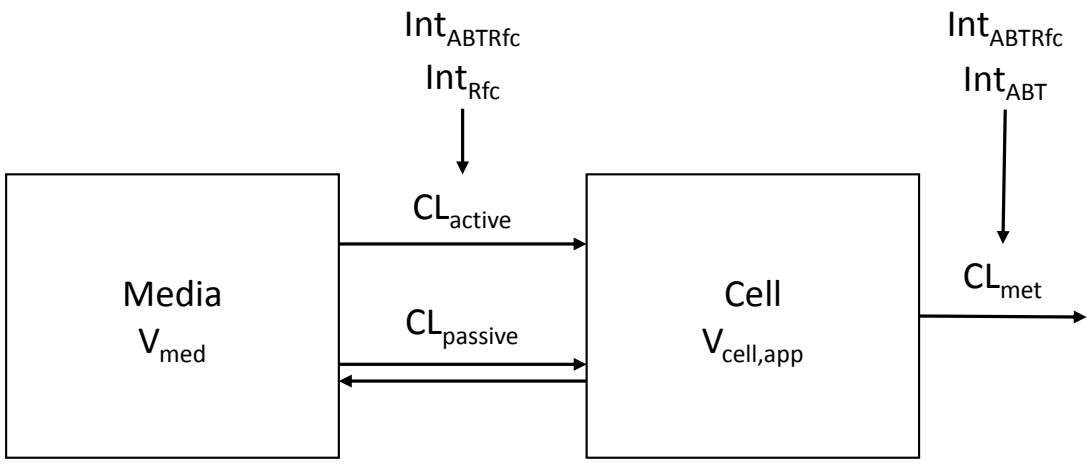

Figure 10 – Two-compartment model used to describe drug uptake (active and passive), metabolism and apparent cell volume.

Differential equations Equation 14 (conventional assay), Equation 15 and Equation 16 (media loss assay) were used to describe the concentrations in both the cell and media over time.

$$\frac{dS_{med}}{dt} = \frac{-CL_{met,app} \cdot S_{med}}{V_{med}} \quad \textbf{Equation 14}$$

$$\frac{dS_{med}}{dt} = \frac{-\left(\left(CL_{active} + CL_{passive}\right) \cdot S_{med}\right) + \left(CL_{passive} \cdot S_{cell}\right)}{V_{med}} \quad \textbf{Equation 15}$$

$$\frac{dS_{cell}}{dt} = \frac{\left(\left(CL_{active} + CL_{passive}\right) \cdot S_{med}\right) - \left(\left(CL_{passive} + CL_{met}\right) \cdot S_{cell}\right)}{V_{app,cell}} \quad \textbf{Equation 16}$$

Where

S_{med} is the concentration in the media, V_{med} is the experimental volume of the media (set at 250 µL) and S_{cell} is the concentration in the cell.

Using this data, additional parameters were calculated as follows. Kp is the ratio of intracellular to media concentrations, and reflects the total drug within the cell, determined by both active uptake processes and intracellular binding (Equation 17).

$$Kp = \frac{V_{app,cell}}{V_{cell}} \quad \textbf{Equation 17}$$

Where $V_{app,cell}$ is the apparent cellular volume of distribution, calculated in the two-compartment model, and V_{cell} is the intracellular volume, calculated assuming 3.9 µL/10^6 cells[97] and a protein conversion of 1x10^6 cells/mg protein (see 3.3.2.1), multiplied by the amount of protein measured in each assay. The ratio of unbound cytosolic drug concentrations, relative to the external medium, is described by the hepatocyte to medium partition co-efficient for unbound drug (Kp_u), and reflects the degree of active uptake (Equation 18).

$$Kp_u = \frac{CL_{active} + CL_{passive}}{CL_{passive}} \qquad \textbf{Equation 18}$$

where CL_{active} and $CL_{passive}$ are the active and passive uptake clearance rates, respectively, estimated by the two-compartment cell model. Due to evidence of internalisation of efflux transporters following hepatocyte isolation[98], efflux was assumed to be negligible. Finally, fu_{cell} was estimated using Equation 19.

$$fu_{cell} = \frac{Kp_u}{Kp} \qquad \textbf{Equation 19}$$

4.3.7. IVIVE

For IVIVE, clearance parameters were scaled to whole body values of the rat using standard physiological scaling factors of 200 mg protein/g liver and 40 g liver/kg bodyweight[123]. Scaling by mg protein was selected since protein content was measured for each *in vitro* assay. These were compared to $CL_{int,\ in\ vivo}$ values (Appendix 7.1) to determine the accuracy of the parameters for prediction of *in vivo* clearance. GMFE and RMSE, described in 3.3.6, were used to assess bias and precision.

4.4. Results

4.4.1. Adaptation of methodology

Methodology was first adapted from that described by Jigorel et al[88] to allow the assay to be performed in 96-well plates. Hepatocyte density and volume, drug volume and shaking speed remained identical. A minor change was made to the sampling volume (75 µL rather than 80 µL) in order to maintain a sample to methanol ratio of 1:3 (as described by Soars et al[1]). The only major change made to both protocols was the centrifugation speed and time, which were halved from 3000g for 30s to 1500g for 15 seconds. This was due to the limitations of the plate centrifuge, and were selected to minimise the delay from the desired time point to sample quenching, while maintaining sufficient separation of cells from the media.

4.4.2. Depletion profiles of the media loss and conventional depletion assay

The diversity of drugs selected in this study resulted in a range of drug depletion profiles in both the media loss and conventional assays. All conventional assay profiles were observed to be monophasic, while those from the media loss assay were predominantly biphasic (Figure 11). Indinavir, midazolam and tolbutamide were the only exceptions, indicating the importance of metabolism (e.g. rate of uptake is equal to or less than that of metabolism). CL_{int} ranges were similar between assay formats at 0.85 – 231 µL/min/mg protein in the media loss assay and 1.5 – 239 µL/min/mg protein in the conventional assay. However, the mean ratio of CL_{int} between the media loss and conventional assay (ML:C) for each compound was 2.81, indicating that clearance is typically greater in the media loss assay. In particular, groups 1 and 2 tended to produce greater CL_{int} values in the media loss assay, with mean ML:C determined to be 5.4 and 1.94, respectively. For groups 3 and 4, a similar CL_{int} value was obtained in both assay formats (ML:C of 0.5 and 1.3, respectively), likely due to metabolism being the predominant route of depletion in both assay formats. Data are summarised in Table 16.

Table 16 – Drug CL_{int} values determined in the media loss and conventional depletion assay. ML:C is the ratio of CL_{int} in the media loss to that in the conventional depletion assay. Data represents mean ± SD (n=3).

Group	Drug	CL_{int} (µL/min/mg)		
		Media Loss	Conventional	ML:C
1	Cerivastatin	47.1 ± 13.9	4.9 ± 2.7	9.7
	Pitavastatin	32.5 ± 1.3	6.3 ± 1.1	5.2
	Rosuvastatin	6.5 ± 5.2	2.2 ± 0.5	2.9
	Valsartan	5.8 ± 3.2	1.5 ± 0.7	3.8
2	Atorvastatin	120 ± 18.9	42.6 ± 7.9	2.8
	Clarithromycin	16.2 ± 3.4	9.1 ± 0.3	1.8
	Indinavir	80.4 ± 17.5	57.4 ± 13.5	1.4
	Repaglinide	44.2 ± 11.3	24.8 ± 8.4	1.8
3	Tolbutamide	0.85 ± 0.39	1.83 ± 0.40	0.5
4	Erythromycin	16.2 ± 6.7	11.4 ± 2.2	1.4
	Midazolam	231 ± 67	239 ± 14	1
	Saquinavir	112 ± 28	73.8 ± 17.9	1.52

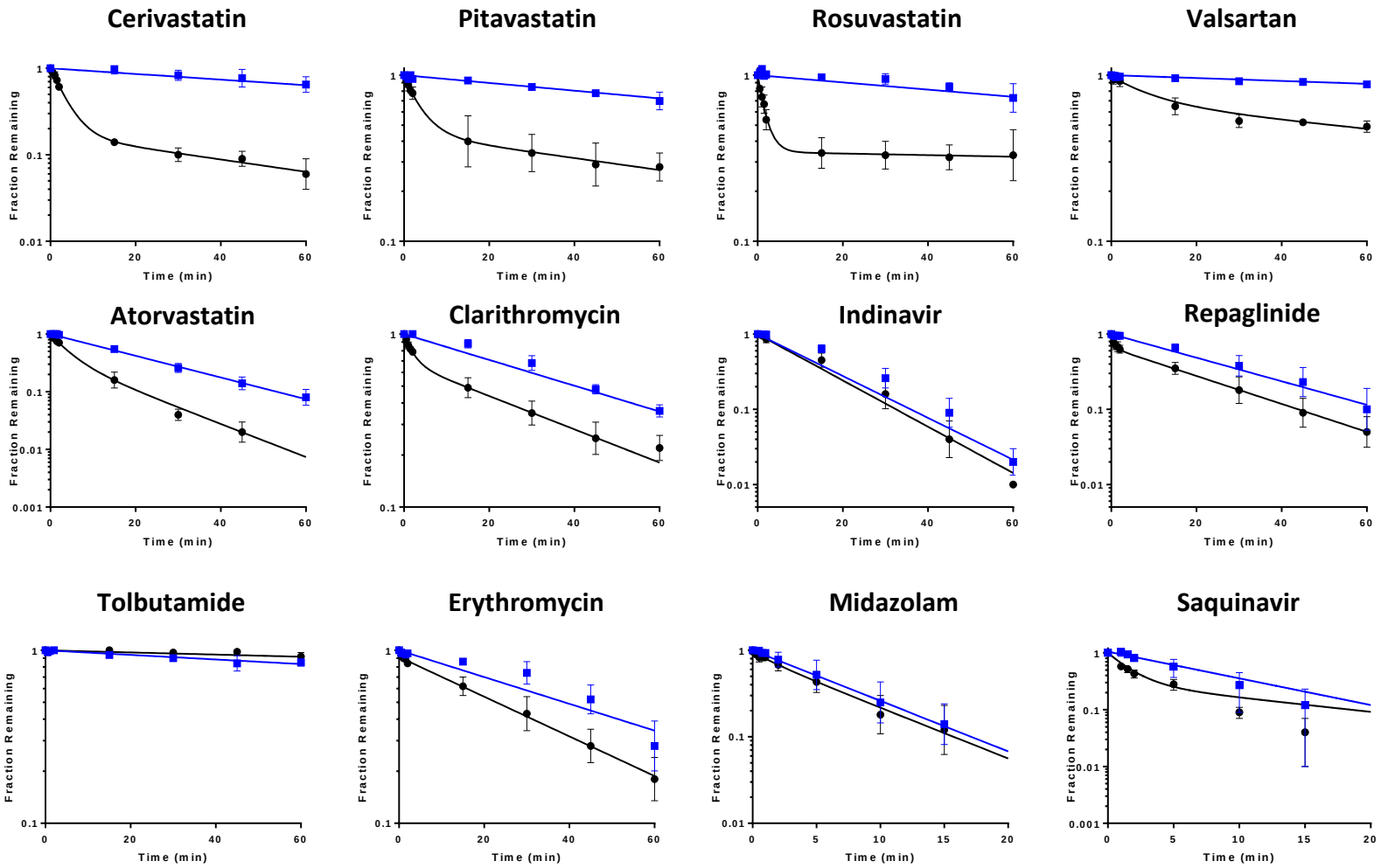

Figure 11 – Substrate depletion-time profiles in rat hepatocytes at 1 µM, with data fitted using Equation 9 or Equation 10. Data were generated using the media loss assay (black symbols) or the conventional depletion assay (blue symbols). Data represents mean ± SD (n=3).

4.4.3. Effects of metabolic and transport inhibitors on depletion profiles

Inhibitors of both uptake and metabolism were investigated to determine the effect on depletion-time profiles and resulting CL_{int} for each of the drugs selected in this study. Representative profiles for each drug group are displayed in Figure 12 (see Appendix 7.9 and 7.10 for all profiles), with CL_{int} values and their change relative to control listed in Table 17 and Table 18 and presented in Figure 13 and Figure 14.

The inclusion of ABT had no effect on the initial uptake phase in the media loss assay, while reduced rate of terminal decay caused by metabolism was evident. Generally this led to reduced CL_{int} in both assay formats, however compounds with low metabolism saw minimal change. The effect of ABT was particularly evident in groups 2 and 4, where all compounds saw a significant reduction ($p < 0.05$) in CL_{int}, with an average CL_{int} reduction of 69 and 75% respectively in the media loss assay, and 82 and 87% respectively in the conventional assay. Of the group 1 compounds, a significant effect ($p < 0.05$) was only noted for pitavastatin in either assay format. For indinavir, the inclusion of ABT also led to a biphasic profile in the media loss assay that was not evident under control conditions. This illustrates the advantage of inhibitors in some cases to allow an estimate of specific clearance parameters (i.e. separating metabolism from uptake).

Inhibition of uptake with the inclusion of Rfc is evident from the concentration-time profiles of drugs relying on active transport, which saw little depletion over time in comparison to control conditions (see Appendix 7.9 and 7.10). On average, CL_{int} was reduced by 78% and 44% for group 1 and 2 compounds, respectively. In comparison, group 3 (tolbutamide) and 4 compounds were unaffected by the inclusion of Rfc (average reduction of 2% was noted for group 4, and an increase in CL_{int} was noted for tolbutamide). Combination of ABT and Rfc typically had a similar or slightly stronger inhibitory effect on the drug in question than the strongest single inhibitor, whether Rfc or ABT

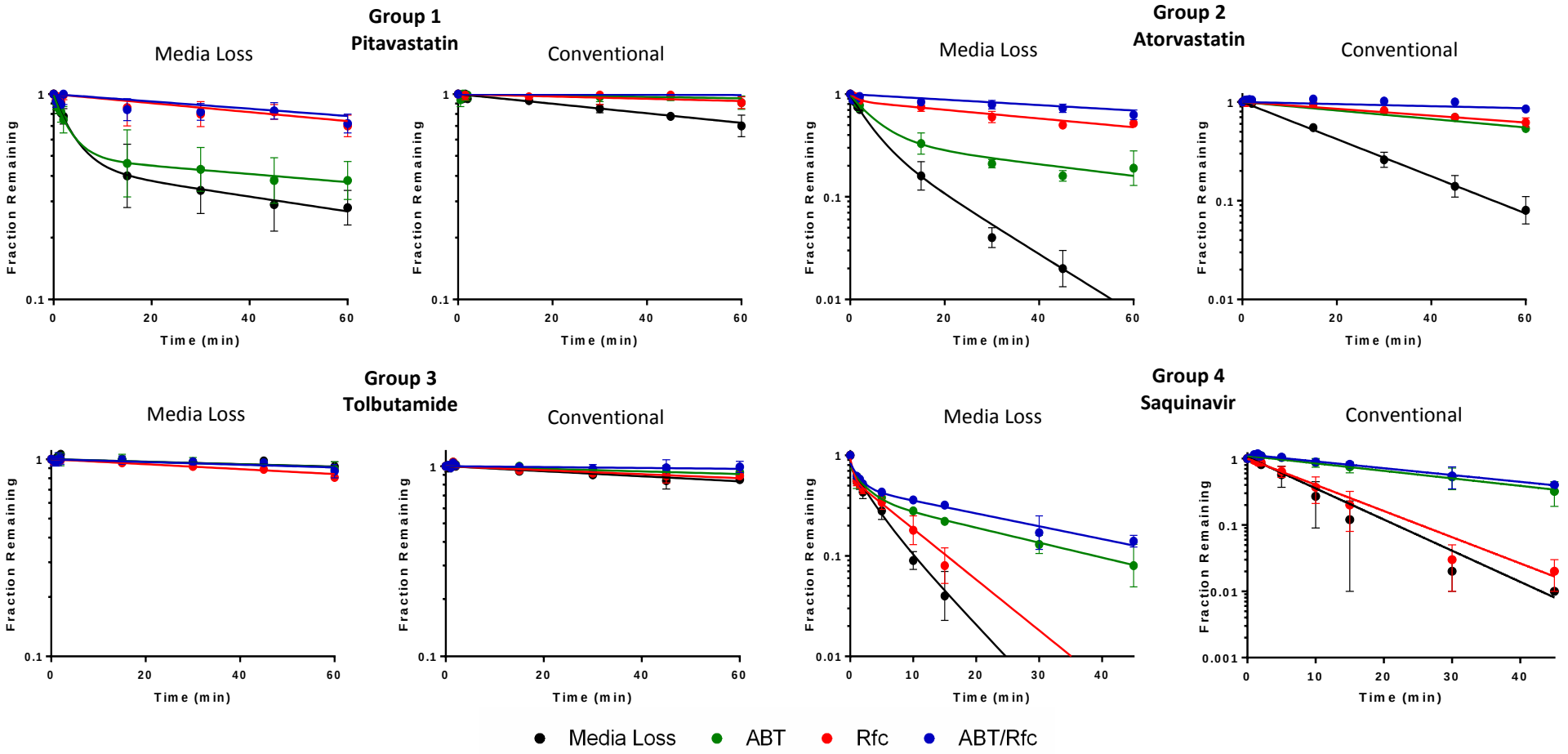

Figure 12 – Representative substrate depletion-time profiles in rat hepatocytes at 1 µM, with data fitted using Equation 9 or Equation **10**. Data were generated using the media loss assay or the conventional depletion assay. Data represents mean ± SD (n=3)

Table 17 - CL_{int} values and the percentage of control values, determined in the media loss assay in the presence of ABT and/or Rfc. Data represents mean ± SD (n=3).

Media Loss								
Group	Drug	CL_{int} (µL/min/mg protein)				% of control		
		Control	ABT	Rfc	ABT+Rfc	ABT	Rfc	ABT+Rfc
1	Cerivastatin	47.1 ± 13.9	30.7 ± 16.5	15.0 ± 2.2	9.7 ± 3.0	65	32*	21*
	Pitavastatin	32.5 ± 1.3	15.1 ± 9.0	2.1 ± 1.8	1.9 ± 1.6	46*	7*	6*
	Rosuvastatin	6.5 ± 5.2	6.5 ± 3.4	1.3 ± 0.9	1.3 ± 0.4	99	19	20
	Valsartan	5.8 ± 3.2	8.0 ± 2.6	1.7 ± 0.5	1.7 ± 1.0	137	29	29
2	Atorvastatin	120 ± 18.9	45.9 ± 7.0	7.1 ± 4.8	4.6 ± 1.0	38*	6*	4*
	Clarithromycin	16.2 ± 3.4	7.2 ± 2.4	17.8 ± 3.0	5.0 ± 3.4	45*	110	31*
	Indinavir	80.4 ± 17.5	12.2 ± 3.3	56.4 ± 22.1	10.9 ± 4.6	15*	70	14*
	Repaglinide	44.2 ± 11.3	11.8 ± 0.4	17.1 ± 6.8	7.6 ± 3.2	27*	39*	17*
3	Tolbutamide	0.85 ± 0.39	0.84 ± 0.52	1.61 ± 0.47	0.87 ± 0.48	99	189	102
4	Erythromycin	16.2 ± 6.7	5.1 ± 1.4	13.1 ± 4.4	3.9 ± 1.5	32*	81	24*
	Midazolam	231 ± 67	32.3 ± 6.5	288 ± 28	33.3 ± 12.2	14*	125	14*
	Saquinavir	112 ± 28	33.3 ± 13.3	97.1 ± 28.4	28.1 ± 9.3	30*	87	25*

* denotes a p value of < 0.05 using Scheffe's test following ANOVA

Table 18 - CL_{int} values and the percentage of control values, determined in the conventional depletion assay in the presence of ABT and/or Rfc. Data represents mean ± SD (n=3).

		Conventional						
Group	Drug	CL_{int} (µL/min/mg protein)				% of control		
		Control	ABT	Rfc	ABT+Rfc	ABT	Rfc	ABT+Rfc
1	Cerivastatin	4.9 ± 2.7	1.2 ± 1.2	5.7 ± 1.5	1.2 ± 1.3	25	118	26
	Pitavastatin	6.3 ± 1.1	0.9 ± 0.2	1.5 ± 0.7	0.4 ± 0.2	14*	25*	6*
	Rosuvastatin	2.2 ± 0.5	2.2 ± 0.4	0.8 ± 0.2	0.8 ± 0.6	97	36*	36*
	Valsartan	1.5 ± 0.7	1.9 ± 1.7	0.5 ± 0.7	0.09 ± 0.02	125	33	6
2	Atorvastatin	42.6 ± 7.9	9.8 ± 0.8	8.1 ± 2.1	2.3 ± 1.4	23*	19*	5*
	Clarithromycin	9.1 ± 0.3	0.5 ± 0.5	8.2 ± 1.5	0.3 ± 0.3	6*	90	4*
	Indinavir	57.4 ± 13.5	6.4 ± 1.4	38.6 ± 4.9	5.5 ± 1.3	11*	67	10*
	Repaglinide	24.8 ± 8.4	8.0 ± 2.6	13.5 ± 6.5	4.2 ± 1.7	32*	54	17*
3	Tolbutamide	1.83 ± 0.40	0.81 ± 0.44	1.46 ± 0.56	0.44 ± 0.35	44	80	24*
4	Erythromycin	11.4 ± 2.2	1.4 ± 0.6	7.1 ± 2.0	0.4 ± 0.3	12*	62*	4*
	Midazolam	239 ± 14	7.1 ± 2.9	246 ± 36	8.0 ± 3.4	3*	103	3*
	Saquinavir	73.8 ± 17.9	18.0 ± 3.5	53.2 ± 13.7	16.6 ± 3.1	24*	72	22*

* denotes a p value of < 0.05 using Scheffe's test following ANOVA

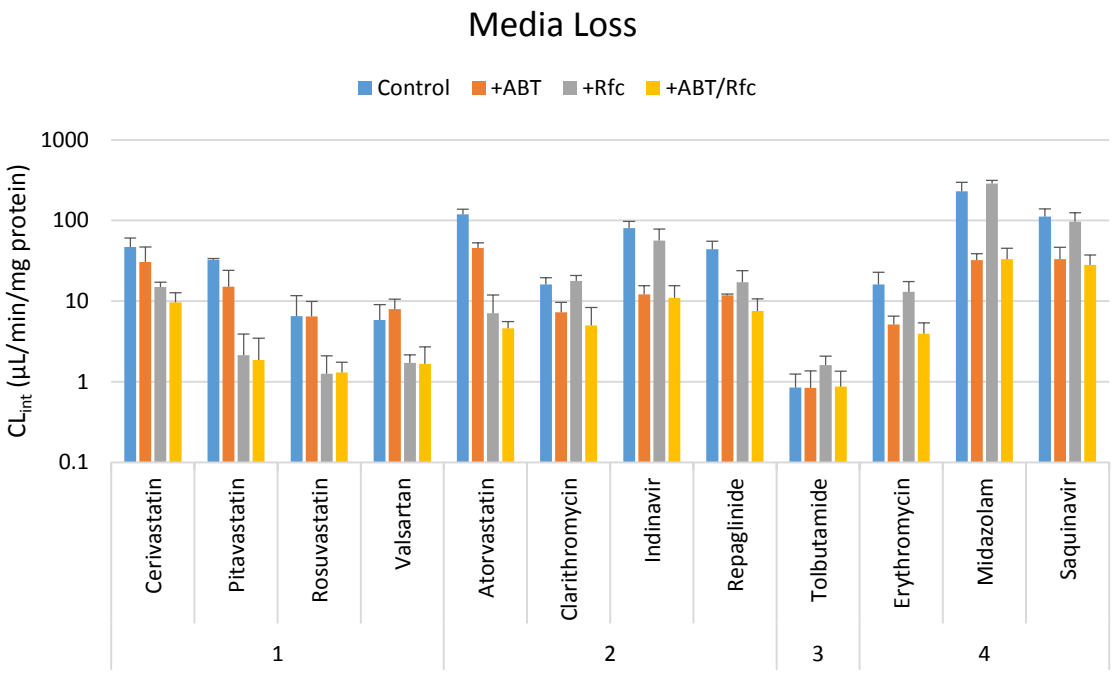

Figure 13 – CL_{int} values determined in the media loss assay under control conditions, and with the inclusion of ABT, Rfc or both ABT and Rfc for each drug selected in this study. Drugs are displayed in the groups described in 4.2. Data represents the mean ± SD (n=3).

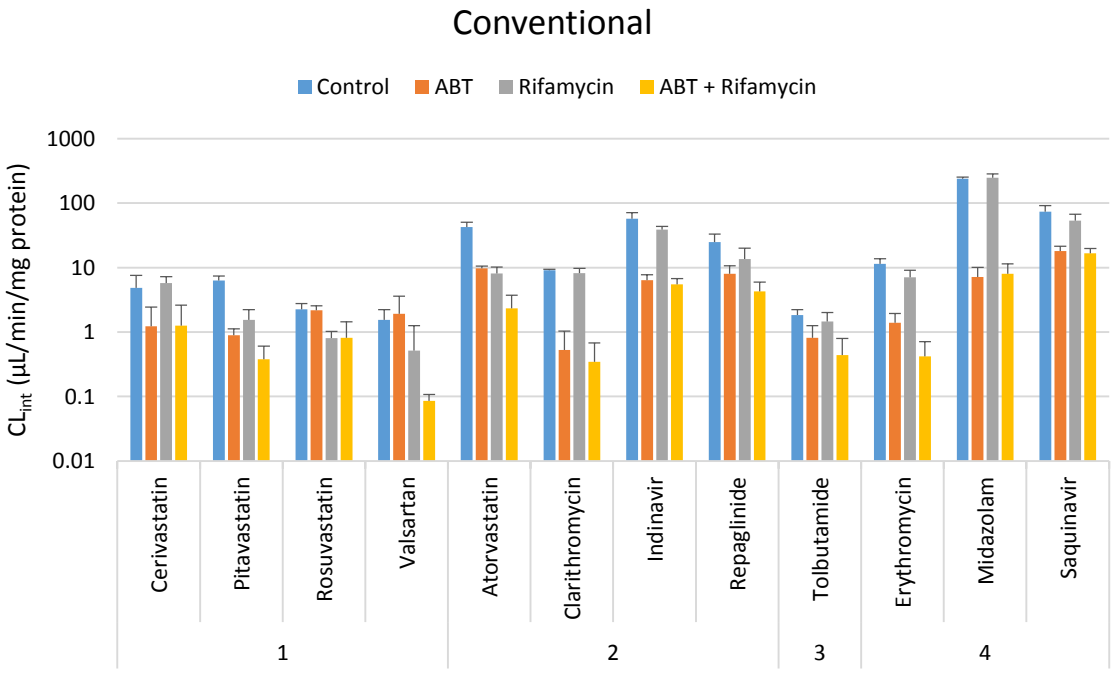

Figure 14 - CL_{int} values determined in the conventional assay under control conditions, and with the inclusion of ABT, Rfc or both ABT and Rfc for each drug selected in this study. Drugs are displayed in the groups described in 4.2. Data represents the mean ± SD (n=3).

4.4.4. Determination of clearance parameters using a two-compartment model

Data for drugs in each assay format were entered into a two-compartment model in order to obtain values for CL_{active}, $CL_{passive}$, CL_{met} and $V_{app,cell}$. The estimated values of these parameters are displayed in Table 19 and Table 20, while all profile fits can be found in Appendix 7.11 and 7.12. Modelled parameters of groups 1, 3 and 4 drugs generally matched the expected characteristics in terms of proportion of active transport and rate of metabolism (Figure 15). However, for group 2 drugs, only atorvastatin conformed to the expected profile, displaying high proportions of active transport along with a high rate of metabolism. For the remaining compounds, although rates of metabolism were in line with expected values, proportions of active transport were low (57 – 62%), indicating that Rfc had limited effect on the clearance of these compounds. A full comparison of grouping between data obtained in this study and previous literature data is illustrated in Figure 16.

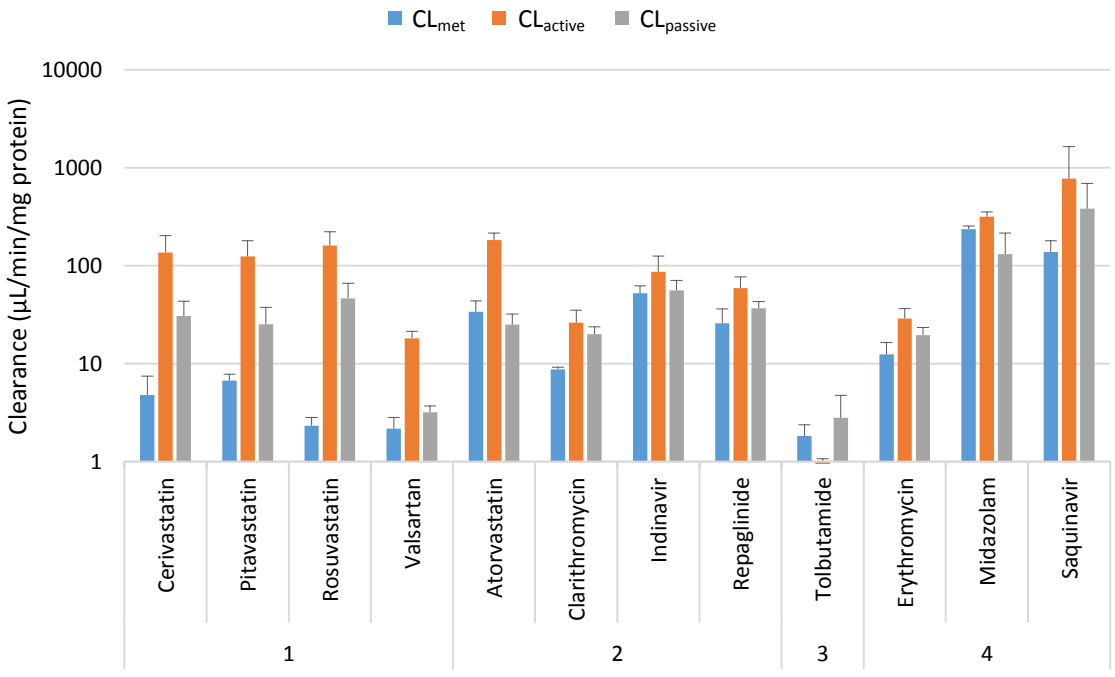

Figure 15 –CL_{met}, CL_{active} and $CL_{passive}$, estimated from data from the media loss and conventional depletion assay using a two-compartment model. Data represents the mean ± SD (n=3), with each experiment modelled independently.

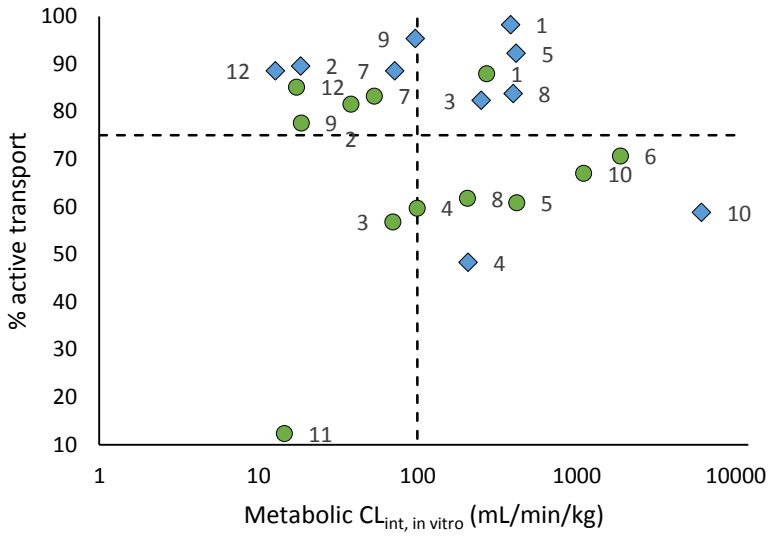

Figure 16 - Percentage Active Transport plotted against metabolic $CL_{int,\ in\ vitro}$ for the classification of drugs into groups 1-4 and comparison of data taken from rat hepatocyte literature data (listed in 7.2, blue symbols), or from data modelled in this study (green symbols). Metabolic clearance data were scaled using standard physiological scaling factors of 200 mg protein/g liver and 40 g liver/kg bodyweight. Labels are as follows: 1) Atorvastatin, 2) Cerivastatin, 3) Clarithromycin, 4) Erythromycin, 5) Indinavir, 6) Midazolam, 7) Pitavastatin, 8) Repaglinide, 9) Rosuvastatin, 10) Saquinavir, 11) Tolbutamide, 12) Valsartan.

Parameters Kp, Kp_u and fu_{cell} were estimated using Equation 17-Equation 19, with values listed in Table 20. $V_{cell,app}$, used to determine Kp, ranged between 1 – 386 µL, while Kp and Kp_u ranged between 3.8 – 254 and 2.3 – 8.3 (Figure 17, excluding tolbutamide which had a Kp and Kp_u of 1.1), respectively, and are indicative of the range of intracellular binding and active transport that occurs with the drugs selected in this study. These values were somewhat lower than has been reported previously by Yabe et al[96] for a similar set of compounds. However, the fu_{cell} of each drug, which ranged between 0.014 – 1 (Figure 18), are similar both in value and rank order[96]. No relationship was seen between either $CL_{passive}$, CL_{active} or Kp_u and the fu_{cell}, indicating binding to be independent of uptake characteristics (Figure 19).

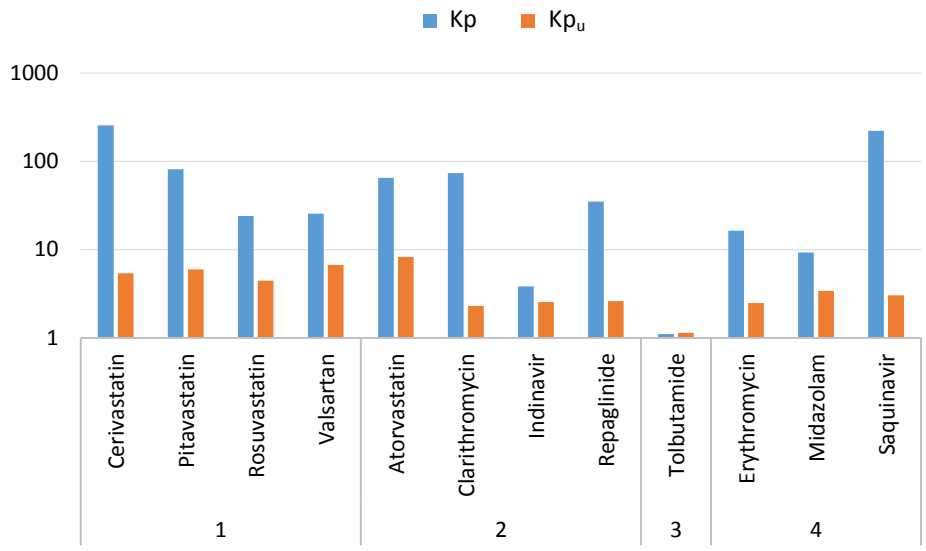

Figure 17 – Values for Kp and Kp_u estimated using data from the media loss and conventional depletion assay using a two-compartment model.

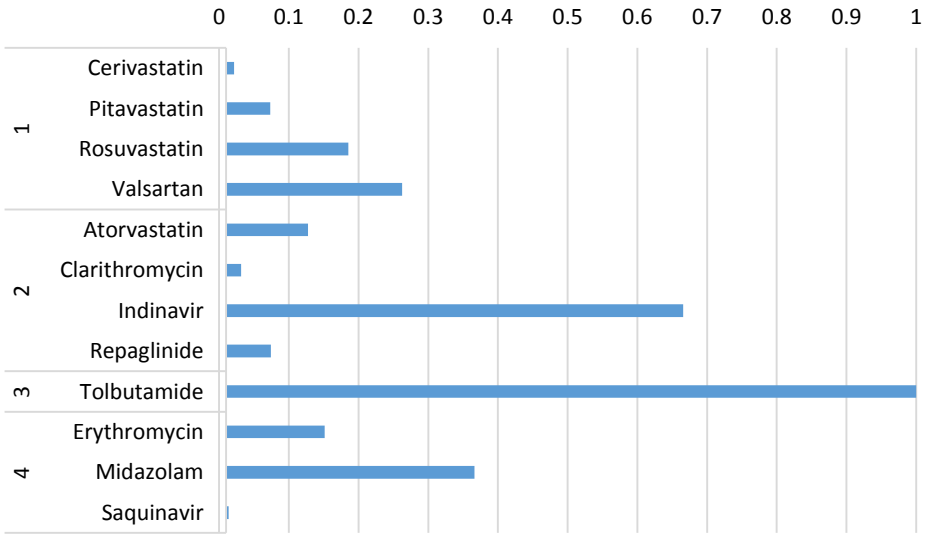

Figure 18 – Values for fu_{cell} estimated using both the Kp and Kp_u, calculated using data from the media loss and conventional depletion assay using a two-compartment model.

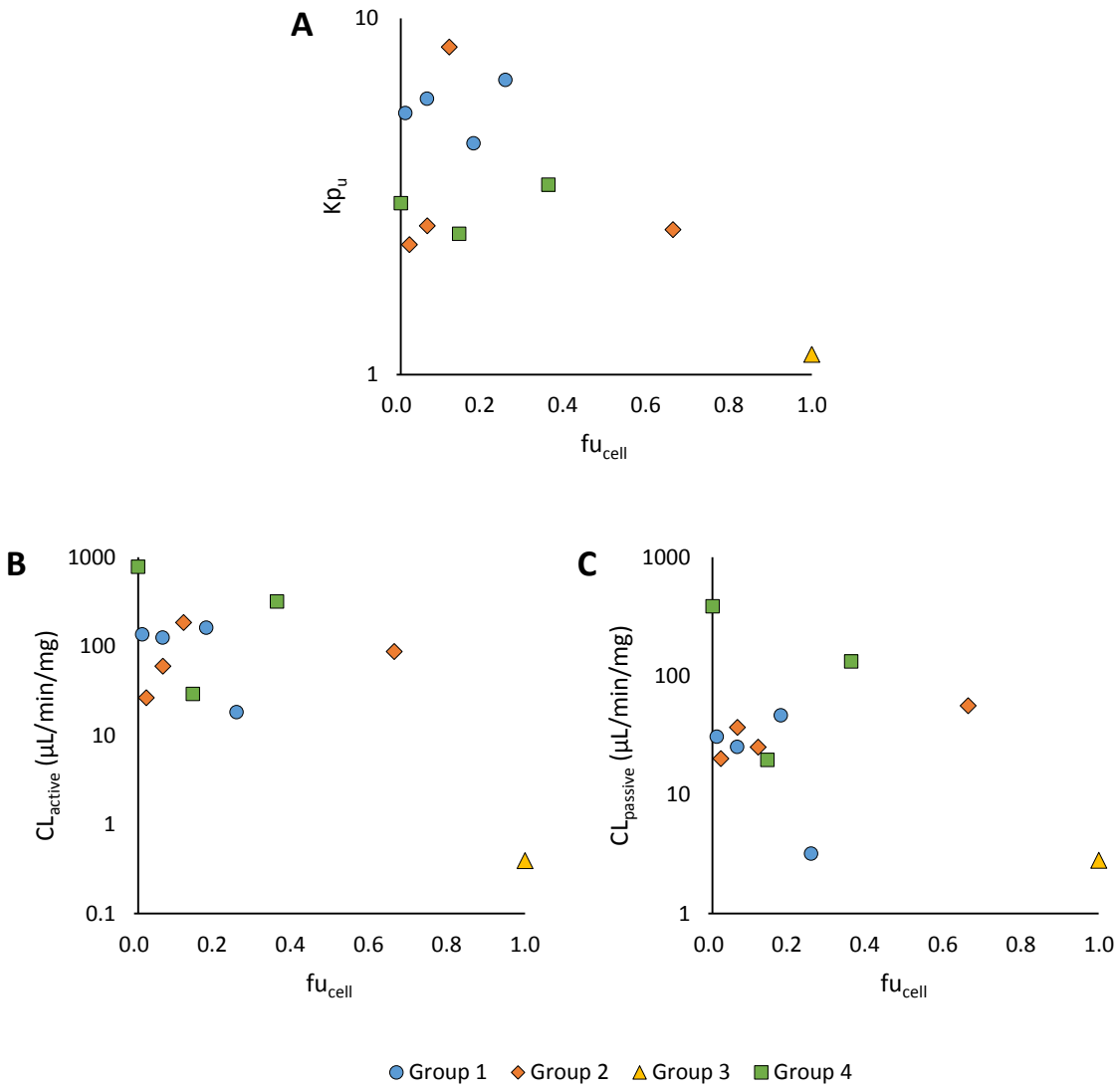

Figure 19 – Uptake, partitioning and binding characteristics calculated for 12 drugs using data from rat media loss and conventional depletion assays, entered into a two-compartment cell model. Relationship between fu_{cell} and Kp_u (A), *in vitro* CL_{active} (B), and *in vitro* $CL_{passive}$. Symbols represent group 1 (blue), 2 (orange), 3 (yellow) and 4 (green). No significant correlations were observed for these relationships.

Inspection of the data for correlations between parameters identified three key relationships; strong, significant relationships were observed between Log $CL_{passive}$ and $LogD_{7.4}$ ($r^2 = 0.69$; $p < 0.01$; Figure 20A), CL_{active} and $CL_{passive}$ ($r^2 = 0.73$; $p < 0.01$; Figure 20B), and CL_{met} and $LogD_{7.4}$ ($r^2 = 0.79$; $p < 0.01$; Figure 20C). These relationships would allow for an initial estimation of the metabolism, passive and active transport rates using only the $LogD_{7.4}$, which is often readily available.

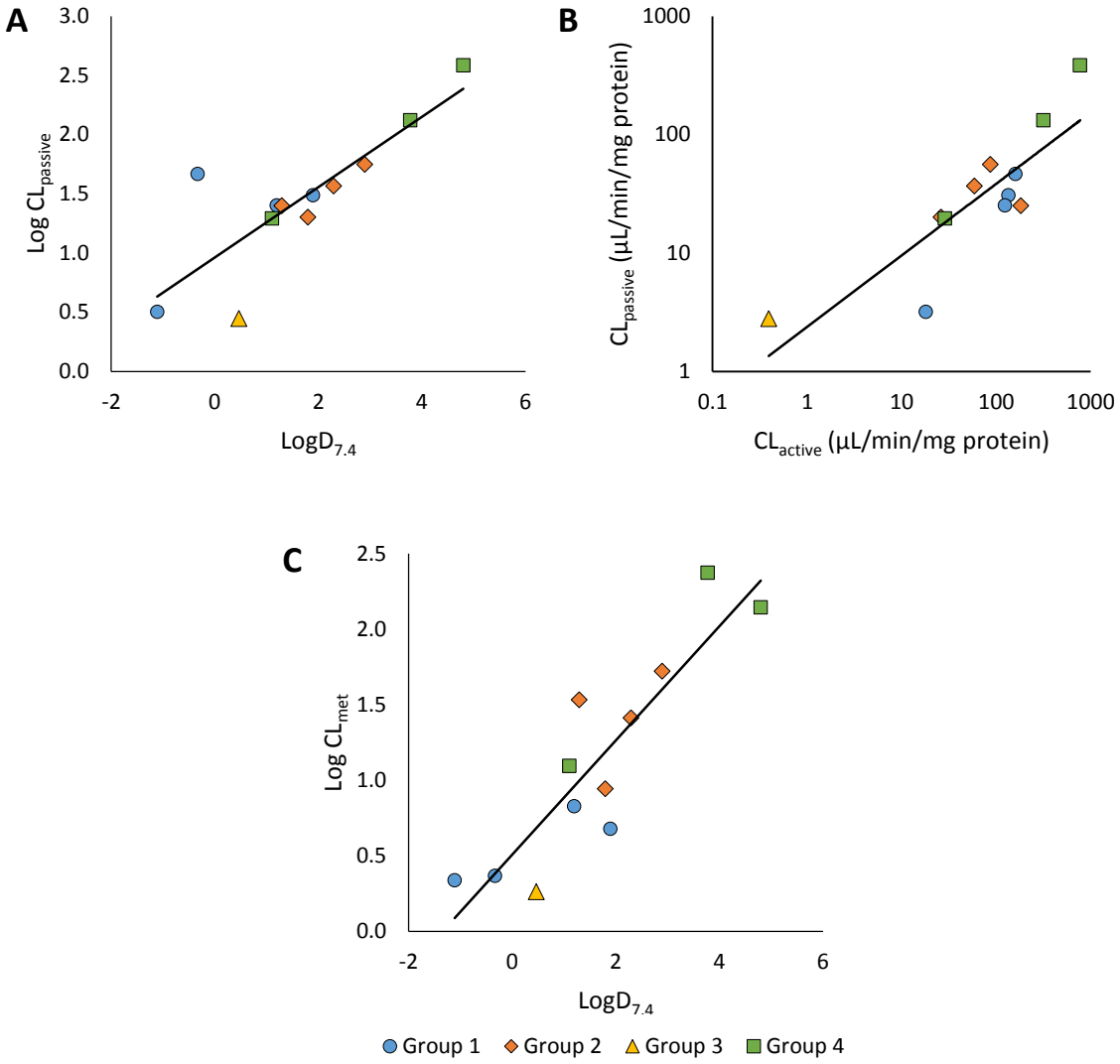

Figure 20 – Uptake and metabolism characteristics calculated for 12 drugs using data from rat media loss and conventional depletion assays, entered into a two-compartment cell model. Relationship between $LogD_{7.4}$ and Log $CL_{passive}$ (A), *in vitro* CL_{active} and $CL_{passive}$ (B), and $LogD_{7.4}$ and Log CL_{met} (C). The solid line in (B) represents the least squares regression of the power function line of best fit, described by $CL_{passive} = 2.382\ CL_{active}^{0.6033}$, while in (A) and (C) it is the linear line of best fit, described by Log $CL_{passive} = 0.297\ LogD_{7.4} + 0.962$ and Log $CL_{met} = 0.378\ LogD_{7.4} + 0.507$, respectively. Symbols represent group 1 (blue), 2 (orange), 3 (yellow) and 4 (green).

Table 19 – Summary of uptake and metabolism parameters calculated using a two-compartment model. Results are displayed as the mean ± SD (n=3).

Group	Drug	CL_{met}	CL_{uptake}	CL_{active}	$CL_{passive}$	% active transport	$LogD_{7.4}$
		µL/min/mg					
1	Cerivastatin	4.8 ± 2.7	167 ± 67.8	136 ± 66.6	30.8 ± 12.6	82	1.9[96]
	Pitavastatin	6.7 ± 1.1	150 ± 56.4	125 ± 55.0	25.2 ± 12.5	83	1.2[96]
	Rosuvastatin	2.3 ± 0.5	207 ± 64.3	161 ± 61.2	46.5 ± 19.8	78	-0.33[96]
	Valsartan	2.2 ± 0.6	21.3 ± 3.3	18.1 ± 3.3	3.2 ± 0.5	85	-1.11[96]
2	Atorvastatin	34.0 ± 9.7	208 ± 34.2	183 ± 33.5	25.1 ± 7.1	88	1.3[96]
	Clarithromycin	8.7 ± 0.5	46.3 ± 9.5	26.3 ± 8.7	20.0 ± 3.8	57	1.8[96]
	Indinavir	52.5 ± 9.7	143 ± 41.2	87.0 ± 38.6	56.1 ± 14.6	61	2.9[150]
	Repaglinide	25.8 ± 10.6	95.8 ± 19.0	59.2 ± 17.9	36.7 ± 6.3	62	2.3[96]
3	Tolbutamide	1.8 ± 0.5	3.2 ± 2.1	0.4 ± 0.7	2.8 ± 1.9	12	0.36[151]
4	Erythromycin	12.4 ± 4.0	48.4 ± 8.6	28.9 ± 7.6	19.5 ± 4.0	60	1.1[96]
	Midazolam	236 ± 18.0	448 ± 91.9	317 ± 36.5	131.6 ± 84.3	71	3.1[152]
	Saquinavir	139 ± 40.9	1160 ± 919	777 ± 866	383 ± 307	67	4.8[96]

Table 20 - Summary of distribution and binding parameters calculated using a two-compartment model. $V_{cell,app}$ results are displayed as the mean ± SD (n=3).

Group	Drug	$V_{cell,app}$	Kp	Kp_u	fu_{cell}
		µL			
1	Cerivastatin	386 ± 287	254	5.4	0.021
	Pitavastatin	60.9 ± 33.4	81.2	5.9	0.073
	Rosuvastatin	54.8 ± 15.2	24.1	4.5	0.185
	Valsartan	31.1 ± 6.9	25.6	6.7	0.263
2	Atorvastatin	1.0 ± 0.3	65.0	8.3	0.128
	Clarithromycin	130 ± 8.8	73.5	2.3	0.031
	Indinavir	3.6 ± 5.5	3.8	2.6	0.666
	Repaglinide	52.1 ± 31.5	35.1	2.6	0.074
3	Tolbutamide	2.1 ± 2.7	1.1	1.1	1.0
4	Erythromycin	24.8 ± 20.8	16.4	2.5	0.151
	Midazolam	5.8 ± 3.6	9.3	3.4	0.366
	Saquinavir	256 ± 188	221	3.0	0.014

4.4.5. IVIVE

To assess uptake and metabolism as a predictor of *in vivo* clearance, a direct cellular scaling approach was used. CL_{int} calculated from the media loss assay ($CL_{int,ML}$, see Table 16), metabolism and uptake data (from data modelling in 4.4.4) were scaled to the level of the whole body using standard physiological scaling factors (Table 21). Clearance ranged between 6 – 1,851, 15 – 1,887 and 26 – 3,587 mL/min/kg for $CL_{int,ML}$, metabolism and uptake, respectively. Although the range would suggest that all three parameters were similar, the average values of 475, 351 and 1,199 mL/min/kg for $CL_{int,ML}$, CL_{met} and CL_{uptake}, respectively, indicates that uptake is generally greater than metabolism, reflected in a higher $CL_{int,ML}$ value compared to CL_{met} alone. Due to the high variability associated with CL_{uptake} for saquinavir, it was omitted from analysis of the range and average values, but not calculation of GMFE and RMSE.

In terms of *in vivo* clearance predictions, CL_{uptake} was seen to have least overall bias and precision according to the GMFE and RMSE values. However, it is evident that the success of each parameter is dependent on the drug group (Figure 21). For example, while 3 out of 4 drugs from group 1 produced accurate predictions of *in vivo* clearance (i.e. within 2-fold)

Table 21 – IVIVE of $CL_{int, ML}$, CL_{met} and CL_{uptake} parameters and assessment of accuracy and precision of parameters when predicting *in vivo* clearance. Data were scaled using standard physiological scaling factors of 200mg protein/g liver and 40 g liver/kg bodyweight. See 7.1 for source(s) of *in vivo* values.

Group	Drug	$CL_{int, ML}$	CL_{met}	CL_{uptake}	$CL_{int, in\ vivo}$	Predicted/Observed		
		mL/min/kg				$CL_{int, ML}$	CL_{met}	CL_{uptake}
1	Cerivastatin	377 ± 111	38 ± 22	1333 ± 542	1517	0.25	0.03	0.88
	Pitavastatin	260 ± 10	54 ± 8.7	1201 ± 451	1165	0.22	0.05	1.03
	Rosuvastatin	52 ± 42	19 ± 4.0	1658 ± 514	1412	0.04	0.01	1.17
	Valsartan	47 ± 26	17 ± 5.1	171 ± 26	1554	0.03	0.01	0.11
2	Atorvastatin	960 ± 151	272 ± 77	1664 ± 274	1593	0.60	0.17	1.04
	Clarithromycin	129 ± 28	70 ± 3.7	371 ± 76	121	1.07	0.58	3.07
	Indinavir	643 ± 140	420 ± 78	1145 ± 330	50	12.9	8.41	22.94
	Repaglinide	353 ± 90	206 ± 85	767 ± 152	496	0.71	0.42	1.55
3	Tolbutamide	6.8 ± 3.1	15 ± 4.4	26 ± 17	7.4	0.92	1.96	3.44
4	Erythromycin	129 ± 54	100 ± 32	387 ± 69	115.5	1.12	0.87	3.35
	Midazolam	1851 ± 536	1887 ± 144	3587 ± 735	1331	1.39	1.42	2.69
	Saquinavir	895 ± 221	1110 ± 327	9282 ± 7351	911	0.98	1.22	10.19
	Mean	475	351	1199*	**GMFE**	3.13	6.40	2.96
					RMSE	779	915	2560

* Excludes saquinavir

using the CL_{uptake}, CL_{met} and $CL_{int,ML}$ values were between 4-100 fold lower than the observed $CL_{int,\ in\ vivo}$. Conversely, all group 4 compounds were over-predicted using the CL_{uptake}, while CL_{met} and $CL_{int,\ ML}$ produced accurate predictions. This highlights the difficulty in the application of a generic cellular IVIVE approach if the properties of the compound are not considered. Of the three terms, $CL_{int,ML}$ produced the most predictions within 2-fold of the observed *in vivo* clearance (58% compared to 42% for both CL_{uptake} and CL_{met}).

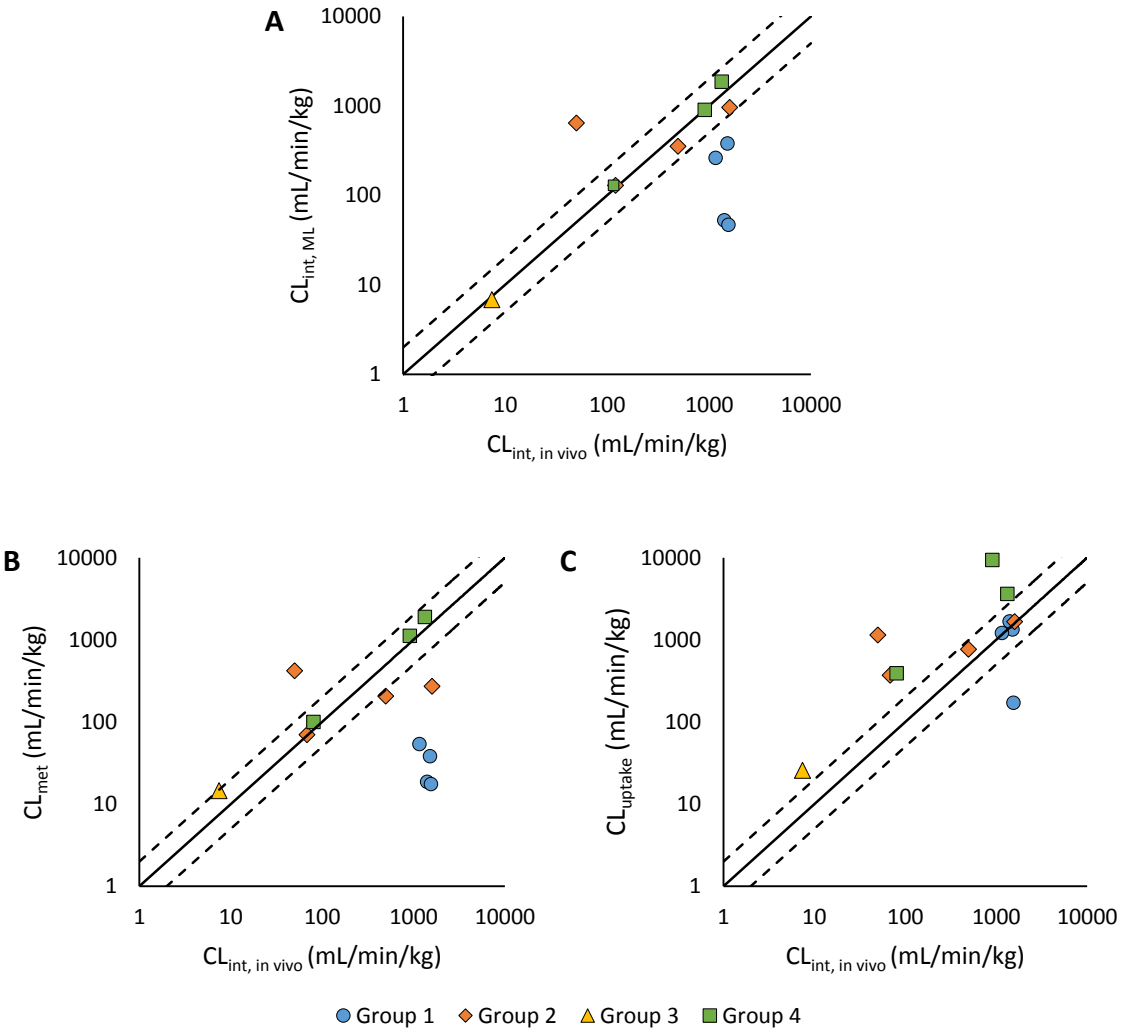

Figure 21 - Observed $CL_{int,\ in\ vivo}$ plotted against $CL_{int,ML}$ (A), CL_{met} (B) and CL_{uptake}(C) scaled using standard physiological scaling factors. Line of unity (solid line), and 2-fold under and over-prediction (dashed line) are displayed. Symbols represent group 1 (blue), 2 (orange), 3 (yellow) and 4 (green), determined from the results of this study (see Figure 16).

4.5. Discussion

Hepatocellular drug uptake assays have now been in use for approximately 20 years, however their labour intensive and low throughput nature has remained an issue preventing their routine and widespread use at early stages of drug development. This chapter aimed to adapt the methodology of the media loss assay to increase throughput and make the assay more informative through the use of inhibitors. It was hypothesised that this approach would allow data modelling to estimate values for individual clearance processes, such as active uptake, passive diffusion and metabolism.

4.5.1. Adaptation of Methodology

While conventional hepatocyte drug depletion assays are routinely performed in multi-well plates, the media loss assay had only previously been performed in individual Eppendorf tubes. This method is not only more demanding in terms of the required reagents (hepatocytes, quantity of drugs etc.), but also limits the feasibility of investigating multiple experimental conditions (for example variations in drug concentration, temperature and inclusion of inhibitors). Since the method as a whole requires two simultaneous assays (the conventional depletion along with the media loss), careful planning is required to avoid clashes in sample times. This necessitates the assays being run successively, rather than simultaneously, if multiple conditions are desired. Time constraints associated with the loss of hepatocyte viability over time therefore limits the number of assays that can be performed. This issue was bypassed through the transition into a 96-well plate format, allowing up to four conditions to be run, in duplicate, simultaneously in both the conventional and media loss format. For the current study this was utilised to investigate various inhibitor conditions, however many more applications are possible.

4.5.2. Depletion profiles of the media loss and conventional depletion assay

Drugs were selected in this study to represent a range of metabolic rates and contributions of active transport, and were divided into four groups based on these properties as determined from previous *in vitro* data. Comparison of profiles obtained from the conventional and media loss assay served to highlight the clear differences

between assays. While all conventional depletion assays were monophasic, the majority of media loss profiles were biphasic, indicating that uptake occurred at a different rate than that of the subsequent metabolism. Indinavir, midazolam and tolbutamide were exceptions, with each displaying monophasic profiles in the media loss assay. This was expected for both midazolam and tolbutamide, which had been selected as low and high clearance controls to confirm that biphasic profiles were not always evident in the media loss assay. However, it was not expected for indinavir, which had been shown previously to be transported predominantly by an active process[153]. In general, compounds from groups 1 and 2 were found to have a markedly higher rate of CL_{int} in the media loss, compared to the conventional depletion, highlighting the importance of uptake to their clearance. CL_{int} for groups 3 and 4 were comparable across formats, indicating metabolism to be the key determinant of clearance rate.

4.5.3. Effects of metabolic and transport inhibitors on depletion profiles

The inclusion of inhibitors was intended to allow the estimation of individual clearance processes. ABT, a broad spectrum CYP inhibitor, was used in an attempt to prevent the majority of phase I metabolism[148], leaving the total rate of uptake as the key determinant of depletion rate. In both assay formats ABT reduced depletion rate, indicating that it successfully inhibited a large degree of metabolism. However, this only affected the terminal phase in the media loss assay, leaving the initial uptake phase unhindered. This method would be suitable as a standalone assay if a measure of total uptake alone was desired through the initial depletion phase. Rfc, a potent OATP inhibitor, was used to prevent active transport of drugs into the hepatocytes. The concentration used in this study has been shown previously to extensively inhibit rat Oatp1 and Oatp2, as well as Ntcp[149]. For the highly transported group 1 compounds, Rfc greatly reduced the uptake phase in the media loss assay. For group 2 compounds, for which a similar effect was expected, only atorvastatin appeared to be highly affected. It is unclear why this may be the case, as previous data would suggest that these are subjected to active transport[96, 97, 153]. It is possible that activity of other families of transporters that are not inhibited by Rfc may enable continued uptake of these particular drugs. Group 3 and 4 compounds were unaffected by the inclusion of Rfc, with no significant difference noted compared to control, as they are expected to enter the cell via passive diffusion. The effect of Rfc was also evident in the conventional depletion

assay, which saw reduced clearance for transported compounds. This is a secondary effect, since drug is prevented from entering the cells, thereby limiting the amount of subsequent metabolism that could take place.

The use of both inhibitors together was intended to leave passive diffusion as the only clearance process. This led to an increase in inhibition compared to use of inhibitors individually. However, it was noted that a degree of depletion was still evident for some compounds in the conventional assay. Since this method can only measure the permanent loss of parent compound due to metabolism, any uptake and intracellular binding events cannot account for the continued depletion in the presence of ABT. Equally, non-specific binding to the plate was measured for each compound, and in all cases found to be negligible and linear over time. The observed depletion, therefore, must be caused by metabolism that is not inhibited by ABT. It is possible that this could include other phase I enzymes, as well as phase II metabolism.

4.5.4. Determination of clearance parameters using a two-compartment model

The two-compartment model used in this study followed a stepwise approach. First, data from the conventional depletion assay was modelled to give estimates of metabolic clearance and the interaction of inhibitors. This was then entered into a two-compartment model, which allowed the estimation of active transport, passive diffusion and an apparent volume of distribution using data from the media loss assay. This method was selected as it was found to reduce the degree of uncertainty for parameters, compared to simultaneously modelling all data from both assay formats.

Data typically followed the expected characteristics for each group, in terms of the proportions of active transport and metabolism, with the exception of the group 2 compounds indinavir, repaglinide and clarithromycin. The lack of effect caused by Rfc led to the percentage of active transport being much lower than the >80% that had been reported previously for each drug[96, 153]. There was also an issue noted for saquinavir, where modelled simulations poorly fitted the observed profile from the media loss assay. It is possible that extensive binding may lead to a higher than expected loss of drug from the media. However, the same issue was not experienced for other high binding drugs used in this study.

Inspection of the data revealed three key relationships which could have further applications. A strong correlation existed between the $LogD_{7.4}$ and the log of the estimated $CL_{passive}$ and CL_{met}. This relationship has been noted previously by Yabe et al[96] for $CL_{passive}$, and may serve as a useful tool for providing initial estimates of both passive diffusion metabolic clearance for novel compounds, should the $LogD_{7.4}$ be known. A second significant relationship was found in this study between CL_{active} and $CL_{passive}$, which had also been investigated by Yabe et al[96] who, although noting a positive correlation, found it did not reach statistical significance. The relationships noted in this study would allow an initial estimation of the metabolic, active transport and passive diffusion clearance rates using only the $LogD_{7.4}$. This could prove useful in assay design and data modelling for novel compounds for which little information is known.

Using the uptake terms (CL_{active} and $CL_{passive}$), along with the $V_{cell,\ app}$ estimated in the model, it was possible to indirectly determine the ratios of total and unbound drug in hepatocytes to that in the medium (Kp and Kp_u, respectively) and therefore the extent of intracellular binding (fu_{cell}). Kp values varied by > 200-fold between tolbutamide and cerivastatin (Kp = 1.1 and 254, respectively), and reflects the difference in both active transport and intracellular binding that occurs for each drug. Kp_u, which reflects the degree of active transport, had much less variation, with a >7-fold range between tolbutamide and atorvastatin (Kp_u = 1.1 and 8.3, respectively). The difference between these two parameters is accounted for by the extent of intracellular binding, defined by fu_{cell}. Compounds extensively bound in hepatocytes included cerivastatin, clarithromycin and saquinavir, while low binding was measured for indinavir and tolbutamide. Values and rank order were in good agreement with that published previously[96, 97]. These terms are essential to understand the specific intracellular processes that govern the clearance characteristics of each drug.

4.5.5. IVIVE

As a continuation of Chapter 3, a cellular scaling approach was adopted to determine the utility of $CL_{int,ML}$, CL_{uptake} and CL_{met} as predictors of *in vivo* clearance. Each term was scaled using standard physiological scaling factors, and assessed for bias and precision by GMFE

and RMSE, respectively. Overall, CL_{uptake} had the lowest bias compared to $CL_{int,ML}$ and CL_{met} (GMFE = 2.96, 3.13 and 6.40, respectively), however it was evident that the accuracy of each term was linked to drug grouping. Group 1 and 2 compounds produced more accurate *in vivo* predictions when using CL_{uptake}, since this appeared to be the predominant clearance process, while groups 3 and 4 benefitted from the use of $CL_{int,ML}$ and CL_{met}. As was noted for the media loss assay in Chapter 3, over-prediction remains a common issue, with CL_{uptake} over-predicting *in vivo* clearance for 50% of the drugs in this study. However, a lower GMFE value was noted compared to $CL_{int,ML}$, indicating an overall improvement following data modelling. While an improvement, the proportion of successful predictions using only a single clearance parameter remains low, and may suggest a more mechanistic approach is required to improve clearance predictions. It must also be considered that the $CL_{int,ML}$ term, while producing slightly greater bias than modelled uptake data, can be estimated using only the media loss assay (without the requirement for a simultaneous conventional assay). This method may therefore be more suitable if a quantitative prediction of $CL_{int,in\ vivo}$ is the sole reason for performing the assay, since fewer reagents and analysis is required, but has the disadvantage of not being able to produce uptake, binding or partitioning information.

4.6. Conclusion

In conclusion, this chapter adapted the media loss assay into a higher throughput format, allowing the inclusion of several inhibitor conditions in order to split the observed intrinsic clearance into individual clearance parameters. Using a two-compartment model, it was possible to directly estimate the rates of active transport, passive diffusion and metabolism, as well as the apparent volume of distribution of the cell. This allowed the indirect estimation of Kp, Kp_u and the fraction of unbound drug in the cell. Together, these provide a detailed account of the parameters governing drug clearance. To continue from the cellular IVIVE approach explored in Chapter 3, metabolism and uptake data were assessed as a predictor of *in vivo* clearance. It was found that the accuracy of each clearance term was strongly linked to the drug grouping, and supports the use of a more mechanistic approach for generation of *in vivo* clearance predictions.

Chapter 5. Use of SCH to assess the validity of integrating multiple system parameters within a single clearance term

5.1. Introduction

For the prediction of *in vivo* clearance, focusing on a single elimination pathway (i.e. uptake or metabolism) has been the most common method within the literature. Indeed, both Chapter 3 and Chapter 4 have primarily focused on the use of individual clearance parameters as predictors of *in vivo* clearance. However, it is becoming increasingly apparent that no single clearance parameter is suitable for the prediction of all compounds. As a result, mechanistic methodologies have been investigated with the purpose of improving predictive accuracy through inclusion of multiple parameters and consideration of their interactions. Approaches within the literature have varied in degree of complexity, from models designed to replicate the body, incorporating the movement of a drug between physiological compartments[91], to the combination of multiple clearance parameters, obtained through different *in vitro* systems, within a single equation clearance term.

An example of this is the so called extended clearance model, which is based on the solved equations of a simple recirculating liver perfusion model[127, 154]. In the *in vitro* setting, where liver blood flow and plasma binding are not considered, this term has been referred to as the total intrinsic clearance ($CL_{int,total}$) as described in Equation 3[127-130].

$$CL_{int,total} = CL_{uptake} \cdot \frac{CL_{met} + CL_{bile}}{CL_{met} + CL_{bile} + CL_{sinusoidal}} \qquad \textbf{Equation 3}$$

$CL_{int,\ total}$ is the basis for the $CL_{int,app}$ term discussed previously (3.3.5), however here CL_{uptake} is assigned as the rate-determining process and efflux clearances are also required, rather than being assumed to be negligible. It should be noted that as with CL_{uptake}, CL_{bile} and $CL_{sinusoidal}$ represent the sum of both active and passive processes. While uptake and metabolism terms required for $CL_{int,total}$ can be obtained from a number of assay formats, the efflux terms CL_{bile} and $CL_{sinusoidal}$ necessitate the use of SCH, widely regarded as the *in vitro* assay of choice due to the repolarisation of cells and correct

localisation of efflux transporters[112]. However, as demonstrated in Chapter 3, uptake rates in SCH are typically much lower than other *in vitro* uptake assays. As a result, low intracellular concentrations have been suggested as the cause of the 10 to 260-fold under-prediction of CL_{bile} that is typically observed in SCH[112]. It is therefore important to assess uptake in SCH and, if required, consider appropriate empirical scaling factors in order to ensure clearance terms within $CL_{int,total}$ are comparable across assay systems. Much less is known regarding $CL_{sinusoidal}$, and is typically disregarded when calculating clearance parameters. However, along with passive rates expected for all compounds, there is now evidence that efflux transporters present in the sinusoidal membrane (for example MRP3 and 4) may contribute to an active component, and therefore warrants further investigation[155-157].

The primary restriction for the use of extended clearance terms remains the large amounts of data that are necessary for the methodology to work. The increased complexity often requires a much greater investment of both time and resources. For example, the novel IVIVE methodology presented by Umehara and Camenisch[129] required three separate *in vitro* methods to be conducted in order to generate an appropriate amount of data. While *in vitro* to *in vivo* correlations were improved, it is unclear whether the improvement was substantial enough to warrant the additional data generation required. It is therefore imperative that these types of experimental approaches are as efficient as possible.

5.2. Aims

The overall aim of this chapter was to transition from cellular IVIVE, demonstrated previously, to a more mechanistic IVIVE approach, incorporating several clearance parameters and methods discussed throughout this thesis.

In order to implement this approach, SCH assays will be performed to measure total efflux rates from both the sinusoidal and canalicular membranes of hepatocytes. In addition, uptake rates will be measured, as these govern the intracellular concentrations which drive efflux processes and must be comparable to data provided from other hepatocyte systems. An assessment will be made to determine if additional empirical scaling is required before use within the extended clearance terms with regards to efflux

parameters. An alternative method of calculating Kp_u to that used in Chapter 4 will also be investigated using influx and efflux data, and comparisons will be made to data from previous chapters.

Along with uptake and metabolism data gathered in Chapter 4, data will be used to calculate $CL_{int,total}$ to estimate the overall clearance from hepatocytes. Using standard physiological scaling methods as well as empirical scaling methods discussed in Chapter 3, the predictive ability of these terms will be compared to using single pathway clearance terms (uptake and metabolism). It is hypothesised that clearance terms implementing multiple clearance parameters will improve accuracy of predictions. However an assessment must be made as to whether the improvement warrants the additional experimentation required.

5.3. Methods

5.3.1. Chemicals

Atorvastatin, indinavir, pitavastatin calcium, rosuvastatin and valsartan were purchased from Sequoia Research Products (Pangbourne, UK). Saquinavir and midazolam were purchased from Roche Products Ltd (Welwyn Garden City, UK). Clarithromycin, dexamethasone, erythromycin, tolbutamide, insulin, L-glutamine and Bradford reagent were purchased from Sigma-Aldrich (Dorset, UK). Cerivastatin and repaglinide were purchased from Carbosynth Limited (Berkshire, UK). Matrigel was purchased from Corning (Wiesbaden, Germany). All other reagents were obtained from Life Technologies (Paisley, UK).

5.3.2. Hepatocyte Isolation and Preparation

Rat hepatocytes were isolated from the livers of male Sprague-Dawley rats weighing between 250 – 300g (Charles River, Margate, Kent, UK). Rats were sacrificed using CO_2 overdose followed by cervical dislocation. Hepatocytes were prepared using an adaptation of the two-step collagenase perfusion method, as described previously[86]. After isolation, hepatocytes were suspended in phenol red free WME, pH 7.4. Cell count and viability were determined using the trypan blue exclusion method. Only preparations

exceeding 85% viability were used. For the preparation of SCH, cells were plated at a density of 300,000 cells per well in 24-well collagen-I coated plates (BD Biosciences, Oxford, UK) in phenol-free WME containing 5% (v/v) fetal bovine serum, 2mM L-glutamine, 100 units/µg per mL penicillin/streptomycin, 1µM dexamethasone and 4 µg/mL insulin. Cells were allowed to adhere for 2 hours at 37°C in an atmosphere containing 5% CO_2. After this time, media was removed and a 0.25 mg/mL matrigel overlay was applied in ice-cold WME containing the same supplements as above. Cells were kept at 37°C in an atmosphere containing 5% CO_2 for the duration of their culture. After the first 24 hours in culture, hepatocytes were cultured in WME containing 2mM L-glutamine, 100 units/µg per mL penicillin/streptomycin, 1µM dexamethasone and 1% (v/v) Insulin-Transferrin-Selenium; media was changed daily.

5.3.3. Fluorescence Microscopy

In order to confirm the formation of functional bile canalicular networks, 5-carboxy-2',7'-dicholofluorescein diacetate (5-CDFDA) was used in conjunction with fluorescence microscopy. 5-CDFDA readily enters hepatocytes and is metabolised to form carboxydichlorofluorescein (CDF), which is a fluorescent substrate of Mrp2. CDF is therefore concentrated within the bile canaliculi. In order to demonstrate the function of efflux transporters, imaging was performed with and without the Mrp inhibitor, MK-571[158]. This does not inhibit the formation of CDF, but prevents the accumulation within the bile ducts, instead retaining the substrate within the cells. Experiments were performed after SCH had been in culture for 3 days. Cells were first pre-incubated for 10 minutes with 0.5 mL of HBSS, with or without MK-571 (20 µM), after which buffer was aspirated from the well and 0.5 mL of 10 µM 5-CDFDA was added. After 10 minutes, wells were aspirated and washed three times with ice cold HBSS. Warm culture medium (200 µL) was then added to wells, and cells were examined using a Zeiss LSM 510 Meta Confocal Microscope (Carl Zeiss Ltd., Cambridge, UK) at an excitation and emission wavelength of 505 and 525 nm, respectively. Images were taken using Combi LSM-FCS and LSM Image Browser v4.0 software (Carl Zeiss Ltd., Cambridge, UK).

5.3.4. Measurement of Uptake and Biliary Efflux using rat SCH

SCH culture and biliary efflux assays were performed based on the recommendations of De Bruyn et al[112]. Experiments were performed after SCH had been in culture for 3 days. Medium was removed and cells were pre-incubated for 10 minutes in 500 µL of either Hank's Balanced Salt Solution (HBSS) containing calcium ions (Ca^{2+}) or Ca^{2+}-free HBSS at 37°C. Cells incubated with Ca^{2+} HBSS retained tight junction activity and a functional bile canalicular network. Drug accumulation is therefore measured from both the cells and the bile, and was used to estimate CL_{uptake}. Cells incubated with Ca^{2+}-free HBSS are unable to retain tight junction function, leading to leakage from the bile network back into the media. Drug accumulation is therefore representative of the cellular concentration only. Following pre-incubation, experiments were initiated by addition of 400 µL of substrate (1 µM) in Ca^{2+} HBSS to the well at 37°C. After 10 minutes, media was removed from the well and cells washed rapidly 3 times with ice cold phosphate buffered saline (PBS) in order to terminate the reaction. In order to lyse cells, 200 µL of water was added to each well, and samples stored at -20°C overnight. Internal standard dissolved in methanol was subsequently added, with samples being stored at -20°C until analysis. For each drug, experiments were performed in duplicate from three separate hepatocyte isolations, with a maximum organic solvent concentration in the incubation medium of 0.1% (v/v). Data were corrected for non-specific binding by subtraction of any measured drug accumulation in wells containing a matrigel overlay but no cells. Protein concentration in cell lysates was measured in untreated wells using the Bradford assay (Biorad, Hemel Hempstead, UK), and was corrected for protein measured in blank wells containing matrigel alone.

5.3.5. Measurement of Sinusoidal Efflux using rat SCH

Sinusoidal efflux assays were performed based on methods outlined by Swift et al[110]. Experiments were performed after SCH had been in culture for 3 days. For sinusoidal efflux studies, medium was removed and cells were pre-incubated for 10 minutes in 400 µL of 1µM substrate solution in Ca^{2+} HBSS at 37°C. Substrate solution was then removed and cells washed 3 times with warm PBS. Cells were then incubated with 300 µL Ca^{2+} HBSS for 10 minutes at 37°C, after which time the media was removed and quenched in methanol containing internal standard. Samples were stored at -20°C until analysis. For each drug, experiments were performed in duplicate from three separate hepatocyte

isolations. The maximum organic solvent concentration in the incubation medium was 0.1% (v/v). Data were corrected for non-specific binding through subtraction of drug accumulation in wells containing a matrigel overlay but no cells. Protein concentration in cell lysates was measured in untreated wells using the Bradford assay, and was corrected for protein measured in blank wells containing matrigel alone.

5.3.6. LC-MS/MS Analysis

A Waters 2795 with a Micromass Quattro Ultima or Quattro Micro triple quadruple mass spectrometer (Waters, Milford, MA) was used for LC-MS/MS analysis. Analytes were centrifuged for 10 min at 2500 rpm and a 10 µL aliquot of the supernatant was analysed by LC-MS/MS. Four mobile phases (A, B, C and D) were used, the composition of each was as follows: A) 90% water; 10% methanol; 0.05% formic acid, B) 90% methanol; 10% water; 0.05% formic acid, C) 90% water; 10% methanol; 10 mM ammonium acetate, D) 90% methanol; 10% water, 10 mM ammonium acetate. A Luna C18 column (3 µm, 50 mm x 4.6 mm) or Luna Phenyl Hexyl column (5µm, 550 x 4.6 mm) was used for chromatographic separation of the analytes (Phenomenex, Torrance, CA), with the flow rate set at 1 mL/min split to 0.25 mL/min before entering the mass spectrometer. For detailed information regarding LC-MS/MS methods for each compound, see Appendix 7.8.

5.3.7. Data Analysis

In vitro CL_{uptake}, CL_{bile} and $CL_{sinusoidal}$ were calculated using Equation 20, Equation 21 and Equation 22, respectively.

$$CL_{uptake} = \frac{Amount\ (cells + bile)}{t\ \cdot [S]_{medium}} \qquad \textbf{Equation 20}$$

$$CL_{bile} = \frac{Amount\ (cells + bile) - Amount\ (cells)}{t\ \cdot [S]} \qquad \textbf{Equation 21}$$

$$CL_{sinusoidal} = \frac{Amount\ (Buffer)}{t\ \cdot [S]} \qquad \textbf{Equation 22}$$

Where t represents the incubation time (10 minutes), $[S]_{medium}$ is the concentration in the medium and [S] was the substrate concentration depending on three methods. For method 1, [S] was taken as the substrate concentration measured in the medium, as is traditionally used when calculating efflux clearance values. In method 2, adapted from the method proposed by Nakakariya et al[143], [S] represents the unbound cellular concentration, calculated using Equation 23.

$$[S]_{cell,unbound} = \frac{Amount\ (cells) \cdot\ fu_{cell}}{Intracellular\ volume} \qquad \textbf{Equation 23}$$

Values for fu_{cell} were taken from results obtained in 4.4.4 (Table 20), and intracellular volume determined assuming 3.9 µL/10^6 cells[97] and a protein conversion of 1x10^6 cells/mg protein (see 3.3.2.1), multiplied by the amount of protein measured in each assay. Finally, in method 3, investigated by Cantrill and Houston[159], [S] represents the product of $[S]_{medium}$ and Kp_u. For this study, Kp_u values from the media loss assay obtained in Chapter 4 were used. However, Equation 24 was applied to investigate an alternative method to calculate Kp_u using both methods 1 and 2 to determine values for CL_{bile} and $CL_{sinusoidal}$.

$$Kp_u = \frac{CL_{uptake}}{CL_{bile} + CL_{sinusoidal}} \qquad \textbf{Equation 24}$$

Kp_u data estimated using this method will be compared to the values obtained in Chapter 4 to assess differences between the methods of estimation.

5.3.8. IVIVE using $CL_{int,total}$

Values for CL_{uptake} and CL_{met}, obtained in Chapter 4, along with CL_{bile} and $CL_{sinusoidal}$ values were scaled using standard physiological scaling factors described in 3.3.2.1, and were used to calculate $CL_{int,total}$ (Equation 3[127-130]).

$$CL_{int,total} = CL_{uptake} \cdot \frac{CL_{met} + CL_{bile}}{CL_{met} + CL_{bile} + CL_{sinusoidal}}$$ **Equation 3**

$CL_{int,total}$ was compared to $CL_{int,\ in\ vivo}$ (see 7.1) to determine the accuracy of the parameters for prediction of *in vivo* clearance. GMFE and RMSE, described in 3.3.6, were used to assess bias and precision. Finally, scaling factors identified in Chapter 3 were applied to CL_{uptake} and CL_{met} data to assess their effects on bias and precision.

5.4. Results

5.4.1. Confirmation of functional bile canaliculi

Figure 22 shows fluorescent images of SCH after incubation with 5-CDFDA with and without the Mrp inhibitor MK-571 at a concentration of 20 µM. In the absence of the inhibitor (Figure 22C and D), CDF fluorescence is clearly localised within the bile cananliculi, indicating the formation of bile canalicular networks with functional Mrp2 transporters. This localisation of CDF within the bile canaliculi is disrupted following treatment of MK-571, however the formation of CDF is not, demonstrated by fluorescence observed within the cells (Figure 22A and B).

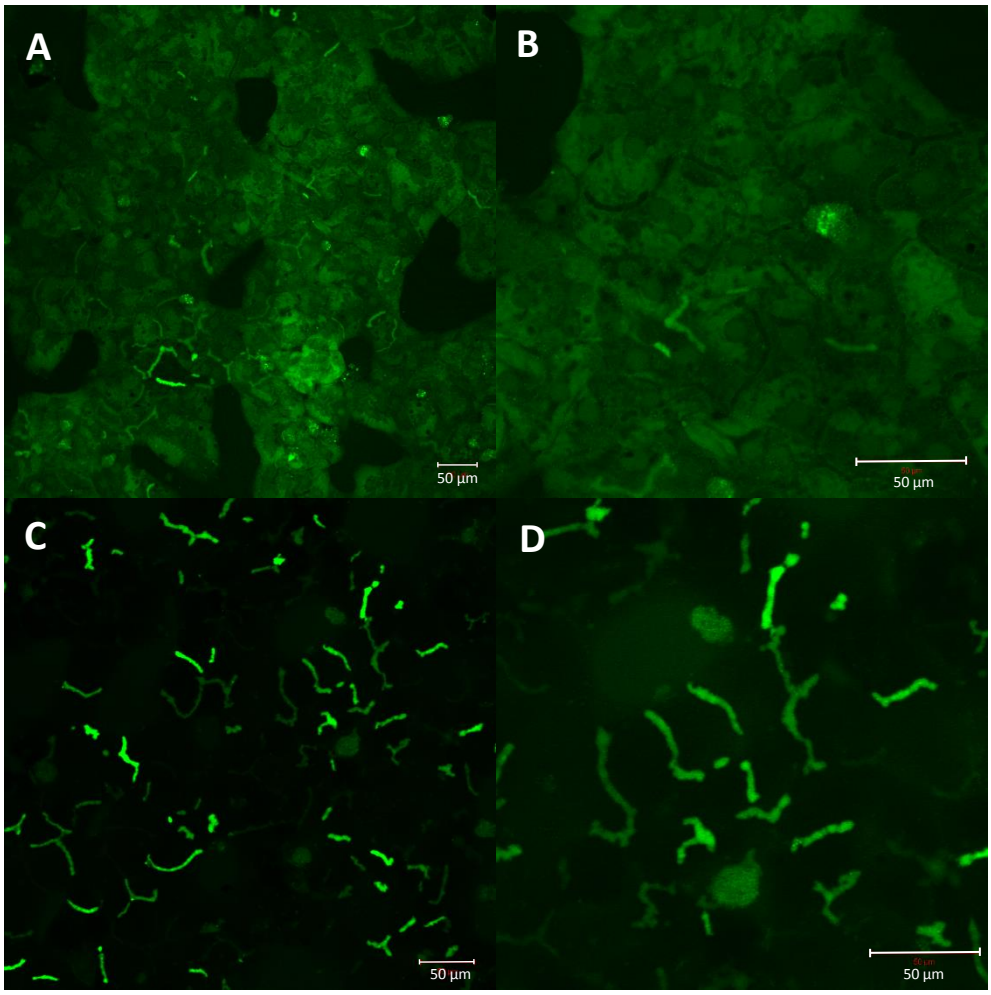

Figure 22 – Representative fluorescent images demonstrating CDF localisation within rat SCH with (A and B) and without (C and D) pre-treatment with the Mrp inhibitor MK-571. Scale bars are indicated.

5.4.2. Measurement of CL_{uptake} using rat SCH

CL_{uptake} was estimated for each drug over 10 minutes at 1 µM, and ranged between 2.7 – 109 µL/min/mg protein. Uptake data were compared with SCH data obtained from the literature in Chapter 3, media loss data produced in Chapter 4 and to *in vivo* clearance values using standard physiological scaling factors. This is of particular interest as uptake governs intracellular drug concentration, which in turn determines the amount of drug available for efflux from either the sinusoidal or basolateral membranes. It is therefore essential to establish if empirical scaling of data from SCH is required.

Only 6 drugs from this study had *in vitro* uptake data in SCH available within the literature (atorvastatin, pitavastatin, repaglinide, rosuvastatin, saquinavir and valsartan). Of the 17 literature studies identified, 14 had lower CL_{uptake} rates than were recorded in the present study. On average, the present study produced CL_{uptake} values approximately 3-fold greater than that observed in the literature (Table 22, Figure 23A). Compared to the media loss assay presented in Chapter 4, CL_{uptake} from SCH in this study were on average 3-fold lower (Figure 23B). This is to be expected, considering the tendency for the media loss assay to produce over-predictions of *in vivo* clearance using uptake data. However, these differences are important to consider when data from different assay formats are used within extended clearance terms.

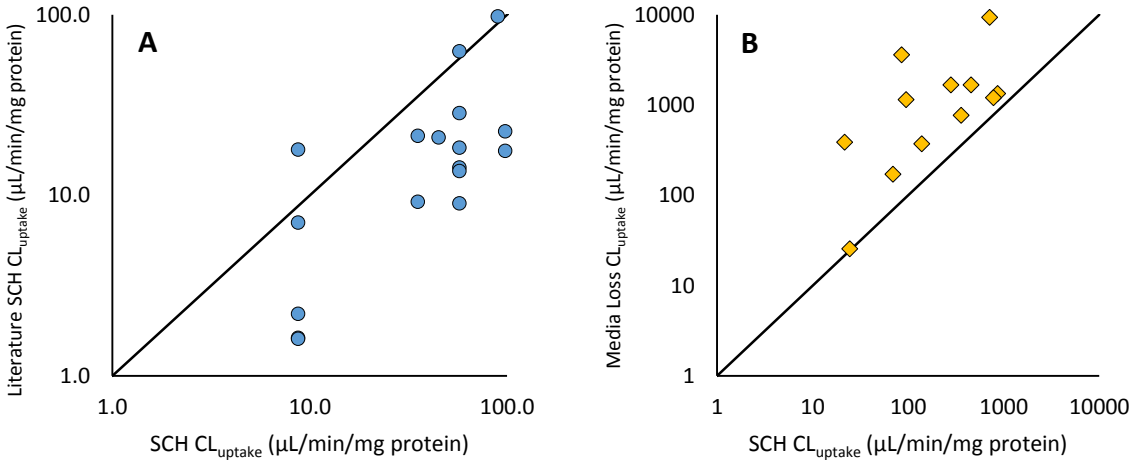

Figure 23 - Comparison of SCH uptake data from the present study to literature SCH CL_{uptake} for 6 drugs for which data were available (Panel A, see Table 22 for individual values) and CL_{uptake} obtained for all 12 compounds used in this study in the media loss assay (Chapter 4, Panel B). Line of unity (solid line) is displayed.

Table 22 - Comparison of CL_{uptake} values from SCH in both the literature and the present study for 6 compounds.

Group	Drug	CL_{uptake}		Fold Difference
		Literature	Present Study	(Present/Literature)
		µL/min/mg protein		
1	Pitavastatin	22.6[160]	97.9	4.33
		17.6[161]		5.56
	Rosuvastatin	14.2[159]	57.4	4.05
		28.5[142]		2.01
		9.0[160]		6.37
		18.3[161]		3.14
		62.5[141]		0.92
		13.6[143]		4.22
	Valsartan	2.2[159]	8.8	3.98
		7.1[160]		1.24
		1.6[161]		5.40
		1.6[141]		5.47
		17.9[143]		0.49
2	Atorvastatin	21.3[159]	35.4	1.66
		9.2[142]		3.84
	Repaglinide	20.8[159]	45.0	2.16
4	Saquinavir	97.6[159]	89.9	0.92
			Average	3.28

When performing IVIVE, SCH data were seen to have much less bias (GMFE = 3.23) than the average value observed for the assay from literature sources in Chapter 3 (GMFE = 14.5). This included 5 of the 12 compounds (42%) having CL_{uptake} values within 2-fold of the observed *in vivo* clearance (Table 23, Figure 24). In comparison, only 7% of drugs were found to be within 2-fold of the observed *in vivo* clearance from literature data in Chapter 3. Precision remained relatively high (RMSE = 764), as was noted for literature SCH data (RMSE = 1032).

Table 23 - IVIVE of CL_{uptake} generated in SCH, with assessment of accuracy and precision when predicting *in vivo* clearance. Data were scaled using standard physiological scaling factors of 200mg protein/g liver and 40 g liver/kg bodyweight. See 7.1 for sources of *in vivo* values.

Group	Drug	CL_{uptake}	Scaled CL_{uptake}	$CL_{int,in\ vivo}$	Predicted/Observed
		µL/min/mg protein	mL/min/kg		
1	Cerivastatin	109 ± 3.7	871 ± 29	1517	0.57
	Pitavastatin	98 ± 10	783 ± 76	1165	0.67
	Rosuvastatin	57 ± 14	459 ± 109	1412	0.33
	Valsartan	8.8 ± 0.9	70 ± 7	1554	0.05
2	Atorvastatin	35 ± 3.8	283 ± 30	1593	0.18
	Clarithromycin	18 ± 5.3	140 ± 43	68	2.06
	Indinavir	12 ± 4.9	96 ± 39	50	1.91
	Repaglinide	45 ± 25	360 ± 202	496	0.73
3	Tolbutamide	3.1 ± 1.4	25 ± 11	7	3.31
4	Erythromycin	2.7 ± 0.1	22 ± 1	81	0.27
	Midazolam	11 ± 13	86 ± 105	1331	0.06
	Saquinavir	90 ± 17	719 ± 133	911	0.79
				GMFE	3.23
				RMSE	764

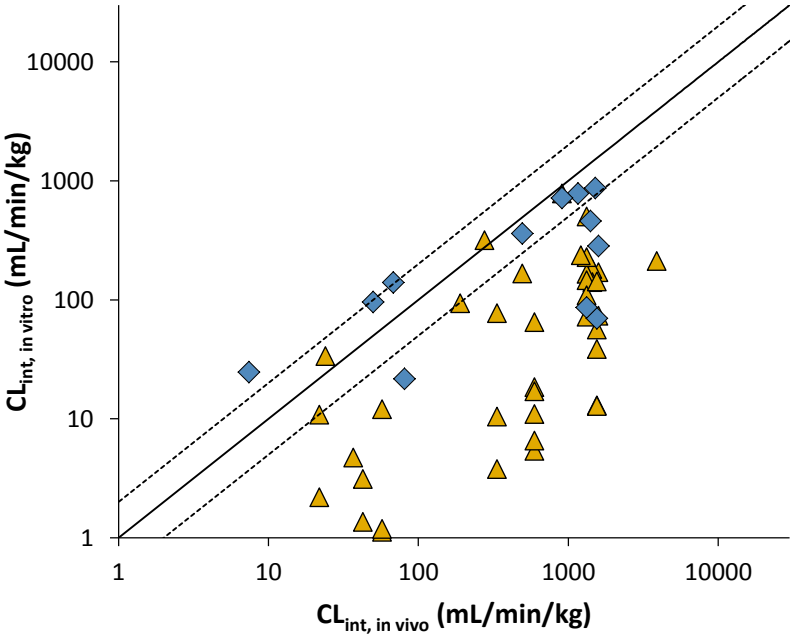

Figure 24 – Comparison of literature $CL_{int,\ in\ vitro}$ (yellow triangle) and $CL_{int,\ in\ vitro}$ from the current study (blue diamonds) against observed $CL_{int,\ in\ vivo}$ for compounds in rat SCH assays scaled using standard physiological scaling factors of 200 mg protein/g liver and 40 g liver/kg bodyweight. Line of unity (solid line), and 2-fold under and over-prediction (dashed line) are displayed.

It is unclear why, in the present study, SCH uptake values do not to display the typical low rates of uptake that is expected of the assay. Nevertheless, it was deemed that empirical scaling of biliary or sinusoidal efflux data prior to input into the extended clearance terms is not be justified. However, it was determined that rates of uptake measured in the media loss assay more accurately represented those seen *in vivo*, demonstrated by the GMFE, and so CL_{uptake} measured in SCH were not considered within the $CL_{int,total}$ model.

5.4.3. Measurement of Biliary Efflux, Sinusoidal Efflux and Kp_u using rat SCH

Estimates of CL_{bile} and $CL_{sinusoidal}$ were generated based on three methods and are summarised in Table 24 and Table 26. Method 1 estimated clearance based on the concentration within the media, which is the traditional method employed for estimating biliary clearance. Excluding both control compounds (tolbutamide and midazolam), CL_{bile} estimated in this way ranged from 0.9 – 9.15 µL/min/mg protein, with the highest values recorded for pitavastatin and rosuvastatin. Values for $CL_{sinusoidal}$ were generally higher, ranging between 1.7 – 23.5 µL/min/mg protein, with the lowest value observed for valsartan, and the highest for repaglinide.

However, in some cases, addition of each efflux parameter was close to, or exceeded, the recorded CL_{uptake}, as shown in Figure 25. Since this is not possible, an alternative methodology for calculating efflux was assessed, adapted from that proposed by Nakakariya et al[143], where rates were calculated based on the unbound intracellular concentration (method 2). CL_{bile} ranged between 0 – 1.95 µL/min/mg, with no biliary efflux noted for cerivastatin, atorvastatin or saquinavir, while the highest value was noted for clarithromycin. $CL_{sinusoidal}$ again typically had greater values, between 0.31 – 8.46 µL/min/mg. The lowest value was recorded for valsartan, while the highest was, as with CL_{bile}, clarithromycin. Data for methods 1 and 2 are summarised in Table 24, and displayed in Figure 26. No significant relationships were noted between CL_{bile} or $CL_{sinusoidal}$ and $LogD_{7.4}$ or $CL_{passive}$ from the media loss assay for any of the methods used in this study (see Appendix 7.14). This would suggest that active transport processes contribute to the observed CL_{bile} and $CL_{sinusoidal}$.

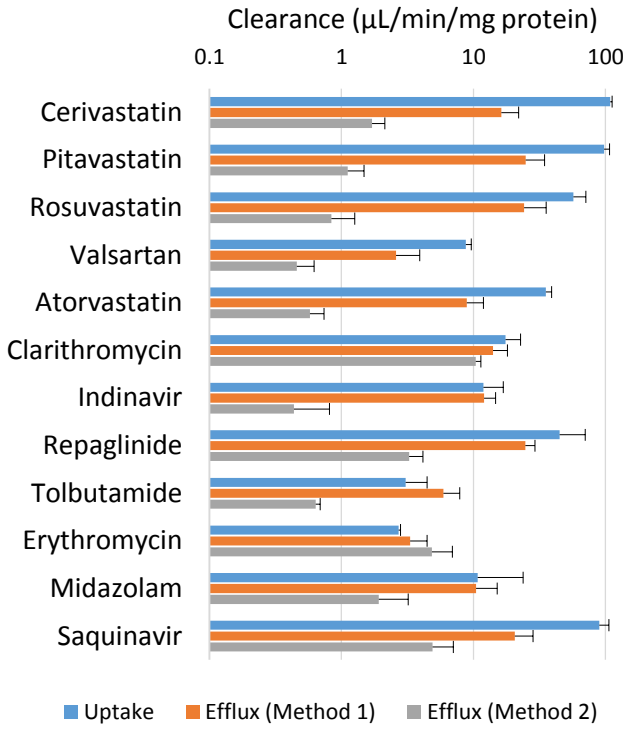

Figure 25 – Uptake and efflux (both biliary and sinusoidal) clearances estimated using Methods 1 and 2. Data represents the mean ± SD (n=3).

Table 24 – CL_{bile} and $CL_{sinusoidal}$ values obtained from rat SCH at 1µM over 10 minutes. CL_{bile} and $CL_{sinusoidal}$ were calculated via two methods, based on media concentrations (method 1) and unbound cell concentrations (method 2). Results are displayed as the mean ± SD (n=3).

Group	Compound	CL_{bile}	$CL_{sinusoidal}$	CL_{bile}	$CL_{sinusoidal}$
		Method 1		Method 2	
		µL/min/mg protein			
1	Cerivastatin	5.99 ± 5.23	10.3 ± 2.29	0 ± 0	1.71 ± 0.43
	Pitavastatin	9.15 ± 8.85	15.8 ± 4.0	0.23 ± 0.27	0.88 ± 0.25
	Rosuvastatin	8.00 ± 10.1	16.2 ± 5.2	0.27 ± 0.33	0.57 ± 0.26
	Valsartan	0.90 ± 1.31	1.70 ± 0.03	0.15 ± 0.15	0.31 ± 0.06
2	Atorvastatin	1.50 ± 2.60	7.41 ± 1.53	0 ± 0	0.58 ± 0.16
	Clarithromycin	3.77 ± 1.60	10.33 ± 3.67	1.95 ± 0.75	8.46 ± 0.6
	Indinavir	2.63 ± 2.65	9.45 ± 0.52	0.06 ± 0.06	0.57 ± 0.22
	Repaglinide	1.33 ± 2.31	23.5 ± 3.9	0.18 ± 0.19	3.08 ± 0.86
3	Tolbutamide	0 ± 0	5.93 ± 1.94	0 ± 0	0.64 ± 0.05
4	Erythromycin	0.98 ± 0.39	2.33 ± 1.1	1.39 ± 0.79	3.46 ± 1.91
	Midazolam	0.04 ± 0.06	10.4 ± 4.7	0 ± 0	1.91 ± 1.3
	Saquinavir	3.08 ± 4.96	17.5 ± 5.8	0 ± 0	4.90 ± 2.14

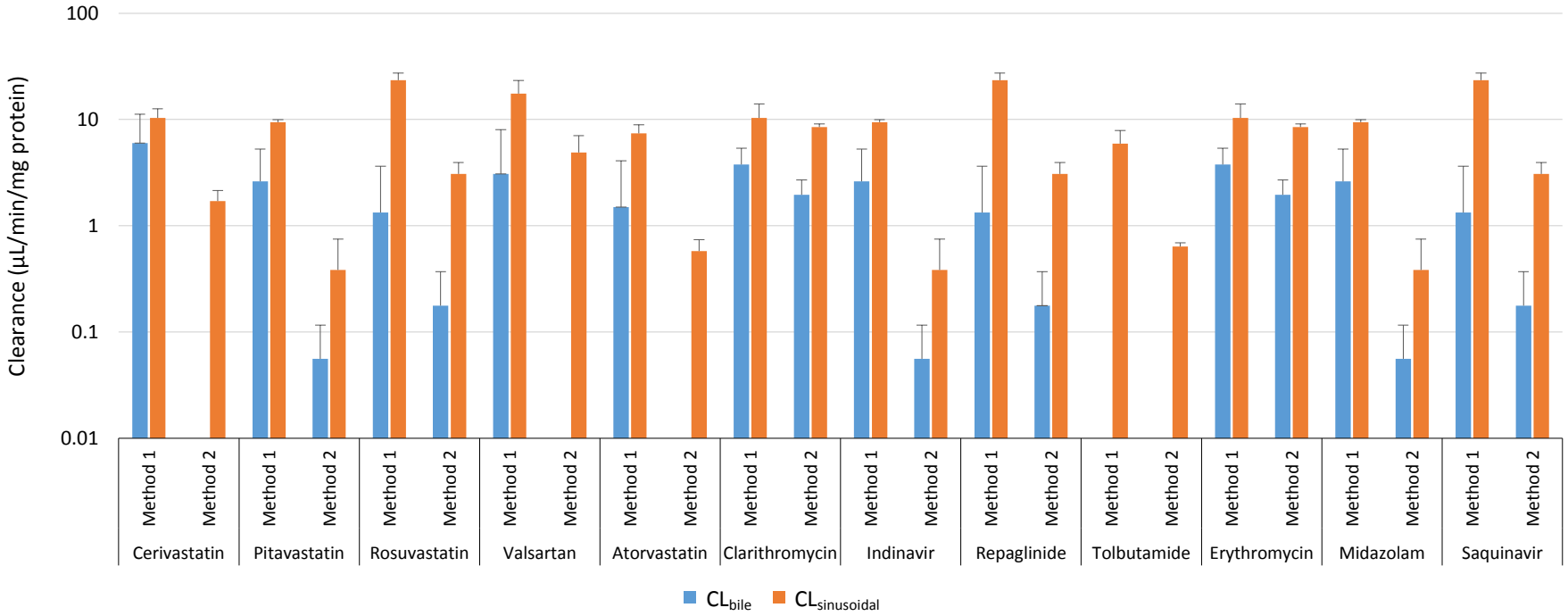

Figure 26 – CL_{bile} and $CL_{sinusoidal}$ calculated using methods 1 and 2. Data represents the mean and SD (n=3).

Method 3, proposed by Cantrill and Houston[159], uses the product of Kp_u and the media concentration as an alternative method to estimate the unbound intracellular concentration for the calculation of efflux clearances. Since no distinction between active and passive transport was made within this study, and efflux processes were not assumed to be negligible, an alternative method for calculating Kp_u was investigated (Equation 24), with the intention to compare values to those generated in Chapter 4 using the media loss assay and Equation 18. Since Kp_u values were dependent on the method of efflux calculation, both method 1 and 2 data were assessed. Kp_u calculated using efflux values from method 1 ranged between 0.39 – 6.9, with lowest values seen for both control compounds midazolam and tolbutamide, while the highest were cerivastatin and saquinavir. Using method 2, Kp_u values were typically higher, ranging between 0.66 – 100 with lowest values seen for erythromycin, while pitavastatin and rosuvastatin displayed the highest. Compared to Kp_u values obtained in the media loss assay (Table 20, 4.4.4), Kp_u calculated using efflux values from method 1 were on average 1.5-fold lower, but had a similar rank order (Table 25, Figure 27). Much higher differences were noted between values from the media loss assay and Kp_u calculated from efflux values using method 2, with an average fold error of 6.99, although again rank order was similar (Table 25, Figure 27).

Kp_u values from the media loss assay were applied within method 3 to calculate CL_{bile} and $CL_{sinusoidal}$ rates (Table 26). Kp_u values estimated using efflux data in Table 25 were not used in order to avoid a circular loop within the methodology. Excluding control compounds, CL_{bile} calculated using method 3 ranged between 0.14 – 1.8 µL/min/mg protein. Consistent with methods 1 and 2, with exception of the control compounds, valsartan produced the lowest CL_{bile} values, while the highest were seen for rosuvastatin. $CL_{sinusoidal}$ ranged between 0.25 – 9.0 µL/min/mg protein, with the lowest value recorded for valsartan, and the highest for repaglinide (Table 26, Figure 28). Both control drugs had particularly high $CL_{sinusoidal}$ values using this method, with 5.2 and 3.1 µL/min/mg protein for tolbutamide and midazolam, respectively.

Table 25 – Comparison of Kp_u values obtained in the media loss (ML) assay with that obtained in the current study using media concentrations (method 1, M_1) or unbound cell concentrations (method 2, M_2) to calculate efflux.

Group	Compound	Kp_u			M_1/ML	M_2/ML
		ML	M_1	M_2	Fold	
1	Cerivastatin	5.4	6.9	67.3	1.3	12.5
	Pitavastatin	5.9	4.8	99.8	0.8	16.9
	Rosuvastatin	4.5	2.7	83.1	0.6	18.5
	Valsartan	6.7	3.8	22.5	0.6	3.4
2	Atorvastatin	8.3	4.0	65.8	0.5	7.9
	Clarithromycin	2.3	1.3	1.7	0.5	0.7
	Indinavir	2.6	1.0	13.3	0.4	5.1
	Repaglinide	2.6	1.8	15.5	0.7	6.0
3	Tolbutamide	1.1	0.5	4.9	0.5	4.5
4	Erythromycin	2.5	0.9	0.7	0.4	0.3
	Midazolam	3.4	0.4	1.2	0.1	0.4
	Saquinavir	3	4.4	23.6	1.5	7.9
				Average	0.65	6.99

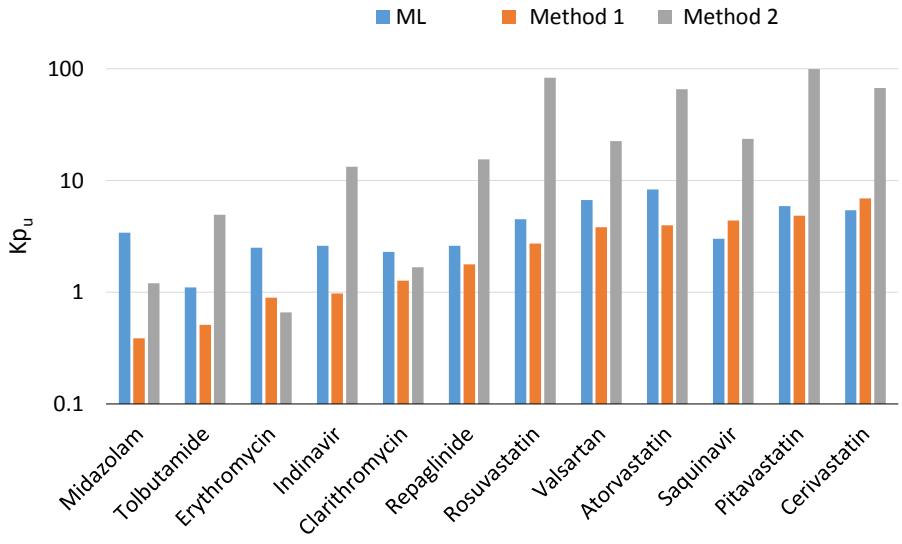

Figure 27 – Kp_u values obtained from the media loss (ML) assay and in the current study using media concentrations (method 1) or unbound cell concentrations (method 2) to calculate efflux.

Table 26 – Kp_u, CL_{bile} and $CL_{sinusoidal}$ values obtained from rat SCH at 1µM over 10 minutes. CL_{bile} and $CL_{sinusoidal}$ were calculated via total intracellular concentration (method 3), using Kp_u values estimated from the media loss assay (Chapter 4). Results are displayed as the mean ± SD (n=3).

Group	Compound	Kp_u	CL_{bile}	$CL_{sinusoidal}$
			Method 3	
			µL/min/mg protein	
1	Cerivastatin	5.4	1.11 ± 0.97	1.91 ± 0.42
	Pitavastatin	5.9	1.54 ± 1.49	2.65 ± 0.68
	Rosuvastatin	4.5	1.80 ± 2.27	3.64 ± 1.17
	Valsartan	6.7	0.14 ± 0.2	0.25 ± 0.004
2	Atorvastatin	8.3	0.18 ± 0.31	0.89 ± 0.18
	Clarithromycin	2.3	1.63 ± 0.7	4.47 ± 1.59
	Indinavir	2.6	1.03 ± 1.04	3.70 ± 0.2
	Repaglinide	2.6	0.51 ± 0.88	8.99 ± 1.5
3	Tolbutamide	1.1	0.00 ± 0.0	5.21 ± 1.7
4	Erythromycin	2.5	0.39 ± 0.16	0.94 ± 0.43
	Midazolam	3.4	0.01 ± 0.02	3.06 ± 1.38
	Saquinavir	3	1.02 ± 1.63	5.78 ± 1.92

In order to assess each method of CL_{bile} estimation, values were compared to observed *in vivo* values (Figure 29). *In vivo* CL_{bile} values could only be obtained for erythromycin, pitavastatin, rosuvastatin and valsartan, and are summarised in Table 27. Use of *in vitro* CL_{bile} calculated based on media concentration (method 1) led to over-prediction of *in vivo* CL_{bile} for pitavastatin, rosuvastatin and valsartan, while erythromycin was under-predicted. Conversely, use of unbound cell concentration (method 2) and Kp_u (method 3) predominantly led to under-predictions of CL_{bile}. Method 3 appeared to produce the most accurate predictions of CL_{bile} (Table 27), with GMFE determined as 2.99 compared to 3.76 (method 1) and 3.36 (method 2).

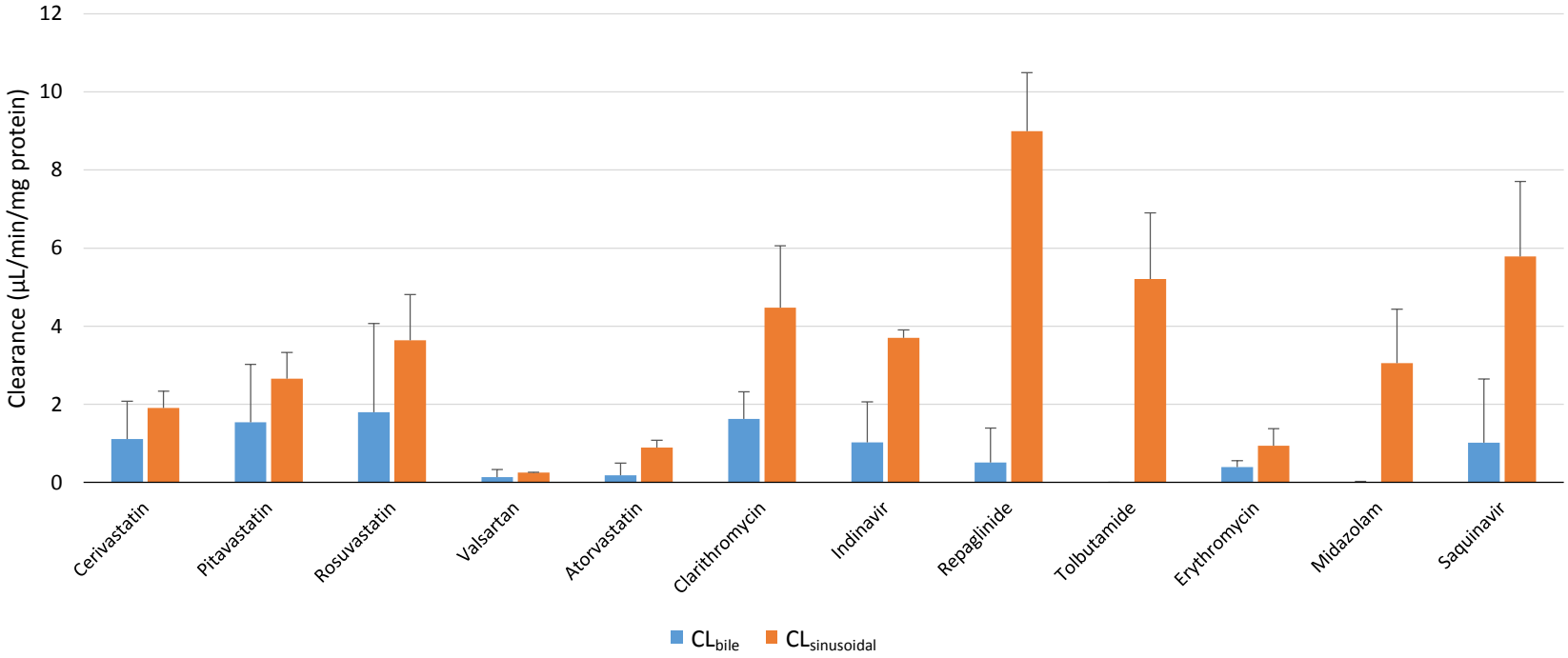

Figure 28 - CL_{bile} and $CL_{sinusoidal}$ calculated using method 3. Data represents the mean and SD (n=3)

Table 27 – Comparison of *in vitro* $CL_{bile,}$ scaled using standard physiological scaling factors of 200 mg protein and 40 g liver/kg bodyweight and calculated using methods 1, 2 and 3, to observed *in vivo* CL_{bile} for four compounds.

Compound	CL_{bile}				Fold Error		
	In vivo	M_1	M_2	M_3	M_1	M_2	M_3
	mL/min/kg						
Erythromycin	17.4[162]	7.84	11.1	3.12	0.45	0.64	0.18
Pitavastatin	4.55[160]	73.2	1.84	12.3	16.09	0.40	2.71
Rosuvastatin	24.3[141]	64	2.16	14.4	2.63	0.09	0.59
Valsartan	3.5[141]	7.2	1.2	1.12	2.06	0.34	0.32
				GMFE	3.76	3.36	2.99

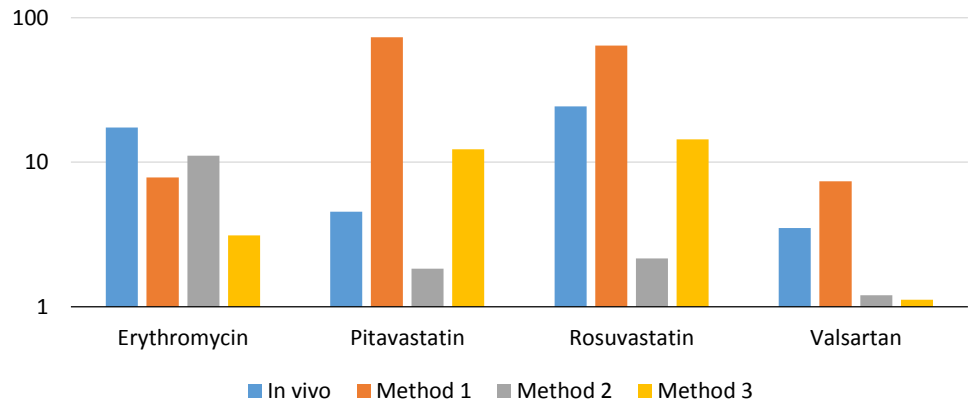

Figure 29 – *In vitro* $CL_{bile,}$ scaled using standard physiological scaling factors of 200 mg protein and 40 g liver/kg bodyweight, calculated using methods 1, 2 and 3, along with observed *in vivo* CL_{bile} for four compounds.

5.4.4. IVIVE using total intrinsic clearance

Following physiological scaling of *in vitro* clearance parameters, $CL_{int,\ total}$ was calculated according to Equation 3, with results displayed in Table 28. In comparison to *in vivo* values (see Table 29), $CL_{int,\ total}$ saw no improvement in GMFE values compared to using uptake data alone when using efflux values calculated using method 1, however marginal improvements were noted when using efflux values calculated using methods 2 and 3. Precision (indicated by the RMSE) was also increased for these methods compared to uptake data. Use of metabolism data alone remains as the clearance parameter with the highest bias. Results are summarised in Table 29, and comparisons between methods and to *in vivo* values are illustrated in Figure 30 and Figure 31, respectively.

As a final analysis, scaling factors identified in Chapter 3 for both CL_{uptake} and CL_{met} were implemented to assess if further improvements could be made to bias and precision. Minimum and maximum physiological scaling factors (3.4.2.1.1) were applicable to both CL_{uptake} and CL_{met}, while mean and median required scaling factors (3.4.2.1.2) were calculated for each parameter individually. Clearance derived scaling factors (3.4.2.1.3)

Table 28 - Summary of $CL_{int,\ total}$ values, calculated using Equation 3, using biliary and sinusoidal efflux data calculated using either methods 1, 2, or 3. Data are scaled using standard physiological scaling factors of 200 mg protein/g liver and 40 g liver/kg bodyweight.

Group	Compound	$CL_{int,\ total}$			$CL_{int,\ in\ vivo}$
		M_1	M_2	M_3	
		mL/min/kg			
1	Cerivastatin	680	982	1006	1517
	Pitavastatin	602	1065	909	1165
	Rosuvastatin	645	1357	880	1412
	Valsartan	110	151	154	1554
2	Atorvastatin	1376	1636	1621	1593
	Clarithromycin	203	207	259	121
	Indinavir	977	1132	1071	50
	Repaglinide	411	685	571	496
3	Tolbutamide	6	19	7	7
4	Erythromycin	330	310	361	116
	Midazolam	3435	3558	3541	1331
	Saquinavir	8262	8966	8913	911

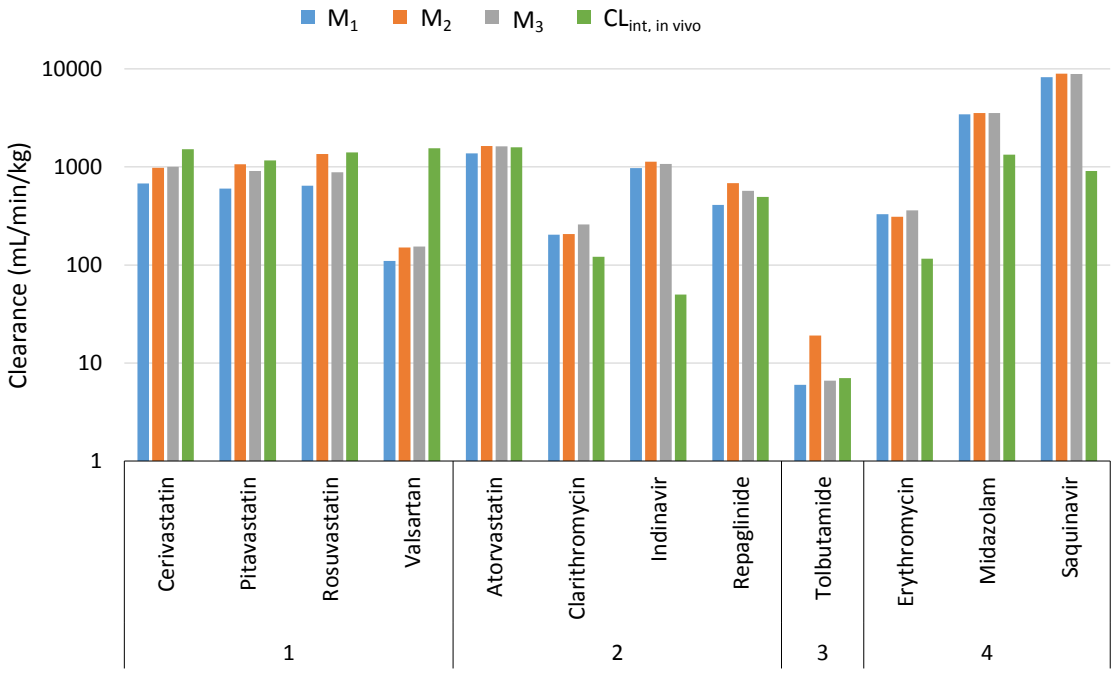

Figure 30 - $CL_{int,\ total}$ values, calculated using Equation 3, using biliary and sinusoidal efflux data calculated using either methods 1, 2 or 3 and scaled using standard physiological scaling factors of 200 mg protein/g liver and 40 g liver/kg bodyweight, as compared to $CL_{int,\ in\ vivo}$ values.

Table 29 – Predicted/observed values for uptake and metabolism data generated in Chapter 4 (Table 21), as well as $CL_{int,total}$ data presented in Table 28, with GMFE and RMSE values for each.

Group	Compound	Uptake	Metabolism	$CL_{int,\ total}$		
				M_1	M_2	M_3
			Predicted/Observed			
1	Cerivastatin	0.88	0.03	0.45	0.65	0.66
	Pitavastatin	1.03	0.05	0.52	0.91	0.78
	Rosuvastatin	1.17	0.01	0.46	0.96	0.62
	Valsartan	0.11	0.01	0.07	0.10	0.10
2	Atorvastatin	1.04	0.17	0.86	1.03	1.02
	Clarithromycin	3.06	0.58	1.68	1.71	2.14
	Indinavir	22.9	8.41	19.58	22.69	21.5
	Repaglinide	1.55	0.42	0.83	1.38	1.15
3	Tolbutamide	3.44	1.96	0.81	2.54	0.89
4	Erythromycin	3.35	0.86	2.86	2.68	3.12
	Midazolam	2.69	1.42	2.58	2.67	2.66
	Saquinavir	10.19	1.22	9.07	9.84	9.78
	GMFE	2.96	6.40	2.99	2.74	2.71
	RMSE	2559	915	2293	2473	2460

were only identified for CL_{uptake}, as no significant correlation was noted for CL_{met}. Since no data were available for calculation of empirical scaling for CL_{bile} and $CL_{sinusoidal}$, data were scaled using physiological scaling factors in all combinations, except for the application of minimum and maximum scaling factors. Of the combinations investigated, the lowest bias (GMFE = 2.63) was recorded for $CL_{int,total}$ using method 2, scaled using the median required empirical scaling factor for uptake and metabolism, while efflux parameters were scaled using standard physiological scaling factors. However, this is almost identical to that recorded for CL_{uptake} (GMFE = 2.66) when scaled by the median or minimum required scaling factors. Overall, the median required empirical scaling factor is recommended as the most suitable scaling factor, as it produces the lowest degree of bias across each of the methods investigated. For the full list of GMFE and RMSE values for each combination, see Table 37 (Appendix 7.15).

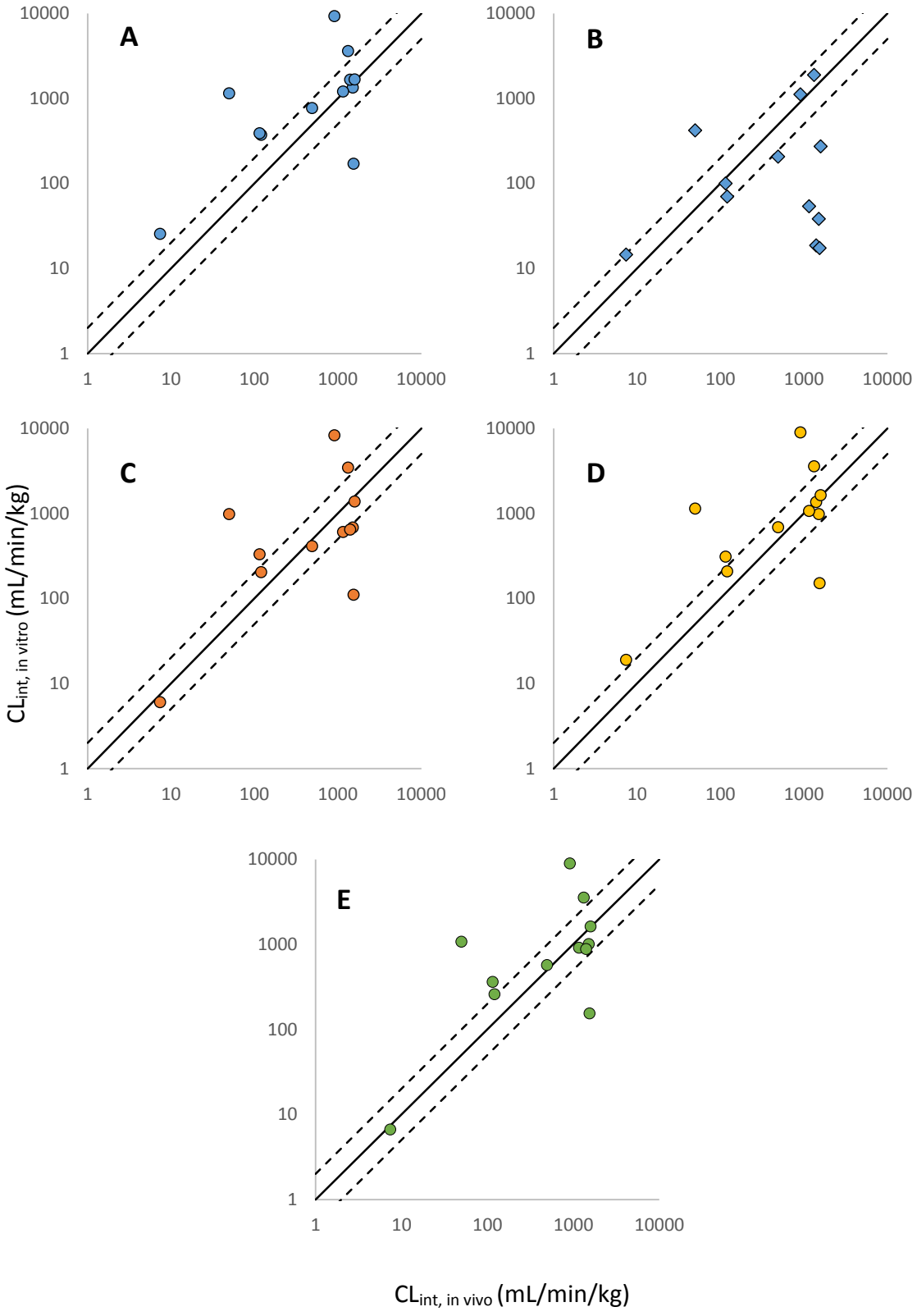

Figure 31 - Observed $CL_{int,\ in\ vivo}$ plotted against CL_{uptake} (A),CL_{met} (B) and $CL_{int,\ total}$ using methods 1 (C), 2 (D) and 3 (E), scaled using standard physiological scaling factors of 200 mg protein/g liver and 40 g liver/kg bodyweight. Line of unity (solid line), and 2-fold under and over-prediction (dashed line) are displayed.

5.5. Discussion

Throughout the literature, prediction of *in vivo* clearance is predominantly performed using single pathway *in vitro* assays, such as metabolic or uptake clearance. However, it has been previously been demonstrated that use of metabolic clearance data alone may lead to a clearance-dependent under-prediction of *in vivo* clearance[83, 131]. Conversely, it has been demonstrated in Chapter 3 that non-cultured (suspension and media loss) hepatocyte uptake systems typically produce over-predictions of *in vivo* clearance, while cultured formats (monolayer and SCH) predominantly produce under-predictions. Mechanistic scaling approaches have been investigated as an alternative, incorporating several clearance parameters to produce an overall clearance value. For this chapter, a simple mechanistic method was used, with the extended clearance term, $CL_{int,\ total}$, being investigated.

5.5.1. Measurement of CL_{uptake} in SCH

Chapter 3 highlighted the consistent under-prediction of uptake using SCH, with GMFE recorded at 14.5% and 93% of compounds under-predicting *in vivo* clearance. However, analysis of CL_{uptake} for the set of 12 compounds in this study found GMFE to be 3.23, with 42% of the drugs being within 2-fold of the observed *in vivo* clearance when scaled using standard physiological scaling factors. When individual drugs were compared directly to literature data, it was found that on average CL_{uptake} in the present study was approximately 3-fold higher. Since reduced uptake had previously been suggested as a reason for the low values of *in vitro* CL_{bile}[112], it was concluded that there was no justification for the empirical scaling of efflux values within this study.

It was speculated that varying experimental conditions could be the source of the observed differences to literature values, however this does not appear to be substantiated. For example, Fukuda et al[141] and Jemnitz et al[142] each measured uptake at 1 µM in SCH, as was used in the present study, but differed in that uptake was measured over a maximum of 2 minutes, as opposed to the 10 minutes. Despite this, CL_{uptake} values from Fukuda et al matched almost exactly with that recorded in this study, while values from Jemnitz et al were 2-fold lower. The strain of rat was also hypothesised to be a potential cause for observed differences, as Jemnitz et al used wistar rats, as

opposed to the Sprague dawley rats used in this study and by Fukuda et al. However, analysis of the literature as a whole has found no difference between the two species in any assay format, and is not regarded as a likely cause. It is evident that no single factor (concentration(s), incubation time, strain of rat) can adequately explain these differences, and so the reason behind the higher than average CL_{uptake} values recorded in this study remains unknown. Despite these observations, in comparison to the media loss assay uptake rates remained lower in both value and overall accuracy in regard to predicting *in vivo* clearance. As such, for this study it was determined that uptake data from the media loss assay were more suitable for application within the $CL_{int,total}$ term. However, SCH should be considered appropriate for future use, should alternative uptake data be unavailable.

5.5.2. Measurement of Biliary Efflux

Biliary excretion has been identified as a primary route of elimination for many clinically used drugs, either directly or through efflux of their metabolites formed during phase II metabolism. SCH have become routine for the *in vitro* prediction of this pathway, however, as has been demonstrated with rates of uptake (Chapter 3), values are typically far below that which is observed *in vivo*[159]. In addition, due to the invasive methods required, *in vivo* biliary clearance data are lacking for many drugs. As such, *in vivo* CL_{bile} could only be found for four of the drugs used in this study (erythromycin, rosuvastatin, pitavastatin and valsartan). Use of method 3 was found to produce the most accurate predictions of CL_{bile} for the 4 compounds for which data was available. Using method 1 for the calculation of efflux clearances led to the over-prediction of CL_{bile} for 3 of the 4 compounds, while methods 2 and 3 primarily under-predicted. However, for methods 2 and 3, it would appear values were not as drastically under-predicted as observed in previous studies. Reported *in vitro* CL_{bile} are typically 10 to 260-fold lower than the observed *in vivo* CL_{bile} (i.e. fold error <0.1), depending on the method used for calculation[112]. The lowest fold error recorded in this study was 0.09 for rosuvastatin using method 2. Over-prediction of rosuvastatin, pitavastatin and valsartan using method 1 is particularly unexpected, given the previous literature. The contradictory observations within this study may be explained by the uptake rates, which on average were higher in this study than have been previously reported, as discussed previously. These results

further supported the conclusion that empirical scaling factors for efflux clearances were not warranted in regard to the integration of data within the extended clearance terms.

An alternative method for generating Kp_u values using efflux data was also investigated. While this is traditionally performed using active and passive uptake rates, assuming negligible efflux, the current methodology allowed for the sinusoidal and biliary effluxes to be taken into account. When calculated using efflux values from method 1, Kp_u was similar in both rank order and value to those obtained in Chapter 4 using the media loss assay. When using efflux values calculated using method 2, Kp_u values were much larger, however a similar rank order was retained. It was therefore concluded that method 1 is the most suitable for future estimations of Kp_u, when there is a lack of distinction between active and passive uptake rates.

5.5.3. Measurement of Sinusoidal Efflux

Sinusoidal efflux is not typically measured *in vitro*, and in the majority of cases is assumed to be negligible. Umehara and Camenisch[129] took this process into consideration when calculating $CL_{int,\ total}$, however the values used were estimated by rearrangement of Equation 3 to make $CL_{sinusoidal}$ the subject. Observed *in vivo* data, CL_{met} data from microsomes, CL_{uptake} data from suspended hepatocytes and CL_{bile} data from SCH were then plugged into the equation to generate $CL_{sinusoidal}$ estimates. Consequently, values were speculative and in some cases unrealistic. For example, the total sinusoidal efflux rate of 247 mL/min/kg for digoxin far exceeded the rate of uptake, metabolism or biliary efflux (76, 4.5 and 12.7 mL/min/kg, respectively). In this study, a similar effect was noted when calculating $CL_{sinusoidal}$ based on media concentrations (method 1). Theoretically, the unbound cell concentration (methods 2 and 3) are the more representative concentration to use in these calculations, since this creates the true gradient driving efflux from the cell. Use of these methods produced more plausible values for $CL_{sinusoidal}$.

Since this cannot be measured *in vivo*, it is difficult to assess how accurate these values are in terms of the *in vivo* environment. It should also be considered that $CL_{sinusoidal}$ is likely to be inflated, due to the methodology used. During a typical assay, passive efflux from the cell into the media would be opposed by the concentration of drug in the media. With

the current methodology, it was necessary to measure efflux in media containing no drug, and the gradient is therefore artificially increased. While total cell concentrations typically exceeded 10μM, the lowest unbound intracellular concentrations were determined to be 0.3 μM. In cases such as these, where media drug concentrations exceed the unbound intracellular concentrations, passive sinusoidal efflux would be expected to be negligible. Depending on the contribution of active transport to overall $CL_{sinusoidal}$, this may or may not have a substantial effect. However, this is a limitation of the assay that could not be avoided. While it was not possible for the present study, this issue could be prevented in future through use of radio-labelled drugs. This would allow preloading of cells with radiolabelled drug, followed by incubation with cold (unlabelled) drug in the buffer solution. Appearance of radiolabelled drug within this buffer would then allow an estimation of $CL_{sinusoidal}$, while maintaining the correct media drug concentration.

5.5.4. IVIVE using $CL_{int,total}$

$CL_{int,\ total}$ was investigated as an alternative to the single pathway IVIVE methods that have been investigated in previous chapters, as well as is most commonly used within the literature. While $CL_{int,total}$ takes into account all clearance processes occurring within the cell in order to determine an overall intrinsic clearance rate, CL_{uptake} is the primary determinant of clearance. It is assumed that permanent removal of drug from the cell occurs via either metabolism or biliary efflux, with drug effluxed from the cell back to the media ($CL_{sinusoidal}$) being the only clearance parameter that can subtract from the overall clearance rate. Therefore, $CL_{int,total} < CL_{uptake}$ when $CL_{sinusoidal} > 0$ (as $CL_{sinusoidal}$ increases, $CL_{int,total}$ decreases). However, both CL_{met} and CL_{bile} have a diminishing effect on $CL_{sinusoidal}$.

Several methods of determining efflux rates were investigated, with each used to determine $CL_{int,total}$. Each variation of $CL_{int,total}$ was compared to single clearance pathways (CL_{uptake} and CL_{met}) for both bias and precision of IVIVE. Uptake and metabolism data were taken from modelled data obtained in Chapter 4. Consideration was given to the use of uptake clearances produced in SCH within the $CL_{int,total}$ model. However, despite the marked improvement noted compared to data obtained from the literature for SCH, uptake clearances produced in the media loss assay produced more accurate results when used within the $CL_{int,total}$ model. While it would be advantageous to estimate all

clearance terms using the same assay format, the loss of CYP activity in SCH necessitates the use of an alternate assay system to determine metabolic clearance[112]. As such, there was no inherent benefit to the application of uptake rates from SCH over that produced in the media loss assay. CL_{uptake} and CL_{met} bias and precision, examined previously in Chapter 4, acted as benchmarks for comparison.

CL_{uptake} had a lower degree of bias than CL_{met} (GMFE = 2.96 compared to 6.40), but also lower precision (RMSE = 2559 compared to 915) when using standard physiological scaling factors. It was observed that $CL_{int,total}$ using methods 2 and 3 for calculation of CL_{bile} and $CL_{sinusoidal}$ provided an improvement in terms of bias and precision over CL_{uptake} and CL_{met}, with GMFE values of 2.74 and 2.71, respectively. Using media concentrations for CL_{bile} and $CL_{sinusoidal}$ resulted in a marginal increase to bias (GMFE = 2.99) compared to CL_{uptake}. All $CL_{int,total}$ terms produced comparable degrees of precision (measured using RMSE) compared to uptake. Overall, $CL_{int,total}$ (calculated using methods 2 or 3) produced predictions with lower bias than either CL_{uptake} or CL_{met}. However, it is unclear if the increase justifies the requirement to perform additional *in vitro* experiments from an IVIVE perspective.

As a final analysis, data from the various scaling approaches discussed in Chapter 3 were used to determine their effect on both GMFE and RMSE of CL_{uptake}, CL_{met} and $CL_{int,total}$. It was observed that use of $CL_{int,total}$, calculated using method 2 and scaled using the median required empirical physiological scaling factor for uptake and metabolism led to the lowest GMFE value of 2.63. This was a marginal improvement over the lowest recorded GMFE for CL_{uptake} alone, determined as 2.66, which was produced when scaled by the median required scaling factor. This provides evidence for the ability of empirical scaling factors outlined in Chapter 3 to improve IVIVE. However, as was noted for standard physiological scaling factors, from a purely IVIVE perspective, use of the CL_{uptake} term may be appropriate, avoiding the necessity for additional *in vitro* assays. However, several key parameters would not be obtained if the complete set of *in vitro* assays were not performed. The utility of this technique will therefore depend on the particular needs of the individual.

5.6. Conclusion

In conclusion, this chapter aimed to implement a mechanistic IVIVE approach, investigating the impact of including multiple clearance parameters for the prediction of *in vivo* clearance. SCH were used to generate biliary and sinusoidal efflux clearance and, along with CL_{uptake} and CL_{met} data from Chapter 4, were used to determine $CL_{int,total}$. $CL_{int,total}$ using CL_{bile} and $CL_{sinusoidal}$ data calculated with the methods 2 and 3 produced a bias lower than when using CL_{uptake} alone. It was also demonstrated that the application of alternative scaling factors can be successful in further reducing the observed bias, and are recommended for IVIVE of both single pathway clearance terms, as well as $CL_{int,total}$. Overall, it was concluded that from a purely IVIVE perspective, use of CL_{uptake} alone would be the most efficient method. However, as well as having marginally reducing bias when predicting *in vivo* clearance (compared to both CL_{uptake} and CL_{met}), use of $CL_{int,total}$ provides a more holistic overview of a drugs elimination pathways,.

Chapter 6. Final Discussion

The overall purpose of this thesis was to investigate the use of hepatocellular transport and metabolism assays for the prediction of *in vivo* clearance. This chapter will provide a brief overview of the studies carried out in this thesis, and discuss the main findings of each. Consideration will also be given to the applications, limitations and future perspectives of the studies that were performed.

6.1. Assessment of the predictive ability of CL_{uptake}

While large scale analyses have been common for metabolic clearance data, no analogous studies have been performed for data from uptake assays using rat or human hepatocytes. As a result, the general consensus within the literature and scientific community has appeared to be the assumption that CL_{uptake} generally under-predicts *in vivo* clearance for both species, as has been demonstrated for metabolic clearance data. With a number of assay formats available, the first aim of this thesis was to provide a holistic analysis of uptake clearance data, and assess the predictive accuracy of each system.

6.1.1. Observations in rat hepatocytes

Several differences were observed between rat and human hepatocytes, which necessitates a separate discussion for each species. With regards to rat hepatocytes, non-cultured formats (suspension and media loss) were generally seen to over-predict *in vivo* clearance, while cultured formats typically produced under-predictions. Of the compounds identified for each assay format, BDDCS Class 2 and/or neutral compounds were identified as being consistently over-predicted in non-cultured formats and, along with class 1 compounds, were frequently predicted well in monolayer. In contrast, far fewer proportions of class 3 and 4 compounds were over-predicted. This led to the hypothesis that rates of passive diffusion could be higher in an *in vitro* setting than that seen *in vivo*, contributing to a higher than expected rate of uptake. In the case of monolayer, where transporter function is expected to decrease over time in culture, it is possible that the increase in rate of diffusion compensates for the reduced transport, resulting in a higher proportion of successful predictions. For non-cultured format, where

active transport may have been maintained to a level similar to that *in vivo*, an over-estimation is feasible. Unfortunately, with the current dataset, it is impossible to explore this hypothesis in detail, as no distinction was made between active and passive uptake. It would also be necessary to compare rates of diffusion across assay formats, with a correction for cell surface area, to identify any variation. In the case of SCH, no additional information can be obtained due to the severity of under-prediction. It is therefore concluded that SCH are highly inappropriate for predicting *in vivo* clearance using uptake data. Selection of an appropriate system must consider the compound in question. If the BDDCS class is known, the suspension, media loss or monolayer assay can be selected as appropriate. If no information if known for the compound, it is recommended that monolayer assays be used to estimate CL_{uptake}.

With this initial analysis as a baseline, the next aim was to explore the effect of various scaling factors. Differences in physiological values were noted in the literature, and combinations used to generate minimum and maximum possible physiological scaling factors. In addition, several empirical scaling factors were calculated using the data collected. Overall, it was concluded that for physiological scaling factors, use of the minimum calculated physiological value produced more accurate predictions for the non-cultured formats, while cultured formats benefitted from the use of the maximum calculated physiological scaling value. Of the static empirical scaling values, the median required scaling factor was seen to produce the largest reduction in bias. The use of CDSF resulted in the lowest observed bias compared to all scaling approaches for each of the 4 assay formats. It is apparent that choice of scaling factor is highly influential over the outcome of predictions and no particular scaling factor can be fully advocated. Based on the current dataset, CDSF may be a useful methodology for *in vitro* data scaling in future, however improvements are still observed for other static empirical scaling methods discussed, and should also be considered.

6.1.2. Observations in human hepatocytes

Although the studies performed throughout this thesis focus on rat hepatocytes, a database of human hepatocytes was generated and analysed in order to create an initial platform for future work along a similar line of investigation. In addition, the analysis

provides valuable information which may be of considerable interest for those routinely using human hepatocytes for assessing uptake. No data were identified for the media loss assay, and so were omitted from this analysis.

The findings for suspension, monolayer and SCH differed from that observed in the rat. For all assay formats, CL_{uptake} had a clear tendency to under-predict the observed *in vivo* clearance. However, GMFE values remained similar to rat for both suspension and monolayer, while SCH was considerably better for human hepatocytes. Another key difference was a lower bias noted for suspension assays compared to monolayer. No clear trends were identified in terms of BDDCS or ionisation character for humans. As with rat, no distinction was made between active and passive uptake and, as such, it cannot be determined if there is a difference in proportion of active transport between species for each compound. From this analysis, it would be recommended that the suspension format be used for human hepatocytes.

Variations in scaling factor and empirical scaling methods described for rat were also investigated for human hepatocytes. Less variation was noted for physiological scaling factors in terms of the range of values, however the ratio between minimum and maximum physiological scaling factor remained consistent. The overall effect on *in vitro* predictions was much less pronounced. Use of the median required scaling factor was beneficial for monolayer and SCH assays, while no change was noted for suspension. Correlations used to determine CDSF were found not to be significant for any of the assay formats in human. Nevertheless, CDSF were applied as it was reasoned that they would act as a non-static empirical scaling factor. No improvement over standard physiological scaling methods was noted for suspension, however large improvements were noted for both monolayer and SCH. Based on these observations, use of median or CDSF scaling methods would be recommended to provide the most accurate *in vivo* predictions.

6.2. Development of the media loss assay

At present, the widespread and routine study of drug uptake is hindered by the labour and time-intensive nature of hepatocyte uptake assays. Of the assays discussed in

Chapter 3, the media loss assay was identified as having the potential to be optimized into a higher throughput system. It was hypothesised that, if this were possible, the assay would be open to a wide range of applications, including experimental conditions which would enable the generation of a number of clearance parameters and drug properties from a single assay.

The move to a higher throughput system was successful through minor changes to the standard protocols presented by both Soars et al.[1] and Jigorel et al.[88], which in turn allowed the assay to be performed in a 96-well plate format, rather than single Eppendorf tubes. The use of multiple wells allows for a variety of different assay conditions. For example, it is now possible to test ranges of concentrations, the effect of the inclusion of inhibitors, or simply to screen several drugs, all within a single assay.

For this thesis, the inclusion of transporter (Rfc) and metabolic (ABT) inhibitors was investigated further. Previous *in vitro* data were used to categorise drugs, for which data were available, into 4 groups, separated by their degree of active transport and rate of metabolism. This ensured a range of rates and contribution of active transport for CL_{met} and CL_{uptake}, respectively, were represented by the compounds selected. The inclusion of inhibitors had a clear effect on the measured CL_{int}, depending on the compound, indicating successful inhibition of either uptake or metabolism. Data were entered into a two-compartmental model, which generated estimated values for the active transport, passive diffusion, metabolic clearance and apparent cellular volume. In turn, these values were used to determine the partitioning parameters Kp and Kp_u, and the fu_{cell}. Compounds generally had both the expected depletion profiles, based on grouping and literature values for proportion of active transport, and degree of intracellular binding. Group 2 compounds indinavir, clarithromycin and repaglinide were exceptions, and did not conform to the expected high degree of active transport that had been previously demonstrated in the literature. It is unclear why this was the case, and may require further investigations using compounds with similar properties. Significant correlations were identified between $LogD_{7.4}$ and $CL_{passive}$ and CL_{met}, as well as between $CL_{passive}$ and CL_{active}. These relationships could allow for initial estimates of compound parameters before commencement of *in vitro* experiments, and are recommended to be used to

determine the likely incubation times required for the assay. For example, high clearance compounds are likely to require only a short incubation time, and so sampling times should be condensed to allow for this.

Finally, data were used in a single parameter IVIVE approach to compare predictions to that typically expected for the media loss assay based on Chapter 3. Using standard physiological scaling factors, the assay was consistent with the findings of the literature analysis. CL_{met} data typically produced under-prediction of *in vivo* clearance, while CL_{uptake} primarily over-predicted. Bias was highest for CL_{met}, while GMFE was lower for CL_{uptake} than values obtained from literature data in Chapter 3 for any assay format. It was noted, however, that prediction accuracy was highly dependent on the compound group. For example, for group 1, which was expected to have high proportions of active transport and only limited rates of metabolism, CL_{uptake} successfully predicted *in vivo* clearance for 3 of the 4 compounds. In contrast, CL_{met} under-predicted by 20- to 200-fold. Conversely, group 4 compounds, expected to have lower proportions of active transport but high rates of metabolism, were all over-predicted using CL_{uptake} but were within 2-fold of the observed *in vivo* clearance when scaling CL_{met}. It is therefore apparent that use of a single clearance parameter may not always be appropriate, and warrants an investigation into using a more mechanistic approach.

Overall, it has been demonstrated that the media loss assay is a highly useful tool for generating several clearance parameters from a single *in vitro* assay for rat hepatocytes. Although this investigation focused on the use of inhibitors to separate out individual processes, the assay is versatile and will accommodate several applications. For example, investigating a range of concentrations would be of interest to further extend on the work performed by Jigorel et al. [88], who generated V_{max} and K_m estimates for uptake using 3 drug concentrations. As an example of the utility of the assay, up to 12 concentrations for 4 separate drugs could be performed within a single assay. Further investigation is also required to determine the suitability of the assay for human hepatocytes. During the development of the assay in its current format, minimum volumes were determined with the intention of reducing the burden on cell number, should the assay be performed with human hepatocytes. With the expense involved with

the use of human hepatocytes, it is important to be efficient with the use of reagents in order to ensure the assay is financially viable. It remains to be seen if depletion profiles can be recorded in human hepatocytes under these optimised conditions, given that rates are typically lower than their rat counterparts.

6.3. Use of SCH to assess the validity of integrating multiple system parameters within a single clearance term

Following from observations of the media loss assay in Chapter 4, it was demonstrated that the accuracy of clearance parameters are highly dependent on properties of a compound. A more mechanistic approach was therefore hypothesised to encompass several clearance terms, and result in an overall higher prediction accuracy. This approach had been demonstrated recently by Umehara and Camenisch[129], who incorporated data from several *in vitro* assays into a total intrinsic clearance term. This was found to have higher correlation to observed *in vivo* clearances compared to individual clearance terms. Therefore, the purpose of this chapter was to generate efflux data using SCH and to combine this with uptake and metabolism data generated in Chapter 4, using the $CL_{int,total}$ term. $CL_{int,total}$ was compared to individual clearance parameters (CL_{met} and CL_{uptake}) to determine if predictions were improved. As a final analysis, the various scaling factors outlined in Chapter 3 were applied to assess if further improvements could be made.

In this study, three methods of calculation were used to determine both biliary and sinusoidal efflux. Method 1 calculated efflux rates based on the total concentration of drug present in the media, which is traditionally used for the calculation of CL_{bile}. Method 2 used the unbound concentration of drug in the cell, and is theoretically more appropriate, since clearance would be driven by the drug available within the cell. Method 3 was based on the method proposed by Cantrill and Houston[159], which also uses unbound cell concentrations, however these were calculated using Kp_u data to determine the driving concentration. In this study, Kp_u values determined in the media loss assay were used. With such limited *in vivo* data available for biliary clearance, and with sinusoidal efflux being challenging to measure, it is difficult to compare these clearance terms to determine which method is more appropriate. Four of the compounds studied had rat *in vivo* biliary clearance rates available in the literature, and sufficed for a

basic comparison. Using media concentrations (method 1), CL_{bile} was seen to over-predict *in vivo* biliary clearance for 3 of the 4 compounds for which data were available. In contrast, using unbound cellular drug concentrations (method 2) or Kp_u (method 3) to calculate efflux rates, CL_{bile} was predominantly under-predicted. Method 3 was observed to produce the least bias, with a GMFE of 2.99. However, all methods used in this study contradict what is generally seen in the literature. Despite the observation that *in vivo* biliary clearance was under-predicted using methods 2 and 3, this was less pronounced than typically seen in the literature (where fold error is expected to be 0.1 – 0.004).

A possible explanation for these observations comes from the recorded uptake rates for SCH within this study, which were much higher in comparison to literature data presented in Chapter 3. Following IVIVE, CL_{uptake} from the SCH assay produced a GMFE of 3.23, with 42% of the compounds predicted within 2-fold of the observed *in vivo* clearance. Direct comparison of drugs for which literature data were available found that the present study produced uptake clearances on average 3-fold higher than have been observed in the literature. It has previously been argued that reduced uptake may contribute to the under-prediction of CL_{bile}, since less drug would be available for efflux than in an *in vivo* environment. It is possible that in the present study this issue was less apparent, leading to the higher than expected biliary clearance rates. However, there is no explanation as to why this may be the case.

Investigation of the $CL_{int,total}$ term found a modest improvement for prediction of *in vivo* clearance in comparison to using single elimination pathways. Use of efflux clearances calculated using methods 2 and 3 produced lower degrees of bias than CL_{uptake} and CL_{met} alone. This largest improvement was observed for method 3 (GMFE = 2.71 compared to 2.96 for CL_{uptake} and 6.40 for CL_{met}). Scaling factors investigated in Chapter 3 were also applied to assess if further improvements could be made to the observed bias. Of the combinations tested, the most improvement (determined from the lowest GMFE value) was noted when using $CL_{int,total}$ (method 3) scaled using the median required empirical scaling factor, producing a GMFE of 2.63. However, using either the minimum physiological or the median required scaling factor, CL_{uptake} had a GMFE of 2.66.

Overall, the recommendations from this chapter are that CL_{uptake} data, generated using the media loss assay, provides the most efficient way to produce predictions of *in vivo* clearance with a relatively low degree of bias. However, predictions using $CL_{int,total}$ on average produce the lowest amount of bias, as well as providing an overview of the potential clearance routes of a drug. If this information, as well as binding/partitioning characteristics are unknown for a particular drug, this method could also provide additional information to guide future studies.

6.4. Summary

While previous studies have analysed the predictive ability of metabolic clearance, this study provides the first extensive investigation into the use of uptake clearance as a predictor of *in vivo* clearance in multiple assay formats. It is evident that, for rat hepatocytes, non-cultured systems have a clear tendency to over-predict *in vivo* clearance, which contrasts with the general expectation of under-prediction associated with predictive pharmacokinetics. However, in cultured hepatocyte assays, as well as *in vitro* experiments using human hepatocytes, the majority of drugs are under-predicted. A number of approaches for scaling of data were analysed, and may prove as useful tools for the scaling of future *in vitro* data.

With evidence from Chapter 3 that use of uptake clearance data as a predictor of *in vivo* clearance generally produces lower bias than the use of metabolic clearance data, the only limitation remaining for the widespread use of uptake assays is the time and resources required. Metabolic assays are particularly popular due to their ease and applicability to rapid screening. A key aim of this thesis was to develop an assay capable of measuring uptake clearance in a higher throughput fashion than is available with the current assay formats. This was successful for the media loss assay, which provided the additional benefit of measuring metabolic clearance within the same assay. Inclusion of transporter and metabolic inhibitors enabled the application of mathematical model, making it possible to estimate several clearance parameters. Prediction of *in vivo* clearance was then shifted from cellular scaling to a mechanistic approach, incorporating data from two *in vitro* assays to take into account multiple clearance pathways. This

method produced a lower degree of bias than was noted for uptake or metabolism data alone, however the improvement was relatively small.

As a final conclusion, the work presented in this thesis provides compelling evidence for the usefulness of hepatocyte uptake data, as well as presenting methods for both the production and scaling of data in order to maximise predictive accuracy. The methods presented are also capable of estimating several key pharmacokinetic parameters. Although these may not always be useful in a quantitative fashion, they remain essential considerations in regards to the overall properties of a compound, and can be used to predict its behaviour within the body. The work carried out also lays the foundation for several future lines of enquiry. Most importantly, a transition from rat to human hepatocytes will be key to determine the usefulness for prediction of human *in vivo* clearance. In conjunction with the human uptake database presented here, a similar set of analyses has the potential to lead to methods suitable for the improvement of human *in vivo* clearance predictions.

References

1. Soars, M.G., K. Grime, J.L. Sproston, P.J. Webborn, and R.J. Riley, *Use of hepatocytes to assess the contribution of hepatic uptake to clearance in vivo.* Drug Metab Dispos, 2007. **35**(6): p. 859-65.
2. Paul, S.M., D.S. Mytelka, C.T. Dunwiddie, C.C. Persinger, B.H. Munos, S.R. Lindborg, and A.L. Schacht, *How to improve R&D productivity: the pharmaceutical industry's grand challenge.* Nat Rev Drug Discov, 2010. **9**(3): p. 203-14.
3. Walker, D.K., *The use of pharmacokinetic and pharmacodynamic data in the assessment of drug safety in early drug development.* Br J Clin Pharmacol, 2004. **58**(6): p. 601-8.
4. Mahmood, I., *Allometric issues in drug development.* J Pharm Sci, 1999. **88**(11): p. 1101-6.
5. Houston, J.B., *Utility of in vitro drug metabolism data in predicting in vivo metabolic clearance.* Biochem Pharmacol, 1994. **47**(9): p. 1469-79.
6. Rane, A., G.R. Wilkinson, and D.G. Shand, *Prediction of hepatic extraction ratio from in vitro measurement of intrinsic clearance.* J Pharmacol Exp Ther, 1977. **200**(2): p. 420-4.
7. Rowland, M., L.Z. Benet, and G.G. Graham, *Clearance concepts in pharmacokinetics.* J Pharmacokinet Biopharm, 1973. **1**(2): p. 123-36.
8. Kola, I. and J. Landis, *Can the pharmaceutical industry reduce attrition rates?* Nat Rev Drug Discov, 2004. **3**(8): p. 711-5.
9. Frevert, U., S. Engelmann, S. Zougbede, J. Stange, B. Ng, K. Matuschewski, L. Liebes, and H. Yee, *Intravital observation of Plasmodium berghei sporozoite infection of the liver.* PLoS Biol, 2005. **3**(6): p. e192.
10. Hagenbuch, B. and P.J. Meier, *Organic anion transporting polypeptides of the OATP/ SLC21 family: phylogenetic classification as OATP/ SLCO superfamily, new nomenclature and molecular/functional properties.* Pflugers Arch, 2004. **447**(5): p. 653-65.
11. Roth, M., A. Obaidat, and B. Hagenbuch, *OATPs, OATs and OCTs: the organic anion and cation transporters of the SLCO and SLC22A gene superfamilies.* Br J Pharmacol, 2012. **165**(5): p. 1260-87.
12. Konig, J., *Uptake transporters of the human OATP family: molecular characteristics, substrates, their role in drug-drug interactions, and functional consequences of polymorphisms.* Handb Exp Pharmacol, 2011(201): p. 1-28.
13. Hagenbuch, B. and C. Gui, *Xenobiotic transporters of the human organic anion transporting polypeptides (OATP) family.* Xenobiotica, 2008. **38**(7-8): p. 778-801.
14. Pang, K.S., A.D. Rodrigues, R. Peter, and SpringerLink, *Enzyme- and Transporter-Based Drug-Drug Interactions*. 2010.
15. Giacomini, K.M., S.M. Huang, D.J. Tweedie, L.Z. Benet, K.L. Brouwer, X. Chu, A. Dahlin, R. Evers, V. Fischer, K.M. Hillgren, K.A. Hoffmaster, T. Ishikawa, D. Keppler, R.B. Kim, C.A. Lee, M. Niemi, J.W. Polli, Y. Sugiyama, P.W. Swaan, J.A. Ware, S.H. Wright, S.W. Yee, M.J. Zamek-Gliszczynski, L. Zhang, and I.T. Consortium, *Membrane transporters in drug development.* Nat Rev Drug Discov, 2010. **9**(3): p. 215-36.
16. Kajosaari, L.I., M. Niemi, M. Neuvonen, J. Laitila, P.J. Neuvonen, and J.T. Backman, *Cyclosporine markedly raises the plasma concentrations of repaglinide.* Clin Pharmacol Ther, 2005. **78**(4): p. 388-99.
17. Nishizato, Y., I. Ieiri, H. Suzuki, M. Kimura, K. Kawabata, T. Hirota, H. Takane, S. Irie, H. Kusuhara, Y. Urasaki, A. Urae, S. Higuchi, K. Otsubo, and Y. Sugiyama, *Polymorphisms of OATP-C (SLC21A6) and OAT3 (SLC22A8) genes: consequences for pravastatin pharmacokinetics.* Clin Pharmacol Ther, 2003. **73**(6): p. 554-65.
18. Koepsell, H. and H. Endou, *The SLC22 drug transporter family.* Pflugers Arch, 2004. **447**(5): p. 666-76.
19. Zolk, O., T.F. Solbach, J. Konig, and M.F. Fromm, *Functional characterization of the human organic cation transporter 2 variant p.270Ala>Ser.* Drug Metab Dispos, 2009. **37**(6): p. 1312-8.

20. Nies, A.T., H. Koepsell, K. Damme, and M. Schwab, *Organic cation transporters (OCTs, MATEs), in vitro and in vivo evidence for the importance in drug therapy.* Handb Exp Pharmacol, 2011(201): p. 105-67.
21. Shu, Y., S.A. Sheardown, C. Brown, R.P. Owen, S. Zhang, R.A. Castro, A.G. Ianculescu, L. Yue, J.C. Lo, E.G. Burchard, C.M. Brett, and K.M. Giacomini, *Effect of genetic variation in the organic cation transporter 1 (OCT1) on metformin action.* J Clin Invest, 2007. **117**(5): p. 1422-31.
22. Stamer, U.M., F. Musshoff, F. Stuber, J. Brockmoller, M. Steffens, and M.V. Tzvetkov, *Loss-of-function polymorphisms in the organic cation transporter OCT1 are associated with reduced postoperative tramadol consumption.* Pain, 2016. **157**(11): p. 2467-2475.
23. Kobayashi, Y., N. Ohshiro, R. Sakai, M. Ohbayashi, N. Kohyama, and T. Yamamoto, *Transport mechanism and substrate specificity of human organic anion transporter 2 (hOat2 [SLC22A7]).* J Pharm Pharmacol, 2005. **57**(5): p. 573-8.
24. Cunningham, R.F., Z.H. Israili, and P.G. Dayton, *Clinical pharmacokinetics of probenecid.* Clin Pharmacokinet, 1981. **6**(2): p. 135-51.
25. Stieger, B., *The role of the sodium-taurocholate cotransporting polypeptide (NTCP) and of the bile salt export pump (BSEP) in physiology and pathophysiology of bile formation.* Handb Exp Pharmacol, 2011(201): p. 205-59.
26. Yanni, S.B., P.F. Augustijns, D.K. Benjamin, Jr., K.L. Brouwer, D.R. Thakker, and P.P. Annaert, *In vitro investigation of the hepatobiliary disposition mechanisms of the antifungal agent micafungin in humans and rats.* Drug Metab Dispos, 2010. **38**(10): p. 1848-56.
27. Ho, R.H., R.G. Tirona, B.F. Leake, H. Glaeser, W. Lee, C.J. Lemke, Y. Wang, and R.B. Kim, *Drug and bile acid transporters in rosuvastatin hepatic uptake: function, expression, and pharmacogenetics.* Gastroenterology, 2006. **130**(6): p. 1793-806.
28. Li, W., *The hepatitis B virus receptor.* Annu Rev Cell Dev Biol, 2015. **31**: p. 125-47.
29. Wakabayashi, K., A. Tamura, H. Saito, Y. Onishi, and T. Ishikawa, *Human ABC transporter ABCG2 in xenobiotic protection and redox biology.* Drug Metab Rev, 2006. **38**(3): p. 371-91.
30. Lee, C.A., M.A. O'Connor, T.K. Ritchie, A. Galetin, J.A. Cook, I. Ragueneau-Majlessi, H. Ellens, B. Feng, M.E. Taub, M.F. Paine, J.W. Polli, J.A. Ware, and M.J. Zamek-Gliszczynski, *Breast cancer resistance protein (ABCG2) in clinical pharmacokinetics and drug interactions: practical recommendations for clinical victim and perpetrator drug-drug interaction study design.* Drug Metab Dispos, 2015. **43**(4): p. 490-509.
31. Jin, M.S., M.L. Oldham, Q. Zhang, and J. Chen, *Crystal structure of the multidrug transporter P-glycoprotein from Caenorhabditis elegans.* Nature, 2012. **490**(7421): p. 566-9.
32. Konig, J., F. Muller, and M.F. Fromm, *Transporters and drug-drug interactions: important determinants of drug disposition and effects.* Pharmacol Rev, 2013. **65**(3): p. 944-66.
33. Fletcher, J.I., M. Haber, M.J. Henderson, and M.D. Norris, *ABC transporters in cancer: more than just drug efflux pumps.* Nat Rev Cancer, 2010. **10**(2): p. 147-56.
34. Fenster, P.E., W.D. Hager, D. Perrier, J.R. Powell, P.E. Graves, and U.F. Michael, *Digoxin-quinidine interaction in patients with chronic renal failure.* Circulation, 1982. **66**(6): p. 1277-80.
35. Brinkmann, U. and M. Eichelbaum, *Polymorphisms in the ABC drug transporter gene MDR1.* Pharmacogenomics J, 2001. **1**(1): p. 59-64.
36. Kurata, Y., I. Ieiri, M. Kimura, T. Morita, S. Irie, A. Urae, S. Ohdo, H. Ohtani, Y. Sawada, S. Higuchi, and K. Otsubo, *Role of human MDR1 gene polymorphism in bioavailability and interaction of digoxin, a substrate of P-glycoprotein.* Clin Pharmacol Ther, 2002. **72**(2): p. 209-19.
37. Konig, J., A.T. Nies, Y. Cui, I. Leier, and D. Keppler, *Conjugate export pumps of the multidrug resistance protein (MRP) family: localization, substrate specificity, and MRP2-mediated drug resistance.* Biochim Biophys Acta, 1999. **1461**(2): p. 377-94.

38. Borst, P., R. Evers, M. Kool, and J. Wijnholds, *The multidrug resistance protein family.* Biochim Biophys Acta, 1999. **1461**(2): p. 347-57.
39. Jedlitschky, G., I. Leier, U. Buchholz, J. Hummel-Eisenbeiss, B. Burchell, and D. Keppler, *ATP-dependent transport of bilirubin glucuronides by the multidrug resistance protein MRP1 and its hepatocyte canalicular isoform MRP2.* Biochem J, 1997. **327 (Pt 1)**: p. 305-10.
40. Cui, Y., J. Konig, J.K. Buchholz, H. Spring, I. Leier, and D. Keppler, *Drug resistance and ATP-dependent conjugate transport mediated by the apical multidrug resistance protein, MRP2, permanently expressed in human and canine cells.* Mol Pharmacol, 1999. **55**(5): p. 929-37.
41. Ellis, L.C., G.M. Hawksworth, and R.J. Weaver, *ATP-dependent transport of statins by human and rat MRP2/Mrp2.* Toxicol Appl Pharmacol, 2013. **269**(2): p. 187-94.
42. Rau, T., B. Erney, R. Gores, T. Eschenhagen, J. Beck, and T. Langer, *High-dose methotrexate in pediatric acute lymphoblastic leukemia: impact of ABCC2 polymorphisms on plasma concentrations.* Clin Pharmacol Ther, 2006. **80**(5): p. 468-76.
43. Weiss, J., D. Theile, N. Ketabi-Kiyanvash, H. Lindenmaier, and W.E. Haefeli, *Inhibition of MRP1/ABCC1, MRP2/ABCC2, and MRP3/ABCC3 by nucleoside, nucleotide, and non-nucleoside reverse transcriptase inhibitors.* Drug Metab Dispos, 2007. **35**(3): p. 340-4.
44. Kivisto, K.T. and M. Niemi, *Influence of drug transporter polymorphisms on pravastatin pharmacokinetics in humans.* Pharm Res, 2007. **24**(2): p. 239-47.
45. Wojnowski, L., B. Kulle, M. Schirmer, G. Schluter, A. Schmidt, A. Rosenberger, S. Vonhof, H. Bickeboller, M.R. Toliat, E.K. Suk, M. Tzvetkov, A. Kruger, S. Seifert, M. Kloess, H. Hahn, M. Loeffler, P. Nurnberg, M. Pfreundschuh, L. Trumper, J. Brockmoller, and G. Hasenfuss, *NAD(P)H oxidase and multidrug resistance protein genetic polymorphisms are associated with doxorubicin-induced cardiotoxicity.* Circulation, 2005. **112**(24): p. 3754-62.
46. Kock, K. and K.L. Brouwer, *A perspective on efflux transport proteins in the liver.* Clin Pharmacol Ther, 2012. **92**(5): p. 599-612.
47. Rowland, M. and T.N. Tozer, *Clinical Pharmacokinetics and Pharmacodynamics: Chapter 5: Elimination*. 4th ed. 2011: Lippincott Williams & Wilkins.
48. Rowland, M. and T.N. Tozer, *Clinical Pharmacokinetics and Pharmacodynamics: Chapter 2: Fundamental Concepts and Terminology*. 4th ed. 2011: Lippincott Williams & Wilkins.
49. Yengi, L.G., L. Leung, and J. Kao, *The evolving role of drug metabolism in drug discovery and development.* Pharm Res, 2007. **24**(5): p. 842-58.
50. Ohtsuki, S., O. Schaefer, H. Kawakami, T. Inoue, S. Liehner, A. Saito, N. Ishiguro, W. Kishimoto, E. Ludwig-Schwellinger, T. Ebner, and T. Terasaki, *Simultaneous absolute protein quantification of transporters, cytochromes P450, and UDP-glucuronosyltransferases as a novel approach for the characterization of individual human liver: comparison with mRNA levels and activities.* Drug Metab Dispos, 2012. **40**(1): p. 83-92.
51. Smith, G., M.J. Stubbins, L.W. Harries, and C.R. Wolf, *Molecular genetics of the human cytochrome P450 monooxygenase superfamily.* Xenobiotica, 1998. **28**(12): p. 1129-65.
52. Nelson, D.R., *The cytochrome p450 homepage.* Hum Genomics, 2009. **4**(1): p. 59-65.
53. Lin, J.H. and A.Y. Lu, *Inhibition and induction of cytochrome P450 and the clinical implications.* Clin Pharmacokinet, 1998. **35**(5): p. 361-90.
54. Hull, M.W. and J.S. Montaner, *Ritonavir-boosted protease inhibitors in HIV therapy.* Ann Med, 2011. **43**(5): p. 375-88.
55. Sinz, M., G. Wallace, and J. Sahi, *Current industrial practices in assessing CYP450 enzyme induction: preclinical and clinical.* AAPS J, 2008. **10**(2): p. 391-400.
56. Mueller, S.C., J. Majcher-Peszynska, B. Uehleke, S. Klammt, R.G. Mundkowski, W. Miekisch, H. Sievers, S. Bauer, B. Frank, G. Kundt, and B. Drewelow, *The extent of induction of CYP3A by St. John's wort varies among products and is linked to hyperforin dose.* Eur J Clin Pharmacol, 2006. **62**(1): p. 29-36.

57. Zanger, U.M. and M. Schwab, *Cytochrome P450 enzymes in drug metabolism: regulation of gene expression, enzyme activities, and impact of genetic variation.* Pharmacol Ther, 2013. **138**(1): p. 103-41.
58. Benowitz, N.L., C.N. Lessov-Schlaggar, G.E. Swan, and P. Jacob, 3rd, *Female sex and oral contraceptive use accelerate nicotine metabolism.* Clin Pharmacol Ther, 2006. **79**(5): p. 480-8.
59. Itoh, M., M. Nakajima, E. Higashi, R. Yoshida, K. Nagata, Y. Yamazoe, and T. Yokoi, *Induction of human CYP2A6 is mediated by the pregnane X receptor with peroxisome proliferator-activated receptor-gamma coactivator 1alpha.* J Pharmacol Exp Ther, 2006. **319**(2): p. 693-702.
60. Kubota, T., C. Nakajima-Taniguchi, T. Fukuda, M. Funamoto, M. Maeda, E. Tange, R. Ueki, K. Kawashima, H. Hara, Y. Fujio, and J. Azuma, *CYP2A6 polymorphisms are associated with nicotine dependence and influence withdrawal symptoms in smoking cessation.* Pharmacogenomics J, 2006. **6**(2): p. 115-9.
61. Fujita, K., W. Yamamoto, S. Endo, H. Endo, F. Nagashima, W. Ichikawa, R. Tanaka, T. Miya, K. Araki, K. Kodama, Y. Sunakawa, M. Narabayashi, K. Miwa, Y. Ando, Y. Akiyama, K. Kawara, T. Kamataki, and Y. Sasaki, *CYP2A6 and the plasma level of 5-chloro-2, 4-dihydroxypyridine are determinants of the pharmacokinetic variability of tegafur and 5-fluorouracil, respectively, in Japanese patients with cancer given S-1.* Cancer Sci, 2008. **99**(5): p. 1049-54.
62. Rahnasto, M., C. Wittekindt, R.O. Juvonen, M. Turpeinen, A. Petsalo, O. Pelkonen, A. Poso, G. Stahl, H.D. Holtje, and H. Raunio, *Identification of inhibitors of the nicotine metabolising CYP2A6 enzyme--an in silico approach.* Pharmacogenomics J, 2008. **8**(5): p. 328-38.
63. Hodgson, E. and R.L. Rose, *The importance of cytochrome P450 2B6 in the human metabolism of environmental chemicals.* Pharmacol Ther, 2007. **113**(2): p. 420-8.
64. Rotger, M., H. Tegude, S. Colombo, M. Cavassini, H. Furrer, L. Decosterd, J. Blievernicht, T. Saussele, H.F. Gunthard, M. Schwab, M. Eichelbaum, A. Telenti, and U.M. Zanger, *Predictive value of known and novel alleles of CYP2B6 for efavirenz plasma concentrations in HIV-infected individuals.* Clin Pharmacol Ther, 2007. **81**(4): p. 557-66.
65. Sachse, C., J. Brockmoller, S. Bauer, and I. Roots, *Cytochrome P450 2D6 variants in a Caucasian population: allele frequencies and phenotypic consequences.* Am J Hum Genet, 1997. **60**(2): p. 284-95.
66. Dahl, M.L., I. Johansson, L. Bertilsson, M. Ingelman-Sundberg, and F. Sjoqvist, *Ultrarapid hydroxylation of debrisoquine in a Swedish population. Analysis of the molecular genetic basis.* J Pharmacol Exp Ther, 1995. **274**(1): p. 516-20.
67. Zhou, S.F., J.P. Liu, and B. Chowbay, *Polymorphism of human cytochrome P450 enzymes and its clinical impact.* Drug Metab Rev, 2009. **41**(2): p. 89-295.
68. Kolars, J.C., K.S. Lown, P. Schmiedlin-Ren, M. Ghosh, C. Fang, S.A. Wrighton, R.M. Merion, and P.B. Watkins, *CYP3A gene expression in human gut epithelium.* Pharmacogenetics, 1994. **4**(5): p. 247-59.
69. Forrester, L.M., C.J. Henderson, M.J. Glancey, D.J. Back, B.K. Park, S.E. Ball, N.R. Kitteringham, A.W. McLaren, J.S. Miles, P. Skett, and et al., *Relative expression of cytochrome P450 isoenzymes in human liver and association with the metabolism of drugs and xenobiotics.* Biochem J, 1992. **281 (Pt 2)**: p. 359-68.
70. Kato, M., *Intestinal first-pass metabolism of CYP3A4 substrates.* Drug Metab Pharmacokinet, 2008. **23**(2): p. 87-94.
71. Scott, E.E. and J.R. Halpert, *Structures of cytochrome P450 3A4.* Trends Biochem Sci, 2005. **30**(1): p. 5-7.
72. Westlind-Johnsson, A., R. Hermann, A. Huennemeyer, B. Hauns, G. Lahu, N. Nassr, K. Zech, M. Ingelman-Sundberg, and O. von Richter, *Identification and characterization of CYP3A4*20, a novel rare CYP3A4 allele without functional activity.* Clin Pharmacol Ther, 2006. **79**(4): p. 339-49.

73. Greenblatt, D.J., P. He, L.L. von Moltke, and M.H. Court, *Chapter 11 The CYP3 Family*, in *Cytochromes P450: Role in the Metabolism and Toxicity of Drugs and other Xenobiotics*. 2008, The Royal Society of Chemistry. p. 354-383.
74. Preissner, S., K. Kroll, M. Dunkel, C. Senger, G. Goldsobel, D. Kuzman, S. Guenther, R. Winnenburg, M. Schroeder, and R. Preissner, *SuperCYP: a comprehensive database on Cytochrome P450 enzymes including a tool for analysis of CYP-drug interactions.* Nucleic Acids Res, 2010. **38**(Database issue): p. D237-43.
75. Yeo, K.R., A. Rostami-Hodjegan, and G.T. Tucker, *Abundance of cytochromes P450 in human liver: a meta-analysis*. 2003, British Pharmacological Society.
76. Kobayashi, K., K. Urashima, N. Shimada, and K. Chiba, *Substrate specificity for rat cytochrome P450 (CYP) isoforms: screening with cDNA-expressed systems of the rat.* Biochem Pharmacol, 2002. **63**(5): p. 889-96.
77. Guengerich, F.P., *Comparisons of catalytic selectivity of cytochrome P450 subfamily enzymes from different species.* Chem Biol Interact, 1997. **106**(3): p. 161-82.
78. Jancova, P., P. Anzenbacher, and E. Anzenbacherova, *Phase II drug metabolizing enzymes.* Biomed Pap Med Fac Univ Palacky Olomouc Czech Repub, 2010. **154**(2): p. 103-16.
79. Jancova, P. and M. Siller, *Phase II Drug Metabolism, Topics on Drug Metabolism*, J. Paxton, Editor. 2012, InTech.
80. Eriksson, L.C., J.W. DePierre, and G. Dallner, *Preparation and properties of microsomal fractions.* Pharmacology & Therapeutics. Part A: Chemotherapy, Toxicology and Metabolic Inhibitors, 1978. **2**(2): p. 281-317.
81. Rodrigues, A.D. and J.H. Lin, *Screening of drug candidates for their drug--drug interaction potential.* Curr Opin Chem Biol, 2001. **5**(4): p. 396-401.
82. Chao, P., A.S. Uss, and K.C. Cheng, *Use of intrinsic clearance for prediction of human hepatic clearance.* Expert Opin Drug Metab Toxicol, 2010. **6**(2): p. 189-98.
83. Hallifax, D., J.A. Foster, and J.B. Houston, *Prediction of human metabolic clearance from in vitro systems: retrospective analysis and prospective view.* Pharm Res, 2010. **27**(10): p. 2150-61.
84. Brown, H.S., A. Chadwick, and J.B. Houston, *Use of isolated hepatocyte preparations for cytochrome P450 inhibition studies: comparison with microsomes for Ki determination.* Drug Metab Dispos, 2007. **35**(11): p. 2119-26.
85. Brouwer, K.L., D. Keppler, K.A. Hoffmaster, D.A. Bow, Y. Cheng, Y. Lai, J.E. Palm, B. Stieger, R. Evers, and I.T. Consortium, *In vitro methods to support transporter evaluation in drug discovery and development.* Clin Pharmacol Ther, 2013. **94**(1): p. 95-112.
86. Berry, M.N. and D.S. Friend, *High-yield preparation of isolated rat liver parenchymal cells: a biochemical and fine structural study.* J Cell Biol, 1969. **43**(3): p. 506-20.
87. Griffin, S.J. and J.B. Houston, *Comparison of fresh and cryopreserved rat hepatocyte suspensions for the prediction of in vitro intrinsic clearance.* Drug Metab Dispos, 2004. **32**(5): p. 552-8.
88. Jigorel, E. and J.B. Houston, *Utility of drug depletion-time profiles in isolated hepatocytes for accessing hepatic uptake clearance: identifying rate-limiting steps and role of passive processes.* Drug Metab Dispos, 2012. **40**(8): p. 1596-602.
89. Jones, H.M., H.A. Barton, Y. Lai, Y.A. Bi, E. Kimoto, S. Kempshall, S.C. Tate, A. El-Kattan, J.B. Houston, A. Galetin, and K.S. Fenner, *Mechanistic pharmacokinetic modeling for the prediction of transporter-mediated disposition in humans from sandwich culture human hepatocyte data.* Drug Metab Dispos, 2012. **40**(5): p. 1007-17.
90. Nordell, P., P. Svanberg, J. Bird, and K. Grime, *Predicting metabolic clearance for drugs that are actively transported into hepatocytes: incubational binding as a consequence of in vitro hepatocyte concentration is a key factor.* Drug Metab Dispos, 2013. **41**(4): p. 836-43.
91. Paine, S.W., A.J. Parker, P. Gardiner, P.J. Webborn, and R.J. Riley, *Prediction of the pharmacokinetics of atorvastatin, cerivastatin, and indomethacin using kinetic models applied to isolated rat hepatocytes.* Drug Metab Dispos, 2008. **36**(7): p. 1365-74.

92. Poirier, A., C. Funk, J.M. Scherrmann, and T. Lave, *Mechanistic modeling of hepatic transport from cells to whole body: application to napsagatran and fexofenadine.* Mol Pharm, 2009. **6**(6): p. 1716-33.
93. Watanabe, T., H. Kusuhara, K. Maeda, H. Kanamaru, Y. Saito, Z. Hu, and Y. Sugiyama, *Investigation of the rate-determining process in the hepatic elimination of HMG-CoA reductase inhibitors in rats and humans.* Drug Metab Dispos, 2010. **38**(2): p. 215-22.
94. Sasabe, H., T. Terasaki, A. Tsuji, and Y. Sugiyama, *Carrier-mediated hepatic uptake of quinolone antibiotics in the rat.* J Pharmacol Exp Ther, 1997. **282**(1): p. 162-71.
95. Hallifax, D. and J.B. Houston, *Uptake and intracellular binding of lipophilic amine drugs by isolated rat hepatocytes and implications for prediction of in vivo metabolic clearance.* Drug Metab Dispos, 2006. **34**(11): p. 1829-36.
96. Yabe, Y., A. Galetin, and J.B. Houston, *Kinetic characterization of rat hepatic uptake of 16 actively transported drugs.* Drug Metab Dispos, 2011. **39**(10): p. 1808-14.
97. Menochet, K., K.E. Kenworthy, J.B. Houston, and A. Galetin, *Simultaneous assessment of uptake and metabolism in rat hepatocytes: a comprehensive mechanistic model.* J Pharmacol Exp Ther, 2012. **341**(1): p. 2-15.
98. Bow, D.A., J.L. Perry, D.S. Miller, J.B. Pritchard, and K.L. Brouwer, *Localization of P-gp (Abcb1) and Mrp2 (Abcc2) in freshly isolated rat hepatocytes.* Drug Metab Dispos, 2008. **36**(1): p. 198-202.
99. Griffin, S.J. and J.B. Houston, *Prediction of in vitro intrinsic clearance from hepatocytes: comparison of suspensions and monolayer cultures.* Drug Metab Dispos, 2005. **33**(1): p. 115-20.
100. Berry, M.N., A.M. Edwards, and G.J. Barritt, *Isolated Hepatocytes: Preparation, Properties and Applications*. 1992, Amsterdam, Netherlands: Elsevier Science Publishers B.V.
101. Riley, R.J., D.F. McGinnity, and R.P. Austin, *A unified model for predicting human hepatic, metabolic clearance from in vitro intrinsic clearance data in hepatocytes and microsomes.* Drug Metab Dispos, 2005. **33**(9): p. 1304-11.
102. Stringer, R., P.L. Nicklin, and J.B. Houston, *Reliability of human cryopreserved hepatocytes and liver microsomes as in vitro systems to predict metabolic clearance.* Xenobiotica, 2008. **38**(10): p. 1313-29.
103. Wood, F.L., J.B. Houston, and D. Hallifax, *Importance of the unstirred water layer and hepatocyte membrane integrity in vitro for quantification of intrinsic metabolic clearance.* Drug Metab Dispos, 2017.
104. Hewitt, N.J., M.J. Lechón, J.B. Houston, D. Hallifax, H.S. Brown, P. Maurel, J.G. Kenna, L. Gustavsson, C. Lohmann, C. Skonberg, A. Guillouzo, G. Tuschl, A.P. Li, E. LeCluyse, G.M. Groothuis, and J.G. Hengstler, *Primary hepatocytes: current understanding of the regulation of metabolic enzymes and transporter proteins, and pharmaceutical practice for the use of hepatocytes in metabolism, enzyme induction, transporter, clearance, and hepatotoxicity studies.* Drug Metab Rev, 2007. **39**(1): p. 159-234.
105. Jigorel, E., M. Le Vee, C. Boursier-Neyret, M. Bertrand, and O. Fardel, *Functional expression of sinusoidal drug transporters in primary human and rat hepatocytes.* Drug Metab Dispos, 2005. **33**(10): p. 1418-22.
106. Li, M., H. Yuan, N. Li, G. Song, Y. Zheng, M. Baratta, F. Hua, A. Thurston, J. Wang, and Y. Lai, *Identification of interspecies difference in efflux transporters of hepatocytes from dog, rat, monkey and human.* Eur J Pharm Sci, 2008. **35**(1-2): p. 114-26.
107. Lundquist, P., G. Englund, C. Skogastierna, J. Loof, J. Johansson, J. Hoogstraate, L. Afzelius, and T.B. Andersson, *Functional ATP-binding Cassette (ABC) Drug Efflux Transporters in Isolated Human and Rat Hepatocytes Significantly Affect Assessment of Drug Disposition.* Drug Metab Dispos, 2014.
108. Paine, A.J., *The maintenance of cytochrome P-450 in rat hepatocyte culture: some applications of liver cell cultures to the study of drug metabolism, toxicity and the induction of the P-450 system.* Chem Biol Interact, 1990. **74**(1-2): p. 1-31.

109. Oorts, M., J. Keemink, N. Deferm, R. Adriaensen, L. Richert, P. Augustijns, and P. Annaert, *Extra collagen overlay prolongs the differentiated phenotype in sandwich-cultured rat hepatocytes.* J Pharmacol Toxicol Methods, 2017. **90**: p. 31-38.
110. Swift, B., N.D. Pfeifer, and K.L. Brouwer, *Sandwich-cultured hepatocytes: an in vitro model to evaluate hepatobiliary transporter-based drug interactions and hepatotoxicity.* Drug Metab Rev, 2010. **42**(3): p. 446-71.
111. Zou, P., X. Liu, S. Wong, M.R. Feng, and B.M. Liederer, *Comparison of in vitro-in vivo extrapolation of biliary clearance using an empirical scaling factor versus transport-based scaling factors in sandwich-cultured rat hepatocytes.* J Pharm Sci, 2013. **102**(8): p. 2837-50.
112. De Bruyn, T., S. Chatterjee, S. Fattah, J. Keemink, J. Nicolai, P. Augustijns, and P. Annaert, *Sandwich-cultured hepatocytes: utility for in vitro exploration of hepatobiliary drug disposition and drug-induced hepatotoxicity.* Expert Opin Drug Metab Toxicol, 2013. **9**(5): p. 589-616.
113. Abe, K., A.S. Bridges, and K.L. Brouwer, *Use of sandwich-cultured human hepatocytes to predict biliary clearance of angiotensin II receptor blockers and HMG-CoA reductase inhibitors.* Drug Metab Dispos, 2009. **37**(3): p. 447-52.
114. Ghibellini, G., L.S. Vasist, E.M. Leslie, W.D. Heizer, R.J. Kowalsky, B.F. Calvo, and K.L. Brouwer, *In vitro-in vivo correlation of hepatobiliary drug clearance in humans.* Clin Pharmacol Ther, 2007. **81**(3): p. 406-13.
115. Turncliff, R.Z., K.A. Hoffmaster, J.C. Kalvass, G.M. Pollack, and K.L. Brouwer, *Hepatobiliary disposition of a drug/metabolite pair: Comprehensive pharmacokinetic modeling in sandwich-cultured rat hepatocytes.* J Pharmacol Exp Ther, 2006. **318**(2): p. 881-9.
116. Yan, L., S. Sheihk-Bahaei, S. Park, G.E. Ropella, and C.A. Hunt, *Predictions of hepatic disposition properties using a mechanistically realistic, physiologically based model.* Drug Metab Dispos, 2008. **36**(4): p. 759-68.
117. Wolf, K.K., A.S. Bridges, J.K. Lee, J.W. Polli, K.R. Brouwer, G.M. Pollack, and K.L.R. Brouwer, *Hepatobiliary Disposition of Morphine and Generated Morphine 3-Glucuronide in Sandwich-Cultured Rat Hepatocytes*, in *15th Annual ISSX North American Regional Meeting*. 2008: San Diego, CA
118. Ansede, J.H. and K.R. Brouwer, *Transport of Naloxone Glucuronide in B-Clear (Sandwich-Cultured Rat Hepatocytes) and its Application as an In Vitro Model for Determining the Directional Transport of Metabolites* in *10th European ISSX Meeting*. 2008: Vienna, Austria.
119. Kostrubsky, S.E., S.C. Strom, A.S. Kalgutkar, S. Kulkarni, J. Atherton, R. Mireles, B. Feng, R. Kubik, J. Hanson, E. Urda, and A.E. Mutlib, *Inhibition of hepatobiliary transport as a predictive method for clinical hepatotoxicity of nefazodone.* Toxicol Sci, 2006. **90**(2): p. 451-9.
120. McRae, M.P., C.M. Lowe, X. Tian, D.L. Bourdet, R.H. Ho, B.F. Leake, R.B. Kim, K.L. Brouwer, and A.D. Kashuba, *Ritonavir, saquinavir, and efavirenz, but not nevirapine, inhibit bile acid transport in human and rat hepatocytes.* J Pharmacol Exp Ther, 2006. **318**(3): p. 1068-75.
121. Treijtel, N., J.C. van Eijkeren, S. Nijmeijer, I.C. de Greef-van der Sandt, and A.P. Freidig, *Clearance and clearance inhibition of the HIV-1 protease inhibitors ritonavir and saquinavir in sandwich-cultured rat hepatocytes and rat microsomes.* Toxicol In Vitro, 2009. **23**(1): p. 185-93.
122. Carlile, D.J., K. Zomorodi, and J.B. Houston, *Scaling factors to relate drug metabolic clearance in hepatic microsomes, isolated hepatocytes, and the intact liver: studies with induced livers involving diazepam.* Drug Metab Dispos, 1997. **25**(8): p. 903-11.
123. Seglen, P.O., *Preparation of isolated rat liver cells.* Methods Cell Biol, 1976. **13**: p. 29-83.
124. Zahlten, R.N. and F.W. Stratman, *The isolation of hormone-sensitive rat hepatocytes by a modified enzymatic technique.* Arch Biochem Biophys, 1974. **163**(2): p. 600-8.
125. Davies, B. and T. Morris, *Physiological parameters in laboratory animals and humans.* Pharm Res, 1993. **10**(7): p. 1093-5.

126. Houston, J.B. and D.J. Carlile, *Prediction of hepatic clearance from microsomes, hepatocytes, and liver slices.* Drug Metab Rev, 1997. **29**(4): p. 891-922.
127. Liu, L. and K.S. Pang, *The roles of transporters and enzymes in hepatic drug processing.* Drug Metab Dispos, 2005. **33**(1): p. 1-9.
128. Shitara, Y., T. Horie, and Y. Sugiyama, *Transporters as a determinant of drug clearance and tissue distribution.* Eur J Pharm Sci, 2006. **27**(5): p. 425-46.
129. Umehara, K. and G. Camenisch, *Novel in vitro-in vivo extrapolation (IVIVE) method to predict hepatic organ clearance in rat.* Pharm Res, 2012. **29**(2): p. 603-17.
130. Varma, M.V., Y.A. Bi, E. Kimoto, and J. Lin, *Quantitative prediction of transporter- and enzyme-mediated clinical drug-drug interactions of organic anion-transporting polypeptide 1B1 substrates using a mechanistic net-effect model.* J Pharmacol Exp Ther, 2014. **351**(1): p. 214-23.
131. Wood, F.L., J.B. Houston, and D. Hallifax, *Clearance prediction methodology needs fundamental improvement: trends common to rat and human hepatocytes/microsomes and implications for experimental methodology.* Drug Metab Dispos, 2017.
132. Wood, F., *Underprediction of metabolic clearance in vitro: Assessing metabolic competence in isolated hepatocytes*. 2015, CAPKR Conference Presentation: University of Manchester.
133. Benet, L.Z., F. Broccatelli, and T.I. Oprea, *BDDCS applied to over 900 drugs.* AAPS J, 2011. **13**(4): p. 519-47.
134. Barter, Z.E., M.K. Bayliss, P.H. Beaune, A.R. Boobis, D.J. Carlile, R.J. Edwards, J.B. Houston, B.G. Lake, J.C. Lipscomb, O.R. Pelkonen, G.T. Tucker, and A. Rostami-Hodjegan, *Scaling factors for the extrapolation of in vivo metabolic drug clearance from in vitro data: reaching a consensus on values of human microsomal protein and hepatocellularity per gram of liver.* Curr Drug Metab, 2007. **8**(1): p. 33-45.
135. Ito, K. and J.B. Houston, *Comparison of the use of liver models for predicting drug clearance using in vitro kinetic data from hepatic microsomes and isolated hepatocytes.* Pharm Res, 2004. **21**(5): p. 785-92.
136. Lundquist, P., J. Loof, A.K. Sohlenius-Sternbeck, E. Floby, J. Johansson, J. Bylund, J. Hoogstraate, L. Afzelius, and T.B. Andersson, *The impact of solute carrier (SLC) drug uptake transporter loss in human and rat cryopreserved hepatocytes on clearance predictions.* Drug Metab Dispos, 2014. **42**(3): p. 469-80.
137. Tchaparian, E.H., J.S. Houghton, C. Uyeda, M.P. Grillo, and L. Jin, *Effect of culture time on the basal expression levels of drug transporters in sandwich-cultured primary rat hepatocytes.* Drug Metab Dispos, 2011. **39**(12): p. 2387-94.
138. Houston, J.B. and A. Galetin, *Methods for predicting in vivo pharmacokinetics using data from in vitro assays.* Curr Drug Metab, 2008. **9**(9): p. 940-51.
139. Naritomi, Y., S. Terashita, A. Kagayama, and Y. Sugiyama, *Utility of hepatocytes in predicting drug metabolism: comparison of hepatic intrinsic clearance in rats and humans in vivo and in vitro.* Drug Metab Dispos, 2003. **31**(5): p. 580-8.
140. Annaert, P.P., R.Z. Turncliff, C.L. Booth, D.R. Thakker, and K.L. Brouwer, *P-glycoprotein-mediated in vitro biliary excretion in sandwich-cultured rat hepatocytes.* Drug Metab Dispos, 2001. **29**(10): p. 1277-83.
141. Fukuda, H., R. Ohashi, M. Tsuda-Tsukimoto, and I. Tamai, *Effect of plasma protein binding on in vitro-in vivo correlation of biliary excretion of drugs evaluated by sandwich-cultured rat hepatocytes.* Drug Metab Dispos, 2008. **36**(7): p. 1275-82.
142. Jemnitz, K., M. Szabo, A. Batai-Konczos, P. Szabo, B. Magda, and Z. Veres, *A Modified Procedure for Estimating the Impact of the Uptake on the Overall Biliary Clearance in Sandwich Culture of Rat Hepatocytes.* Drug Metab Lett, 2015. **9**(1): p. 17-27.
143. Nakakariya, M., M. Ono, N. Amano, T. Moriwaki, K. Maeda, and Y. Sugiyama, *In vivo biliary clearance should be predicted by intrinsic biliary clearance in sandwich-cultured hepatocytes.* Drug Metab Dispos, 2012. **40**(3): p. 602-9.
144. Fagerholm, U., *Prediction of human pharmacokinetics--evaluation of methods for prediction of hepatic metabolic clearance.* J Pharm Pharmacol, 2007. **59**(6): p. 803-28.

145. Chiba, M., Y. Ishii, and Y. Sugiyama, *Prediction of hepatic clearance in human from in vitro data for successful drug development.* AAPS J, 2009. **11**(2): p. 262-76.
146. Menochet, K., K.E. Kenworthy, J.B. Houston, and A. Galetin, *Use of mechanistic modeling to assess interindividual variability and interspecies differences in active uptake in human and rat hepatocytes.* Drug Metab Dispos, 2012. **40**(9): p. 1744-56.
147. Watanabe, T., H. Kusuhara, K. Maeda, Y. Shitara, and Y. Sugiyama, *Physiologically based pharmacokinetic modeling to predict transporter-mediated clearance and distribution of pravastatin in humans.* J Pharmacol Exp Ther, 2009. **328**(2): p. 652-62.
148. Parrish, K.E., J. Mao, J. Chen, A. Jaochico, J. Ly, Q. Ho, S. Mukadam, and M. Wright, *In vitro and in vivo characterization of CYP inhibition by 1-aminobenzotriazole in rats.* Biopharm Drug Dispos, 2016. **37**(4): p. 200-11.
149. Fattinger, K., V. Cattori, B. Hagenbuch, P.J. Meier, and B. Stieger, *Rifamycin SV and rifampicin exhibit differential inhibition of the hepatic rat organic anion transporting polypeptides, Oatp1 and Oatp2.* Hepatology, 2000. **32**(1): p. 82-86.
150. Smith, D.A., D.E. Thurston, A.A. Alex, and C. Royal Society of, *Metabolism, Pharmacokinetics and Toxicity of Functional Groups : Impact of Chemical Building Blocks on ADMET*. RSC Drug Discovery v.1. 2010.
151. Wenlock, M.C., T. Potter, P. Barton, and R.P. Austin, *A method for measuring the lipophilicity of compounds in mixtures of 10.* J Biomol Screen, 2011. **16**(3): p. 348-55.
152. Kansy, M., H. Fischer, K. Kratzat, F. Senner, B. Wagner, and I. Parrilla, *High-Throughput Artificial Membrane Permeability Studies in Early Lead Discovery and Development*, in *Pharmacokinetic Optimization in Drug Research*. 2007, Verlag Helvetica Chimica Acta. p. 447-464.
153. De Bruyn, T., P.F. Augustijns, and P.P. Annaert, *Hepatic Clearance Prediction of Nine Human Immunodeficiency Virus Protease Inhibitors in Rat.* J Pharm Sci, 2016. **105**(2): p. 846-53.
154. Sirianni, G.L. and K.S. Pang, *Organ clearance concepts: new perspectives on old principles.* J Pharmacokinet Biopharm, 1997. **25**(4): p. 449-70.
155. Ferslew, B.C., K. Kock, A.S. Bridges, and K.L. Brouwer, *Role of Multidrug Resistance-associated Protein 4 (MRP4) in the Basolateral Efflux of Hepatically-Derived Enalaprilat.* Drug Metab Dispos, 2014.
156. Fukuda, Y., K. Takenaka, A. Sparreboom, S.B. Cheepala, C.P. Wu, S. Ekins, S.V. Ambudkar, and J.D. Schuetz, *Human immunodeficiency virus protease inhibitors interact with ATP binding cassette transporter 4/multidrug resistance protein 4: a basis for unanticipated enhanced cytotoxicity.* Mol Pharmacol, 2013. **84**(3): p. 361-71.
157. Zhou, S.F., L.L. Wang, Y.M. Di, C.C. Xue, W. Duan, C.G. Li, and Y. Li, *Substrates and inhibitors of human multidrug resistance associated proteins and the implications in drug development.* Curr Med Chem, 2008. **15**(20): p. 1981-2039.
158. Agarwal, S., D. Pal, and A.K. Mitra, *Both P-gp and MRP2 mediate transport of Lopinavir, a protease inhibitor.* Int J Pharm, 2007. **339**(1-2): p. 139-47.
159. Cantrill, C. and J.B. Houston, *Understanding the Interplay Between Uptake and Efflux Transporters Within In Vitro Systems in Defining Hepatocellular Drug Concentrations.* J Pharm Sci, 2017.
160. Abe, K., A.S. Bridges, W. Yue, and K.L. Brouwer, *In vitro biliary clearance of angiotensin II receptor blockers and 3-hydroxy-3-methylglutaryl-coenzyme A reductase inhibitors in sandwich-cultured rat hepatocytes: comparison with in vivo biliary clearance.* J Pharmacol Exp Ther, 2008. **326**(3): p. 983-90.
161. Li, N., P. Singh, K.M. Mandrell, and Y. Lai, *Improved extrapolation of hepatobiliary clearance from in vitro sandwich cultured rat hepatocytes through absolute quantification of hepatobiliary transporters.* Mol Pharm, 2010. **7**(3): p. 630-41.
162. Grime, K. and S.W. Paine, *Species differences in biliary clearance and possible relevance of hepatic uptake and efflux transporters involvement.* Drug Metab Dispos, 2013. **41**(2): p. 372-8.

163. De Bruyn, T., *Transporter-based Boosting of HIV Protease Inhibitors*, in *Faculty of Pharmaceutical Sciences*. 2014, KU Leuven: Leuven.
164. Lau, Y.Y., H. Okochi, Y. Huang, and L.Z. Benet, *Pharmacokinetics of atorvastatin and its hydroxy metabolites in rats and the effects of concomitant rifampicin single doses: relevance of first-pass effect from hepatic uptake transporters, and intestinal and hepatic metabolism.* Drug Metab Dispos, 2006. **34**(7): p. 1175-81.
165. Watanabe, T., K. Maeda, T. Kondo, H. Nakayama, S. Horita, H. Kusuhara, and Y. Sugiyama, *Prediction of the hepatic and renal clearance of transporter substrates in rats using in vitro uptake experiments.* Drug Metab Dispos, 2009. **37**(7): p. 1471-9.
166. Horiuchi, I., Y.I. Mori, M. Taguchi, F. Ichida, T. Miyawaki, and Y. Hashimoto, *Mechanisms responsible for the altered pharmacokinetics of bosentan: analysis utilizing rats with bile duct ligation-induced liver dysfunction.* Biopharm Drug Dispos, 2009. **30**(6): p. 326-33.
167. Lave, T., S. Dupin, C. Schmitt, R.C. Chou, D. Jaeck, and P. Coassolo, *Integration of in vitro data into allometric scaling to predict hepatic metabolic clearance in man: application to 10 extensively metabolized drugs.* J Pharm Sci, 1997. **86**(5): p. 584-90.
168. Huang, L., A. Chen, J. Roberts, B. Janosky, X. Be, L. Berry, and M.H. Lin, *Use of uptake intrinsic clearance from attached rat hepatocytes to predict hepatic clearance for poorly permeable compounds.* Xenobiotica, 2012. **42**(9): p. 830-40.
169. Sawada, Y., M. Hanano, Y. Sugiyama, and T. Iga, *Prediction of the disposition of beta-lactam antibiotics in humans from pharmacokinetic parameters in animals.* J Pharmacokinet Biopharm, 1984. **12**(3): p. 241-61.
170. Muraoka, I., T. Hasegawa, M. Nadai, L. Wang, S. Haghgoo, O. Tagaya, and T. Nabeshima, *Biliary and renal excretions of cefpiramide in Eisai hyperbilirubinemic rats.* Antimicrob Agents Chemother, 1995. **39**(1): p. 70-4.
171. Lee, A.K., J.H. Lee, J.W. Kwon, W.B. Kim, S.G. Kim, S.H. Kim, and M.G. Lee, *Pharmacokinetics of clarithromycin in rats with acute renal failure induced by uranyl nitrate.* Biopharm Drug Dispos, 2004. **25**(6): p. 273-82.
172. Yamano, K., K. Yamamoto, H. Kotaki, S. Takedomi, H. Matsuo, Y. Sawada, and T. Iga, *Correlation between in vivo and in vitro hepatic uptake of metabolic inhibitors of cytochrome P-450 in rats.* Drug Metab Dispos, 1999. **27**(11): p. 1225-31.
173. Peris-Ribera, J.E., F. Torres-Molina, M.C. Garcia-Carbonell, J.C. Aristorena, and J.M. Pla-Delfina, *Pharmacokinetics and bioavailability of diclofenac in the rat.* J Pharmacokinet Biopharm, 1991. **19**(6): p. 647-65.
174. Reyes-Gordillo, K., P. Muriel, G. Castaneda-Hernandez, and L. Favari, *Pharmacokinetics of diclofenac in rats intoxicated with CCL4, and in the regenerating liver.* Biopharm Drug Dispos, 2007. **28**(8): p. 415-22.
175. Zhang, J., P. Li, H.F. Guo, L. Liu, and X.D. Liu, *Pharmacokinetic-pharmacodynamic modeling of diclofenac in normal and Freund's complete adjuvant-induced arthritic rats.* Acta Pharmacol Sin, 2012. **33**(11): p. 1372-8.
176. Kim, Y.C., E.Y. Oh, S.H. Kim, and M.G. Lee, *Pharmacokinetics of diclofenac in rat model of diabetes mellitus induced by alloxan or steptozotocin.* Biopharm Drug Dispos, 2006. **27**(2): p. 85-92.
177. Sohlenius-Sternbeck, A.K., C. Jones, D. Ferguson, B.J. Middleton, D. Projean, E. Floby, J. Bylund, and L. Afzelius, *Practical use of the regression offset approach for the prediction of in vivo intrinsic clearance from hepatocytes.* Xenobiotica, 2012. **42**(9): p. 841-53.
178. Harrison, L.I. and M. Gibaldi, *Pharmacokinetics of digoxin in the rat.* Drug Metab Dispos, 1976. **4**(1): p. 88-93.
179. Liu, L., E. Mak, R.G. Tirona, E. Tan, P.M. Novikoff, P. Wang, A.W. Wolkoff, and K.S. Pang, *Vascular binding, blood flow, transporter, and enzyme interactions on the processing of digoxin in rat liver.* J Pharmacol Exp Ther, 2005. **315**(1): p. 433-48.
180. Lam, J.L., H. Okochi, Y. Huang, and L.Z. Benet, *In vitro and in vivo correlation of hepatic transporter effects on erythromycin metabolism: characterizing the importance of transporter-enzyme interplay.* Drug Metab Dispos, 2006. **34**(8): p. 1336-44.

181. Yamano, K., K. Yamamoto, H. Kotaki, Y. Sawada, and T. Iga, *Quantitative prediction of metabolic inhibition of midazolam by itraconazole and ketoconazole in rats: implication of concentrative uptake of inhibitors into liver.* Drug Metab Dispos, 1999. **27**(3): p. 395-402.
182. Jaisue, S., J.P. Gerber, and A.K. Davey, *Pharmacokinetics of fexofenadine following LPS administration to rats.* Xenobiotica, 2010. **40**(11): p. 743-50.
183. Matsuda, Y., Y. Konno, T. Hashimoto, M. Nagai, T. Taguchi, M. Satsukawa, and S. Yamashita, *In vivo assessment of the impact of efflux transporter on oral drug absorption using portal vein-cannulated rats.* Drug Metab Dispos, 2013. **41**(8): p. 1514-21.
184. Watanabe, M., M. Kobayashi, J. Ogura, N. Takahashi, H. Yamaguchi, and K. Iseki, *Alteration of pharmacokinetics of grepafloxacin in type 2 diabetic rats.* J Pharm Pharm Sci, 2014. **17**(1): p. 25-33.
185. Suzuki, T., Y. Kato, H. Sasabe, M. Itose, G. Miyamoto, and Y. Sugiyama, *Mechanism for the tissue distribution of grepafloxacin, a fluoroquinolone antibiotic, in rats.* Drug Metab Dispos, 2002. **30**(12): p. 1393-9.
186. Gardiner, P. and S.W. Paine, *The impact of hepatic uptake on the pharmacokinetics of organic anions.* Drug Metab Dispos, 2011. **39**(10): p. 1930-8.
187. Cheng, F.C., T.R. Tsai, Y.F. Chen, L.C. Hung, and T.H. Tsai, *Pharmacokinetic study of levofloxacin in rat blood and bile by microdialysis and high-performance liquid chromatography.* J Chromatogr A, 2002. **961**(1): p. 131-6.
188. Hurtado, F.K., B. Weber, H. Derendorf, G. Hochhaus, and T. Dalla Costa, *Population pharmacokinetic modeling of the unbound levofloxacin concentrations in rat plasma and prostate tissue measured by microdialysis.* Antimicrob Agents Chemother, 2014. **58**(2): p. 678-86.
189. Yano, I., T. Ito, M. Takano, and K. Inui, *Evaluation of renal tubular secretion and reabsorption of levofloxacin in rats.* Pharm Res, 1997. **14**(4): p. 508-11.
190. Vuppugalla, R., Y. Zhang, S. Chang, A.D. Rodrigues, and P.H. Marathe, *Impact of nonlinear midazolam pharmacokinetics on the magnitude of the midazolam-ketoconazole interaction in rats.* Xenobiotica, 2012. **42**(11): p. 1058-68.
191. Lau, C.E., F. Ma, Y. Wang, and C. Smith, *Pharmacokinetics and bioavailability of midazolam after intravenous, subcutaneous, intraperitoneal and oral administration under a chronic food-limited regimen: relating DRL performance to pharmacokinetics.* Psychopharmacology (Berl), 1996. **126**(3): p. 241-8.
192. Hirano, M., K. Maeda, S. Matsushima, Y. Nozaki, H. Kusuhara, and Y. Sugiyama, *Involvement of BCRP (ABCG2) in the biliary excretion of pitavastatin.* Mol Pharmacol, 2005. **68**(3): p. 800-7.
193. Fujino, H., I. Yamada, J. Kokima, H. Hirano, H. Matsumoto, and M. Yoneda, *Studies on the Metabolic Fate of NK-104, a New Inhibitor of HMG-CoA Reductase. In Vitro Metabolism and Plasma Protein Binding in Animals and Human.* Drug Metabolism and Pharmacokinetics, 1999. **14**: p. 415-424.
194. Kivisto, K.T., *Comments on "Multiple transporters affect the disposition of atorvastatin and its two active hydroxy metabolites: Application of in vitro and ex situ systems".* J Pharmacol Exp Ther, 2006. **316**(3): p. 1386; author reply 1387.
195. Belpaire, F.M., F. de Smet, L.J. Vynckier, A.M. Vermeulen, M.T. Rosseel, M.G. Bogaert, and L. Chauvelot-Moachon, *Effect of aging on the pharmcokinetics of atenolol, metoprolol and propranolol in the rat.* J Pharmacol Exp Ther, 1990. **254**(1): p. 116-22.
196. Rodgers, T., D. Leahy, and M. Rowland, *Tissue distribution of basic drugs: accounting for enantiomeric, compound and regional differences amongst beta-blocking drugs in rat.* J Pharm Sci, 2005. **94**(6): p. 1237-48.
197. Sawada, Y., M. Hanano, Y. Sugiyama, and T. Iga, *Prediction of the disposition of nine weakly acidic and six weakly basic drugs in humans from pharmacokinetic parameters in rats.* J Pharmacokinet Biopharm, 1985. **13**(5): p. 477-92.
198. Komura, H., A. Kawase, and M. Iwaki, *Application of substrate depletion assay for early prediction of nonlinear pharmacokinetics in drug discovery: assessment of nonlinearity of metoprolol, timolol, and propranolol.* J Pharm Sci, 2005. **94**(12): p. 2656-66.

199. Harashima, H., Y. Sawada, Y. Sugiyama, T. Iga, and M. Hanano, *Analysis of nonlinear tissue distribution of quinidine in rats by physiologically based pharmacokinetics.* J Pharmacokinet Biopharm, 1985. **13**(4): p. 425-40.
200. Fremstad, D., *Increased plasma binding and decreased blood cell binding of quinidine in blood from anuric rats.* Acta Pharmacol Toxicol (Copenh), 1977. **41**(2): p. 148-60.
201. Fremstad, D., S. Jacobsen, and K.M. Lunde, *Influence of serum protein binding on the pharmacokinetics of quinidine in normal and anuric rats.* Acta Pharmacol Toxicol (Copenh), 1977. **41**(2): p. 161-76.
202. Moriwaki, T., H. Yasui, and A. Yamamoto, *Pharmacokinetic analysis of ramatroban using a recirculatory model with enterohepatic circulation by measuring portal and systemic blood concentration difference in Sprague-Dawley and Eisai hyperbilirubinemic rats.* Pharm Res, 2004. **21**(6): p. 1055-64.
203. Choi, J.S., I. Choi, and D.H. Choi, *Effects of nifedipine on the pharmacokinetics of repaglinide in rats: possible role of CYP3A4 and P-glycoprotein inhibition by nifedipine.* Pharmacol Rep, 2013. **65**(5): p. 1422-30.
204. Li, F., J. Lu, and X. Ma, *CYP3A4-mediated lopinavir bioactivation and its inhibition by ritonavir.* Drug Metab Dispos, 2012. **40**(1): p. 18-24.
205. Kitamura, S., K. Maeda, Y. Wang, and Y. Sugiyama, *Involvement of multiple transporters in the hepatobiliary transport of rosuvastatin.* Drug Metab Dispos, 2008. **36**(10): p. 2014-23.
206. Inoue, M., Y. Morino, and S. Nagase, *Transhepatic transport of taurocholic acid in normal and mutant analbuminemic rats.* Biochim Biophys Acta, 1985. **833**(2): p. 211-6.
207. Hayashi, H. and Y. Sugiyama, *4-phenylbutyrate enhances the cell surface expression and the transport capacity of wild-type and mutated bile salt export pumps.* Hepatology, 2007. **45**(6): p. 1506-16.
208. Matthew, D.E. and J.B. Houston, *Drug metabolizing capacity in vitro and in vivo--II. Correlations between hepatic microsomal monooxygenase markers in phenobarbital-induced rats.* Biochem Pharmacol, 1990. **40**(4): p. 751-8.
209. Choi, M.R., M.H. Kwon, Y.Y. Cho, H.D. Choi, Y.C. Kim, and H.E. Kang, *Pharmacokinetics of tolbutamide and its metabolite 4-hydroxy tolbutamide in poloxamer 407-induced hyperlipidemic rats.* Biopharm Drug Dispos, 2014. **35**(5): p. 264-74.
210. Uchimura, T., M. Kato, T. Saito, and H. Kinoshita, *Prediction of human blood-to-plasma drug concentration ratio.* Biopharm Drug Dispos, 2010. **31**(5-6): p. 286-97.
211. Yamao, T., H. Nakagami, K. Furuhama, T. Onodera, Y. Kurosaki, T. Nakayama, and T. Kimura, *Pharmacokinetics of tolbutamide following intravenous and oral administrations in rats with obstructive jaundice.* Biol Pharm Bull, 1994. **17**(5): p. 691-5.
212. Mustafa, S., P. Venkatesh, K. Pasha, R. Mullangi, and N.R. Srinivas, *Altered intravenous pharmacokinetics of topotecan in rats with acute renal failure (ARF) induced by uranyl nitrate: do adenosine A1 antagonists (selective/non-selective) normalize the altered topotecan kinetics in ARF?* Xenobiotica, 2006. **36**(12): p. 1239-58.
213. Choi, D.H., W.G. Shin, and J.S. Choi, *Drug interaction between oral atorvastatin and verapamil in healthy subjects: effects of atorvastatin on the pharmacokinetics of verapamil and norverapamil.* Eur J Clin Pharmacol, 2008. **64**(5): p. 445-9.
214. Lee, Y.S., J.N. Yoon, I.S. Yoon, M.G. Lee, and H.E. Kang, *Pharmacokinetics of verapamil and its metabolite norverapamil in rats with hyperlipidaemia induced by poloxamer 407.* Xenobiotica, 2012. **42**(8): p. 766-74.
215. Nicolai, J., T. De Bruyn, L. Thevelin, P. Augustijns, and P. Annaert, *Transport-Metabolism Interplay of Atazanavir in Rat Hepatocytes.* Drug Metab Dispos, 2016. **44**(3): p. 389-97.
216. Lundquist, P., J. Loof, U. Fagerholm, I. Sjogren, J. Johansson, S. Briemm, J. Hoogstraate, L. Afzelius, and T.B. Andersson, *Prediction of In Vivo Rat Biliary Drug Clearance from an In Vitro Hepatocyte Efflux Model.* Drug Metab Dispos, 2014.
217. de Moraes, N.G.M.R.-H., A; Galetin, A., *Mechanistic Modelling of Atorvastatin Uptake and Acid – Lactone Inter-conversion in Plated Rat and Human Hepatocytes*, in *ISSX*. 2012: Noordwijk aan Zee.

218. Kotani, N., K. Maeda, T. Watanabe, M. Hiramatsu, L.K. Gong, Y.A. Bi, T. Takezawa, H. Kusuhara, and Y. Sugiyama, *Culture period-dependent changes in the uptake of transporter substrates in sandwich-cultured rat and human hepatocytes.* Drug Metab Dispos, 2011. **39**(9): p. 1503-10.
219. Parker, A.J. and J.B. Houston, *Rate-limiting steps in hepatic drug clearance: comparison of hepatocellular uptake and metabolism with microsomal metabolism of saquinavir, nelfinavir, and ritonavir.* Drug Metab Dispos, 2008. **36**(7): p. 1375-84.
220. Nezasa, K., K. Higaki, M. Takeuchi, M. Nakano, and M. Koike, *Uptake of rosuvastatin by isolated rat hepatocytes: comparison with pravastatin.* Xenobiotica, 2003. **33**(4): p. 379-88.
221. Cantrill, C., *In House Data*. 2013: University of Manchester.
222. Griffin, L.M., P.B. Watkins, C.H. Perry, R.L. St Claire, 3rd, and K.L. Brouwer, *Combination lopinavir and ritonavir alter exogenous and endogenous bile acid disposition in sandwich-cultured rat hepatocytes.* Drug Metab Dispos, 2013. **41**(1): p. 188-96.
223. Liu, X., J.P. Chism, E.L. LeCluyse, K.R. Brouwer, and K.L. Brouwer, *Correlation of biliary excretion in sandwich-cultured rat hepatocytes and in vivo in rats.* Drug Metab Dispos, 1999. **27**(6): p. 637-44.
224. Camenisch, G. and K. Umehara, *Predicting human hepatic clearance from in vitro drug metabolism and transport data: a scientific and pharmaceutical perspective for assessing drug-drug interactions.* Biopharm Drug Dispos, 2012. **33**(4): p. 179-94.
225. Gertz, M., A. Harrison, J.B. Houston, and A. Galetin, *Prediction of human intestinal first-pass metabolism of 25 CYP3A substrates from in vitro clearance and permeability data.* Drug Metab Dispos, 2010. **38**(7): p. 1147-58.
226. Weber, C., L. Banken, H. Birnboeck, and R. Schulz, *Effect of the endothelin-receptor antagonist bosentan on the pharmacokinetics and pharmacodynamics of warfarin.* J Clin Pharmacol, 1999. **39**(8): p. 847-54.
227. Weber, C., R. Schmitt, H. Birnboeck, G. Hopfgartner, S.P. van Marle, P.A. Peeters, J.H. Jonkman, and C.R. Jones, *Pharmacokinetics and pharmacodynamics of the endothelin-receptor antagonist bosentan in healthy human subjects.* Clin Pharmacol Ther, 1996. **60**(2): p. 124-37.
228. Mück, W., *Clinical pharmacokinetics of cerivastatin.* Clin Pharmacokinet, 2000. **39**(2): p. 99-116.
229. Bauer, L.A., C. Wareing-Tran, W.A. Edwards, V. Raisys, L. Ferreri, R. Jack, E.P. Dellinger, and D. Simonowitz, *Cimetidine clearance in the obese.* Clin Pharmacol Ther, 1985. **37**(4): p. 425-30.
230. Gugler, R., B. Muller-Liebenau, and A. Somogyi, *Altered disposition and availability of cimetidine in liver cirrhotic patients.* Br J Clin Pharmacol, 1982. **14**(3): p. 421-30.
231. Paixao, P., L.F. Gouveia, and J.A. Morais, *Prediction of drug distribution within blood.* Eur J Pharm Sci, 2009. **36**(4-5): p. 544-54.
232. Jaehde, U., F. Sorgel, A. Reiter, G. Sigl, K.G. Naber, and W. Schunack, *Effect of probenecid on the distribution and elimination of ciprofloxacin in humans.* Clin Pharmacol Ther, 1995. **58**(5): p. 532-41.
233. Lettieri, J.T., M.C. Rogge, L. Kaiser, R.M. Echols, and A.H. Heller, *Pharmacokinetic profiles of ciprofloxacin after single intravenous and oral doses.* Antimicrob Agents Chemother, 1992. **36**(5): p. 993-6.
234. Paixao, P., *In Silico Prediction of Human Oral Bioavailability. Artificial Neural Networks and Physiologically Based Models*, in *Especialidade de Biofarmácia e Farmacocinética* 2010, Universidade De Lisboa.
235. Legg, B., S.K. Gupta, M. Rowland, R.W. Johnson, and L.R. Solomon, *Cyclosporin: pharmacokinetics and detailed studies of plasma and erythrocyte binding during intravenous and oral administration.* Eur J Clin Pharmacol, 1988. **34**(5): p. 451-60.
236. Lappin, G., Y. Shishikura, R. Jochemsen, R.J. Weaver, C. Gesson, B. Houston, B. Oosterhuis, O.J. Bjerrum, M. Rowland, and C. Garner, *Pharmacokinetics of fexofenadine: evaluation of*

a microdose and assessment of absolute oral bioavailability. Eur J Pharm Sci, 2010. **40**(2): p. 125-31.
237. Tse, F.L., J.M. Jaffe, and A. Troendle, *Pharmacokinetics of fluvastatin after single and multiple doses in normal volunteers.* J Clin Pharmacol, 1992. **32**(7): p. 630-8.
238. Tse, F.L., D.F. Nickerson, and W.S. Yardley, *Binding of fluvastatin to blood cells and plasma proteins.* J Pharm Sci, 1993. **82**(9): p. 942-7.
239. Smith, D.E., E.T. Lin, and L.Z. Benet, *Absorption and disposition of furosemide in healthy volunteers, measured with a metabolite-specific assay.* Drug Metab Dispos, 1980. **8**(5): p. 337-42.
240. Hammarlund, M.M., L.K. Paalzow, and B. Odlind, *Pharmacokinetics of furosemide in man after intravenous and oral administration. Application of moment analysis.* Eur J Clin Pharmacol, 1984. **26**(2): p. 197-207.
241. Sohlenius-Sternbeck, A.K., L. Afzelius, P. Prusis, J. Neelissen, J. Hoogstraate, J. Johansson, E. Floby, A. Bengtsson, O. Gissberg, J. Sternbeck, and C. Petersson, *Evaluation of the human prediction of clearance from hepatocyte and microsome intrinsic clearance for 52 drug compounds.* Xenobiotica, 2010. **40**(9): p. 637-49.
242. Brown, H.S., M. Griffin, and J.B. Houston, *Evaluation of cryopreserved human hepatocytes as an alternative in vitro system to microsomes for the prediction of metabolic clearance.* Drug Metab Dispos, 2007. **35**(2): p. 293-301.
243. Jonsson, A., J.C. Chan, T. Rydberg, S. Vaaler, B. Hallengren, C.S. Cockram, J.A. Critchley, and A. Melander, *Pharmacodynamics and pharmacokinetics of intravenous glibenclamide in Caucasian and Chinese patients with type-2 diabetes.* Eur J Clin Pharmacol, 2000. **55**(10): p. 721-7.
244. George, S., A. McBurney, and A. Cole, *Possible protein binding displacement interaction between glibenclamide and metolazone.* Eur J Clin Pharmacol, 1990. **38**(1): p. 93-5.
245. Rogers, H.J., R.G. Spector, P.J. Morrison, and I.D. Bradbrook, *Pharmacokinetics of intravenous glibenclamide investigated by a high performance liquid chromatographic assay.* Diabetologia, 1982. **23**(1): p. 37-40.
246. Ensing, K., R.A. de Zeeuw, G.D. Nossent, G.H. Koeter, and P.J. Cornelissen, *Pharmacokinetics of ipratropium bromide after single dose inhalation and oral and intravenous administration.* Eur J Clin Pharmacol, 1989. **36**(2): p. 189-94.
247. Heizmann, P., M. Eckert, and W.H. Ziegler, *Pharmacokinetics and bioavailability of midazolam in man.* Br J Clin Pharmacol, 1983. **16 Suppl 1**: p. 43S-49S.
248. Pentikainen, P.J., L. Valisalmi, J.J. Himberg, and C. Crevoisier, *Pharmacokinetics of midazolam following intravenous and oral administration in patients with chronic liver disease and in healthy subjects.* J Clin Pharmacol, 1989. **29**(3): p. 272-7.
249. Schwocho, L.R. and H.N. Masonson, *Pharmacokinetics of CS-866, a new angiotensin II receptor blocker, in healthy subjects.* J Clin Pharmacol, 2001. **41**(5): p. 515-27.
250. Luo, Z., Y. Zhang, J. Gu, P. Feng, and Y. Wang, *Pharmacokinetic Properties of Single- and Multiple-Dose Pitavastatin Calcium Tablets in Healthy Chinese Volunteers.* Curr Ther Res Clin Exp, 2015. **77**: p. 52-7.
251. Singhvi, S.M., H.Y. Pan, R.A. Morrison, and D.A. Willard, *Disposition of pravastatin sodium, a tissue-selective HMG-CoA reductase inhibitor, in healthy subjects.* Br J Clin Pharmacol, 1990. **29**(2): p. 239-43.
252. Cheymol, G., J.M. Poirier, P.A. Carrupt, B. Testa, J. Weissenburger, J.C. Levron, and E. Snoeck, *Pharmacokinetics of beta-adrenoceptor blockers in obese and normal volunteers.* Br J Clin Pharmacol, 1997. **43**(6): p. 563-70.
253. McGinnity, D.F., M.G. Soars, R.A. Urbanowicz, and R.J. Riley, *Evaluation of fresh and cryopreserved hepatocytes as in vitro drug metabolism tools for the prediction of metabolic clearance.* Drug Metab Dispos, 2004. **32**(11): p. 1247-53.
254. Walle, T., E.C. Conradi, U.K. Walle, T.C. Fagan, and T.E. Gaffney, *4-Hydroxypropranolol and its glucuronide after single and long-term doses of propranolol.* Clin Pharmacol Ther, 1980. **27**(1): p. 22-31.

255. Watson, R.G., W. Bastain, K.A. Larkin, J.R. Hayes, J.A. McAinsh, and R.G. Shanks, *A comparative pharmacokinetic study of conventional propranolol and long acting preparation of propranolol in patients with cirrhosis and normal controls.* Br J Clin Pharmacol, 1987. **24**(4): p. 527-35.
256. Regardh, C.G., G. Johnsson, L. Jordo, P. Lungborg, B.A. Persson, and O. Ronn, *Plasma concentrations and beta-blocking effects in normal volunteers after intravenous doses of metoprolol and propranolol.* J Cardiovasc Pharmacol, 1980. **2**(6): p. 715-23.
257. Cid, E., F. Mella, L. Lucchini, M. Carcamo, and J. Monasterio, *Plasma concentrations and bioavailability of propranolol by oral, rectal, and intravenous administration in man.* Biopharm Drug Dispos, 1986. **7**(6): p. 559-66.
258. Cheymol, G., J.M. Poirier, J. Barre, A. Pradalier, and J. Dry, *Comparative pharmacokinetics of intravenous propranolol in obese and normal volunteers.* J Clin Pharmacol, 1987. **27**(11): p. 874-9.
259. Bowman, S.L., S.A. Hudson, G. Simpson, J.F. Munro, and J.A. Clements, *A comparison of the pharmacokinetics of propranolol in obese and normal volunteers.* Br J Clin Pharmacol, 1986. **21**(5): p. 529-32.
260. Sowinski, K.M., J.J. Lima, B.S. Burlew, J.D. Massie, and J.A. Johnson, *Racial differences in propranolol enantiomer kinetics following simultaneous i.v. and oral administration.* Br J Clin Pharmacol, 1996. **42**(3): p. 339-46.
261. Bleske, B.E., L.S. Welage, S. Rose, G.L. Amidon, and M.J. Shea, *The effect of dosage release formulations on the pharmacokinetics of propranolol stereoisomers in humans.* J Clin Pharmacol, 1995. **35**(4): p. 374-8.
262. Olanoff, L.S., T. Walle, U.K. Walle, T.D. Cowart, and T.E. Gaffney, *Stereoselective clearance and distribution of intravenous propranolol.* Clin Pharmacol Ther, 1984. **35**(6): p. 755-61.
263. Fremstad, D., O.G. Nilsen, L. Storstein, J. Amlie, and S. Jacobsen, *Pharmacokinetics of quinidine related to plasma protein binding in man.* Eur J Clin Pharmacol, 1979. **15**(3): p. 187-92.
264. Woo, E. and D.J. Greenblatt, *Pharmacokinetic and clinical implications of quinidine protein binding.* J Pharm Sci, 1979. **68**(4): p. 466-70.
265. Obach, R.S., F. Lombardo, and N.J. Waters, *Trend analysis of a database of intravenous pharmacokinetic parameters in humans for 670 drug compounds.* Drug Metab Dispos, 2008. **36**(7): p. 1385-405.
266. Martin, P.D., M.J. Warwick, A.L. Dane, C. Brindley, and T. Short, *Absolute oral bioavailability of rosuvastatin in healthy white adult male volunteers.* Clin Ther, 2003. **25**(10): p. 2553-63.
267. Mancinelli, L.M., L. Frassetto, L.C. Floren, D. Dressler, S. Carrier, I. Bekersky, L.Z. Benet, and U. Christians, *The pharmacokinetics and metabolic disposition of tacrolimus: a comparison across ethnic groups.* Clin Pharmacol Ther, 2001. **69**(1): p. 24-31.
268. Iwasaki, K., Y. Miyazaki, Y. Teramura, A. Kawamura, Z. Tozuka, T. Hata, and N. Undre, *Binding of tacrolimus (FK506) with human plasma proteins re-evaluation and effect of mycophenolic acid.* Res Commun Mol Pathol Pharmacol, 1996. **94**(3): p. 251-7.
269. Zahir, H., G. McCaughan, M. Gleeson, R.A. Nand, and A.J. McLachlan, *Factors affecting variability in distribution of tacrolimus in liver transplant recipients.* Br J Clin Pharmacol, 2004. **57**(3): p. 298-309.
270. Stangier, J., C.A. Su, and W. Roth, *Pharmacokinetics of orally and intravenously administered telmisartan in healthy young and elderly volunteers and in hypertensive patients.* J Int Med Res, 2000. **28**(4): p. 149-67.
271. Flesch, G., P. Muller, and P. Lloyd, *Absolute bioavailability and pharmacokinetics of valsartan, an angiotensin II receptor antagonist, in man.* Eur J Clin Pharmacol, 1997. **52**(2): p. 115-20.
272. Abernethy, D.R., I.W. Wainer, J.A. Longstreth, and N.S. Andrawis, *Stereoselective verapamil disposition and dynamics in aging during racemic verapamil administration.* J Pharmacol Exp Ther, 1993. **266**(2): p. 904-11.

273. Eichelbaum, M., G. Mikus, and B. Vogelgesang, *Pharmacokinetics of (+)-, (-)- and (+/-)-verapamil after intravenous administration.* Br J Clin Pharmacol, 1984. **17**(4): p. 453-8.
274. Obach, R.S., *Prediction of human clearance of twenty-nine drugs from hepatic microsomal intrinsic clearance data: An examination of in vitro half-life approach and nonspecific binding to microsomes.* Drug Metab Dispos, 1999. **27**(11): p. 1350-9.
275. Nordell, P., S. Winiwarter, and C. Hilgendorf, *Resolving the distribution-metabolism interplay of eight OATP substrates in the standard clearance assay with suspended human cryopreserved hepatocytes.* Mol Pharm, 2013. **10**(12): p. 4443-51.
276. Izumi, S., Y. Nozaki, T. Komori, O. Takenaka, K. Maeda, H. Kusuhara, and Y. Sugiyama, *Comparison of the Predictability of Human Hepatic Clearance for Organic Anion Transporting Polypeptide Substrate Drugs Between Different In Vitro-In Vivo Extrapolation Approaches.* J Pharm Sci, 2017.
277. Bi, Y.A., R.J. Scialis, S. Lazzaro, S. Mathialagan, E. Kimoto, J. Keefer, H. Zhang, A.M. Vildhede, C. Costales, A.D. Rodrigues, L.M. Tremaine, and M.V.S. Varma, *Reliable Rate Measurements for Active and Passive Hepatic Uptake Using Plated Human Hepatocytes.* AAPS J, 2017. **19**(3): p. 787-796.
278. Shitara, Y., T. Itoh, H. Sato, A.P. Li, and Y. Sugiyama, *Inhibition of transporter-mediated hepatic uptake as a mechanism for drug-drug interaction between cerivastatin and cyclosporin A.* J Pharmacol Exp Ther, 2003. **304**(2): p. 610-6.
279. Sogame, Y., A. Kitamura, M. Yabuki, and S. Komuro, *A comparison of uptake of metformin and phenformin mediated by hOCT1 in human hepatocytes.* Biopharm Drug Dispos, 2009. **30**(8): p. 476-84.
280. Hirano, M., K. Maeda, Y. Shitara, and Y. Sugiyama, *Contribution of OATP2 (OATP1B1) and OATP8 (OATP1B3) to the hepatic uptake of pitavastatin in humans.* J Pharmacol Exp Ther, 2004. **311**(1): p. 139-46.
281. Kimoto, E., K. Yoshida, L.M. Balogh, Y.A. Bi, K. Maeda, A. El-Kattan, Y. Sugiyama, and Y. Lai, *Characterization of Organic Anion Transporting Polypeptide (OATP) Expression and Its Functional Contribution to the Uptake of Substrates in Human Hepatocytes.* Mol Pharm, 2012.
282. Pfeifer, N.D., K. Yang, and K.L. Brouwer, *Hepatic basolateral efflux contributes significantly to rosuvastatin disposition I: characterization of basolateral versus biliary clearance using a novel protocol in sandwich-cultured hepatocytes.* J Pharmacol Exp Ther, 2013. **347**(3): p. 727-36.
283. Oda, K. and K. Yamano, *Effect of telaprevir on the metabolism and hepatic uptake of tacrolimus (FK506).* Biopharm Drug Dispos, 2014. **35**(9): p. 501-12.
284. Bayliss, M.K., J.A. Bell, W.N. Jenner, G.R. Park, and K. Wilson, *Utility of hepatocytes to model species differences in the metabolism of loxtidine and to predict pharmacokinetic parameters in rat, dog and man.* Xenobiotica, 1999. **29**(3): p. 253-68.
285. Rinaldini, L.M.J., *The Isolation of Living Cells from Animal Tissues.* International Review of Cytology, 1958. **7**: p. 587-647.
286. Molina, D.K. and V.J. DiMaio, *Normal organ weights in men: part II-the brain, lungs, liver, spleen, and kidneys.* Am J Forensic Med Pathol, 2012. **33**(4): p. 368-72.
287. Szakacs, T., Z. Veres, and L. Vereczkey, *In vitro-in vivo correlation of the pharmacokinetics of vinpocetine.* Pol J Pharmacol, 2001. **53**(6): p. 623-8.
288. Brown, H.S., A.J. Wilby, J. Alder, and J.B. Houston, *Comparative use of isolated hepatocytes and hepatic microsomes for cytochrome P450 inhibition studies: transporter-enzyme interplay.* Drug Metab Dispos, 2010. **38**(12): p. 2139-46.
289. Blanchard, N., E. Alexandre, C. Abadie, T. Lave, B. Heyd, G. Mantion, D. Jaeck, L. Richert, and P. Coassolo, *Comparison of clearance predictions using primary cultures and suspensions of human hepatocytes.* Xenobiotica, 2005. **35**(1): p. 1-15.
290. Jacobson, L., B. Middleton, J. Holmgren, S. Eirefelt, M. Frojd, A. Blomgren, and L. Gustavsson, *An optimized automated assay for determination of metabolic stability using hepatocytes: assay validation, variance component analysis, and in vivo relevance.* Assay Drug Dev Technol, 2007. **5**(3): p. 403-15.

291. Bi, Y.A., X. Qiu, C.J. Rotter, E. Kimoto, M. Piotrowski, M.V. Varma, A.F. Ei-Kattan, and Y. Lai, *Quantitative assessment of the contribution of sodium-dependent taurocholate co-transporting polypeptide (NTCP) to the hepatic uptake of rosuvastatin, pitavastatin and fluvastatin.* Biopharm Drug Dispos, 2013. **34**(8): p. 452-61.
292. Lau, Y.Y., E. Sapidou, X. Cui, R.E. White, and K.C. Cheng, *Development of a novel in vitro model to predict hepatic clearance using fresh, cryopreserved, and sandwich-cultured hepatocytes.* Drug Metab Dispos, 2002. **30**(12): p. 1446-54.
293. Hallifax, D., H.C. Rawden, N. Hakooz, and J.B. Houston, *Prediction of metabolic clearance using cryopreserved human hepatocytes: kinetic characteristics for five benzodiazepines.* Drug Metab Dispos, 2005. **33**(12): p. 1852-8.
294. Hallifax, D., A. Galetin, and J.B. Houston, *Prediction of metabolic clearance using fresh human hepatocytes: comparison with cryopreserved hepatocytes and hepatic microsomes for five benzodiazepines.* Xenobiotica, 2008. **38**(4): p. 353-67.
295. Floby, E., J. Johansson, J. Hoogstraate, N.J. Hewitt, J. Hill, and A.K. Sohlenius-Sternbeck, *Comparison of intrinsic metabolic clearance in fresh and cryopreserved human hepatocytes.* Xenobiotica, 2009. **39**(9): p. 656-62.

Chapter 7. Appendix

7.1. Rat *In Vivo* Database

Table 30 - *In vivo* rat data collated from the literature and used to determine average values used in this report.

Drug	Dose	Strain	Route	fu_p	Rb	fu_b	CL_p	CL_b	CL_R	CL_H	CL_{int}[2]	Reference
	mg/kg						mL/min/kg					
Amprenavir	10	Wistar	Bolus	0.32	0.87	0.37	20.9	24.0	0.0	24.0	85.8	[163]
Atazanavir	10	Wistar	Bolus	0.08	0.85	0.09	31.2	36.7	0.0	36.7	658.8	[163]
Atorvastatin	2	SDR	Bolus	0.04[1]	1.47	0.04[1]	47.5	32.3	0.0	32.3	1332.4	[164]
	1	SDR	Bolus	0.03	1.30	0.02	47.0	36.2	0.0	36.2	2300.5	[91]
	1 µmol	SDR	Bolus	0.06	1.20	0.05	42.0	35.0	0.0	35.0	1145.7	[93]
Benazeprilat	0.5	SDR	Bolus	0.25	0.67	0.37	30.9	46.1	24.0	22.1	77.5	[165]
Bosentan	0.024 /min	Wistar	Infusion	0.02[1]	1.04[1]	0.02[1]	31.7	30.5	0.0[1]	30.5	2925.7	[166]
	0.06 /min	Wistar	Infusion	0.02[1]	1.04[1]	0.02[1]	20.1	19.3	0.0[1]	19.3	1594.4	[166]
	40 / min	Wistar	Infusion	0.02[1]	1.04[1]	0.02[1]	29.2	28.1	0.0[1]	28.1	2605.5	[166]
	0	"Roro"	Bolus	0.02	1.04[1]	0.02[1]	57.2	55.0	0.0[1]	55.0	6111.1	[167]
	1	SDR	Bolus	0.01	1.04	0.01	15.3	14.7	0.0	14.7	1719.2	[168]
Candesartan	0.08	Rat	Bolus	0.01	0.58	0.01	2.4	4.1	0.2	3.9	372.9	[165]
Cefmetazole	0.1	SDR	Bolus	0.60	0.69	0.87	37.5	54.3	24.0	30.3	50.3	[165]
	1	SDR	Bolus	0.74	0.66	1.00	9.6	14.5	4.7[1]	9.8	10.9	[141]
	20	Not stated	Bolus	0.56	0.68[1]	0.83	40.3	59.7	11.8	47.8	110.7	[169]
Cefoperazone	1	SDR	Bolus	0.43	0.57	0.75	13.4	23.5	3.2[1]	20.3	33.8	[141]
	20	Not stated	Bolus	0.74	0.57[1]	1.00	22.5	39.5	5.4	34.0	51.6	[169]
Cefpiramide	20	SDR	Bolus	0.32[1]	0.55	0.58	8.2	14.8	3.9	10.9	21.1	[170]
	Not stated	SDR	Bolus	0.10	0.55	0.18	9.5	17.3	5.2[1]	12.1	76.7	[161]
	20	Not stated	Bolus	0.54	0.55	0.98	9.5	17.3	6.1	11.2	12.9	[169]

Cerivastatin	1	SDR	Bolus	0.03	0.70	0.04	27.0	38.6	0.0	38.6	1515.6	[91]
Clarithromycin	20	SDR	Bolus	0.29	1.09[1]	0.26	32.5	29.7	5.0	24.1	121.0	[171]
	10	SDR	Bolus	0.69	1.09	0.63	17.8	16.3	7.5	8.8	15.3	[172]
Darunavir	10	Wistar	Bolus	0.30	0.67	0.45	19.4	29.0	0.0	29.0	91.2	[163]
Diclofenac	2.5	Wistar	Bolus	0.03[1]	0.55	0.05[1]	16.3	29.6	0.0	29.6	925.8	[173]
	3.2	Wistar	Bolus	0.03[1]	0.55	0.05[1]	71.1	129.2	0.2[1]	129.0	0.0	[174]
	10	SDR	Bolus	0.03[1]	0.55	0.05[1]	5.0	9.1	0.0[1]	9.1	219.6	[175]
	5	SDR	Bolus	0.02	0.55	0.04	13.6	24.7	0.0	24.7	821.3	[176]
	5	SDR	Bolus	0.03	0.55	0.05	15.2	27.6	0.1	27.6	750.2	[176]
	1	SDR	Bolus	0.01	0.55	0.02	9.9	18.0	0.0[1]	18.0	1341.5	[177]
Digoxin	1	SDR	Bolus	0.64[1]	1.04[1]	0.62[1]	16.0	15.4	2.5	12.9	24.1	[178]
	N/A	SDR	N/A	0.64	1.04	0.62						[179]
Enalaprilat	0.5	SDR	Bolus	0.42	0.75	0.56	17.1	22.8	17.4	5.4	10.2	[165]
Erythromycin	10	Wistar	Bolus	0.78[1]	1.30[1]	0.60[1]	61.4	47.2	6.3	40.9	115.5	[180]
	50	SDR	Bolus	0.78	1.30	0.60	32.6	25.1	3.3[1]	21.8	46.3	[181]
Fexofenadine	10	SDR	Bolus	0.34[1]	0.94[1]	0.36[1]	34.4	36.5	4.3	25.3	94.7	[182]
	0.0016	SDR	Bolus	0.34[1]	0.94[1]	0.36[1]	10.3	10.9	3.7	7.2	21.6	[136]
	1	SDR	Bolus	0.34[1]	0.99	0.34	39.3	39.7	7.1	32.6	141.7	[183]
	1	Wistar	Bolus	0.34	0.90	0.38	69.3	77.4	19.0	58.4	372.3	[92]
	10	Wistar	Bolus	0.34	0.90	0.38	52.8	59.0	9.2	49.8	263.0	[92]
	1	Wistar	Infusion	0.34	0.90	0.38	56.7	63.4	8.7	54.6	318.9	[92]
	10	Wistar	Infusion	0.34	0.90	0.38	33.3	37.2	5.4	31.8	123.7	[92]
	30	Wistar	Infusion	0.34	0.90	0.38	41.6	46.5	5.1	41.3	186.6	[92]
Fluvastatin	0.5 µmol	SDR	Bolus	0.01	0.53	0.02	22.3	42.0	0.0	42.0	3893.2	[93]
Gerpafloxacin	10	Wistar	Bolus	0.60	1.51	0.40	39.3	26.1	0.9	25.2	84.6	[184, 185]
Indinavir	10	Wistar	Bolus	0.49	0.49	1	17.4	35.4	2.1	33.3	49.9	[163]
Indomethacin	Not stated	SDR	Bolus	0.00	0.60	0.01	0.3	0.4	0.0	0.6	120.7	[186]

Levofloxacin	3	SDR	Bolus	0.64[1]	0.55	1.00	6.9	12.6	4.3	8.3	9.1	[187]
	7	Wistar	Bolus	0.55	0.55	0.99	14.0	25.5	8.7	16.8	20.4	[188]
	2.85	Wistar	Bolus	0.74	0.55	1.00	30.1	54.8	18.6	36.1	56.6	[189]
Lopinavir	10	Wistar	Bolus	0.02	0.62	0.03	29.1	47.0	0.0	47.0	2608.2	[163]
Losartan	Not stated	SDR	Bolus	0.02	0.80	0.02	4.7	5.8	0.0	5.8	329.1	[186]
Midazolam				0.053[1]	1[1]	0.053[1]	56.6	56.6	0.0	56.6	2065	[190]
				0.053[1]	1[1]	0.053[1]	41.6	41.6	0.0	41.6	1129	[191]
				0.053[1]	1[1]	0.053[1]	44.0	44.0	0.0	44.0	1245	[135]
				0.053	1[1]	0.053	31.9	31.9	0.0	31.9	884	[177]
Napsagatran	5	Wistar	Bolus	0.67	0.56	1.00	59.0	105.4	14.6	44.4	79.9	[92]
	3.6	Wistar	Infusion	0.67	0.56	1.00	50.1	89.5	12.2	37.9	61.0	[92]
	30	Wistar	Infusion	0.67	0.56	1.00	89.5	159.8	24.3	65.2	187.4	[92]
Nelfinavir	10	Wistar	Bolus	0.04	0.85	0.04	31.4	36.9	0.0	36.9	1426.3	[163]
Olmesartan	0.08	SDR	Bolus	0.01	0.84	0.01	3.2	3.8	0.0	3.8	395.7	[165]
	Not stated	SDR	Bolus	0.01	0.84[1]	0.01	2.7	3.2	0.0[1]	3.2	274.6	[161]
Pitavastatin	0.2	SDR	Bolus	0.01	0.54	0.01	9.6	17.8	0.0	17.8	1803.2	[165]
	0	SDR	Infusion	0.01[1]	0.59[1]	0.02[1]	6.3	10.5	0.0	10.5	706.0	[192]
	1 µMol	SDR	Infusion	0.01	0.65	0.02	18.2	28.0	0.0	28.0	1851.9	[93]
	1	Wistar	Infusion	0.01[1]	0.59[1]	0.02[1]	11.6	19.5	0.0[1]	19.5	1463.9	[193]
Pravastatin	0.67/76	SDR	Infusion	0.51	0.77	0.66	94.6	123.0	32.5	90.5	1439.0	[165]
	5	Lewis	Bolus	0.00	0.67[1]	0.89	653.3	0.0	1.0	974.5	0.0	[194]
	0.5 µmol	SDR	Bolus	0.68	0.59	1.00	36.6	62.0	2.5	59.5	147.0	[93]
	1	SDR	Bolus	0.67	0.65	1.00	43.7	67.2	0.0	67.2	205.2	[141]
Propranolol	Various	Wistar	Infusion	0.09[1]	1.01[1]	0.08[1]			0.0	100.0	0.0	[135]
	Not stated	"Roro"	Bolus	0.09[1]	1.01[1]	0.08[1]	92.9	92.0	0.0	92.0	14375.0	[167]
	1	SDR	Bolus	0.09	1.20	0.08	112.4	93.7	0.0	93.7	19191.0	[168]
	1	Wistar	Not Stated	0.10	1.01[1]	0.10	99.8	98.8	0.0	98.8	85712.6	[195]

	1	Wistar	Not Stated	0.11	1.01[1]	0.11	54.0	53.5	0.0	53.5	1054.9	[195]
	1	Wistar	Not Stated	0.09	1.01[1]	0.09	55.6	55.0	0.0	55.0	1315.9	[195]
				0.07	1.03	0.07						[196]
	Not stated	Not stated	Not stated	0.08	0.80	0.10	92.0	115.0	0.0	32.6	494.7	[197]
	1	Wistar	Bolus	0.09	1.01[1]	0.09	70.3	69.6	0.0	69.6	2551.1	[198]
Quinidine	30	Wistar	Bolus	0.30	1.48	0.20	75.6	51.1	1.4	49.7	487.5	[199]
	25	Wistar	Bolus	0.31	1.84	0.17	18.5	10.1	0.3	9.8	65.2	[200, 201]
	Not stated	Not stated	Not stated	0.33	1.40	0.23	33.8	24.1	0.0	24.1	137.1	[197]
Ramatroban	2	SDR	Bolus	0.01	0.63	0.02	28.1	44.6	0.0	44.6	4377.6	[202]
	Not stated	SDR	Bolus	0.04	0.80	0.05	15.7	19.6	0.0	19.6	525.8	[186]
Repaglinide	0.2	SDR	Bolus	0.01	0.56	0.02	5.2	9.3	0.0	9.3	490.3	[203]
	0.2	SDR	Bolus	0.01	0.56	0.02	5.3	9.5	0.0	9.5	500.7	[204]
Ritonavir	10	Wistar	Bolus	0.04	0.70	0.05	21.0	30.0	0.0	30.0	810.8	[163]
	1	SDR	Bolus	0.04	1.00	0.04	30.0	30.0	0.0	30.0	996.7	[177]
Rosuvastatin	0.5	SDR	Bolus	0.05	0.63	0.08	80.1	127.0	8.4	118.6		[165]
	667 pmol	SDR	Infusion	0.06[1]	0.67[1]	0.08	50.6	75.9	18.9[1]	56.9	1571.9	[205]
	1	SDR	Bolus	0.08	0.70	0.11	94.5	135.0	65.0	70.0	2102.1	[168]
	1	SDR	Bolus	0.04	0.67[1]	0.06	28.0	41.8	10.4[1]	31.4	784.8	[141]
	3 µmol	SDR	Bolus	0.06[1]	0.67[1]	0.08	41.9	62.8	12.8	50.0	1189.5	[136]
	1	SDR	Infusion	0.04								[143]
	0	SDR	Infusion	0.12	0.67	0.08	40.7	60.9	15.2[1]	45.7	1002.4	[161]
Saquinavir	5	Wistar	Bolus	0.05	0.82	0.06	29.6	36.1	0.0	36.1	911.2	[163]
Taurocholate	8 µmol	SDR	Bolus	0.24	0.60	0.40	29.8	49.7	0.0	49.7	246.7	[206]
	70 ng/min	SDR	Infusion	0.24[1]	0.60[1]	0.40[1]	29.4	49.0	0.0	49.0	240.2	[207]
Telmisartan	Not Stated	SDR	Bolus	0.01	0.90	0.01	6.8	7.5	0.0	7.5	1216.2	[186]
Temocaprilat	0.5	SDR	Bolus	0.06	0.78	0.08	41.3	53.0	7.8	45.2	1005.5	[165]
Tipranavir	10	Wistar	Bolus	0.00	0.62	0.00	1.4	2.2	0.0	2.2	1124.7	[163]

Tolbutamide	10	SDR	Infusion	0.04[1]	0.75[1]	0.06[1]	0.4	0.5	0.0[1]	0.5	9.1	[208]
	10	SDR	Bolus	0.05	0.75[1]	0.06[1]	0.2	0.3	0.0	0.3	5.0	[209]
	Not stated	Not stated	Not stated		0.75							[210]
	13	Wistar	Bolus	0.04	0.75[1]	0.05	0.4	0.3	0.0[1]	0.6	10.4	[211]
	Not stated	Not stated	Not Stated	0.27	0.75	0.36	1.4	1.8	0.0[1]	1.8	5.2	[197]
Topotecan	Not stated	SDR	Bolus	0.65[1]	1.00	0.65	40.2	40.2	26.2[1]	13.9	25.0	[161]
	5	Wistar	Bolus	0.65[1]	1.00	0.65	31.2	31.2	20.4	10.8	18.8	[212]
Valsartan	0.5	SDR	Bolus	0.01	0.70	0.01	15.7	22.3	0.4	21.9	2002.3	[165]
	1	SDR	Bolus	0.00	0.60	0.01	4.2	7.0	0.1[1]	6.9	1106.5	[141]
Verapamil	3	SDR	Bolus	0.00	0.90[1]	0.07	22.8	25.3	0.1	25.2	451.0	[213]
	10	SDR	Bolus	0.08	0.90[1]	0.09	45.5	50.5	0.2	50.3	1183.2	[214]
	Not stated	Not stated	Not stated	0.05	0.85	0.06						[210]
	5	SDR	Bolus	0.06	0.95	0.07	43.4	45.6	0.2	45.4	1256.6	[172]
	5	SDR	Bolus	0.063	0.90[1]	0.07	45.7	50.7	0.2[1]	50.5	1459.9	[181]

[1]Values were calculated using data obtained from other studies or, where more than one data source was available, a mean of these values. These values were not directly stated in the referenced source.

[2]Calculated using the re-arranged well-stirred model (Equation 1, Methods)

SDR: Sprague-Dawley Rat

7.2. Rat *In Vitro* Database

Table 31 - Rat hepatocyte *in vitro* data collated from the literature and used in the literature analysis in this report.

Drug	Concentration(s)	Incubation Time(s)	Strain	Assay	CL_{int}[1]	Wholy body CL_{int}	Reference
	µM	*min*			*µL/min/mg*	*mL/min/kg*	
Amprenavir	1	1	Wistar	Suspension	258	2066	[153]
Atazanavir	1	1	Wistar	Suspension	213	1704	[153]
	0.1-15	0.5	Wistar	Suspension	234	1870	[215]
Atorvastatin	0.01-100	0-1.5 & 0-90	SDR	Suspension	1505	12043	[96]
	1	0-0.66 & 1-90	SDR	Suspension	392	3136	[91]
	1	0-0.75 & 1-120	SDR	Suspension	611	4888	[90]
	0.1	0.5-2.5	SDR	Suspension	193	1540	[93]
	1	0-90	SDR	Media Loss	30.0	240	[216]
	0.1, 1, 10	0-90	SDR	Media Loss	459	3672	[88]
	0.1-100	0.5-90	SDR	Monolayer	136	1085	[217]
	1	0-90	SDR	Monolayer	30.0	240	[216]
	1 + 100	0.5-2	Wistar	Monolayer	329	2632	[142]
	1	1-5	SDR	SCH	21.3	171	[159]
	1 + 100	0.5 + 2	Wistar	SCH	9.2	73.6	[142]
Benazeprilat	10	-	SDR	Suspension	4.7	37.6	[165]
Bosentan	0.01-100	0-1.5 & 0-90	SDR	Suspension	36.2	290	[96]
	1	0-90	SDR	Media Loss	18.0	144	[216]
	0.1-300	0.5-2	SDR	Monolayer	81.2	650	[97]
	1	0-90	SDR	Monolayer	11.5	92.0	[216]
	0.1	0-30	SDR	Monolayer	97.0	776	[168]
	1	0-30	SDR	Monolayer	76.0	608	[168]

Candesartan	0.1	-	SDR	Suspension	72.5	580	[165]
Cefmetazole	2	2-10	SDR	SCH	0.14	1.12	[161]
	1	2-15	SDR	SCH	1.5	12.0	[141]
	25	15	SDR	SCH	0.15	1.18	[143]
Cefoperazone	2	10	SDR	SCH	0.17	1.36	[161]
	1	2-15	SDR	SCH	0.39	3.12	[141]
	20	15	SDR	SCH	0.06	0.51	[143]
Cefpiramide	10	10	SDR	SCH	0.59	4.72	[161]
	10	15	SDR	SCH	0.05	0.38	[143]
Cerivastatin	0.01-100	0-1.5 & 0-90	SDR	Suspension	309	2470	[96]
	1	0-0.66 & 1-90	SDR	Suspension	471	3768	[91]
Clarithromycin	0.01-100	0-1.5 & 0-90	SDR	Suspension	61.6	493	[96]
	0.1, 1, 10	0-90	SDR	Media Loss	68.0	544	[88]
Darunavir	1	1	Wistar	Suspension	198	1586	[153]
Diclofenac	1	0-30	SDR	Monolayer	100	800	[168]
Digoxin	0.1-3.75	0-1	SDR	Suspension	97.0	776	[179]
	0.01	0-15	SDR	Monolayer	2.65	21.2	[218]
	1	2-15	SDR	SCH	4.2	33.6	[141]
Enalaprilat	10	-	SDR	Suspension	1.19	9.5	[165]
Erythromycin	0.01-100	0-1.5 & 0-90	SDR	Suspension	23.6	189	[96]
	0.1, 1, 10	0-90	SDR	Media Loss	35	280	[88]
Fexofenadine	0.01-100	0-1.5 & 0-90	SDR	Suspension	174	1390	[96]
	1	0-90	SDR	Media Loss	6.0	48.0	[216]
	0.1, 1, 10	0-90	SDR	Media Loss	117	936	[88]
	1	0-0.25 & 0-90	SDR	Media Loss	1.9	15.4	[107]
	0.1-300	0-2	SDR	Monolayer	11.0	88.0	[159]
	1	0-90	SDR	Monolayer	3.0	24.0	[216]

	Not stated	Not stated	Wistar	Monolayer	13.8	110	[92]
	1	1-10	SDR	SCH	3.06	24.5	[159]
Fluvastatin	0.1	0.5-2.5	SDR	Suspension	243	1946	[93]
	1, 100	0.5-2	SDR	Monolayer	746	5968	[142]
	1, 100	0.5, 2	Wistar	SCH	26.5	212	[142]
Grepafloxacin	5	0.25-0.75	SDR	Suspension	68.3	547	[94]
Indinavir	1	1	Wistar	Suspension	90.9	727.2	[153]
Indomethacin	1	0-0.66 & 1-90	SDR	Suspension	836	6688	[91]
Levofloxacin	5	0.25-0.75	SDR	Suspension	33.4	267	[94]
Lopinavir	1	1	Wistar	Suspension	669	5352	[153]
Losartan	1	0-90	SDR	Media Loss	197	1576	[186]
Napsagatran	-	-	Wistar	Monolayer	4.34	34.8	[92]
Nelfinavir	1-200	0.1-0.6	SDR	Suspension	2974	23792	[219]
	1	1	Wistar	Suspension	494	3951	[153]
Olmesartan	0.01-100	0-1.5 & 0-90	SDR	Suspension	11.5	91.7	[96]
	0.1	-	SDR	Suspension	45.2	362	[165]
	2-30	5-20	Wistar	SCH	0.47	3.8	[160]
	2	10	SDR	SCH	1.30	10.4	[161]
	1	15	SDR	SCH	9.63	77.0	[143]
Pitavastatin	0.01-100	0-1.5 & 0-90	SDR	Suspension	216	1726	[96]
	0.1	0.5-2.5	SDR	Suspension	444	3554	[93]
	0.1	0-60	SDR	Suspension	519	4152	[165]
	0.1, 1, 10	0-90	SDR	Media Loss	1705	13640	[88]
	0.1-300	0.5-2	SDR	Monolayer	73.8	591	[97]
	0.5-5	5-20	Wistar	SCH	22.6	181	[160]
	2	10	SDR	SCH	17.6	141	[161]
Pravastatin	0.01-100	0-1.5 & 0-90	SDR	Suspension	33.4	267	[96]

	0.1	0.5-2.5	SDR	Suspension	21.6	173	[93]
	0.1	Not Stated	SDR	Suspension	34.3	274	[165]
	0.1-400	0-0.33	SDR	Suspension	30.1	241	[220]
	0.1-300	0-2	SDR	Monolayer	11.6	93.0	[97]
	1 + 100	0.5-2	Wistar	Monolayer	26.0	208	[142]
	0.1	0-15	SDR	Monolayer	6.1	49.0	[218]
	1	1-5	SDR	SCH	1.4	11.0	[159]
	1 + 100	0.5 & 2	Wistar	SCH	2.3	18.4	[142]
	0.5-30	5-20	Wistar	SCH	0.7	5.4	[160]
	10	10	SDR	SCH	0.8	6.6	[161]
	10	2-15	SDR	SCH	8.1	64.9	[141]
	0.5	15	SDR	SCH	2.1	17.0	[143]
Propranolol	1	0-30	SDR	Monolayer	220	1760	[168]
Quinidine	1	1-5	SDR	SCH	39.5	316	[159]
Ramatroban	1	0-90	SDR	Media Loss	385	3080	[186]
Repaglinide	0.01-100	0-1.5 & 0-90	SDR	Suspension	357	2858	[96]
	0.1, 1, 10	0-90	SDR	Media Loss	49.3	394	[88]
	0.1-300	0.5-2	SDR	Monolayer	50.7	406	[97]
	1	1-5	SDR	SCH	20.8	167	[221]
Ritonavir	0.01-100	0-1.5 & 0-90	SDR	Suspension	991	7928	[96]
	1-200	0.1-0.6	SDR	Suspension	1138	9104	[219]
	1	1	Wistar	Suspension	596	4764	[153]
	0.1-30	0-2	SDR	Monolayer	37.9	303	[159]
Rosuvastatin	0.01-100	0-1.5 & 0-90	SDR	Suspension	425	3401	[96]
	0.1-400	0-0.33	SDR	Suspension	210	1680	[220]
	0.1	Not Stated	SDR	Suspension	201	1608	[165]
	0.1, 1, 10	0-90	SDR	Media Loss	1657	13256	[88]

	0.1-300	0-2	SDR	Monolayer	84.9	680	[97]
	1 + 100	0.5-2	Wistar	Monolayer	590	4720	[142]
	0.1	0-15	SDR	Monolayer	3.5	27.8	[218]
	0.1	0-30	SDR	Monolayer	135	1080	[168]
	1	0-30	SDR	Monolayer	112	896	[168]
	1	1-5	SDR	SCH	14.2	113	[159]
	1 + 100	0.5 & 2	Wistar	SCH	28.5	228	[142]
	0.5-5	5-20	Wistar	SCH	9.0	72.1	[160]
	2	10	SDR	SCH	18.3	146	[161]
	1	2-15	SDR	SCH	62.5	500	[141]
	0.5	15	SDR	SCH	13.6	109	[143]
Saquinavir	0.01-100	0-1.5 & 0-90	SDR	Suspension	430	3440	[96]
	0.1-200	0.1-0.6	SDR	Suspension	562	4496	[219]
	1	1	Wistar	Suspension	286	2290	[153]
	0.1, 1, 10	0-90	SDR	Media Loss	1469	11752	[88]
	1	1-5	SDR	SCH	97.6	780	[159]
Taurocholate	1	0.25-0.75	Wistar	Suspension	91.8	734	[222]
	1	0-15	SDR	Monolayer	6.7	53.5	[218]
	0.2	0-30	SDR	Monolayer	188	1504	[168]
	1	0-10	Wistar	Monolayer	84.6	677	[223]
Telmisartan	0.01-100	0-1.5 & 0-90	SDR	Suspension	658	5265	[96]
	0.1	Not Stated	SDR	Suspension	112	896	[165]
	1	0-90	SDR	Media Loss	2160	17280	[186]
	0.1-300	0.5-2	SDR	Monolayer	103	822	[97]
	1	1-5	SDR	SCH	29.6	237	[159]
Temocaprilat	6.3	-	SDR	Suspension	18.6	149	[165]
Tipranavir	1	1	Wistar	Suspension	462	3695	[153]

Tolbutamide	1	0-30	SDR	Monolayer	7.8	62.4	[168]
Topotecan	2	10	SDR	SCH	1.35	10.8	[161]
	5	15	SDR	SCH	0.27	2.18	[143]
Valsartan	0.01-100	0-1.5 & 0-90	SDR	Suspension	34.0	272	[96]
	0.1-300	0.5-2	SDR	Monolayer	31.7	254	[97]
	1	1-5	SDR	SCH	2.21	17.7	[159]
	0.5-5	5-20	Wistar	SCH	1.6	13.0	[160]
	10	10	SDR	SCH	1.6	12.8	[161]
	1	2-15	SDR	SCH	17.9	143	[141]
	1	15	SDR	SCH	7.1	56.4	[143]
Verapamil	1	0-30	SDR	Monolayer	190	1520	[168]

7.3. Human *In Vivo* Database

Table 32 - In vivo human data collated from the literature and used to determine average values used in this report.

Drug	Dose	Route	fu_p	R_b	fu_b	CL_p	CL_b	CL_R	CL_H	CL_{int}^2	Reference
	mg					*mL/min/kg*					
Aliskiren					0.70				11.3	35.6	[224]
Atorvastatin			0.02	0.55	0.04	8.9	16.2	0.0	16.2	2070.6	[225]
Bosentan			0.04	0.55	0.06	1.9	3.5	0.0	3.5	65.6	[226]
	10-750	Infusion	0.04	0.55	0.06	1.9	3.5	0.0	3.5	66.0	[227]
Cerivastatin			0.01	0.55	0.01	3.3	6.1	0.0	6.1	672.4	[228]
Cimetidine	600	Infusion		0.97	0.70	10.3	10.6	8.7	1.9	35.6	[229]
		Infusion		0.97	0.70	7.1	7.3	5.1	2.2	35.6	[230]
			0.81	0.97	0.84	8.3	8.6	5.3	3.3	4.6	[231]
Ciprofloxacin	200	Infusion		1.07	0.70	9.1	8.5	5.2	3.3	35.6	[232]
	300	Infusion	0.70	1.07	0.65	8.3	7.7	5.0	2.8	4.9	[233]
	400	Infusion	0.70	1.07	0.65	8.2	7.6	4.6	3.1	5.5	[233]
			0.60	1.07	0.56	7.6	7.1	3.6	3.6	7.6	[234]
Cyclosporine A	7 (/kg/day)	Infusion	0.07	1.30	0.05	9.8	7.5	0.0	7.5	226.7	[235]
			0.07	1.36	0.05	5.4	4.0	0.0	4.0	98.9	[225]
					0.04				4.7	152.0	[101]
Digoxin					0.82				4.6	7.3	[224]
Fexofenadine	0.1	Infusion	0.30	0.55	0.55	2.9	5.3	1.7	3.6	8.0	[236]
Fluvastatin	2		0.01	0.57	0.01	9.2	16.2	0.0	16.2	5246.1	[237]
			0.01	0.57							[238]
Furosemide	40	Infusion		0.55	0.70	2.0	3.5	2.4	1.2	35.6	[239]
	40	Bolus		0.55	0.70	2.5	4.6	3.3	1.3	35.6	[240]
				0.01	0.55	0.02	2.0	3.6	2.4	1.2	72.3	[234]

			0.02								[241]
			0.01	0.55	0.02	1.7	3.1		11.3	35.6	[242]
Glyburide	1.25	Infusion	0.02	0.56	0.04	1.1	1.9	0.0	1.9	55.0	[243]
	1.25	Infusion	0.02	0.56	0.04	1.1	1.9	0.0	1.9	55.0	[243]
			0.02	0.56							[244]
			0.02	0.56	0.04	1.3	2.3	0.0	2.3	69.7	[234]
	1	Infusion	0.02	0.56	0.04	1.3	2.3	0.0	2.3	69.7	[245]
Ipratropium	2	Infusion	0.91	0.89	1.00	31.4	35.3	17.7	17.7	119.8	[246]
Ketoconazole					0.02				3.9	300.3	[224]
Midazolam	0.15 (/kg)			0.53	0.70	4.6	8.6		11.3	35.6	[247]
	7.5	Bolus	0.02		0.70	5.6			11.3	35.6	[248]
			0.03	0.55	0.06	6.2	11.2		11.3	35.6	[225]
			0.02		0.70				6.6	35.6	[82]
			0.02	0.67	0.03						[177]
			0.02	0.80	0.03						[234]
Olmesartan	16	Bolus	0.00	0.58	0.01	0.3	0.5	0.2	0.3	42.4	[249]
Pitavastatin	1	Oral	0.04	0.58	0.07	0.7	1.3	0.0	1.2	19.0	[250]
	2	Oral	0.04	0.58	0.07	0.8	1.4	0.0	1.4	21.8	[250]
Pravastatin	9.9		0.52	0.55	0.95	13.5	24.5	11.5	13.1	37.7	[251]
Propranolol	0.108 (/kg)	Infusion	0.10		0.70	11.6			11.3	35.6	[252]
					0.70				16.0	35.6	[253]
			0.13	0.83	0.16	13.0	15.7	0.0	15.7	410.9	[242]
			0.13	0.89	0.15	16.0	18.0	0.0	18.0	935.8	[234]
	0.05 (/kg)	Bolus			0.70	16.8			11.3	35.6	[254]
					0.70	13.6			11.3	35.6	[255]
	10	Bolus			0.70	11.9			11.3	35.6	[256]
	2.2	Infusion			0.70	8.8			11.3	35.6	[257]

	8	Infusion	0.12		0.70	18.3			11.3	35.6	[258]
	8	Infusion			0.70	19.7			11.3	35.6	[258]
	10	Infusion	0.10		0.70	11.9			11.3	35.6	[259]
		Infusion		0.87	0.17		12.0	0.0	12.0	167.0	[260]
		Infusion		0.87	0.15		10.1	0.0	10.1	131.8	[260]
	10	Infusion			0.70	15.4			11.3	35.6	[261]
	0.1 (/kg)	Infusion	0.19		0.70		14.9	0.0	14.9	35.6	[262]
Quinidine		Infusion	0.22		0.70	2.3			11.3	35.6	[263]
			0.25		0.70						[264]
			0.26	0.87	0.30	3.9	4.4	0.8	3.6	14.8	[225]
			0.13	0.88	0.15	4.7	5.3	1.0	4.4	37.6	[234]
			0.13	0.87	0.15	5.2	6.0	1.1	4.9	43.0	[242]
Repaglinide			0.02	0.60	0.03	7.8	13.0	0.0	13.0	1397.9	[265]
			0.02	0.60	0.03	7.8	12.9	0.0	12.9	1378.8	[225]
Rosuvastatin	8		0.12	1.45	0.08	10.5	7.2	2.0	5.2	84.5	[266]
Tacrolimus	0.015 (/kg ideal weight)	Infusion			0.70		0.7	0.0	0.7	35.6	[267]
	0.015 (/kg ideal weight)	Infusion			0.70		0.8	0.0	0.8	35.6	[267]
	0.015 (/kg ideal weight)	Infusion			0.70		0.7	0.0	0.7	35.6	[267]
			0.01		0.70						[268]
			0.13	35.00	0.00						[225]
			0.47	107.20	0.00						[269]
Telmisartan	40	Bolus	0.01	0.78	0.01	11.5	14.7	0.0	14.7	7887.8	[270]
Valsartan	20	Bolus	0.05	0.55	0.09	0.5	0.9	0.3	0.6	7.3	[271]
Verapamil	20	Infusion	0.07		0.70	17.2			11.3	35.6	[272]
	20	Infusion	0.07		0.70	12.6			11.3	35.6	[272]
			0.06	0.90	0.06	14.3	15.9	0.0	15.9	1046.6	[273]
					0.70				15.0	35.6	[253]

	0.10	0.77	0.13						[274]
	0.09	0.89	0.10	11.7	13.1	0.0	13.1	344.7	[225]
	0.10		0.70	15.0			11.3	35.6	[82]

7.4. Human *In Vitro* Database

Table 33 - Human hepatocyte *in vitro* data collated from the literature and used in the literature analysis in this report.

Drug	Source	Donor(s)	Concentration(s)	Incubation Time(s)	Assay	CL_{int} [1]	Wholy body CL_{int}	Reference
			µM	*min*		*µl/min/mg*	*mL/min/kg*	
Aliskiren	Cryopreserved	10 donors	1-100		Suspension	22.7	58.3	[224]
Atorvastatin	Cryopreserved	UMJ donor	1	120	Suspension	74.0	190.0	[275]
	Cryopreserved	IRK donor	1	120	Suspension	85.0	218.3	[275]
	Cryopreserved	10 donors	1-100		Suspension	78.0	200.3	[224]
	Cryopreserved	VRR (Pooled)	1	0-60	Suspension	50.9	130.7	[276]
	Cryopreserved	OJE	1	0-60	Suspension	172.0	441.7	[276]
Bosentan	Cryopreserved	UMJ donor	1	120	Suspension	41.9	107.6	[275]
	Cryopreserved	IRK donor	1	120	Suspension	33.9	87.1	[275]
	Cryopreserved	11 donors	1	0-2	Suspension	25.4	65.1	[277]
	Cryopreserved	VRR (Pooled)	1	0-60	Suspension	24.5	62.9	[276]
	Cryopreserved	OJE	1	0-60	Suspension	65.8	169.0	[276]
	Cryopreserved	HU4122	0.1 -300	30s- 90	Monolayer	27.6		[146]
	Cryopreserved	HH1025	1	0-5	Monolayer	28.9	74.1	[277]
	Cryopreserved	2 donors	1-2	0.5-30	SCH	13.9	35.7	[89]
	Cryopreserved	HH1025	1	0-5	SCH	28.5	73.1	[277]
Cerivastatin	Cryopreserved	HH-088	Various	30s-120s	Suspension	354.2	909.6	[278]
	Cryopreserved	HH-106	Various	30s-120s	Suspension	277.1	711.6	[278]
	Cryopreserved	HH-117	Various	30s-120s	Suspension	144.4	370.8	[278]
	Cryopreserved	11 donors	1	0-2	Suspension	65.2	167.4	[277]
	Cryopreserved	VRR (Pooled)	1	0-60	Suspension	46.4	119.2	[276]

	Cryopreserved	OJE	1	0-60	Suspension	134.0	344.1	[276]
	Cryopreserved	HH1025	1	0-5	Monolayer	44.2	113.5	[277]
	Cryopreserved	2 donors	1-2	0.5-30	SCH	34.6	88.9	[89]
	Cryopreserved	HH1025	1	0-5	SCH	38.4	98.5	[277]
Cimetidine	Cryopreserved	10 donors	1-100		Suspension	2.6	6.7	[224]
Ciprofloxacin	Cryopreserved	10 donors	1-100		Suspension	11.8	30.3	[224]
Cyclosporin A	Cryopreserved	10 donors	1-100		Suspension	61.1	156.9	[224]
Digoxin	Cryopreserved	10 donors	1-100		Suspension	10.6	27.2	[224]
Fexofenadine	Cryopreserved	UMJ donor	1	120	Suspension	1.0	2.5	[275]
	Cryopreserved	IRK donor	1	120	Suspension	0.9	2.3	[275]
	Fresh		1	45	Suspension	11.4	29.3	[136]
	Cryopreserved		1	45	Suspension	1.9	4.9	[136]
	Cryopreserved	11 donors	1	0-2	Suspension	5.1	13.1	[277]
	Cryopreserved	VRR (Pooled)	1	0-60	Suspension	12.4	31.8	[276]
	Cryopreserved	OJE	1	0-60	Suspension	12.5	32.1	[276]
	Fresh		1	5-60	Monolayer	8.9	22.9	[136]
	Cryopreserved		1	5-60	Monolayer	0.8	2.1	[136]
	Cryopreserved	HH1025	1	0-5	Monolayer	1.0	2.5	[277]
	Cryopreserved	HH1025	1	0-5	SCH	2.8	7.3	[277]
Fluvastatin	Cryopreserved	RTH	1	30-90s	Suspension	63.0	161.8	[277]
	Cryopreserved	11 donors	1	0-2	Suspension	75.1	192.9	[277]
	Cryopreserved	VRR (Pooled)	1	0-60	Suspension	133.0	341.5	[276]
	Cryopreserved	OJE	1	0-60	Suspension	156.0	400.6	[276]
	Cryopreserved	HH1025	1	0-5	Monolayer	44.2	113.5	[277]
	Cryopreserved	2 donors	1-2	0.5-30	SCH	65.0	166.9	[89]
	Cryopreserved	HH1025	1	0-5	SCH	75.4	193.5	[277]
Furosemide	Cryopreserved	10 donors	1-100		Suspension	13.8	35.4	[224]

Glyburide	Cryopreserved	UMJ donor	1	120	Suspension	230.0	590.6	[275]
	Cryopreserved	IRK donor	1	120	Suspension	220.0	565.0	[275]
	Cryopreserved	VRR (Pooled)	1	0-60	Suspension	44.9	115.3	[276]
	Cryopreserved	OJE	1	0-60	Suspension	176.0	452.0	[276]
Ipratropium	Fresh		1	45	Suspension	25.0	64.2	[136]
	Fresh		1	5-60	Monolayer	18.3	47.0	[136]
	Cryopreserved		1	5-60	Monolayer	11.2	28.8	[136]
Ketoconazole	Cryopreserved	10 donors	1-100		Suspension	616.5	1583.1	[224]
Metformin	Cryopreserved	6 donors	20-10000	20	Suspension	0.4	1.0	[279]
Midazolam	Cryopreserved	RTH	1	30-90s	Suspension	172.0	441.7	[277]
Olmesartan	Fresh		5	10	SCH	1.4	3.7	[113]
Pitavastatin	Cryopreserved	UMJ donor	1	120	Suspension	163.0	418.6	[275]
	Cryopreserved	IRK donor	1	120	Suspension	133.0	341.5	[275]
	Cryopreserved	RTH	1	30-90s	Suspension	69.0	177.2	[277]
	Cryopreserved	OCF		30s-5	Suspension	61.3	157.4	[280]
	Cryopreserved	094		30s-5	Suspension	113.0	290.2	[280]
	Cryopreserved	ETR		30s-5	Suspension	39.2	100.7	[280]
	Cryopreserved	11 donors	1	0-2	Suspension	52.3	134.3	[277]
	Cryopreserved	VRR (Pooled)	1	0-60	Suspension	66.9	171.8	[276]
	Cryopreserved	OJE	1	0-60	Suspension	256.0	657.4	[276]
	Cryopreserved	HU4122	0.1 -300	30s- 90	Monolayer	53.9	138.4	[146]
	Cryopreserved	HH1025	1	0-5	Monolayer	44.2	113.5	[277]
	Fresh		5	10	SCH	19.7	50.5	[113]
	Cryopreserved	HH1025	1	0-5	SCH	56.8	145.9	[277]
Pravastatin	Cryopreserved	UMJ donor	1	120	Suspension	3.8	9.8	[275]
	Cryopreserved	IRK donor	1	120	Suspension	4.7	12.1	[275]
	Cryopreserved	Hu4163	1	0.5-3	Suspension	2.0	5.0	[281]

	Cryopreserved	Lot 109	1	0.5-3	Suspension	2.4	6.1	[281]
	Cryopreserved	10 donors	1-100		Suspension	37.0	95.0	[224]
	Cryopreserved	11 donors	1	0-2	Suspension	1.9	4.9	[277]
	Cryopreserved	VRR (Pooled)	1	0-60	Suspension	3.7	9.6	[276]
	Cryopreserved	OJE	1	0-60	Suspension	17.7	45.5	[276]
	Cryopreserved	HU4122	0.1 -300	30s- 90	Monolayer	3.0	7.6	[146]
	Cryopreserved	HH1025	1	0-5	Monolayer	1.2	3.1	[277]
	Cryopreserved	Hu4163	1	1.5	SCH	3.4	8.8	[281]
	Cryopreserved	Lot 109?	1	1.5	SCH	2.5	6.3	[281]
	Cryopreserved	2 donors	1-2	0.5-30	SCH	1.9	4.9	[89]
	Fresh		5	10	SCH	0.9	2.3	[113]
	Cryopreserved	HH1025	1	0-5	SCH	1.2	3.1	[277]
Propranolol	Cryopreserved	10 donors	1-100		Suspension	227.2	583.4	[224]
Quinidine	Cryopreserved	10 donors	1-100		Suspension	133.3	342.3	[224]
Repaglinide	Cryopreserved	11 donors	1	0-2	Suspension	54.8	140.7	[277]
	Cryopreserved	VRR (Pooled)	1	0-60	Suspension	94.0	241.4	[276]
	Cryopreserved	OJE	1	0-60	Suspension	128.0	328.7	[276]
	Cryopreserved	HU4122	0.1 -300	30s- 90	Monolayer	89.0	228.6	[146]
	Cryopreserved	HH1025	1	0-5	Monolayer	44.2	113.5	[277]
	Cryopreserved	2 donors	1-2	0.5-30	SCH	119.0	305.6	[89]
	Cryopreserved	HH1025	1	0-5	SCH	30.3	77.9	[277]
Rosuvastatin	Cryopreserved	UMJ donor	1	120	Suspension	12.5	32.2	[275]
	Cryopreserved	IRK donor	1	120	Suspension	8.3	21.4	[275]
	Cryopreserved	RTH	1	30-90s	Suspension	12.0	30.8	[277]
	Cryopreserved	Hu4163	1	0.5-3	Suspension	7.8	20.0	[281]
	Cryopreserved	Lot 109	1	0.5-3	Suspension	11.2	28.8	[281]
	Cryopreserved	11 donors	1	0-2	Suspension	13.1	33.6	[277]

	Cryopreserved	VRR (Pooled)	1	0-60	Suspension	12.6	32.4	[276]
	Cryopreserved	OJE	1	0-60	Suspension	40.6	104.3	[276]
	Cryopreserved	HU4122	0.1 -300	30s- 90	Monolayer	9.6	24.7	[146]
	Cryopreserved	HU4199	0.1 -300	30s- 90	Monolayer	1.8	4.7	[146]
	Cryopreserved	HU8089	0.1 -300	30s- 90	Monolayer	1.6	4.1	[146]
	Fresh		1	5-60	Monolayer	16.5	42.4	[136]
	Cryopreserved		1	5-60	Monolayer	3.9	10.0	[136]
	Cryopreserved	HH1025	1	0-5	Monolayer	8.4	21.5	[277]
	Cryopreserved	Hu4163	1	1.5	SCH	8.2	20.9	[281]
	Cryopreserved	Lot 109?	1	1.5	SCH	10.8	27.7	[281]
	Cryopreserved	2 donors	1-2	0.5-30	SCH	11.0	28.2	[89]
	Fresh		5	10	SCH	8.0	20.5	[113]
	Cryopreserved	KQG		10	SCH	0.4	1.0	[218]
	Cryopreserved	HH190		10	SCH	0.4	1.0	[218]
	Cryopreserved	Hu0930		10	SCH	0.3	0.7	[218]
	Cryopreserved			0.1	SCH	1.4	3.6	[282]
	Cryopreserved	HH1025	1	0-5min	SCH	15.2	39.0	[277]
Tacrolimus	Cryopreserved	HC1-15, HC5-25, HC3-18	1	0.25	Monolayer	82.1		[283]
Telmisartan	Cryopreserved	11 donors	1	0-2	Suspension	80.0	205.4	[277]
	Cryopreserved	VRR (Pooled)	1	0-60	Suspension	222.0	570.1	[276]
	Cryopreserved	OJE	1	0-60	Suspension	545.0	1399.6	[276]
	Cryopreserved	HU4122	0.1 -300	30s- 90	Monolayer	109.3	280.7	[146]
	Cryopreserved	HH1025	1	0-5	Monolayer	44.2	113.5	[277]
	Cryopreserved	HH1025	1	0-5	SCH	84.1	216.0	[277]
Valsartan	Cryopreserved	UMJ donor	1	120	Suspension	5.0	12.9	[275]
	Cryopreserved	IRK donor	1	120	Suspension	5.3	13.7	[275]
	Cryopreserved	10 donors	1-100		Suspension	13.6	34.9	[224]

	Cryopreserved	11 donors	1	0-2	Suspension	4.1	10.5	[277]
	Cryopreserved	VRR (Pooled)	1	0-60	Suspension	9.4	24.0	[276]
	Cryopreserved	OJE	1	0-60	Suspension	16.8	43.1	[276]
	Cryopreserved	HU4122	0.1 -300	30s- 90	Monolayer	2.9	7.6	[146]
	Cryopreserved	Lot 77?		0.5-1.5	Monolayer	7.6	19.4	[92]
	Cryopreserved	HH1025	1	0-5	Monolayer	1.3	3.4	[277]
	Cryopreserved	2 donors	1-2	0.5-30	SCH	2.7	6.9	[89]
	Fresh		5	10	SCH	2.8	7.1	[113]
	Cryopreserved	HH1025	1	0-5	SCH	2.8	7.3	[277]
Verapamil	Cryopreserved	10 donors	1-100		Suspension	101.7	261.2	[224]

7.5. Calculation of minimum and maximum scaling factors

Table 34 – Literature values used to calculate rat and human minimum and maximum scaling factors.

Scaling Factor	Hepatocellularity	Protein Conversion Factor	Protein Content	Liver Weight	Resultant Scaling Factor
	10^6 cells/g liver	*mg protein/10^6 cells*	***mg protein/g liver***	***g liver/kg bodyweight***	***(Mg protein/kg bodyweight)x10^{-3}***
Rat					
Minimum	98[124]	1	**98**	**35.3**[284]	**3.46**
Maximum	194[285]	1.78[123]	**345**	**45**[5]	**15.5**
Human					
Minimum	86[134]	0.67[160]	**57.6**	**20.4**[286]	**1.18**
Maximum	135[287]	1[89]	**135**	**25.7**[125]	**3.47**

7.6. Rat *In Vitro* vs. *In Vivo* Graphs

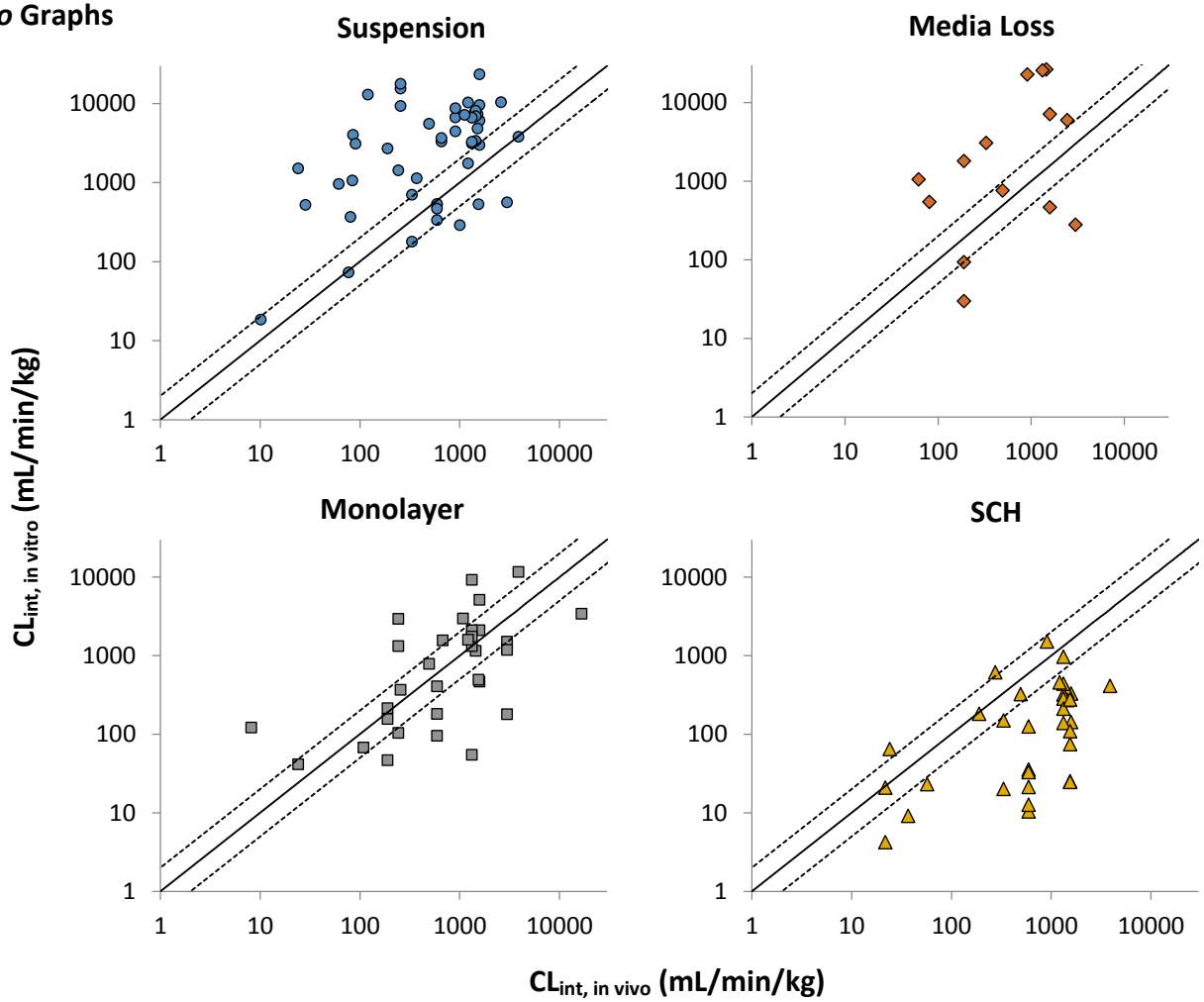

Figure 32 - Predicted $CL_{int,\ in\ vitro}$ against observed $CL_{int,\ in\ vivo}$ for compounds in rat hepatocyte assays scaled using maximum physiological scaling factors found in the literature. Line of unity (solid line), and 2-fold under and over-prediction (dashed line) are

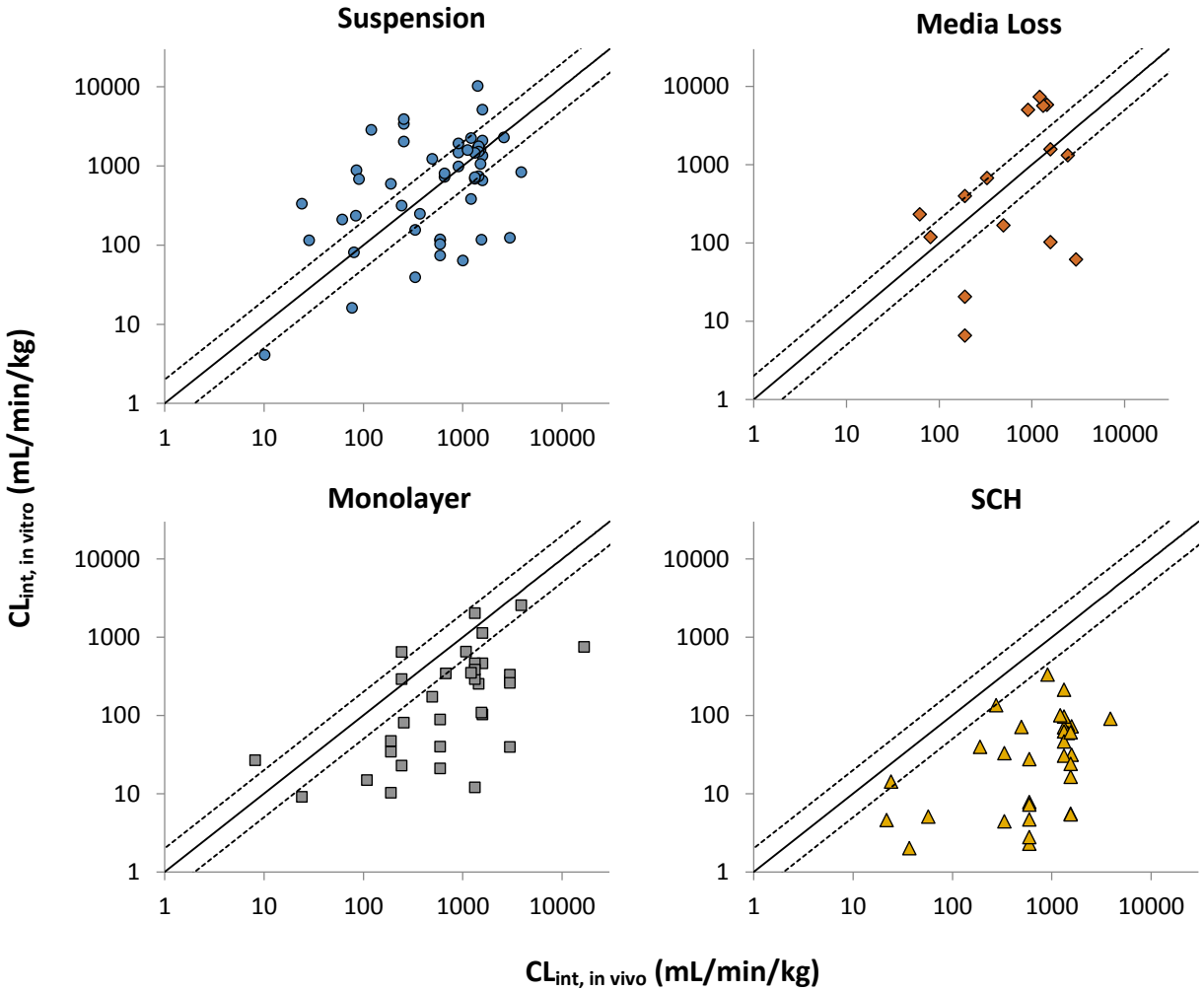

Figure 33 - Predicted $CL_{int,\ in\ vitro}$ against observed $CL_{int,\ in\ vivo}$ for compounds in rat hepatocyte assays scaled using minimum physiological scaling factors found in the literature. Line of unity (solid line), and 2-fold under and over-prediction (dashed line) are displayed.

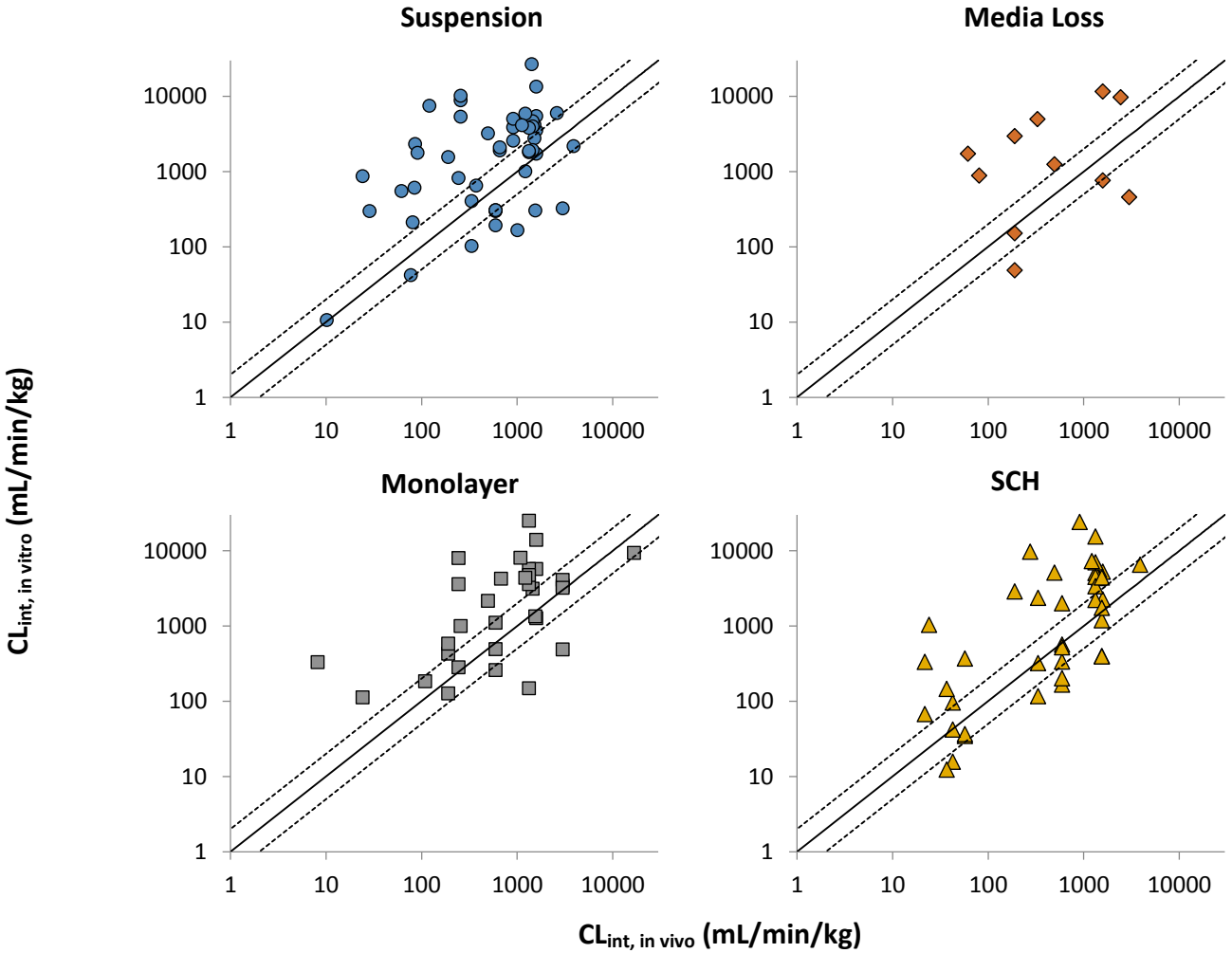

Figure 34 - Predicted $CL_{int,\ in\ vitro}$ against observed $CL_{int,\ in\ vivo}$ for compounds in rat hepatocyte assays scaled using the mean required scaling factor, calculated from the in vitro data. Line of unity (solid line), and 2-fold under and over-prediction (dashed line) are displayed.

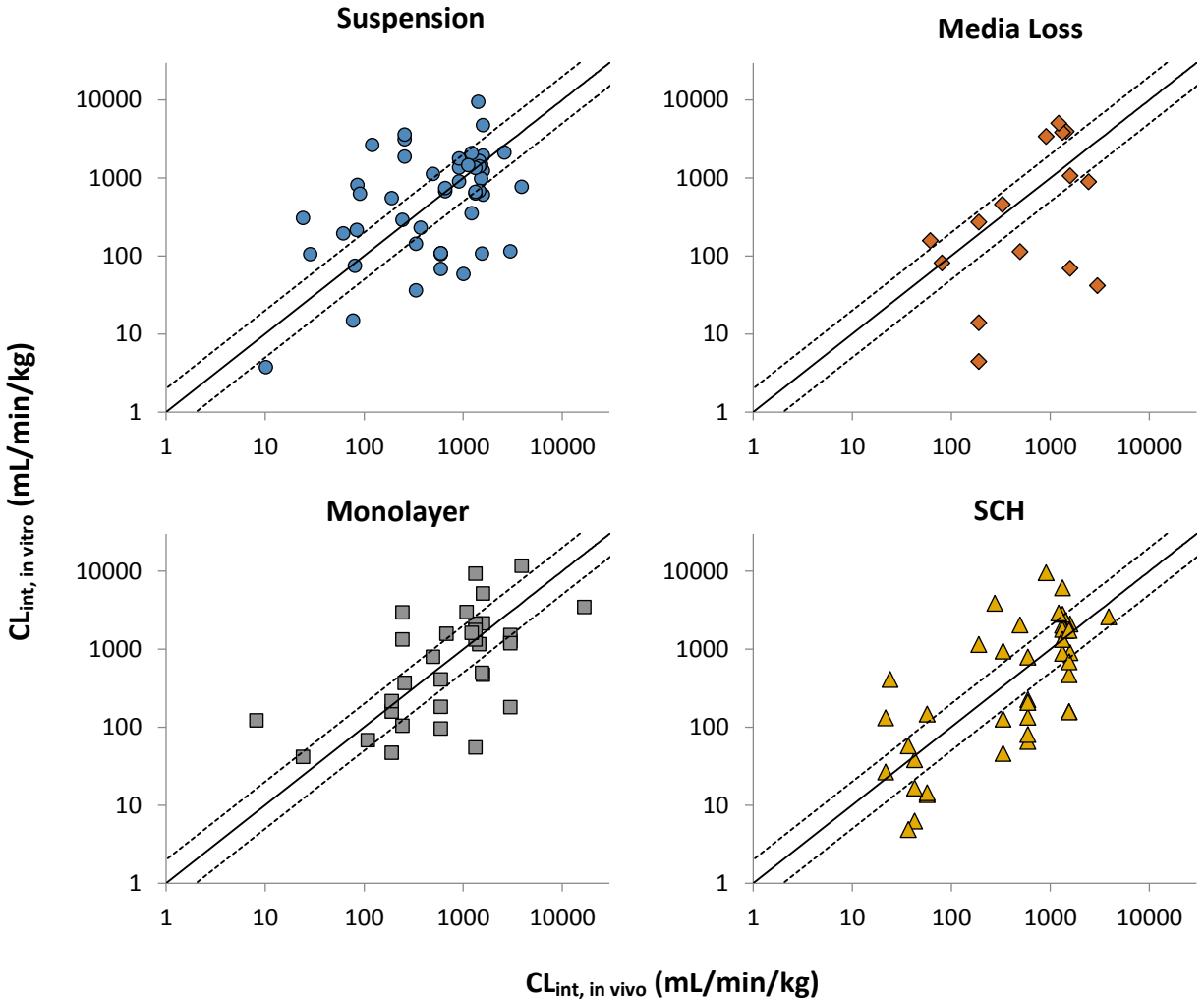

Figure 35 - Predicted $CL_{int,\ in\ vitro}$ against observed $CL_{int,\ in\ vivo}$ for compounds in rat hepatocyte assays scaled using the median required scaling factor, calculated from the *in vitro* data. Line of unity (solid line), and 2-fold under and over-prediction (dashed line) are displayed.

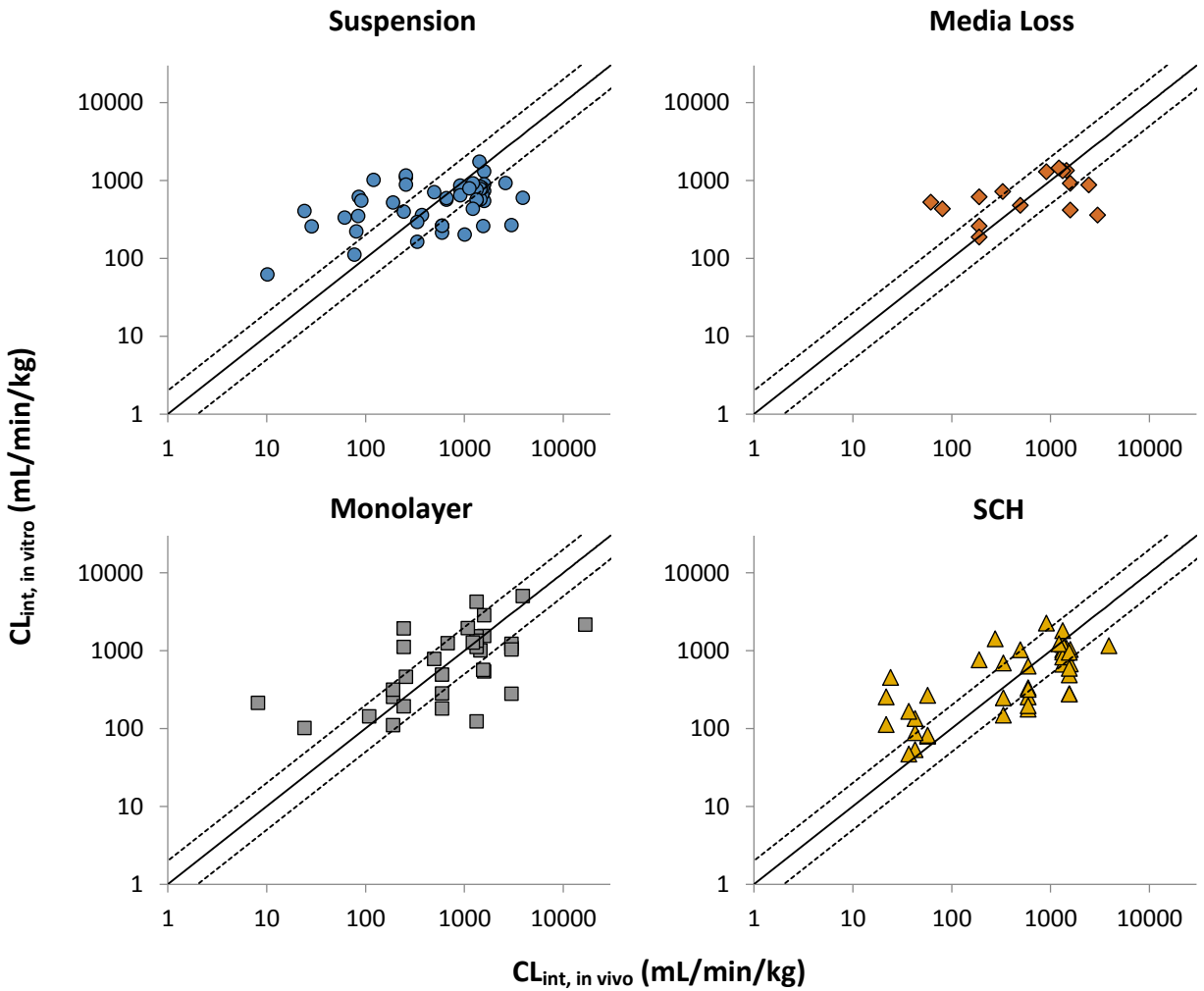

Figure 36 - Predicted $CL_{int,\ in\ vitro}$ against observed $CL_{int,\ in\ vivo}$ for compounds in rat hepatocyte assays scaled using clearance derived scaling factors, calculated from the *in vitro* data. Line of unity (solid line), and 2-fold under and over-prediction (dashed line) are displayed.

Table 35 - List of values used to calculate $CL_{int, app}$ in rat hepatocytes. Values in bold represent the mean value of the data collated.

Compound	CL_{total}	CL_{active}	$CL_{passive}$	% active	CL_{met}	$CL_{int, app}$	Reference(s)
	µl/min/mg				*µl/min/mg*		
Amprenavir	**258.2**	**180.5**	**77.7**		**52**	**103.5**	
	258.20	180.5	77.7	69.9	52[1]		[163]
Atazanavir	**223.4**	**147.1**	**76.3**		**136**	**143.1**	
	213.0	194.5	18.50	91.30			[163]
	233.75	99.75	134.00	42.67	136		[215]
Atorvastatin	**675.2**	**662.9**	**12.3**		**47.4**	**536**	
	1505.4	1500.0	5.4	98.5			[96]
	392.0	375.0	17.0	95.7	4.30		[91]
	611.0	590.0	21.0	96.6	25.00		[90]
	192.5	186.6	5.95	96.9[1]			[93]
					113.0		[88]
Bosentan	**36.2**	**18.7**	**17.5**		**7.7**	**11.0**	
	36.2	18.7	17.5	48.9			[96]
					9		[168]
					6.3		[168]
Cerivastatin	**389.9**	**349**	**40.9**		**2.3**	**20.8**	
	308.7	285	23.7	86.7			[96]
	471	413	58	87.7	2.3		[91]
Clarithromycin	**61.6**	**50.7**	**10.9**		**31.5**	**45.7**	
	61.6	50.7	10.9	81.8			[96]
					46		[88]
					16.9		[288]
Darunavir	**198.2**	**163.3**	**34.8**		**120**	**153.6**	

	198.2	163.3	34.8	82.4	120		[163]
Erythromycin	**23.6**	**11.4**	**12.2**		**26**	**16.1**	
	23.6	11.4	12.2	47.7			[96]
					26		[88]
Fexofenadine	**173.8**	**167**	**6.8**		**17**	**124.4**	
	173.8	167	6.8	94.3			[96]
					17		[88]
Indinavir	**90.9**	**83.8**	**7.1**		**52.2**	**80.0**	
	90.9	83.8	7.1	92.2	52.2[2]		[163]
Indomethacin	**836**	**599**	**237**		**1**	**3.5**	
	836	599	237	71.6	1		[91]
Lopinavir	**669**	**599.4**	**69.6**		**11564**	**665.0**	
	669	599.4	69.6	89.6	11564		[163]
Nelfinavir	**1734**	**1439.9**	**294.1**		**1290**	**1412**	
	2974	2670	304	89.8	1290		[219]
	493.9	209.7	284.2	42.5			[163]
Pitavastatin	**393**	**347.9**	**45.1**		**9**	**65.4**	
	215.8	197	18.8	87.9			[96]
	519	456.2	62.8	87.9			[165]
	444.2	390.5	53.7	87.9			[93]
					7.1		[88]
Repaglinide	**357.2**	**299**	**58.2**		**49.9**	**164.9**	
	357.2	299	58.2	84.6			[96]
					49.9		[88]
Ritonavir	**908.2**	**805.8**	**102.4**		**734**	**797.0**	
	991	873	118	87.5			[96]
		1138	1070	68.0	94	734	[219]

	595.5	474.3	121.2	79.6			[163]
							[177]
Rosuvastatin	**278.7**	**265.6**	**13.18**		**12.1**	**133.5**	
	425.1	418	7.08	97.7			[96]
	201	188.9	12.1	94			[165]
	210	190	20.4	90.3			[220]
					3.3		[88]
					14		[168]
					19		[168]
Saquinavir	**573.0**	**336.9**	**236.3**		**763.8**	**373.4**	
	430	239	191	52.1			[96]
	286.3	195.7	90.6	68.4			[163]
					1675		[88]
					130.4		In House Data
Tipranavir	**461.9**	**324.8**	**137.2**		**6534**	**452.5**	
	461.9	324.8	137.2	70.3	6534		[163]
Valsartan	**34.0**	**30.1**	**3.9**		**1.6**		
	34.0	30.1	3.9	79.4	1.6[2]		[96]

[1]Data taken as an average of other available literature values in order to calculate CL_{active} and $CL_{passive}$

[2]Data taken from microsomes

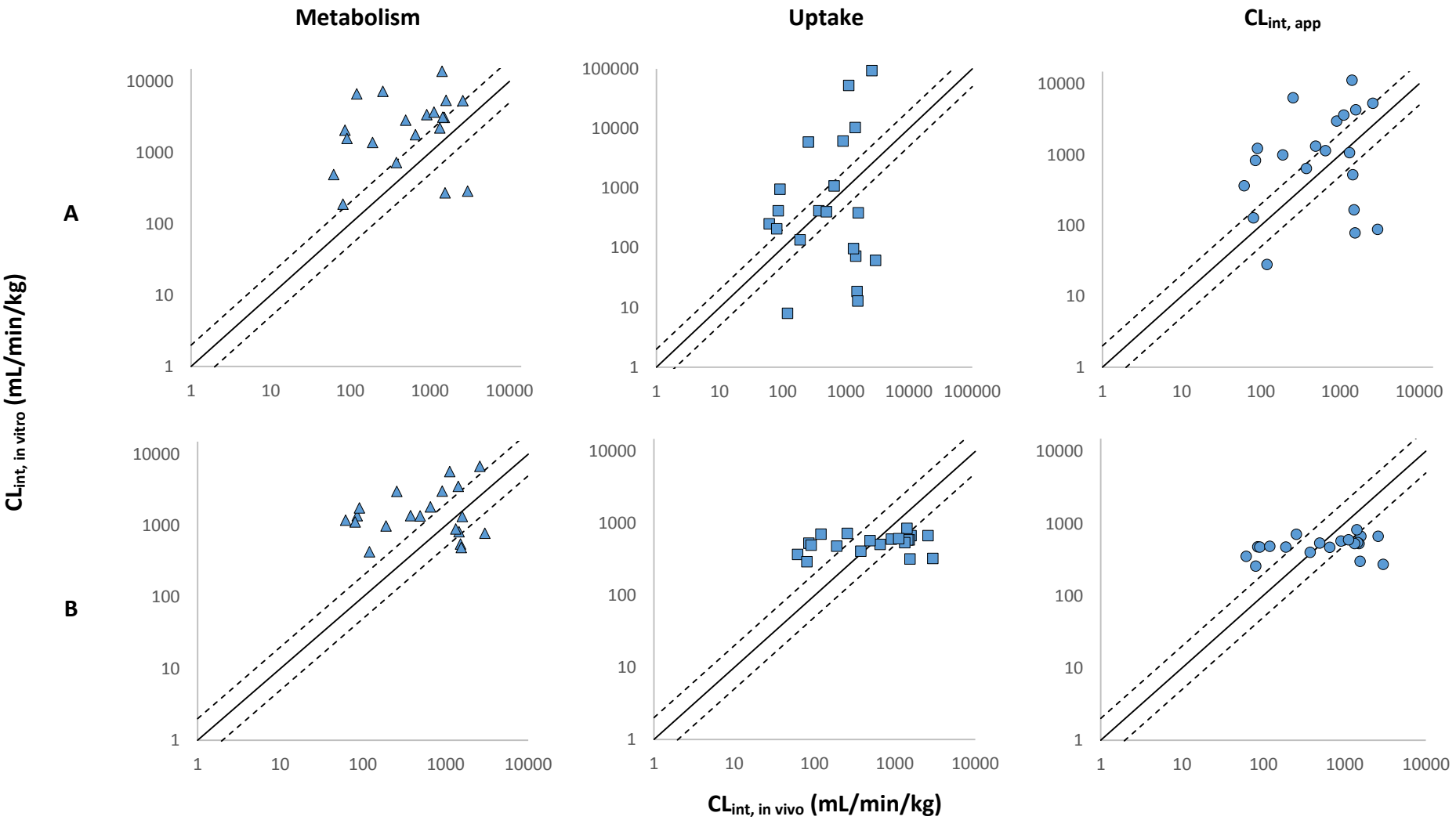

Figure 37 - Predicted $CL_{int,\ in\ vitro}$ against observed $CL_{int,\ in\ vivo}$ for 20 compounds in rat hepatocyte assays scaled using metabolic, uptake or $CL_{int,\ app}$ terms scaled using standard physiological scaling factors (A) or Median required scaling factor (metabolism), CDSF (uptake) or both ($CL_{int,app}$) (B). Line of unity (solid line), and 2-fold under and over-prediction (dashed line) are displayed.

7.7. Human *In Vitro* vs. *In Vivo* Graphs

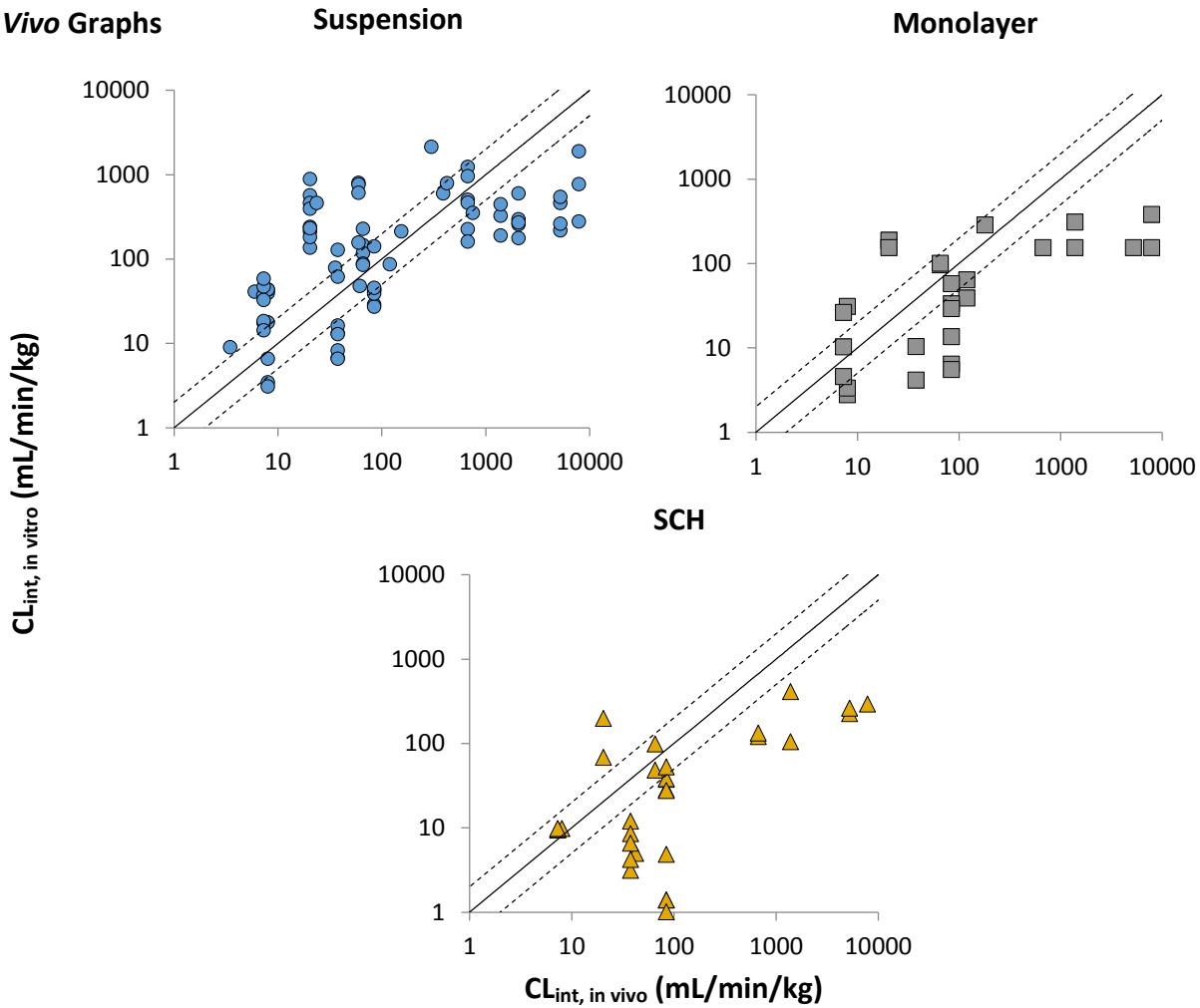

Figure 38 - Predicted $CL_{int,\ in\ vitro}$ against observed $CL_{int,\ in\ vivo}$ for compounds in human hepatocyte assays scaled using maximum physiological scaling factors found in the literature. Line of unity (solid line), and 2-fold under and over-prediction (dashed line) are displayed.

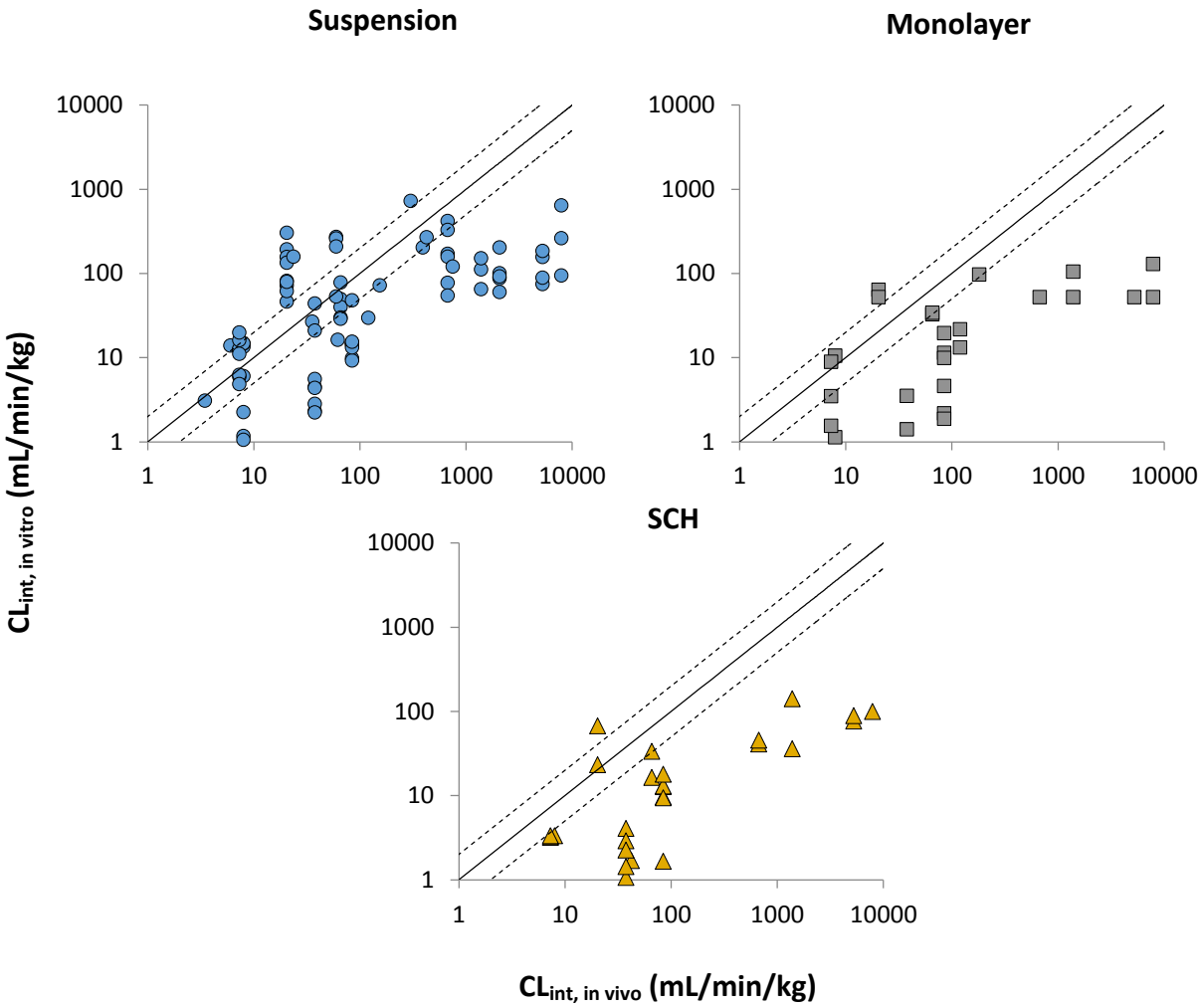

Figure 39 - Predicted $CL_{int,\ in\ vitro}$ against observed $CL_{int,\ in\ vivo}$ for compounds in human hepatocyte assays scaled using minimum physiological scaling factors found in the literature. Line of unity (solid line), and 2-fold under and over-prediction (dashed line) are displayed.

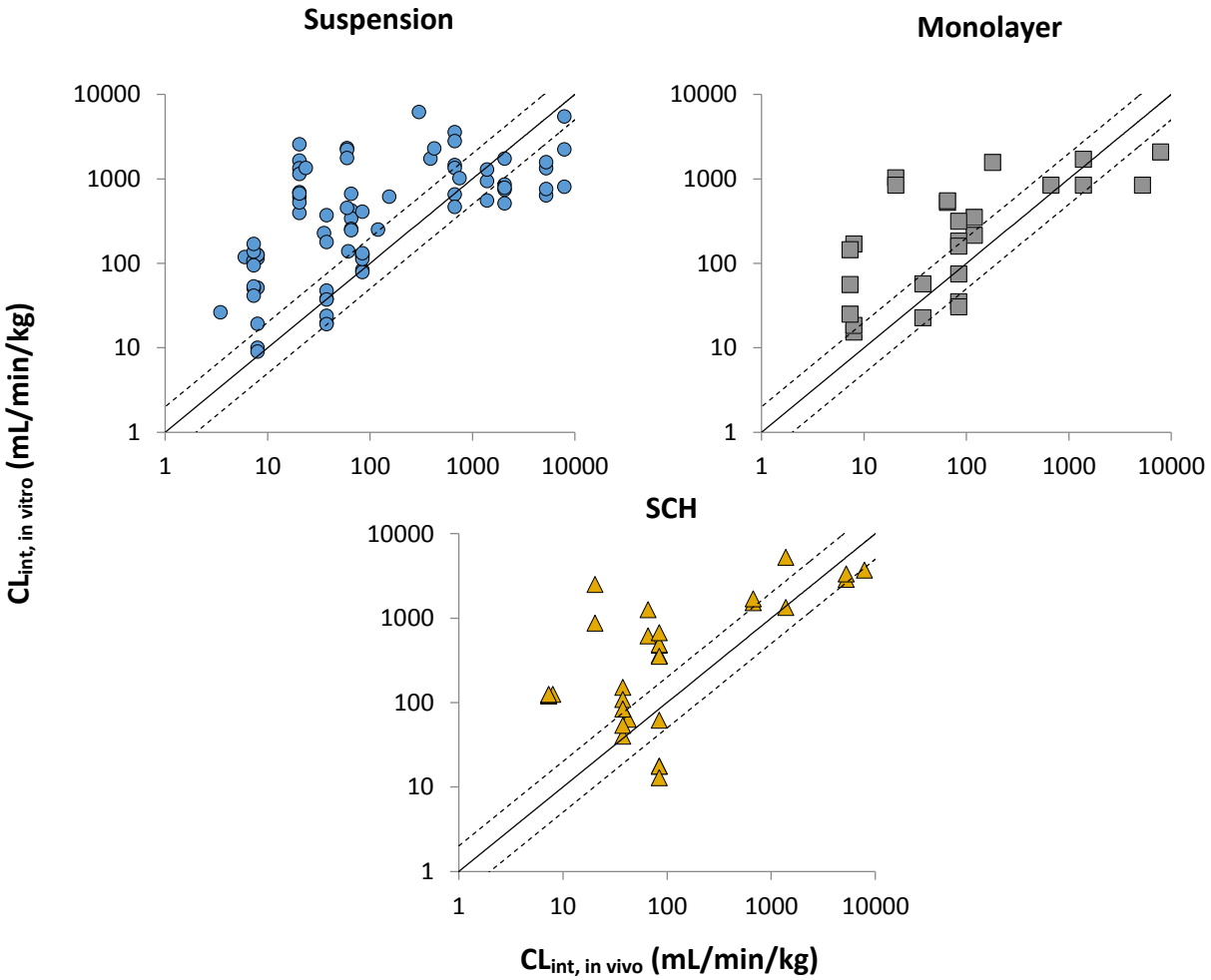

Figure 40 - Predicted $CL_{int,\ in\ vitro}$ against observed $CL_{int,\ in\ vivo}$ for compounds in human hepatocyte assays scaled using the mean required scaling factor, calculated from the *in vitro* data. Line of unity (solid line), and 2-fold under and over-prediction (dashed line) are displayed.

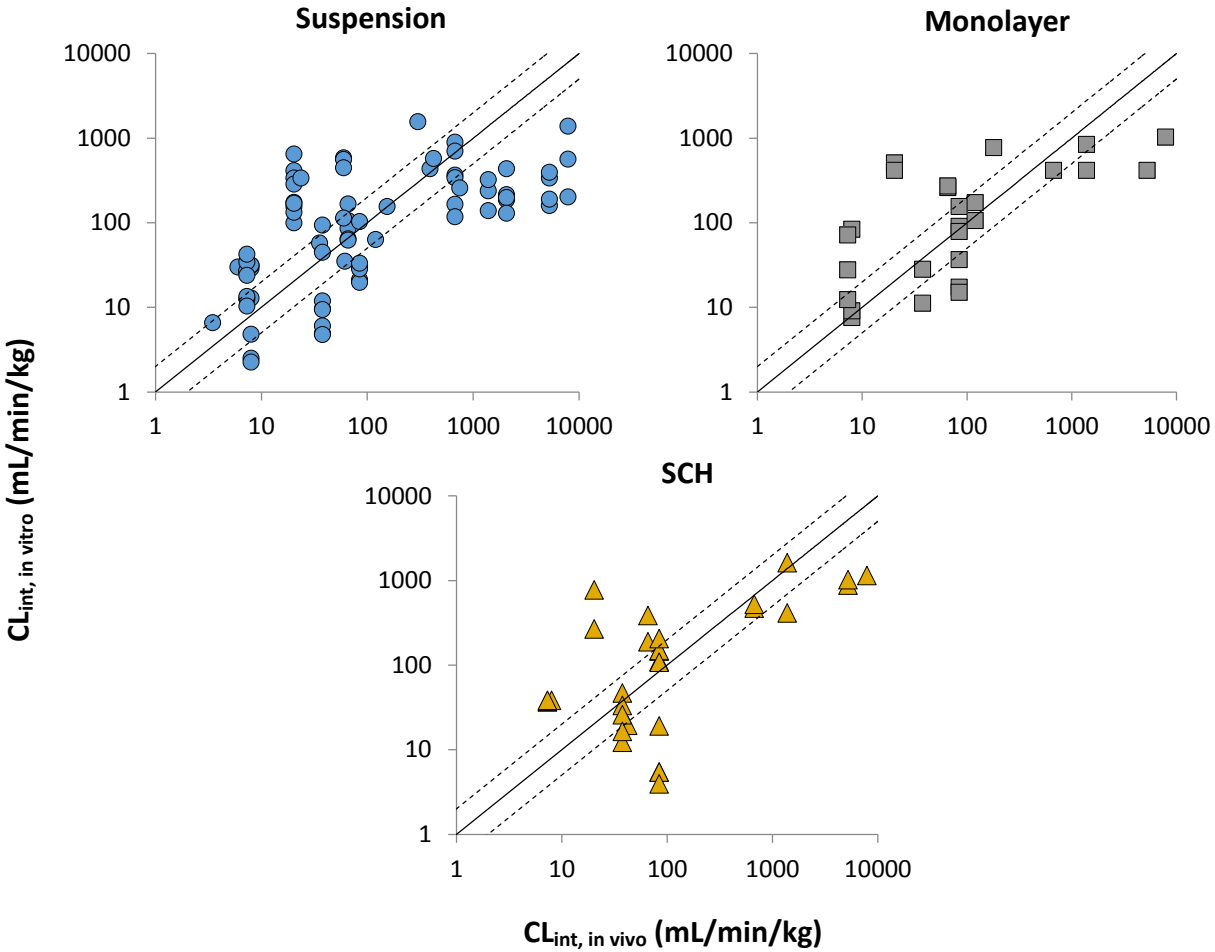

Figure 41 - Predicted $CL_{int,\ in\ vitro}$ against observed $CL_{int,\ in\ vivo}$ for compounds in human hepatocyte assays scaled using the median required scaling factor, calculated from the *in vitro* data. Line of unity (solid line), and 2-fold under and over-prediction (dashed line) are displayed.

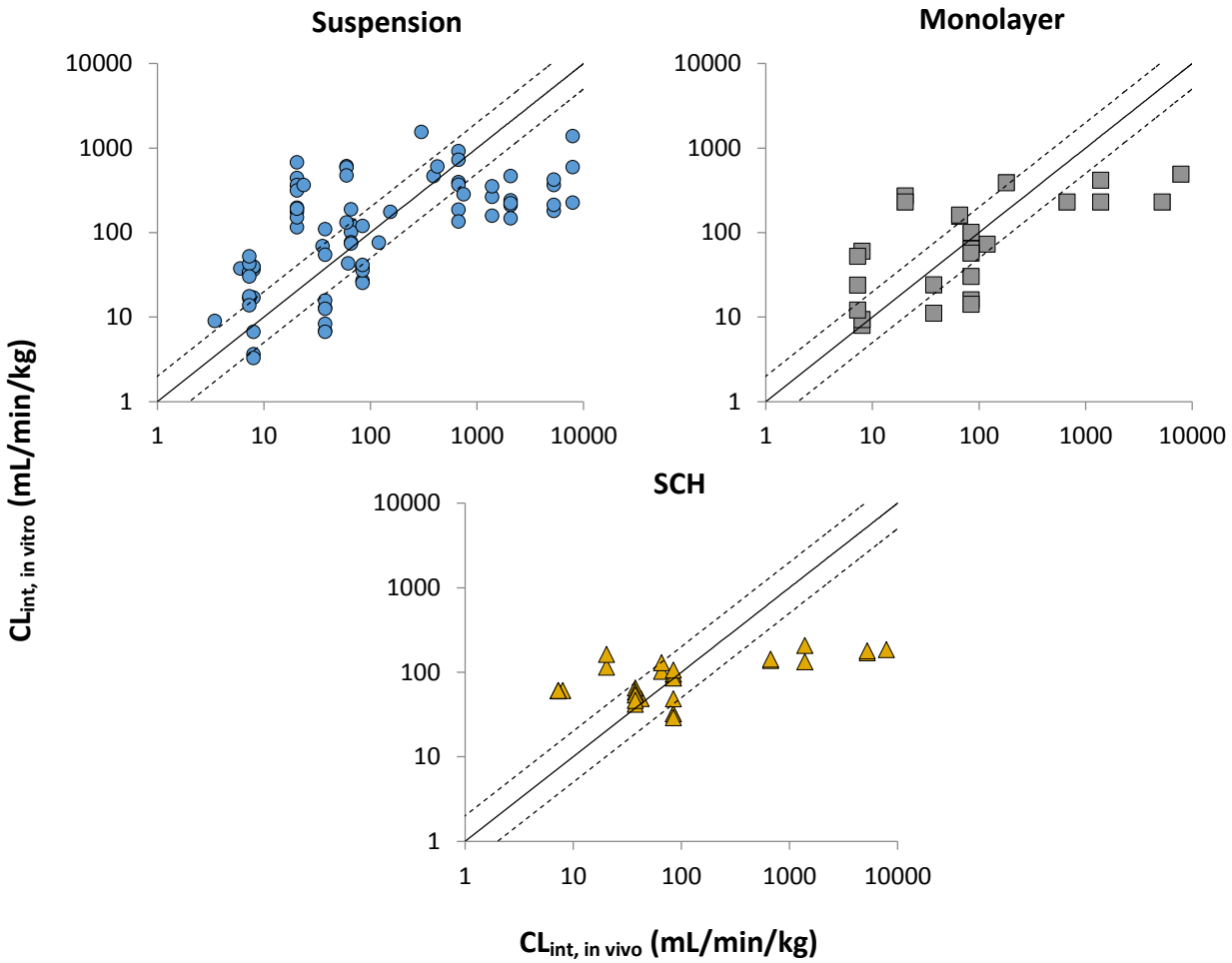

Figure 42 - Predicted $CL_{int,\ in\ vitro}$ against observed $CL_{int,\ in\ vivo}$ for compounds in human hepatocyte assays scaled using CDSF, calculated from the *in vitro* data. Line of unity (solid line), and 2-fold under and over-prediction (dashed line) are displayed.

Table 36 - List of values used to calculate $CL_{int,\ app}$ in human hepatocytes. Values in bold represent the mean value if there are multiple sources available.

	CL_{uptake}	CL_{active}	$CL_{passive}$	% active transport	CL_{met}	$CL_{int,app}$	Reference(s)
	µL/min/mg				*µL/min/mg*		
Atorvastatin	**92.0**	**78.0**	**14.0**		**0.5**	**2.9**	
	74.0	61.0	13.0	82.4	0.6		[275]
	85.0	72.0	13.0	84.0	0.3		[275]
	78.0	55.3	22.7	70.9			[224]
	50.9	42.1	8.8	82.7			[276]
	172.0	159.7	12.3	92.8			[276]
Bosentan	**38.3**	**28.4**	**9.9**		**1.3**	**4.3**	
	41.9	32.0	9.9	76.0	1.0		[275]
	33.9	24.0	9.9	71.0	0.9		[275]
	25.4	13.3	12.1	52.3			[277]
	24.5	21.8	2.7	89.1			[276]
	65.8	50.7	15.1	77.1			[276]
					1.7		[289]
					1.5		[289]
Cerivastatin	**170.2**	**132.2**	**38.0**		**3.9**	**15.8**	
	354.2	284.0	70.2	80.2			[278]
	277.1	212.0	65.1	76.5			[278]
	144.4	97.3	47.1	67.4			[278]
	65.2	32.5	32.7	49.8			[277]
	46.4	44.5	1.9	95.9			[276]
	134.0	122.9	11.1	91.7			[276]
					6.1		[241]
					1.7		[290]

Cimetidine	**2.6**	**1.2**	**1.4**		**7.1**	**2.2**	
	2.6	1.2	1.4	46.2			[224]
					13.0		[241]
					1.2		[253]
Furosemide	**13.8**	**4.4**	**9.4**		**30.0**	**10.5**	
	13.8	4.4	9.4	31.9			[224]
					30.0[2]		[241]
Glyburide	**167.7**	**113.3**	**54.4**		**6.8**	**18.7**	
	230.0	130.0	100.0	56.0	8.9		[275]
	220.0	120.0	100.0	55.0	5.6		[275]
	44.9	38.8	6.1	86.4			[276]
	176.0	164.4	11.6	93.4			[276]
					6.0		[102]
Irbesartan	**75.9**	**71.0**	**4.9**		**9.7**	**50.5**	
	33.7	32.9	0.8	97.7			[276]
	118.0	109.1	8.9	92.4			[276]
					8.3		[241]
					14.3		[177]
					6.4		[290]
Midazolam	**172.0**	**0.0**	**175.0**		**15.3**	**14.1**	
	172.0	0.0	175.0	0.0			[291]
					14.0		[241]
					14.0		[102]
					16.0		[177]
					11.3		[289]
					12.7		[289]
					7.0		[292]

					54.8		[293]
					14.0		[253]
					11.0		[253]
					4.0		[294]
					9.8		[295]
Pitavastatin	**106.0**	**96.7**	**9.1**		**1.2**	**11.8**	
	163.0	150.0	13.0	92.0	1.1		[275]
	133.0	120.0	13.0	90.0	1.2		[275]
	69.0	61.0	8.0	88.0			[291]
	61.3	54.9	6.1[1]	89.5[1]			[280]
	113.0	101.2	11.3[1]	89.5[1]			[280]
	39.2	35.1	3.9[1]	89.5[1]			[280]
	52.3	40.2	12.1	76.9			[277]
	66.9	63.4	3.5	94.7			[276]
	256.0	244.7	11.3	95.6			[276]
Pravastatin	**9.1**	**6.8**	**2.3**		**0.6**	**1.8**	
	3.8	3.1	0.7	81.0	0.4		[275]
	4.7	4.0	0.7	85.0	0.8		[275]
	2.0	1.5	0.4	79.4			[281]
	2.4	1.9	0.5	79.4			[281]
	37.0	22.8	14.2	61.6			[224]
	1.9	1.2	0.7	63.0			[277]
	3.7	3.4	0.3	91.1			[276]
	17.7	16.8	0.9	94.9			[276]
Propranolol	**227.2**	**118.4**	**108.8**		**12.3**	**23.0**	
	227.2	118.4	108.8	52.1			[224]
					7.8		[241]

					5.5		[102]
					19.9		[177]
					10.0		[292]
					10.0		[253]
					15.0		[253]
					19.0		[253]
					11.0		[290]
Quinidine	**133.3**	**90.3**	**43.0**		**4.9**	**13.6**	
	133.3	90.3	43.0	67.7			[224]
					4.5		[241]
					3.2		[177]
					7.0		[242]
Rosuvastatin	**14.6**	**13.6**	**1.0**		**0.1**	**1.3**	
	12.5	12.0	0.5	96.0	0.1		[275]
	8.3	7.8	0.5	94.0	0.1		[275]
	22.8[1]	21.2	1.6[1]	92.6[1]			[136]
	5.4[1]	5.0	0.4[1]	92.6[1]			[136]
	12.0	10.7	1.3	89.0			[291]
	7.8	7.2	0.6	92.6			[281]
	11.2	10.4	0.8	92.6			[281]
	13.1	11.3	1.8	86.4			[277]
	12.6	12.0	0.6	95.5			[276]
	40.6	38.3	2.3	94.4			[276]
Valsartan	**9.0**	**7.2**	**1.9**		**0.1**	**0.6**	
	5.0	4.6	0.4	92.0	0.2		[275]
	5.3	4.9	0.4	92.0	0.1		[275]
	13.6	6.3	7.3	46.3			[224]

	4.1	3.3	0.8	80.4			[277]
	9.4	8.1	1.2	86.8			[276]
	16.8	15.7	1.1	93.6			[276]
Verapamil	**101.7**	**0.0**	**101.7**		**21.6**	**17.8**	
	101.7	0.0	101.7	0.0			[224]
					13.0		[241]
					6.3		[102]
					23.1		[177]
					16.0		[292]
					18.0		[253]
					42.0		[253]
					43.0		[253]
					11.0		[290]

[1]Data taken as an average of other available literature values in order to calculate CL_{active} and $CL_{passive}$
[2]Data taken from microsomes

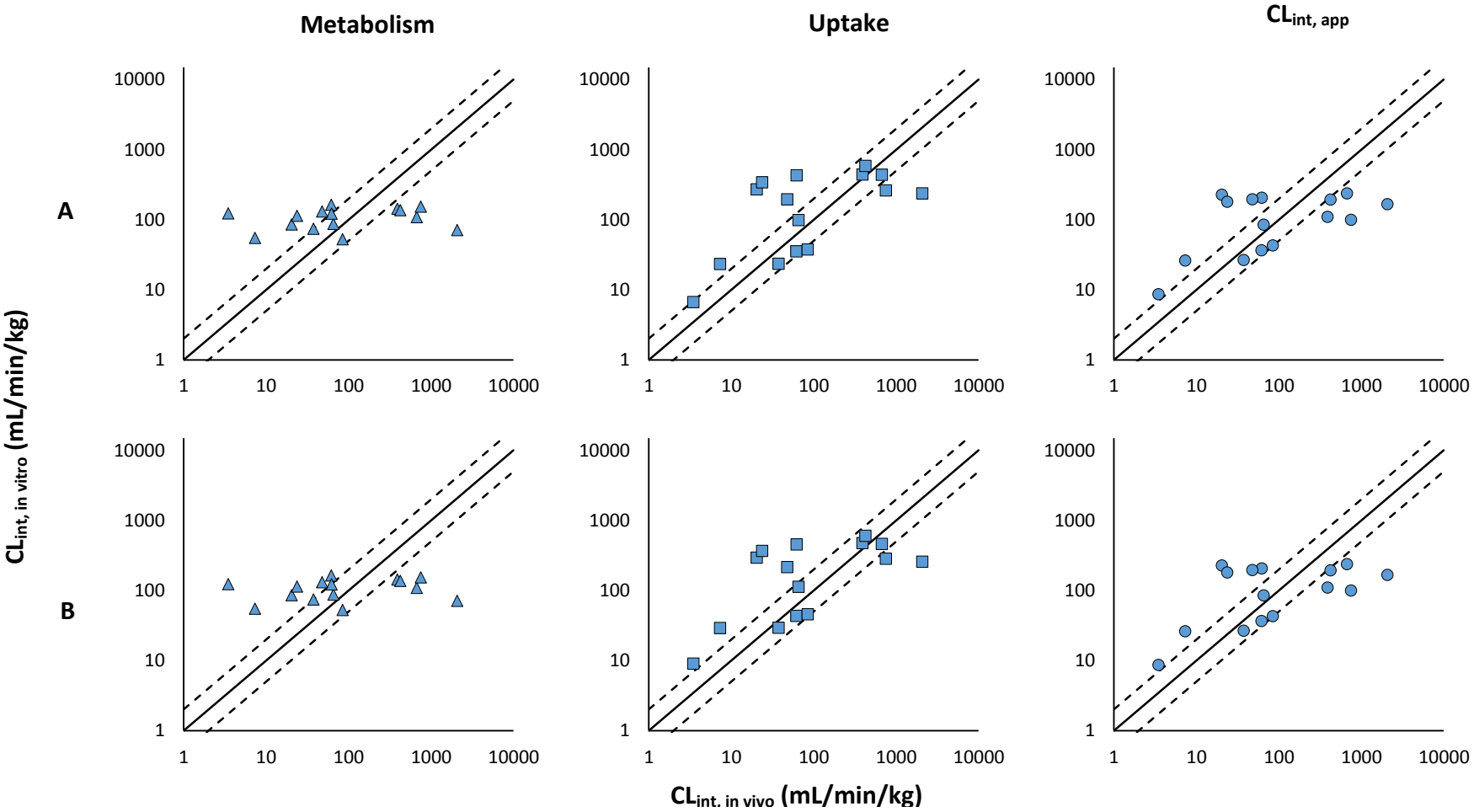

Figure 43 - Predicted $CL_{int,\ in\ vitro}$ against observed $CL_{int,\ in\ vivo}$ for 15 compounds in human hepatocyte assays scaled using metabolic, uptake or $CL_{int,\ app}$ terms scaled using standard physiological scaling factors (A) or Median required scaling factor (metabolism), CDSF (uptake) or both ($CL_{int,app}$) (B). Line of unity (solid line), and 2-fold under and over-prediction (dashed line) are displayed.

7.8. LC-MS/MS Methods

Quattro Micro Triple Quadruple Mass Spectrometer

Compounds: Saquinavir / Indinavir

Mass Spectrometer Settings:

ESI +ve mode

Source temp: 125ºC Desolvation temp: 350ºC

Cone gas: 150 L/hr Desolvation gas: 600 L/hr

Capillary voltage : 3.5kV

Saquinavir

Mass transitions : 671.45>570.45

Cone voltage: 45V Collision voltage: 45eV

Indinavir

Mass transitions : 614.45>421.25

Cone voltage: 40V Collision voltage: 40eV

Liquid Chromatography Settings:

Luna 5u Phenyl Hexyl 50x4.6mm column from Phenomenex

Gradient elution at 1ml/min, split post column to deliver 0.25ml/min to MS

	A	B	C	D	Curve
0 min	70	30	-	-	1
1 min	35	65	-	-	11
3 min	10	90	-	-	6
4.9min	-	100	-	-	1
5 min	70	30	-	-	1
5.9min	70	30	-	-	1

Where A = 90% H2O, 10% MeOH + 0.05% formic acid

B = 10% H2O, 90% MeOH + 0.05% formic acid

C = 90% H2O, 10% MeOH + 1mM ammonium acetate

D = 10% H2O, 90% MeOH + 1mM ammonium acetate

Retention times: Saquinavir = 3.2min

Indinavir = 2.9min

Micromass Quattro Ultima

Compound: Atorvastatin

Mass Spectrometer Settings:

ESI +ve mode

Source temp: 125ºC Desolvation temp: 350ºC

Cone gas: 150 L/hr Desolvation gas: 600 L/hr

Capillary voltage : 3.5kV

Atorvastatin

Mass transitions : 559.4>440.5

Cone voltage: 85V Collision voltage: 21eV

Buspirone (IS)

Mass transitions : 386.25>122.2

Cone voltage: 60V Collision voltage: 30eV

Liquid Chromatography Settings:

Luna 5u C18 50x4.6mm column from Phenomenex

Gradient elution at 1ml/min, split post column to deliver 0.25ml/min to MS

	A	B	C	D	Curve
0 min	-	-	30	70	1
5 min	-	-	30	70	1

Where A = 90% H2O, 10% MeOH + 0.05% formic acid

B = 10% H2O, 90% MeOH + 0.05% formic acid

C = 90% H2O, 10% MeOH + 1mM ammonium acetate

D = 10% H2O, 90% MeOH + 1mM ammonium acetate

Retention times: Atorvastatin= 1.6min

Buspirone = 2.4min

Compound: Cerivastatin

Mass Spectrometer Settings:

ESI +ve mode

Source temp: 125ºC Desolvation temp: 350ºC

Cone gas: 150 L/hr Desolvation gas: 600 L/hr

Capillary voltage : 3.5kV

Cerivastatin

Mass transitions : 460.25>356.2

Cone voltage: 70V Collision voltage: 35eV

Atorvastatin (IS)

Mass transitions : 559.25>440.4

Cone voltage: 60V Collision voltage: 21eV

Liquid Chromatography Settings:

Luna 5u C18 50x4.6mm column from Phenomenex

Gradient elution at 1ml/min, split post column to deliver 0.25ml/min to MS

	A	B	C	D	Curve
0 min	75	-	25	-	1
1 min	-	82	18	-	11
3 min	-	70	-	30	11
4 min	-	30	-	70	11
5.7min	75	-	25	-	11
6.4min	75	-	25	-	11

Where A = 90% H2O, 10% MeOH + 0.05% formic acid

B = 10% H2O, 90% MeOH + 0.05% formic acid

C = 90% H2O, 10% MeOH + 1mM ammonium acetate

D = 10% H2O, 90% MeOH + 1mM ammonium acetate

Retention times: Cerivastatin = 4.35min

IS = 3.4min

Compound: Clarithromycin

Mass Spectrometer Settings:

ESI +ve mode

Source temp: 125ºC Desolvation temp: 350ºC

Cone gas: 150 L/hr Desolvation gas: 600 L/hr

Capillary voltage : 3.5kV

Clarithromycin

Mass transitions : 748.4>158.15

Cone voltage: 50V Collision voltage: 31eV

Diazepam (IS)

Mass transitions : 285.05>257.05

Cone voltage: 60V Collision voltage: 21eV

Liquid Chromatography Settings:

Luna 5u C18 50x4.6mm column from Phenomenex

Gradient elution at 1ml/min, split post column to deliver 0.25ml/min to MS

	A	B	C	D	Curve
0 min	-	-	100	-	1
1 min	-	-	100	-	1
3 min	-	60	30	10	1
4.75min	-	-	-	100	1
5.6min	-	-	100	-	1

Where A = 90% H2O, 10% MeOH + 0.05% formic acid

B = 10% H2O, 90% MeOH + 0.05% formic acid

C = 90% H2O, 10% MeOH + 1mM ammonium acetate

D = 10% H2O, 90% MeOH + 1mM ammonium acetate

Retention times: Clarithromycin = 2.8min

IS = 4.2min

Compound: Erythromycin

Mass Spectrometer Settings:

ESI +ve mode

Source temp: 125ºC Desolvation temp: 350ºC

Cone gas: 150 L/hr Desolvation gas: 600 L/hr

Capillary voltage : 3.5kV

Erythromycin

Mass transitions : 734.35>158.15

Cone voltage: 45V Collision voltage: 35eV

Midazolam (IS)

Mass transitions : 326.0>291.2

Cone voltage: 70V Collision voltage: 25eV

Liquid Chromatography Settings:

Luna 5u Phenyl Hexyl 50x4.6mm column from Phenomenex

Gradient elution at 1ml/min, split post column to deliver 0.25ml/min to MS

	A	B	C	D	Curve
0 min	-	-	100	-	1
1 min	-	-	100	-	1
3 min	-	-	30	70	1
4.75min	-	-	-	100	1
5.6min	-	-	100	-	1

Where A = 90% H2O, 10% MeOH + 0.05% formic acid

B = 10% H2O, 90% MeOH + 0.05% formic acid

C = 90% H2O, 10% MeOH + 1mM ammonium acetate

D = 10% H2O, 90% MeOH + 1mM ammonium acetate

Retention times: Erythromycin= 4.5min

IS = 4.3min

Compound: Pitavastatin

Mass Spectrometer Settings:

ESI +ve mode

Source temp: 125ºC Desolvation temp: 350ºC

Cone gas: 150 L/hr Desolvation gas: 600 L/hr

Capillary voltage : 3.5kV

Pitavastatin

Mass transitions : 422.4>290.3

Cone voltage: 40V Collision voltage: 25eV

Buspirone (IS)

Mass transitions : 386.25>122.2

Cone voltage: 60V Collision voltage: 30eV

Liquid Chromatography Settings:

Luna 5u C18 50x4.6mm column from Phenomenex

Gradient elution at 1ml/min, split post column to deliver 0.25ml/min to MS

	A	B	C	D	Curve
0 min	100	-	-	-	1
1 min	100	-	-	-	11
3 min	5	85	10	-	1
4 min	-	90	5	5	1
5 min	100	-	-	-	1

Where A = 90% H2O, 10% MeOH + 0.05% formic acid

B = 10% H2O, 90% MeOH + 0.05% formic acid

C = 90% H2O, 10% MeOH + 1mM ammonium acetate

D = 10% H2O, 90% MeOH + 1mM ammonium acetate

Retention times: Pitavastatin= 3.2min

IS = 2.3min

Compound: Repaglinide

Mass Spectrometer Settings:

ESI +ve mode

Source temp: 125ºC Desolvation temp: 350ºC

Cone gas: 150 L/hr Desolvation gas: 600 L/hr

Capillary voltage : 3.5kV

Repaglinide

Mass transitions : 453.25>230.2

Cone voltage: 80V Collision voltage: 25eV

Midazolam (IS)

Mass transitions : 326.0>291.2

Cone voltage: 70V Collision voltage: 25eV

Liquid Chromatography Settings:

Luna 5u C18 50x4.6mm column from Phenomenex

Gradient elution at 1ml/min, split post column to deliver 0.25ml/min to MS

	A	B	C	D	Curve
0 min	-	-	100	-	1
1 min	-	-	100	-	11
3 min	-	-	30	70	1
4.75min	-	-	-	100	1
5.6min	-	-	100	-	1

Where A = 90% H2O, 10% MeOH + 0.05% formic acid

B = 10% H2O, 90% MeOH + 0.05% formic acid

C = 90% H2O, 10% MeOH + 1mM ammonium acetate

D = 10% H2O, 90% MeOH + 1mM ammonium acetate

Retention times: Repaglinide= 4.5min

IS = 4.3min

Compound: Repaglinide

Mass Spectrometer Settings:

ESI +ve mode

Source temp: 125ºC Desolvation temp: 350ºC

Cone gas: 150 L/hr Desolvation gas: 600 L/hr

Capillary voltage : 3.5kV

Rosuvastatin

Mass transitions : 482.3>258.2

Cone voltage: 65V Collision voltage: 30eV

Buspirone (IS)

Mass transitions : 386.25>122.2

Cone voltage: 60V Collision voltage: 30eV

Liquid Chromatography Settings:

Luna 5u C18 50x4.6mm column from Phenomenex

Gradient elution at 1ml/min, split post column to deliver 0.25ml/min to MS

	A	B	C	D	Curve
0 min	-	-	100	-	1
1 min	-	-	100	-	11
3 min	20	-	-	80	6
4 min	-	-	-	100	11
5.7min	-	-	100	-	11
6.4min	-	-	100	-	11

Where A = 90% H2O, 10% MeOH + 0.05% formic acid

B = 10% H2O, 90% MeOH + 0.05% formic acid

C = 90% H2O, 10% MeOH + 1mM ammonium acetate

D = 10% H2O, 90% MeOH + 1mM ammonium acetate

Retention times: Rosuvastatin= 4.4min

IS = 3.6min

Compound: Tolbutamide

Mass Spectrometer Settings:

ESI -ve mode

Source temp: 125ºC Desolvation temp: 350ºC

Cone gas: 150 L/hr Desolvation gas: 600 L/hr

Capillary voltage : 3.0kV

Tolbutamide

Mass transitions : 269>170

Cone voltage: 75V Collision voltage: 17eV

Warfarin (IS)

Mass transitions : 306.95>160.95

Cone voltage: 25V Collision voltage: 20eV

Liquid Chromatography Settings:

Luna 5u Phenyl Hexyl 50x4.6mm column from Phenomenex

Gradient elution at 1ml/min, split post column to deliver 0.25ml/min to MS

	A	B	C	D	Curve
0 min	100	-	-	-	1
1 min	100	-	-	-	1
2.75min	30	70	-	-	1
4.75min	-	100	-	-	1
5.6min	100	-	-	-	1

Where A = 90% H2O, 10% MeOH + 0.05% formic acid

B = 10% H2O, 90% MeOH + 0.05% formic acid

C = 90% H2O, 10% MeOH + 1mM ammonium acetate

D = 10% H2O, 90% MeOH + 1mM ammonium acetate

Retention times: Tolbutamide= 3.5min

IS = 4.2min

Compound: Valsartan

ESI +ve mode

Source temp: 125ºC Desolvation temp: 350ºC

Cone gas: 150 L/hr Desolvation gas: 600 L/hr

Capillary voltage : 3.5kV

Valsartan

Mass transitions : 436.45>235.25

Cone voltage: 35V Collision voltage: 15eV

Buspirone (IS)

Mass transitions : 386.25>122.2

Cone voltage: 60V Collision voltage: 30eV

Liquid Chromatography Settings:

Luna 5u C18 50x4.6mm column from Phenomenex

Gradient elution at 1ml/min, split post column to deliver 0.25ml/min to MS

	A	B	C	D	Curve
0 min	100	-	-	-	1
1 min	100	-	-	-	11
3 min	-	15	-	85	1
4 min	-	15	-	85	1
5 min	100	-	-	-	1

Where A = 90% H2O, 10% MeOH + 0.05% formic acid

B = 10% H2O, 90% MeOH + 0.05% formic acid

C = 90% H2O, 10% MeOH + 1mM ammonium acetate

D = 10% H2O, 90% MeOH + 1mM ammonium acetate

Retention times: Valsartan= 3.1min

IS = 2.3m

7.9. Conventional Depletion Profiles

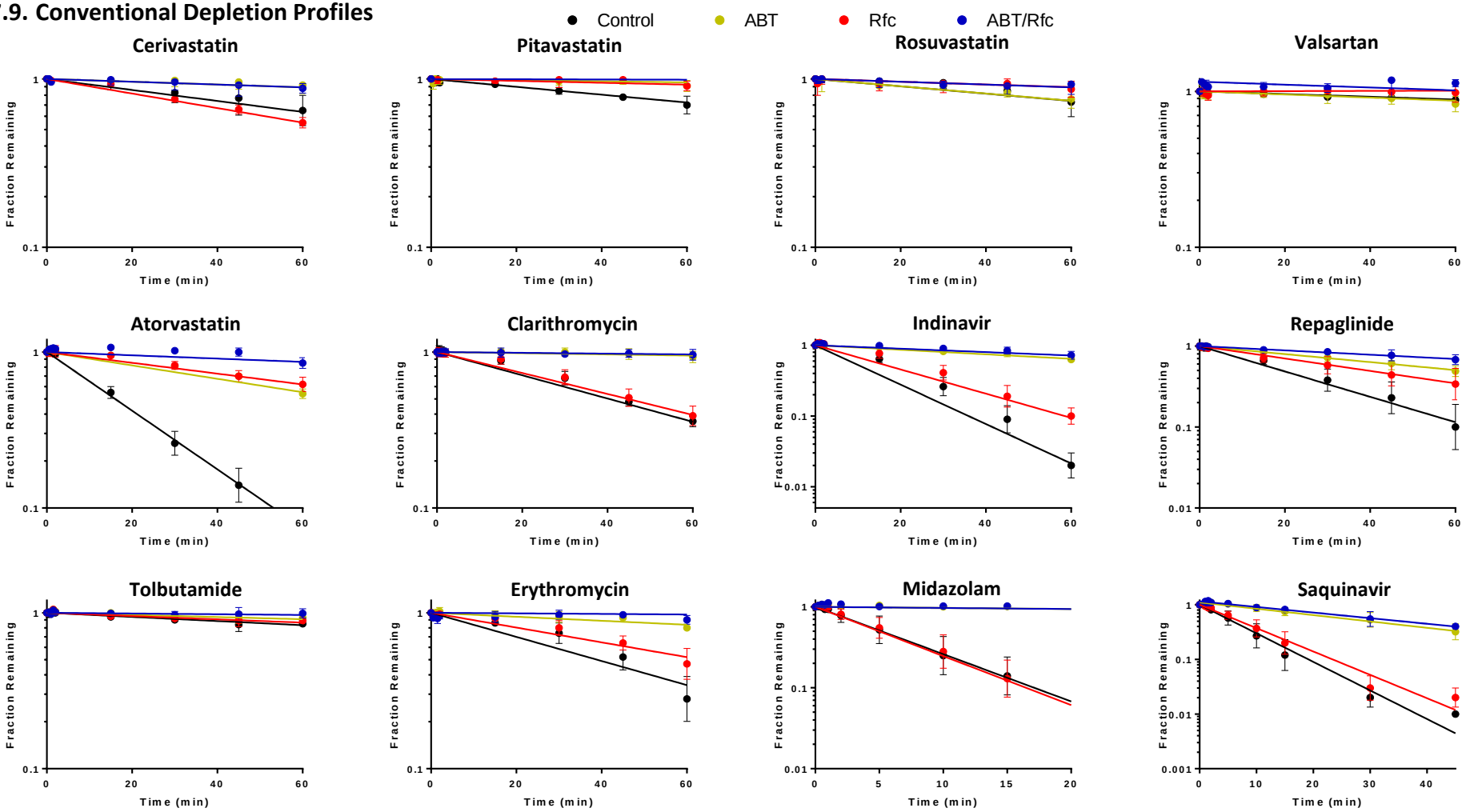

Figure 44 - Substrate depletion-time profiles in rat hepatocytes at 1 µM in the conventional depletion assay. Data fitted using Equation 9 and represents mean ± SD (n=3).

7.10. Media Loss Profiles

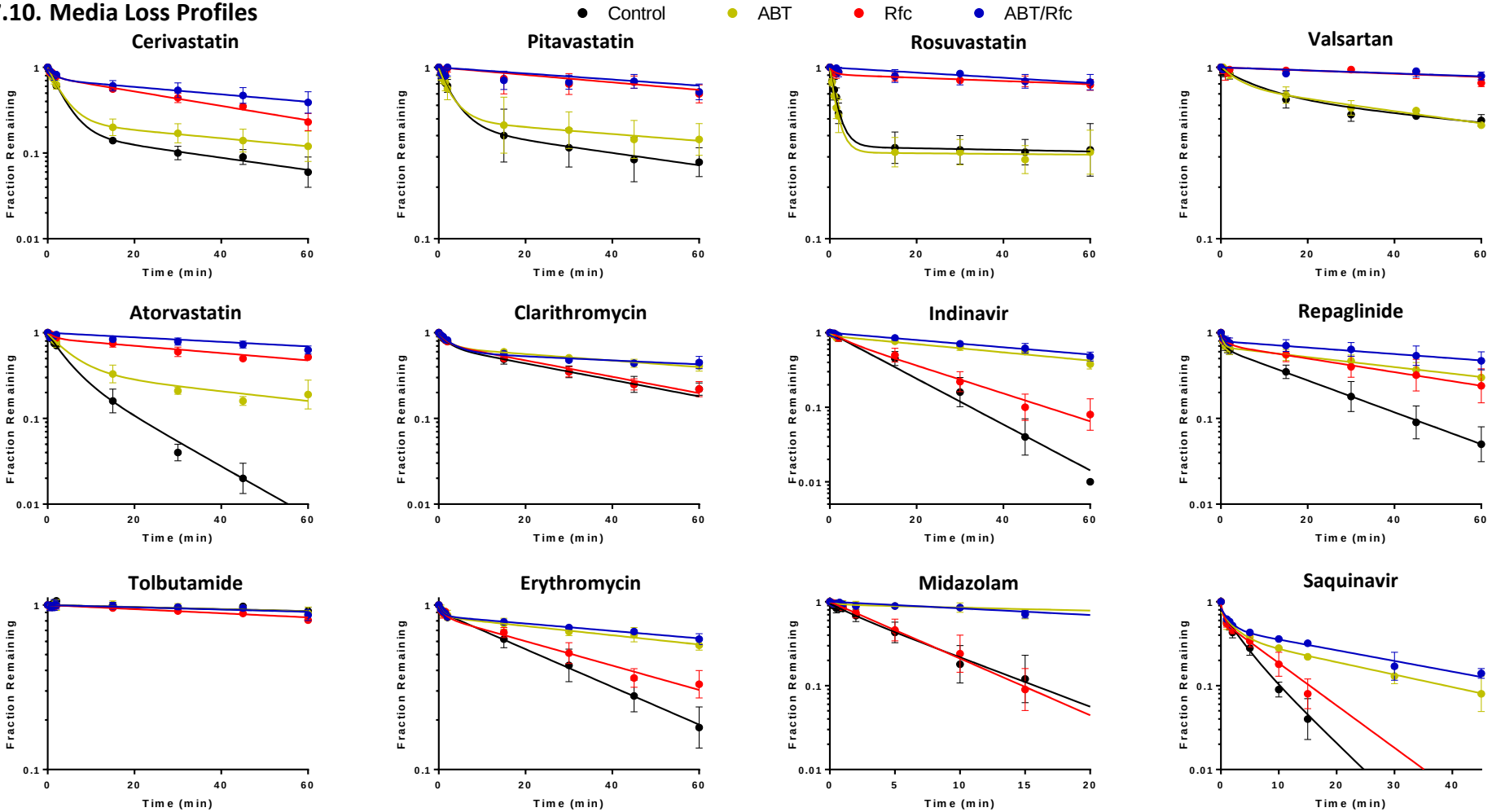

Figure 45 - Substrate depletion-time profiles in rat hepatocytes at 1 µM in the media loss assay. Data fitted using Equation 9 or Equation 10, as appropriate for a biphasic or monophasic fit. Data represents mean ± SD (n=3).

7.11. Conventional Depletion Profiles (Modelled)

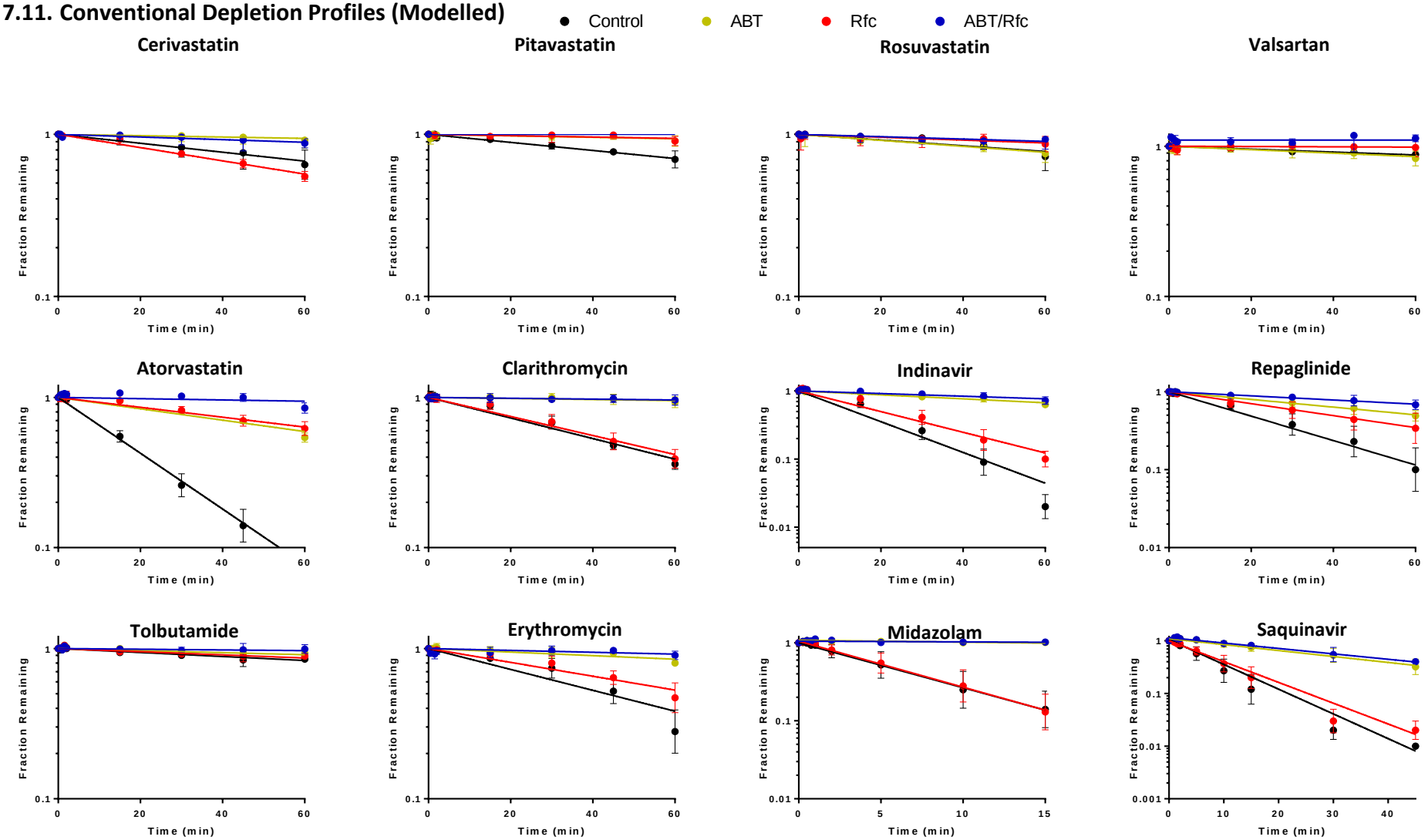

Figure 46 - Substrate depletion-time profiles in rat hepatocytes at 1 µM in the conventional depletion assay. Data fits were generated using a two-compartment model, described for the conventional depletion assay by Equation 14. Data represents mean ± SD (n=3).

7.12. Media Loss Profiles (Modelled)

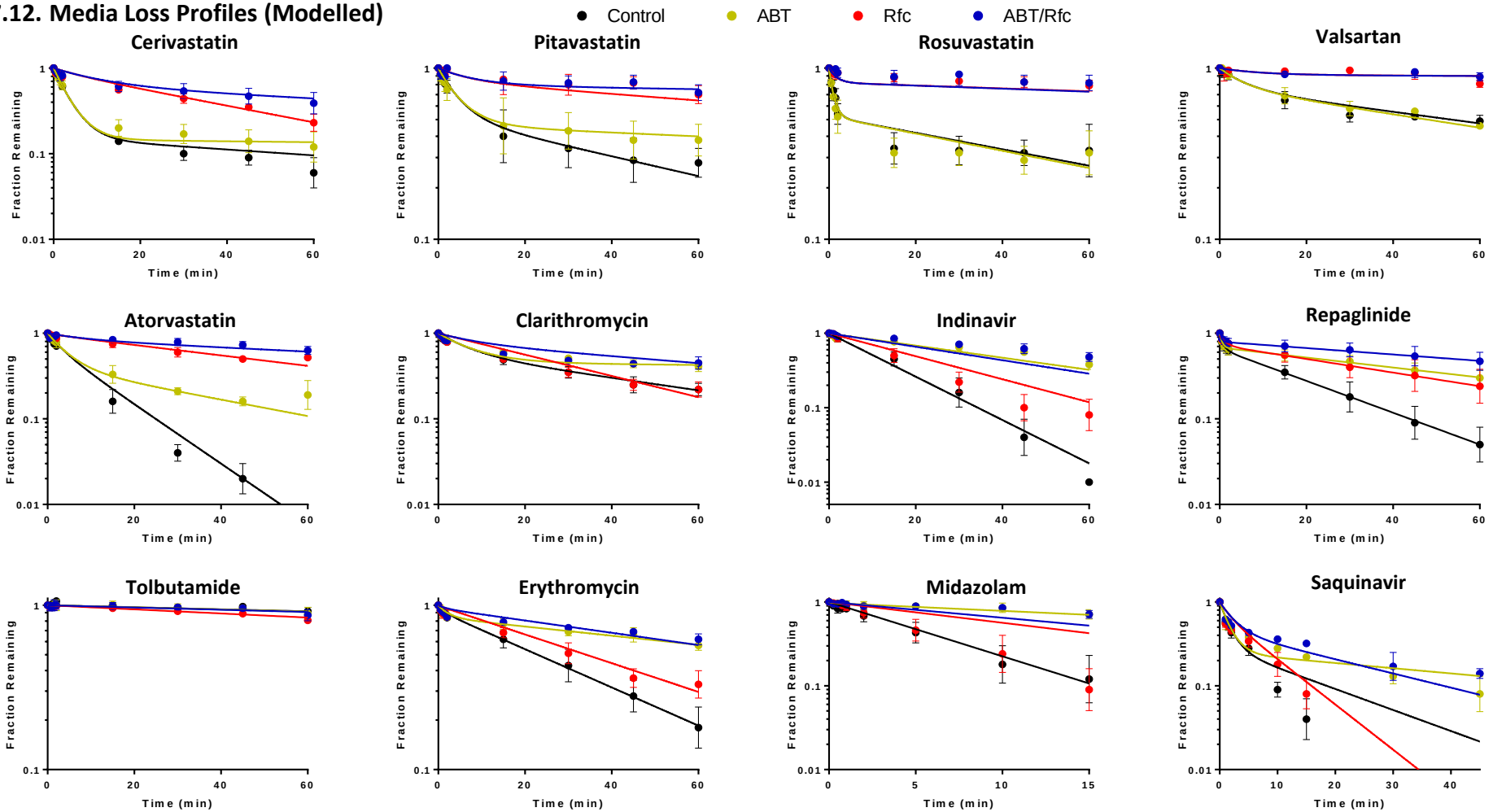

Figure 47 - Substrate depletion-time profiles in rat hepatocytes at 1 µM in the media loss assay. Data fits were generated using a two-compartment model, described for the media loss assay by Equation 14 to Equation **16**. Data represents mean ± SD (n=3).

7.13. Model Script

7.13.1. Step 1 – Modelling of Conventional Depletion Assay

CL_inter.m

```
function clact = cl_inter(theta, GammaABT, GammaRIF,GammaABTRIF)

ABTINT=theta(2)^(GammaABT);
RIFINT=theta(3)^(GammaRIF);
ABTRIFINT=theta(4)^(GammaABTRIF);

clact = theta(1)*ABTINT*RIFINT*ABTRIFINT;
```

Jac.m

```
function J = Jac(THETA,data_all,mic_prot,volumes,doses)

t_all = data_all(:,1);
exp_id = data_all(:,3);

h=0.00001;
h2=0.0000001;

for z=1:length(THETA)
    %% Forward
    THETA1=THETA;
    THETA1(z)=THETA1(z)*(1+h)+h2;

    FF1 = modelrun_all(t_all, exp_id, THETA1, mic_prot, volumes, doses);

    %%    Backward
    THETA1=THETA;
    THETA1(z)=THETA(z)*(1-h)-h2;

    FF2 = modelrun_all(t_all, exp_id, THETA1, mic_prot, volumes, doses);

    J(z,:)=(FF1-FF2)./(2*THETA(z)*h+2*h2);
end
J;


%% Differentiation using complex-step derivative approximation
%
% THETA;
% nTHETA=numel(THETA);                    % size of independent
% h=nTHETA*eps;                           % differentiation step size
%
% for z=1:length(THETA)
%     THETA1=THETA;                           % reference point
%     THETA1(z)=THETA1(z)+h*1i;               % increment in kth
independent variable
%
%     FF1 = modelrun_all(t_all, exp_id, THETA1, mic_prot, volumes,
doses);
%
```

```
%     J(z,:)=imag(FF1)/h;                                % complex step
differentiation
% end
% J;
```

Modelfit.m

```
%% Model - Estimation

%% INPUT - Fixed parameters
% Doses [Amt in nM] in experimental conditions (Control,ABT,Rfc,ABTRfc)
doses=[x1,x2,x3,x4].*250;

% Microsomal protein [Amt in mg] in experimental conditions
(Control,ABT,Rfc,ABTRfc)
mic_prot=[x1 x2 x3 x4];

% Volumes
Vinc=250; % [mL]

%% INPUT - Estimated parameters: Initial estimates
CLmet=x;
IntABT=x;
IntRIF=x;
IntABTRIF=x;
lowerbound=zeros(1,4);
upperbound=[10^6,10^6,10^6,10^6];


%% Import and curate data
data_conv=load('alldata_conv.txt');
data_all=[data_conv];

volumes=[Vinc];
theta0=[CLmet,IntABT,IntRIF,IntABTRIF];


%% Optimisation
options=optimset('Diagnostics','on','Display','iter','MaxFunEvals',10000,
'Maxiter',10000,'TolX',1e-10);
%
options=optimset('LargeScale','off','Diagnostics','on','Display','iter','
MaxFunEvals',1000,'Maxiter',1000,'TolX',1e-8);
[theta,resnorm] =
lsqnonlin(@obj_fun,theta0,lowerbound,upperbound,options,...
                  data_all,mic_prot,volumes,doses);

theta
THETA=theta;    % Estimation

% prediction
t_all = data_all(:,1);
exp_id = data_all(:,3);
pred = modelrun_all(t_all, exp_id, THETA, mic_prot, volumes, doses);

%data
data=data_all(:,2);
```

```
res=data-pred;              % residual (data-prediction)

wt_pred=pred;
for k=1:length(wt_pred);
    if pred(k)==0
        wt_pred(k)=1;
    end
end
OF=sum((res.^2)./(wt_pred.^2)); % objective function this must be equal
to "resnom" or f(x) at the last iteration of the LSQnonlin
%OF=sum(res.^2); % objective function this must be equal to "resnom" or
f(x) at the last iteration of the LSQnonlin

J = Jac(THETA,data_all,mic_prot,volumes,doses);

nparam=length(THETA);

FIM=zeros(nparam);
for i=1:length(J)
    v=wt_pred(i)^2;
    FIM=((J(:,i)*J(:,i)')/v) + FIM;
end
FIM=FIM/(sum((res.^2)./wt_pred.^2)/(length(J)-nparam))

%FIM=FIM/(sum(res.^2)/(length(J)-nparam));

dt=det(FIM)           % determinant
Cov=inv(FIM)          % Var-Cov

se=sqrt(diag(Cov));
se=se'                % se
cv=se./THETA*100      % cv se(%)

%% SIMULATING: Final parameter estimates
t_end=max(data_all(:,1));

t_sim=[0:0.01:t_end*1.10]';

t_sim_all=[t_sim;t_sim;t_sim;t_sim];
exp_id_all=[ones(length(t_sim),1);ones(length(t_sim),1).*2;ones(length(t_
sim),1).*3;...
    ones(length(t_sim),1).*4];

C_sim=modelrun_all(t_sim_all, exp_id_all, THETA, mic_prot, volumes,
doses);
```

Modelrun_all.m

```
function F=modelrun_all(t_all, exp_id, theta, mic_prot, volumes, inicon)

dose_all=inicon;

% Fixed volumes
Vinc=volumes(1);    % [uL]

% model run all
%% Depletion
obs_comp=1;
% Depletion: Control
```

```
clmeti = cl_inter(theta,0,0,0);
theta=[clmeti,theta(2:end)];
inicon=[dose_all(1)/Vinc];
t_data=t_all(exp_id(:,1)==1,:);
C1=oderun(t_data,theta,mic_prot(1),volumes,inicon,obs_comp);

% Depletion: +ABT
clmeti = cl_inter(theta,1,0,0);
theta=[clmeti,theta(2:end)];
inicon=[dose_all(2)/Vinc];
t_data=t_all(exp_id(:,1)==2,:);
C2=oderun(t_data,theta,mic_prot(2),volumes,inicon,obs_comp);

% Depletion: +RIF
clmeti = cl_inter(theta,0,1,0);
theta=[clmeti,theta(2:end)];
inicon=[dose_all(3)/Vinc];
t_data=t_all(exp_id(:,1)==3,:);
C3=oderun(t_data,theta,mic_prot(3),volumes,inicon,obs_comp);

% Depletion: +ABT&RIF
clmeti = cl_inter(theta,0,0,1);
theta=[clmeti,theta(2:end)];
inicon=[dose_all(4)/Vinc];
t_data=t_all(exp_id(:,1)==4,:);
C4=oderun(t_data,theta,mic_prot(4),volumes,inicon,obs_comp);


%% Return simulated data
F=[C1;C2;C3;C4];
```

Obj_fun.m

```
function F = obj_fun(theta,data_all,mic_prot,volumes,doses)

%% Run simulation
t_all = data_all(:,1);
exp_id = data_all(:,3);

pred = modelrun_all(t_all, exp_id, theta, mic_prot, volumes, doses);


%% Objective function
data = data_all(:,2); % Observed data

nt=length(data(1,:)); % N time points

if any(theta < 0)
    F=1000000*ones(1,nt);
else
    FF_wt=pred;
    for k=1:length(FF_wt);
        if FF_wt(k)==0
            FF_wt(k)=1;
        end
    end

     F=(data-pred)./FF_wt;
end
F;
```

Ode_model1.m

```
function dC = odemodel1(t,C,theta,mic_prot,volumes)

dC=zeros(1,1);

CLmet_tot=theta(1)*mic_prot;

Vinc=volumes(1); % [uL]

% Conventional
dC(1) = (-CLmet_tot*C(1))/Vinc;
```

Oderun.m

```
function F=oderun(t_all, theta, mic_prot, volumes, inicon, obs_comp)

options = odeset();

[t C] = ode45(@odemodel1,t_all,inicon,options,theta,mic_prot,volumes);


F=C(:,obs_comp);
%plot(t,C);
%legend('Conv.','Media','Cell');
```

7.13.2. Step 2 – Modelling the Media Loss Assay

CL_inter.m

```
function clact = cl_inter(fixed_params, GammaABT, GammaRIF, GammaABTRIF)

CLmet_tot=fixed_params(1);
ABT=fixed_params(2);
RIF=fixed_params(3);
RIFABT=fixed_params(4);

ABTINT=ABT^(GammaABT);
RIFINT=RIF^(GammaRIF);
ABTRIFINT=RIFABT^(GammaABTRIF);

clact = CLmet_tot*ABTINT*RIFINT*ABTRIFINT;
```

Jac.m

```
function J = Jac(THETA,data_all,mic_prot,volumes,doses, fixed_params)

t_all = data_all(:,1);
exp_id = data_all(:,3);
```

```
h=0.00001;
h2=0.0000001;

for z=1:length(THETA)
    %% Forward
    THETA1=THETA;
    THETA1(z)=THETA1(z)*(1+h)+h2;

    FF1 = modelrun_all(t_all, exp_id, THETA1, mic_prot, volumes, doses,
fixed_params);

    %%    Backward
    THETA1=THETA;
    THETA1(z)=THETA(z)*(1-h)-h2;

    FF2 = modelrun_all(t_all, exp_id, THETA1, mic_prot, volumes, doses,
fixed_params);

    J(z,:)=(FF1-FF2)./(2*THETA(z)*h+2*h2);
end
J;


%% Differentiation using complex-step derivative approximation
%
% THETA;
% nTHETA=numel(THETA);                    % size of independent
% h=nTHETA*eps;                           % differentiation step size
%
% for z=1:length(THETA)
%     THETA1=THETA;                           % reference point
%     THETA1(z)=THETA1(z)+h*1i;               % increment in kth
independent variable
%
%     FF1 = modelrun_all(t_all, exp_id, THETA1, mic_prot, volumes,
doses);
%
%     J(z,:)=imag(FF1)/h;                                % complex step
differentiation
% end
% J;
```

Modelfit.m

```
%% Model - Estimation

%% INPUT - Fixed parameters
% Doses [Amt in nM] in experimental conditions (Control,ABT,Rfc,ABTRfc)
doses=[x1,x2,x3,x4].*250;

% Microsomal protein [Amt in mg] in experimental conditions
(Control,ABT,Rfc,ABTRfc)
mic_prot=[x1 x2 x3 x4];

% Volumes
Vinc=250; % [mL]
```

```
%% INPUT - Model parameters
% FIXED parameters
CLmet_tot=[Value calculated in Step 1];   % uL/min/mg
IntABT=[Value calculated in Step 1];
IntRIF=[Value calculated in Step 1];
IntABTRIF=[Value calculated in Step 1];


% Estimated parameters
CLupt=x;
CLdif=x;        % uL/min/mg
Vcell=x;

lowerbound=zeros(1,3);
upperbound=[10^6,10^6,10^6];


%% Import and curate data
data_medloss=load('alldata_medloss.txt');
data_all=data_medloss;

volumes=[Vmed];
theta0=[CLupt,CLdif,Vcell];
fixed_params=[CLmet_tot, IntABT, IntRIF,IntABTRIF];

%% Optimisation
options=optimset('Diagnostics','on','Display','iter','MaxFunEvals',1000,'
Maxiter',1000,'TolX',1e-10);
%
options=optimset('LargeScale','off','Diagnostics','on','Display','iter','
MaxFunEvals',1000,'Maxiter',1000,'TolX',1e-8);
[theta,resnorm] =
lsqnonlin(@obj_fun,theta0,lowerbound,upperbound,options,...
                  data_all,mic_prot,volumes,doses,fixed_params);

theta
THETA=theta;    % Estimation

% prediction
t_all = data_all(:,1);
exp_id = data_all(:,3);
pred = modelrun_all(t_all, exp_id, THETA, mic_prot, volumes, doses,
fixed_params);

%data
data=data_all(:,2);

res=data-pred;              % residual (data-prediction)

wt_pred=pred;
for k=1:length(wt_pred);
    if pred(k)==0
        wt_pred(k)=1;
    end
end
OF=sum((res.^2)./(wt_pred.^2)); % objective function this must be equal
to "resnom" or f(x) at the last iteration of the LSQnonlin
%OF=sum(res.^2); % objective function this must be equal to "resnom" or
f(x) at the last iteration of the LSQnonlin

J = Jac(THETA,data_all,mic_prot,volumes,doses, fixed_params);
```

```
nparam=length(THETA);

FIM=zeros(nparam);
for i=1:length(J)
    v=wt_pred(i)^2;
    FIM=((J(:,i)*J(:,i)')/v) + FIM;
end
FIM=FIM/(sum((res.^2)./wt_pred.^2)/(length(J)-nparam))

%FIM=FIM/(sum(res.^2)/(length(J)-nparam));

dt=det(FIM)          % determinant
Cov=inv(FIM)         % Var-Cov

se=sqrt(diag(Cov));
se=se'               % se
cv=se./THETA*100     % cv se(%)

%% SIMULATING: Final parameter estimates
t_end=max(data_all(:,1))+5;

t_sim=[0:0.01:t_end]';

t_sim_all=[t_sim;t_sim;t_sim;t_sim];
exp_id_all=[ones(length(t_sim),1);ones(length(t_sim),1).*2;ones(length(t_
sim),1).*3;...
    ones(length(t_sim),1).*4];

C_sim=modelrun_all(t_sim_all, exp_id_all, THETA, mic_prot, volumes,
doses, fixed_params);
```

Modelrun_all.m

```
function F=modelrun_all(t_all, exp_id, theta, mic_prot, volumes, inicon,
fixed_params)

dose_all=inicon;

% Fixed volumes
Vmed=volumes(1);   % [uL]
Vcel=theta(3);   % [uL]

% model run all
%% Media loss
obs_comp=2;
% Media loss: Control
clmeti = cl_inter(fixed_params,0,0,0);
theta=[theta(1:end)];
inicon=[0,dose_all(1)/Vmed,0];
t_data=t_all(exp_id(:,1)==1,:);
C1=oderun(t_data,theta,mic_prot(1),volumes,inicon,obs_comp,clmeti);

% Media loss: +ABT
clmeti = cl_inter(fixed_params,1,0,0);
theta=[theta(1:end)];
inicon=[0,dose_all(2)/Vmed,0];
t_data=t_all(exp_id(:,1)==2,:);
C2=oderun(t_data,theta,mic_prot(2),volumes,inicon,obs_comp,clmeti);
```

```
% Media loss: +RIF
clmeti = cl_inter(fixed_params,0,1,0);
theta=[0,theta(2:end)];
inicon=[0,dose_all(3)/Vmed,0];
t_data=t_all(exp_id(:,1)==3,:);
C3=oderun(t_data,theta,mic_prot(3),volumes,inicon,obs_comp,clmeti);

% Media loss: +ABT&RIF
clmeti = cl_inter(fixed_params,1,1,0);
theta=[0,theta(2:end)];
inicon=[0,dose_all(4)/Vmed,0];
t_data=t_all(exp_id(:,1)==4,:);
C4=oderun(t_data,theta,mic_prot(4),volumes,inicon,obs_comp,clmeti);



%% Return simulated data
F=[C1;C2;C3;C4];
```

Obj_fun.m

```
function F = obj_fun(theta,data_all,mic_prot,volumes,doses,fixed_params)

%% Run simulation
t_all = data_all(:,1);
exp_id = data_all(:,3);

pred = modelrun_all(t_all, exp_id, theta, mic_prot, volumes, doses,
fixed_params);


%% Objective function
data = data_all(:,2); % Observed data

nt=length(data(1,:)); % N time points

if any(theta < 0)
    F=1000000*ones(1,nt);
else
    FF_wt=pred;
    for k=1:length(FF_wt);
        if FF_wt(k)==0
            FF_wt(k)=1;
        end
    end

     F=(data-pred)./FF_wt;
end
F;
```

Odemodel1.m

```
function dC = odemodel1(t,C,theta,mic_prot,volumes,clmeti)

dC=zeros(3,1);
```

```
CLmet_tot=clmeti*mic_prot;
CLupt=theta(1)*mic_prot;
CLdif=theta(2)*mic_prot;

Vcell=theta(3); % [uL]
Vmed=volumes(1); % [uL]

% Conventional
dC(1) = 0;

% Media: Media
dC(2) = (-(CLupt + CLdif)*C(2) + CLdif*C(3))/Vmed;

% Media: Cell
dC(3) = ( (CLupt + CLdif)*C(2) - CLdif*C(3) - (CLmet_tot*C(3)))/Vcell;

%
```

Oderun.m

```
function F=oderun(t_all, theta, mic_prot, volumes, inicon, obs_comp,
clmeti)

options = odeset();

[t C] =
ode45(@odemodel1,t_all,inicon,options,theta,mic_prot,volumes,clmeti);


F=C(:,obs_comp);
%plot(t,C);
%legend('Conv.','Media','Cell');
```

7.14. Correlations between CL_{bile} and $CL_{sinusoidal}$ to $LogD_{7.4}$ and $CL_{passive}$

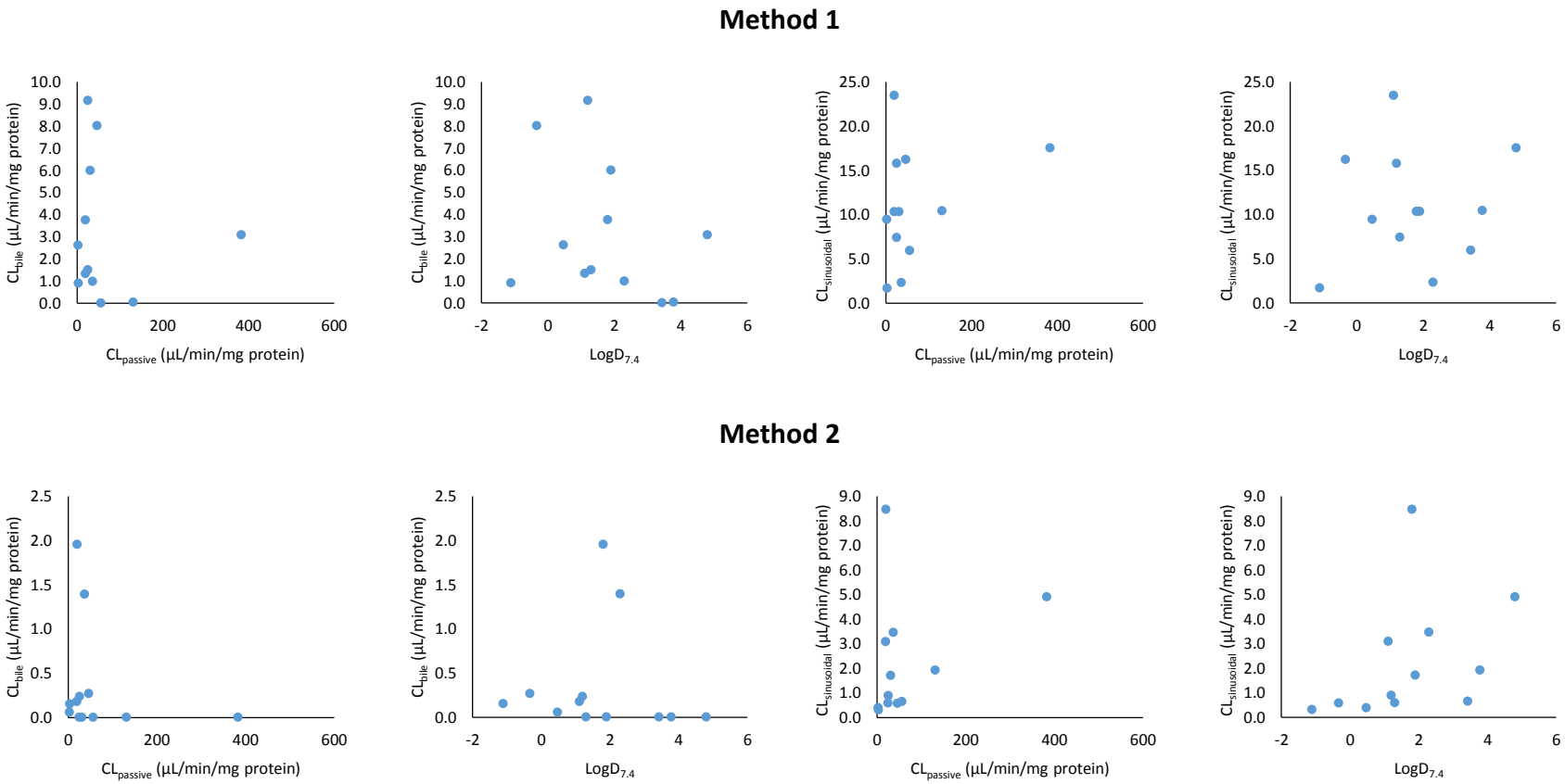

Figure 48 – Correlations between CL_{bile} or $CL_{sinusoidal}$, estimated using methods 1 and 2, with $CL_{passive}$ data generated in the media loss assay (Chapter 4) or $LogD_{7.4}$ (Table 19). No significant relationships were noted.

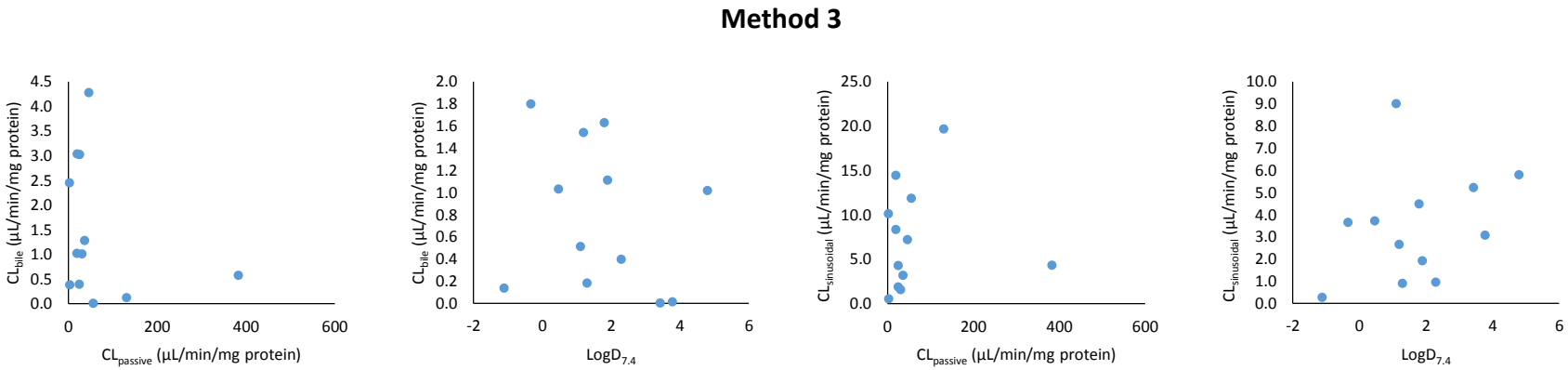

Figure 49 - Correlations between CL_{bile} or $CL_{sinusoidal}$, estimated using method 3, with $CL_{passive}$ data generated in the media loss assay (Chapter 4) or $LogD_{7.4}$ (Table 19). No significant relationships were noted.

7.15. Determining the GMFE and RMSE for clearance parameters using combinations of scaling factor

Table 37 - Effect of scaling factors on the GMFE and RMSE for CL_{uptake}, CL_{met}, and $CL_{int,total}$ using combinations of physiological or empirical scaling factors

Parameter		Scaling Method																			
	CL_{uptake}	Phys		Mean		Median		Min		Max		CDSF		CDSF		CDSF		CDSF		CDSF	
	CL_{met}	Phys		Mean		Median		Min		Max		Phys		Mean		Median		Min		Max	
	CL_{bile}	Phys		Phys		Phys		Min		Max		Phys		Phys		Phys		Min		Max	
	$CL_{sinusoidal}$	Phys		Phys		Phys		Min		Max		Phys		Phys		Phys		Min		Max	
		GMFE	RMSE	GMFE	RMSE	GMFE	RMSE	GMFE	RMSE	GMFE	RMSE	GMFE	RMSE	GMFE	RMSE	GMFE	RMSE	GMFE	RMSE	GMFE	RMSE
CL_{uptake} only		2.97	2559	7.01	8132	2.66	1114	2.66	915	5.05	21798	3.11	689								
CL_{met} only		6.43	2416	12.9	21798	6.3	2416	10.45	946	5.72	1158										
$CL_{int,total}$	Method 1	2.97	2293	6.76	8069	2.89	1134	3.61	1088	3.42	4682	3.41	802	3.17	705	3.33	755	3.41	802	3.41	802
	Method 2	2.75	2473	6.97	8121	2.63	1113	2.73	1097	4.35	5115	3.04	723	3.11	690	3.08	698	3.04	723	3.04	723
	Method 3	2.69	2460	6.91	8113	2.65	1121	3.05	1110	3.83	5064	3.04	747	3.11	692	3.08	712	3.04	747	3.04	747

Phys; Physiological scaling factor of 200 mg protein/g liver and 40g liver/kg bodyweight for rat

Min/Max; Minimum and maximum possible physiological scaling factor, see Table 34 (Appendix 7.5)

CDSF; Clearance-Derived Scaling Factor, determined by the CL_{uptake} for data from the media loss assay (see 3.4.2.1.3)

Mean/Median; Mean and Median required scaling factors for CL_{uptake} or CL_{met} (see 3.4.2.1.2)